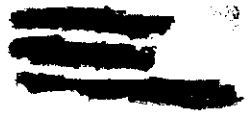

FIXED-BASE FLIGHT SIMULATOR STUDIES OF VTOL AIRCRAFT HANDLING QUALITIES IN HOVERING AND LOW-SPEED FLIGHT

DAVID P. MILLER
EDWARD W. VINJE

UNITED AIRCRAFT RESEARCH LABORATORIES

FOREWORD

This report was prepared for the United States Air Force by the United Aircraft Research Laboratories, East Hartford, Connecticut.

The work reported herein was performed by the United Aircraft Research Laboratories under the sponsorship of the Air Force Flight Dynamics Laboratory, Research and Technology Division, Air Force Systems Command, Wright-Patterson Air Force Base, Ohio. The research was conducted under Subcontract S-67-2 to the Cornell Aeronautical Laboratory as part of Part III of the VTOL Integrated Flight Control Systems Program (VIFCS), Contract AF 33(615)-3736, Project 698 DC. The RTD project engineer was Mr. Wilfred Klotzback and the CAL project engineer was Mr. Charles Chalk.

This manuscript was submitted 18 January 1968 for publication as an RTD Technical Report. It is also published as United Aircraft Research Laboratories Report F910482-12.

This technical report has been reviewed and is approved.

C. B. Westbrook
Chief, Control Criteria Branch
Flight Control Division
Air Force Flight Dynamics Laboratory

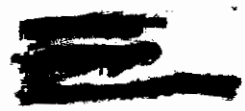

ABSTRACT

A systematic investigation of VTOL longitudinal and lateral handling qualities in hovering and low-speed flight was conducted in a fixed-base simulator. The effects of rate damping and attitude stability augmentation on handling qualities for a range of speed-stability and drag parameters, turbulence levels, and several other factors were studied. Pilots selected optimum control sensitivity, prepared written comments and assigned pilot opinion ratings for each configuration. The results for minimum satisfactory handling qualities are correlated with the aircraft and stability augmentation parameters and compared with existing and suggested requirements for VTOL handling qualities. Suggested criteria for aircraft dynamic characteristics and minimum response to control inputs that are based on the flight simulator data are presented. Root-mean-square performance data for a precision hovering task were obtained for a range of aircraft, stability augmentation and turbulence level parameters. Pilot model adapted parameters for a multiloop representation of the hovering task were computed from these rms performance data and correlated with pilot opinion.

Results show that the stability augmentation and optimum control sensitivity requirements for satisfactory handling qualities are dependent on the gust sensitivity of the aircraft. The generalized results show little correlation with existing or suggested criteria. Instead they indicate that the aircraft speed-stability parameters must be considered in the development of handling qualities specifications. The rms hovering performance was dependent primarily on position-loop disturbances. Changes in pitch-loop dynamics and disturbance level had little effect on hovering performance even when they resulted in large changes in pilot opinion rating. Results of the studies of pilot model adapted parameters show that pilot opinion correlates well with a combination of adapted lead and aircraft gust sensitivity.

TABLE OF CONTENTS

TABLE OF CONTENTS (Cont'd.)

ILLUSTRATIONS

ILLUSTRATIONS (Cont'd)

ILLUSTRATIONS (Cont'd.)

TABLES

TABLES (Cont'd.)

SYMBOLS

b	Bandwidth of longitudinal control backlash, in. (see Table V)
f_d	Damped frequency of oscillation, cycles/sec
g	Gravitational constant, 32.2 ft/sec^2
I_x, I_y, I_z	Moments of inertia in roll, pitch, and yaw, slug-ft^2
I_{xz}	Product of inertia, slug-ft^2
j	$\sqrt{-1}$
K_{P_θ}	Pilot adaptive pitch-loop gain, in./rad
K_{P_x}	Pilot adaptive position-loop gain, rad/ft
L	Rolling moment divided by I_x, rad/sec^2
L_{δ_o}	Lateral control sensitivity at which the extended optimum line crosses the zero-damping axis, (rad/sec^2)/in. (see Fig. 7)
m	Aircraft mass, slugs
M	Pitching moment divided by I_y, rad/sec^2
M_{RA}	Authority of pitch rate stabilization system, rad/sec^2 (see Fig. 32)
M_{δ_o}	Longitudinal control sensitivity at which the extended optimum line crosses the zero-damping axis, (rad/sec^2)/in. (see Fig. 4)
N	Yawing moment divided by I_z, rad/sec^2
PM	Phase margin, an indicator of closed-loop stability expressed as the phase lag of the aircraft open-loop dynamics, plus the phase contribution from the pilot model, plus 180 degrees, deg
PM_x	Phase margin for the position loop, deg
PM_θ	Phase margin for the pitch loop, deg
PR	Cooper pilot rating for hovering and maneuvering task (see Table I)

SYMBOLS (Cont'd.)

PR_H	Cooper pilot rating for precision hovering task (see Table I)
p	Roll rate, rad/sec
q	Pitch rate, rad/sec
$q/u_g \Big\vert_{\substack{\theta \to \delta_e \\ x \to \theta_x}}$	Closed-loop hovering-task model equation for aircraft pitch rate response to turbulence where $\theta \to \delta_e$ indicates the pitch loop is closed on the longitudinal stick command and $x \to \theta_x$ indicates that the position loop is closed on the attitude command angle (see Eq.(B-16))
r	Yaw rate, rad/sec
s	Laplace operator, 1/sec
S_P	Slope of longitudinal optimum control sensitivity line, in./(rad/sec)
S_R	Slope of lateral optimum control sensitivity line, in./(rad/sec)
S_{u_g}	Turbulence power spectrum, ft^2/sec
t	Time, sec
T_{L_x}	Pilot adapted pitch-loop rate sensing (lead) parameter, sec
T_{L_θ}	Pilot adapted position-loop rate sensing (lead) parameter, sec
T_N	Neuromuscular lag, sec
$1/T_{sp}$	Frequency domain location of the first-order pole in the open-loop pitch dynamics, 1/sec
u	Velocity along the x axis, ft/sec
$u/u_g \Big\vert_{\substack{\theta \to \delta_e \\ x \to \theta_x}}$	Closed-loop hovering-task model equation for aircraft longitudinal-velocity response to turbulence, where $\theta \to \delta_e$ indicates that the pitch loop is closed on the longitudinal stick command and $x \to \theta_x$ indicates that the position loop is closed on the attitude command angle (see Eq. (B-20))

SYMBOLS (Cont'd.)

u_g	Longitudinal component of gust velocity, ft/sec
v	Velocity along y axis, ft/sec
v_g	Lateral component of gust velocity, ft/sec
w	Velocity along z axis, ft/sec
W	Gross weight of aircraft, lb
x	Conventional longitudinal axis notation for the body-axis system
$x/u_g \Big\vert_{\substack{\theta \rightarrow \delta_e \\ x \rightarrow \theta_x}}$	Closed-loop hovering-task model equation for aircraft position response to turbulence where $\theta \rightarrow \delta_e$ indicates the pitch loop is closed on the longitudinal stick command and $x \rightarrow \theta_x$ indicates that the position loop is closed on the attitude command angle, (see Eq. (B-19))
$x/\theta_x \Big\vert_{\theta \rightarrow \delta_e}$	Open-loop position response to an attitude command where $\theta \rightarrow \delta_e$ indicates the pitch loop is closed on the longitudinal stick command (see Eq. (B-10))
X	Forces along x axis divided by mass of aircraft, ft/sec^2
y	Conventional lateral axis notation for the body-axis system
Y	Forces along y axis divided by mass of aircraft, ft/sec^2
Y_{p_θ}	Pitch-loop quasi-linear pilot model (see Eq. (10))
Y_{p_x}	Position-loop quasi-linear pilot model
$Y_{x_{\delta_e}}$	Transfer function for open-loop position response to a longitudinal stick command (see Eq. (B-5))
$Y_{x_{u_g}}$	Transfer function for open-loop position response to turbulence (see Eq. (B-6))
$Y_{\theta_{\delta_e}}$	Transfer function for open-loop pitch response to a longitudinal stick command (see Eq. (B-2))
$Y_{\theta_{u_g}}$	Transfer function for open-loop pitch response to turbulence (see Eq. (B-3))

SYMBOLS (Cont'd.)

z	Conventional vertical axis notation for the body-axis system
Z	Forces along z axis divided by mass of aircraft, ft/sec^2
δ_a	Lateral displacement of control stick, in.
δ_c	Displacement of collective stick for height control, in.
δ_e	Longitudinal displacement of control stick, in.
δ_r	Displacement of pedals for yaw control, in.
δ_T	Displacement of engine throttle control, in.
Δ_1	Characteristic equation for the open-loop pitch dynamics (see Eq. (B-4))
Δ_2	Characteristic equation for the open-loop position dynamics (see Eq. (B-11))
Δ_3	Characteristic equation for the closed-loop hovering task model (see Eq. (B-15))
ζ	Damping ratio of oscillatory roots
θ	Euler pitch attitude angle, rad
$\theta/u_g \Big\vert_{\substack{\theta \rightarrow \delta_e \\ x \rightarrow \theta_x}}$	Closed-loop hovering-task model equation for pitch attitude response to turbulence where $\theta \rightarrow \delta_e$ indicates that the pitch loop is closed on the longitudinal stick command and $x \rightarrow \theta_x$ indicates that the position loop is closed on the attitude command angle (see Eq. (B-14))
θ_R	Pitch attitude angle change required within 1 sec following 1 in. longitudinal control input, rad
θ_x	Position loop command angle, rad
σ	Denotes rms value of subscripted variable for hovering task (see Eq. (B-23))
σ_{u_g}	RMS turbulence, ft/sec

τ_c	First-order time constant of control lag, sec
τ_x	Pilot x-loop transport lag, sec
τ_θ	Pilot θ-loop transport lag, sec
ϕ	Euler roll attitude angle, rad
ϕ_R	Roll attitude angle change required within 1 sec following 1 in. lateral control input, rad
ψ	Euler yaw attitude angle, rad
ω	Frequency of oscillation, rad/sec
ω_B	Break frequency of first-order filter for generating turbulence, rad/sec (see Eq. (2))
ω_c	Crossover frequency, that frequency at which the gain of the product of the pilot model and open-loop aircraft dynamics is equal to 1, a measure of closed-loop frequency response, rad/sec
ω_d	Damped frequency of oscillation, rad/sec
ω_n	Natural frequency of oscillation, rad/sec

Subscripts

REF	Denotes reference or base value of a variable
q, u	Denotes partial derivative of a parameter with respect to the subscript shown (e.g., pitch rate damping $M_q = \partial M/\partial q$) when used with M or X. Denotes rms pitch rate and rms longitudinal velocity (position rate), respectively, when used with σ.
x, θ	Denotes quantities pertaining to position and pitch loops, respectively
δ_e	Denotes quantity pertaining to longitudinal control stick activity

Subscripts (cont'd.)

δ_a	Denotes quantity pertaining to lateral control stick activity
δ_r	Denotes quantity pertaining to directional control pedal activity
ϵ	Denotes error between desired and actual value of a variable

Superscripts

$(\dot{})$	Denotes first derivative with respect to time, d/dt
$(\ddot{})$	Denotes second derivative with respect to time, d^2/dt^2

SECTION I

INTRODUCTION

Within a few years the military services and air transport carriers are expected to procure nonrotary-wing V/STOL aircraft for operational use. These vehicles must be designed so that they satisfy mission-performance requirements which are especially stringent because of the unique capabilities of V/STOL aircraft. Military tacticians, for example, can be expected to call for the utmost in performance from such aircraft. The performance, efficiency, and reliability requirements levied on the propulsive, aerodynamic and structural characteristics of such aircraft will be severe. Yet, despite these considerations, the aircraft will have to be safe and relatively easy to fly if the pilot is to perform the complex and demanding tasks which will be asked of him and his aircraft. The performance and handling qualities specifications which will be applied during the procurement of such V/STOL aircraft (but which have not yet been developed) must insure that these demanding requirements are satisfied. In doing so, however, the specifications must not be so restrictive that they add unnecessary complexity and cost to the vehicle. In addition, the specifications must be in a form that can be easily interpreted and applied by the designer of the aircraft. Finally, they must also be expressed so that the procuring agency can determine by flight tests if the specifications have been met by the manufacturer.

An official specification for V/STOL aircraft handling qualities does not yet exist and its development has been impaired by the lack of extensive flight experience with such aircraft. Consequently, research is being continued using ground-based and in-flight simulators to obtain the needed information. The majority of this research has dealt with hovering and low-speed flight. Experimental handling qualities data have generally been derived from three sources: (1) ground-based simulation, (2) in-flight simulation, and (3) flight tests with prototype V/STOL aircraft. Ground-based simulation is economical; however, the lack of important motion and visual cues may have a significant effect on some of the data. Moving-base simulators have not achieved their full usefulness since methods for scaling and washing out motion effects (especially important for VTOL transition studies) are still being developed. In-flight simulations have been performed using helicopters and other VTOL aircraft equipped with variable-stability systems, and good data have been obtained by Princeton University (Ref. 1), National Research Council of Canada (Ref. 2) and the NASA (Refs. 3 and 4). These simulations have generally provided good visual and motion cues but have not provided the capability for simulating translational forces (aircraft drag and gust forces). Flight tests with prototype V/STOL aircraft have, of course, also been conducted. Unfortunately, most of the data and experience obtained from prototype V/STOL aircraft in the past have not been documented in the open literature.

The usefulness of data from the above studies has been impaired somewhat by widely differing experimental conditions. Most of them have also been conducted with specific limited objectives, and the results lack the generality which is needed for the development of specifications. The biggest deficiency, however, has been that too little effort has gone into understanding how fundamental flight characteristics influence a pilot's opinion of and ability to control a given configuration. Achieving this understanding is important because so many factors influence handling qualities. Such factors as dynamic characteristics of the aircraft, control system characteristics, sensitivity of the aircraft to external disturbances, motion and visual cues given the pilot, and pilot's confidence in the overall aircraft are just a few. Systematic flight test evaluation of all these factors is impractical because of the prohibitive cost of such a program. Moreover, the relative importance of any one of them depends on the particular flight vehicle, its environment, and the flight task. The necessary emphasis has not been given to the determination of common, basic handling qualities characteristics which result from these factors and are the source for pilot opinion. Recently, however, analytical studies (Refs. 5 and 6) have indicated that the effects of some of these factors on pilot opinion can be described in terms of only one or two generalized parameters. While this has been an important step in understanding V/STOL handling qualities, little has been done to experimentally validate these results.

In undertaking this study then, it was believed that isolating the effects of some of the fundamental flight characteristics affecting handling qualities would be necessary to obtain information required for the development of handling qualities specifications for VTOL aircraft. To accomplish this, the general approach taken in both the analytical and flight simulator experiments was to represent the flight characteristics of a generalized VTOL aircraft in hovering and low-speed flight with stability derivatives. This method has been used successfully in previous studies at the United Aircraft Research Laboratories (UARL) in which good correlation with flight test data was achieved (Ref. 7). The primary objectives of the study reported herein were: (1) to relate the stability augmentation requirements for satisfactory handling qualities in hovering and low-speed flight to several principal aircraft stability derivatives and the level of turbulence, (2) to determine possible correlation of measured rms performance data from a simulated hovering task with pilot opinion of handling qualities, and (3) to examine the basis for pilot opinion by computing pilot-adapted parameters using measured rms hovering performance data in conjunction with closed-loop model analysis techniques.

SECTION II

BACKGROUND OF EXPERIMENTAL PROGRAM

This section contains a general discussion of the experimental program. In Part A, the equations of motion, the method for simulating turbulence and the experimental equipment are described. Parts B and C contain descriptions of the hovering and low-speed maneuvering experiments and the precision-hovering experiments, respectively. The range of parameters, experimental conditions, instructions to pilots, and data reduction techniques are discussed in both Parts B and C.

A. Details of Experimental Program

1. Equations of Motion

Equations governing pitch, roll, and yaw attitude and longitudinal, lateral, and vertical displacement degrees of freedom for hovering and low-speed flight were programmed on an analog computer. The equations were written assuming small perturbations from hovering flight. They had the general form

$$
\left.
\begin{aligned}
&M_u u + M_\theta \theta + M_q q - \dot{q} = -M_{\delta_e}\delta_e - M_u u_g \\
&L_v v + L_\phi \phi + L_p p - \dot{p} = -L_{\delta_a}\delta_a - L_v v_g \\
&N_v v + N_r r - \dot{r} = -N_{\delta_r}\delta_r - N_v v_g \\
&X_u u - qw + rv - g\sin\theta - \dot{u} = -X_u u_g - X_{\delta_e}\delta_e \\
&Y_v v - ru + pw + g\sin\phi\cos\theta - \dot{v} = -Y_v v_g \\
&Z_w w - pv + qu + g\cos\phi\cos\theta - \dot{w} = 0 \\
&\dot{\theta} = q\cos\phi - r\sin\phi \\
&\dot{\phi} = p + q\sin\phi\tan\theta + r\cos\phi\tan\theta \\
&\dot{\psi} = (q\sin\phi + r\cos\phi)\sec\theta
\end{aligned}
\right\} \qquad (1)
$$

The various terms and symbols are described in the List of Symbols. The equations have been normalized with aircraft mass and moments of inertia. Stability derivatives on the left side of the equations describe the aerodynamic, propulsive and stability augmentation forces and moments. Terms on the right side describe the control moments and the forces and moments induced by the simulated turbulence. During the course of this study, flight simulator studies of the XC-142 and XV-4B aircraft were also conducted. For these simulations, additional stability derivatives were included in the equations of motion (listed in Tables A-VIII and A-IX). Also, as described subsequently, the vertical (z) degree of freedom was not simulated in the generalized hovering and low-speed maneuvering experiments, and the vertical (z) and directional (ψ) degrees of freedom were not simulated in the rms hovering performance experiments.

2. Simulation of Turbulence

Turbulence has an important influence on handling qualities of VTOL aircraft in low-speed flight. The method selected for simulating turbulence was similar to that used successfully in the flight test studies of handling qualities with the Princeton HUP-1 helicopter (Ref. 1). Turbulence was simulated by passing the output of a random noise generator having a relatively uniform low-frequency power spectral distribution through a first-order filter with a break frequency ω_B of 0.314 rad/sec. That is, the signal was unattenuated at frequencies up to ω_B and then attenuated at 20 db per decade at higher frequencies. The transfer function of the filter had the form

$$\frac{u_g}{\text{GENERATOR OUTPUT}} = \frac{\sigma_{u_g}\sqrt{2\omega_B / S_{RN}}}{s + \omega_B} \qquad (2)$$

where σ_{u_g} is the root-mean-square value of the random component of the wind and S_{RN} is the power spectral density of the output of the random noise generator at low frequencies. The resulting simulated turbulence had a power spectral density given by

$$S_{u_g}(\omega) = \frac{2\omega_B \sigma_{u_g}^2}{\omega_B^2 + \omega^2} \qquad (3)$$

With a break frequency of 0.314 rad/sec and an rms turbulence level of 5.1 ft/sec, the simulated turbulence had a frequency content similar to that simulated in the flight tests of the Princeton HUP-1 variable stability tandem-rotor helicopter reported in Ref. 1. In this reference, the pilots describe this simulated turbulence as corresponding to a medium-turbulent day.

Lateral gust disturbances were not simulated in the Princeton studies. However, it was felt that for the UARL studies small lateral gust disturbances should be provided. This would cause the pilot to direct some attention to

controlling the lateral and directional degrees of freedom but would not seriously affect his evaluation of the longitudinal handling qualities. The lateral component v_g was assumed to be 25% of the longitudinal component u_g. The two components were in phase. For the studies in which lateral handling qualities were evaluated, the longitudinal component u_g was 25% of the lateral component v_g.

Previous studies were conducted at UARL to investigate the effect of variations in the frequency of the simulated turbulence model on handling qualities (Ref. 8). It was found that for a gust-sensitive configuration the handling qualities were much more sensitive to the rms level of turbulence than to the power spectral distribution. A 50% change in the break frequency ω_B of the filter from 0.314 rad/sec had no significant effect on the rms hovering position error or pilot opinion of handling qualities. Likewise, substituting a filter with a 40 db/dec attenuation above the break frequency had no significant effect on handling qualities as long as the rms turbulence level was held constant.

3. Flight Simulator

The experimental program was conducted in the V/STOL Aircraft Flight Simulator located in the Simulation Laboratory at UARL. This facility consists of a full-scale fixed-base Sikorsky S-61 helicopter cockpit with Norden contact analog display system. It is used by UARL and the Sikorsky Aircraft Division of United Aircraft for studying the performance and handling qualities of a wide range of helicopter and V/STOL aircraft configurations. Figure 1 shows the interior of the cockpit, the conventional helicopter-type controls and the contact analog display.

A conventional floor-mounted control stick was used for attitude control. It could be used without a force gradient, in which case there was, effectively, no inherent friction present, or it could be used with a longitudinal and lateral force gradient of about 1.5 lb/in. The full longitudinal and lateral travels of the control stick were $\pm$6.63 in. and $\pm$6.50 in., respectively. For height control, required in the XC-142 and XV-4B aircraft studies, a conventional helicopter-type collective stick with adjustable friction was used. The floor pedals for yaw control did not have a force gradient and the inherent friction was negligible.

Although the simulator is equipped with a wide range of conventional and VTOL aircraft instruments, only a few of these were used. The simulated hovering and low-speed flight task was a VFR task and the pilot derived almost all of his information from the contact analog display screen. Altitude and airspeed were displayed on instruments that contained the lags and low sensitivity scaling normally present in standard aircraft instruments. Therefore, neither of these instruments were of much value for the hovering and low-speed flight task. Auxiliary instruments were also provided to allow the pilot to center his controls and null accelerations while in the initial condition

mode of computer operation. This assured that the aircraft would be trimmed when the compute mode was initiated and thus prevented the aircraft from rapidly diverging. A more detailed description of the flight simulator is given in Ref. 9.

4. Display

The Norden contact analog display system provides the pilot with an inside-out video picture of the motion of the aircraft relative to the earth. A number of different displays are possible since, in addition to the earth elements (the ground grid, horizon, and sky), a commandable pathway, two earth position markers, and two general-purpose screen elements are available. Figure 2 shows the contact analog display for the VTOL hovering and low-speed flight task. The cross indicated the position of the nose of the aircraft relative to the horizon and remained fixed at the center of the viewing screen. The square traversed vertically and horizontally on the screen to serve as a sensitive position indicator. Thus the square provided information analogous to that which the pilot would derive by looking at an object beneath the aircraft. When the square was at the center of the screen (coinciding with the cross), the aircraft was located directly over a reference hovering position. As the aircraft maneuvered 50 ft forward and rearward with respect to the nominal reference hovering position, the square travelled to the bottom and top edges of the screen, respectively. Similarly, as the aircraft maneuvered 65 ft to the right and left with respect to the nominal reference hovering position, the square travelled to the left and right edges of the screen, respectively. The size of the square was equivalent to a hovering displacement of 7 ft. In addition to the square or precise position reference, a course position reference was provided by the ground position indicator (also shown in Fig. 2). When the aircraft was located directly over the reference hovering position (square coincident with the cross) the ground position indicator was approximately 135 ft ahead of the aircraft for a simulated hovering altitude of 40 ft. When maneuvering, the sweep rate of the ground grid provided an indication of maneuvering velocity. In addition, when changing altitude the apparent size of the ground grid squares also changed. The pitch and roll displacement of the horizon grid line was also scaled so as to produce true angles as viewed from the nominal pilot seating position. Yawing the aircraft resulted in a corresponding rotation of the grid plane.

5. Pilots

As in previous exploratory studies of this type conducted at UARL (Refs. 7, 8, 9 and 10), the principal investigators served as the evaluation pilots. Both are licensed private pilots and had flown a variety of aircraft. One also had limited helicopter experience. Prior to this investigation, both pilots had accumulated several hundred hours evaluation time on the flight simulator. Previous studies (Ref. 7) have shown good agreement between results of these studies and published handling qualities data from flight

tests. In addition, the Chief Test Pilot for Cornell Aeronautical Laboratory, Nello Infanti, also participated for approximately 14 hours in this investigation. Although his participation was somewhat limited, his comments on the effects of various parameters on handling qualities (Table A-IV) show good agreement with those of the UARL pilots.

B. Hovering and Low-Speed Maneuvering Experiments

A series of hovering and low-speed maneuvering experiments was conducted to investigate the effects of speed-stability and drag parameters, level of turbulence and several other factors on handling qualities. The purpose of the experiments was to relate the stability augmentation requirements for satisfactory handling qualities to these factors. The data are discussed in Section III and presented in detail in Appendix A in tabular form.

1. Range of Parameters

The range of parameters was selected to encompass those of present VTOL aircraft and also those believed possible for future aircraft. The principal aerodynamic stability derivatives examined were the speed-stability parameters (M_{ug} and L_{vg}) and the drag parameters (X_u and Y_v). The stability augmentation parameters were angular rate damping stabilization (M_q and L_p) and attitude stabilization (M_θ and L_ϕ). The parameters used to represent turbulence were its longitudinal and lateral components expressed in root-mean-square (rms) values. The range of parameters was as follows:

Speed-Stability Parameters, per sec^3	$0 \leq M_{ug} \leq 1.0,\ 0 \geq L_{vg} \geq -1.0$
Drag Parameters, per sec	$0 \geq X_u \geq -0.3,\ 0 \geq Y_v \geq -0.3$
Rate Damping Stabilization, per sec	$-1 \geq M_q \geq -6.0,\ -1.0 \geq L_p \geq -4.0$
Attitude Stabilization, per sec^2	$0 \geq M_\theta \geq -5.0,\ 0 \geq L_\phi \geq -6.0$
RMS Turbulence Level, ft/sec	$0 \leq \sigma_{u_g} \leq 10.3,\ 0 \leq \sigma_{v_g} \leq 10.3$

The longitudinal and lateral control sensitivities were selected by the pilots but these parameters were always less than 1.0 (rad/sec^2)/in. Directional stability derivatives were held constant and had the following values:

$$N_v = 0.002 \text{ per sec},\ N_r = -1 \text{ per sec},\ N_{\delta_r} = 0.20 \text{ per sec}^2$$

The parameters used in the simulation of XC-142 and XV-4B aircraft are tabulated in Section VI. These aircraft simulations included additional

longitudinal, lateral and directional parameters and also those for the vertical degree of freedom.

2. Experimental Conditions

For the series of generalized flight simulator studies, the following conditions apply:

(1) Five degrees of freedom of the aircraft were simulated; the pilots were not required to control the vertical or plunge degree of freedom. For VTOL aircraft in hovering flight, the longitudinal and lateral degrees of freedom are generally weakly coupled to the vertical degree of freedom (Ref. 11). In previous studies at UARL, it was found that the addition of the vertical degree of freedom affected the pilot's opinion of the longitudinal or lateral handling qualities only when the vertical degree of freedom is very lightly damped ($|Z_w| \lesssim 0.5$ per sec) and/or the longitudinal or lateral handling qualities are very poor (PR > 5). Since the stability augmentation requirements for minimum satisfactory handling qualities (PR = 3.5) were of primary interest in this series of experiments, the vertical degree of freedom was not included. This facilitated the evaluation of the large number of configurations that were to be examined.

(2) The control sensitivity selected by the pilots was effective over the full range of travel of the control stick ($\pm$6.63 in. longitudinally and $\pm$6.50 in. laterally). Pilots did not normally use the full control available, especially when the sensitivity was adjusted to near the optimum value. Therefore, the pilot ratings and comments were not affected by limitations in control power.

(3) Except for the experiments in which the effects of stick-force gradient were evaluated, the longitudinal and lateral handling qualities evaluations were made with essentially a free control stick (a small amount of inherent friction was present).

(4) The longitudinal and lateral handling qualities were evaluated separately and in a different series of experiments. For the longitudinal experiments, the lateral and directional parameters ($L_v g$, Y_v, N_v, etc.) were held constant. The lateral and directional stability augmentation was at a level that insured satisfactory lateral and directional

handling qualities. For the lateral experiments this situation was reversed. The lateral parameters used in the longitudinal studies and the longitudinal parameters used in the lateral studies are listed in Table A-I.

(5) The sequence of experiments was planned so that the basic configuration (designated by a speed-stability and drag parameter) was held constant for each group of experiments. Within each group, the parameter under investigation (rate damping, attitude stabilization, etc.) was varied randomly from run to run. The pilot was generally aware of the type of parameter being varied but was not informed of the basic configuration.

3. Instructions to Pilot

a. Task

The pilots were instructed to maintain hovering position at the reference hovering point and to maneuver about the hovering point. The nominal reference position of the ground position indicator was 135 ft ahead of the aircraft for the hovering altitude of 40 ft. The maneuvers required rapid translation followed by momentarily holding position at points within an area bounded by distances of approximately $\pm$50 ft longitudinally and $\pm$65 ft laterally from the nominal reference hovering position.

The pilot developed longitudinal and lateral acceleration by pitching and rolling of the aircraft which tilted the thrust vector. Only the random components of the wind were introduced into the aircraft equations of motion. Thus, it was assumed that the pilot would use auxiliary means, such as partial wing tilt or thrust deflection, to trim the mean head wind while maneuvering around the hover point.

b. Recording of Data

For each configuration, the pilots were instructed to:

(1) Select a control sensitivity using an uncalibrated lever located overhead in the cockpit. The control sensitivity was to be the best compromise between the requirements of the hovering and maneuvering portions of the task. For each case the sensitivity was initially set at a low value and the pilot advanced the lever until he obtained the desired control sensitivity. The control sensitivity was recorded at the analog computer console and the value remained unknown to the pilot.

(2) Record written comments on the handling qualities of the configuration. The pilots were to emphasize unfavorable aspects of handling qualities.

(3) Assign a pilot rating based on the Cooper pilot opinion scale (Table I). This rating was to be based on the handling qualities of both the hovering and maneuvering portions of the task.

4. Data Reduction

a. Optimum Control Sensitivity

When evaluating the handling qualities of each configuration, the pilots selected the control sensitivity (either longitudinal or lateral depending upon the series of experiments) that they considered optimum to perform the hovering and low-speed maneuvering task. Generally, for each configuration (a given value of speed-stability and drag parameter) this was done at four or more levels of rate damping. The values of rate damping and corresponding optimum sensitivities were then plotted as shown in Sketch II-A.

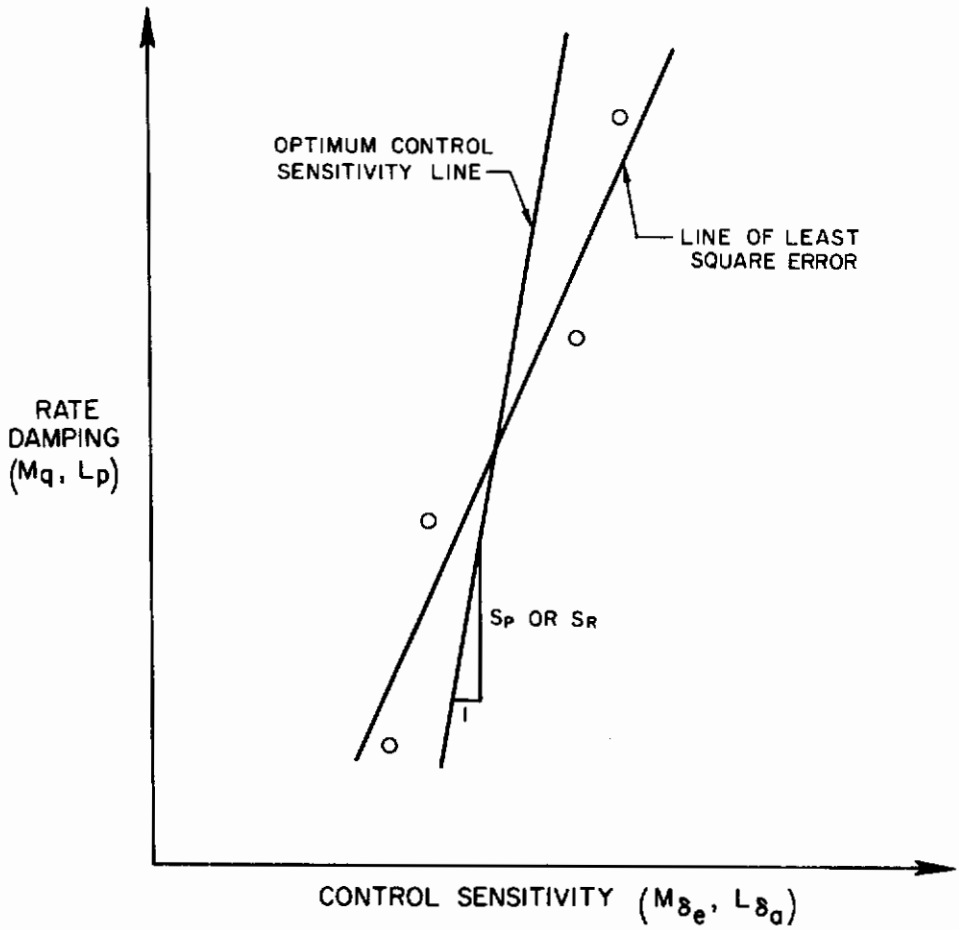

SKETCH II-A

TABLE I

COOPER PILOT RATING SYSTEM

Operating Conditions	Adjective Rating	Numerical Rating	Description	Primary Mission Accomplished	Can Be Landed
Normal Operation	Satisfactory	1	Excellent, includes optimum	Yes	Yes
		2	Good, Pleasant to fly	Yes	Yes
		3	Satisfactory, but with some mildly unpleasant characteristics	Yes	Yes
Emergency Operation	Unsatisfactory	4	Acceptable, but with unpleasant characteristics	Yes	Yes
		5	Unacceptable for normal operation	Doubtful	Yes
		6	Acceptable for emergency condition only[1]	Doubtful	Yes
No Operation	Unacceptable	7	Unacceptable even for emergency condition[1]	No	Doubtful
		8	Unacceptable - dangerous	No	No
		9	Unacceptable - uncontrollable	No	No
	Catastrophic	10	Motions possibly violent enough to prevent pilot escape	No	No

[1] Failure of a stability augmenter.

As a first step, a line of least square error was fitted to the data points. The slopes of these lines were then averaged for all of the longitudinal configurations and separately for all of the lateral configurations. The average slopes of the longitudinal (S_P) and the lateral (S_R) optimum control sensitivity lines were found to be -32.3 and -21.5 in./(rad/sec), respectively. As a second step, lines having these average values of slope were refit to the data (see Sketch II-A). In this latter step, only the mean square error of the sensitivities was minimized. These lines are termed the "optimum control sensitivity lines." Therefore, the intercepts of the optimum control sensitivity lines with the zero-damping axis (see Sketch II-A) were computed from

$$M_{\delta_O} = \frac{1}{N}\left[\sum_{i=1}^{N} M_{\delta_{e_i}} - \frac{1}{S_P}\sum_{j=1}^{N} M_{q_i}\right] \tag{4}$$

$$L_{\delta_O} = \frac{1}{N}\left[\sum_{j=1}^{N} L_{\delta_{a_j}} - \frac{1}{S_R}\sum_{j=1}^{N} L_{p_j}\right] \tag{5}$$

where i and j are indices of the N number of data points for the given configuration.

b. Pilot Ratings and Comments

In the series of experiments in which the effects of speed-stability and drag parameters were evaluated, each configuration was usually evaluated by two pilots. For these cases, the Cooper pilot ratings were averaged for the two pilots and crossplotted to develop plots of rate damping versus speed stability having lines of constant values of pilot ratings. These results are presented subsequently as a series of four plots each having a different value of drag parameter. This is done for both longitudinal and lateral results.

The pilots made written comments on the handling qualities of each configuration. These comments are summarized in Tables A-II and A-III in Appendix A. To condense this summary as much as possible, emphasis was placed on summarizing unfavorable comments on the handling qualities rather than favorable comments.

C. Precision Hovering Experiments

A series of precision hovering experiments was conducted to measure the effect of several factors on rms hovering performance. Only longitudinal motion of the aircraft and the pilot's control activity were measured. The principal factors investigated were speed-stability and drag parameters, rms turbulence level, rate and attitude stabilization and stick force gradient. These rms hovering performance data were used in conjunction with closed-loop model analyses to investigate trends in pilot-adapted parameters (lead and gain) with the factors. It was hoped that this would lead to better understanding of how the various factors affect handling qualities. The rms data are discussed in Section IV.

1. Range of Parameters

The parameters of the configurations for which rms performance data were measured are listed in Table A-V. Most of the configurations were variations on a basic combination of parameters. The "basic" configuration had the following parameters: $M_u g = 0.67$, $X_u = -0.1$, $M_q = -3$, $\sigma_{u_g} = 5.1$ and SFG = 0. The variations of parameters from the basic values were:

Study	Values of Parameter
Drag Parameter, X_u, per sec	0, -0.05, -0.1, -0.2, -0.3
Speed-Stability Parameter, $M_u g$, per sec^3	0, 0.33, 0.67, 1.0
Rate Damping, M_q, per sec	-1, -3, -5
RMS Turbulence Level, σ_{u_g}, ft/sec	2.6, 3.9, 5.1, 7.7
Stick Force Gradient, SFG, lb/in.	0, 1.5

Pitch attitude stabilization M_θ was also evaluated for other configurations (Table A-V). In addition, several specialized configurations were evaluated to examine the generality of some preliminary conclusions resulting from the closed-loop pilot model studies. These configurations are identified in Table A-V, and the parameters and rms data for the configurations are shown in Table A-VI.

2. Experimental Conditions

For the rms hovering performance experiments the following conditions applied:

(1) Four degrees of freedom of the aircraft were simulated; the pilot was not required to control direction or height of the aircraft. Only attitude and translation were simulated because the closed-loop model for which the data were obtained represented only the inner (or pitch) loop and the outer (or position) loop of the aircraft (Section V).

(2) Control sensitivity was effective over the full range of travel of the control. The rms measurements were not affected by limitations in control power.

(3) The rms data are based on runs of 100-sec duration each. Ten or more runs were made with each configuration.

3. Instructions to Pilots

For each configuration, the pilots were instructed to:

(1) Select a control sensitivity considered optimum for performing the precision hovering task.

(2) Assign a pilot rating (Cooper scale) and record written comments that apply specifically to the hovering task.

(3) Perform the simulated hovering task for the duration of the rms recording period. The pilot was to minimize hovering position error.

The pilot derived the aircraft position error information from the relative positions of the square and the cross on the contact analog display (Fig. 2). As discussed previously, this provided the pilot with very sensitive position error and error rate information. The equivalent sensitivity would be obtained in flight only if the pilot were hovering near the ground and could observe the position of a part of the aircraft (such as a landing gear) relative to an object on the ground.

4. Data Reduction

Measurements were made of the root-mean-square values of pitch attitude (σ_θ), pitch rate (σ_q), hovering position error (σ_x), longitudinal velocity (σ_u), and control motion (σ_{δ_e}). These data were used in conjunction with closed-loop pilot-model analyses to compute the adapted pilot-model parameters. However, since the closed-loop analyses modeled the aircraft response to a random component of wind with a mean value of zero, the measured rms data had to be corrected for the small mean wind component usually present in the simulated turbulence. The mean wind ($\bar{u}_g$) for the 10 or more runs (100-sec duration each) was generally less than $|0.5|$ ft/sec. Therefore the

correction was usually small. To reduce the measured data to the values listed in Table A-VI, the following steps were followed:

(1) The rms values were computed for each run (100-sec duration) and then averaged for the total number of runs, N (10 or more).

(2) The mean wind correction was applied to rms turbulence level, pitch attitude and control motion using

$$\sigma'_{u_g} = \sqrt{(\sigma_{u_g})^2_{MEAS.} - (\bar{u}_g)^2} \tag{6}$$

$$\sigma'_{\theta} = \sqrt{(\sigma_{\theta})^2_{MEAS.} - \left(\frac{X_u \cdot \bar{u}_g}{g}\right)^2} \tag{7}$$

$$\sigma'_{\delta_e} = \sqrt{(\sigma_{\delta_e})^2_{MEAS.} - \left(\frac{M_{u_g} \cdot \bar{u}_g}{g M_{\delta_e}}\right)^2} \tag{8}$$

Similar corrections to σ_q, σ_x and σ_u were not required because they are unaffected by a mean-wind component.

(3) Finally, although this correction did not affect the values of the pilot model parameters recovered from the rms data, all of the rms values were corrected to the nominal rms turbulence level selected for the series of experiments. For example, for experiments having a nominal rms turbulence level of 5.1 ft/sec, rms pitch attitude was corrected by

$$\sigma_{\theta} = \frac{(5.1)}{\sigma'_{v_g}} \sigma'_{\theta} \tag{9}$$

Usually the measured turbulence level σ_{u_g} was within 10% of the nominal value. These corrections allowed comparison of the data for different configurations.

SECTION III

RESULTS FOR HOVERING AND LOW-SPEED MANEUVERING TASK

The data obtained in the flight simulator program for the hovering and low-speed maneuvering task are presented in this section. Results for the effects of speed-stability and drag parameters, rate damping and attitude stability augmentation, and level of turbulence on handling qualities are discussed. Optimum control sensitivities selected by the pilots, pilot ratings and pilot comments are summarized for both longitudinal and lateral evaluations. Detailed tabulations of these data for each configuration are presented in Tables A-II and A-III. Results are also presented from limited studies of stick force gradient, control lag and backlash, and authority of the rate stabilization system. Conclusions drawn from these data regarding their applicability to a general handling qualities criteria for VTOL aircraft are discussed in Section VII.

A. Speed-Stability and Drag Parameters

1. Longitudinal Handling Qualities

a. Control Sensitivity

For the range of parameters investigated, the data show that the speed-stability parameter, $M_u g$, had a greater effect on optimum longitudinal control sensitivity ($M\delta_e$) than the drag parameter, X_u. Typical results are presented in Fig. 3 on plots of pitch rate damping M_q versus control sensitivity, $M\delta_e$. These results show that for constant X_u (-0.3), $M\delta_e$ nearly doubled for an increase in $M_u g$ from 0 to 1.0 (Fig. 3(a)). For constant $M_u g$ (0.33), $M\delta_e$ initially decreased as X_u became more negative, then increased as X_u approached -0.3. The total increase was less than 20% (Fig. 3(b)).

A summary of the effects of $M_u g$ and X_u on control sensitivity for the complete range of parameters investigated is shown in Fig. 4. It shows contours of the longitudinal control sensitivity, $M\delta_o$, at which the extrapolated optimum control sensitivity line crosses the zero-damping axis. These contours were developed by crossplotting the experimentally determined intercepts for 16 combinations of $M_u g$ and X_u (nine of these combinations were investigated in a previous study, Ref. 7). The intercepts of the optimum control sensitivity lines have been determined by fairing a straight line of constant slope ($\partial M_q / \partial M\delta_e = -32.3$) through the data. Thus, the optimum control sensitivity at any level of M_q may be estimated by adding $-M_q/32.3$ to the intercept value. An analysis of the data on which the contours of Fig. 4 are

based indicates the following results:

(1) When the magnitude of X_u was less than 0.2, increasing $M_u g$ had little effect on M_{δ_e} at low values of $M_u g$ (less than 0.3) because the control sensitivity required for attitude control while maneuvering was adequate for controlling the small increase in pitch attitude disturbances and for trimming the small speed-stability effects when maneuvering.

(2) For values of $M_u g$ greater than 0.3 and the magnitude of X_u less than 0.2, control sensitivity increased rapidly with $M_u g$ to counteract the effects of gust disturbances on attitude and, to a smaller extent, reduce the control travel required to trim the $M_u g$ effect when maneuvering.

(3) At high values of $M_u g$, control sensitivity decreased slightly for a change in X_u from 0 to about -0.2 due to increased translational damping when maneuvering. For low-drag configurations, maneuvering speeds tend to be relatively high so that rapid rotation of pitch attitude is required to arrest translational velocity when attempting to stop over a preselected point.

(4) Control sensitivities generally increased as X_u changed from -0.2 to -0.3 because large, rapid attitude changes were required to offset the increased gust-induced longitudinal forces when hovering.

b. Pilot Rating

The effects of the speed-stability parameter $M_u g$ and the drag parameter X_u on pilot ratings are summarized in Fig. 5. Contours of constant Cooper pilot rating were derived from the data for 16 combinations of $M_u g$ and X_u. The contours are presented on four plots of M_q versus $M_u g$. Each plot has a separate value of X_u (0, -0.1, -0.2, -0.3).

The results presented in Fig. 5 show that at given values of M_q and X_u, there was a significant deterioration in pilot rating with increasing $M_u g$, especially for values greater than 0.6. The effect of X_u was not as large. However, pilot rating generally improved for changes in X_u from 0 to -0.1, then tended to deteriorate as X_u approached -0.3. The plot for X_u of -0.3 shows that only unsatisfactory pilot ratings (PR > 3.5) were obtained for these configurations. Based on pilot comments, the primary reasons for these effects are as follows:

(1) Pilot rating deteriorated with increasing $M_u g$ because gust disturbances on pitch attitude increased, and to a much lesser degree, because the pitch attitude dynamics became slightly less stable and higher in frequency.

(2) Pilot ratings for $X_u = -0.1$ were generally better than those for $X_u = 0$ because the translational damping produced by the drag made it easier to control the position of the aircraft when maneuvering.

(3) Pilot ratings were unsatisfactory for X_u of -0.3 because of the large gust-induced disturbances in position. The unsatisfactory ratings are not indicative of the pitch control characteristics which were considerably better than those for position.

2. Lateral Handling Qualities

a. Control Sensitivity

The effects of the lateral speed-stability parameter, $L_v g$, and the lateral drag parameter, Y_v, on lateral optimum control sensitivity were similar to those of the corresponding longitudinal parameters. The effects of speed stability were slightly greater than those of the drag parameter for the range of parameters investigated. Typical results for one pilot are shown in Fig. 6 on plots of roll rate damping, L_p, versus control sensitivity, L_{δ_a}. These results show an increase in L_{δ_a} of less than 50% for a change in $L_v g$ from 0 to -1.0 ($Y_v = -0.1$), and an increase in L_{δ_a} of less than 25% for a change in Y_v from 0 to -0.3 ($L_v g = -0.67$).

A summary of the effects of $L_v g$ and Y_v on control sensitivity for the complete range of parameter combinations is shown in Fig. 7. The format of the plot is the same as that for the longitudinal results in Fig. 4. It displays contours of the lateral control sensitivity, L_{δ_0}, at which the extrapolated optimum control sensitivity line crosses the zero-damping axis. The average slope of the lateral optimum control sensitivity lines, $\partial L_p / \partial L_{\delta_a}$, is -21.5. Therefore, the lateral optimum control sensitivity at any level of L_p may be estimated by adding $-L_p/21.5$ to the intercept value. An analysis of the data on which the contours of Fig. 7 are based indicates the following:

(1) Optimum control sensitivity was nearly constant for values of $L_v g$ between 0 and about -0.5 and Y_v between 0 and -0.2. This was because the basic L_{δ_a} for attitude control while maneuvering was adequate for controlling changes in the level of gust-induced disturbances and also satisfied the trim requirements. However, gust effects and trim requirements accounted for the increase in L_{δ_a} as $L_v g$ approached -1.0 and Y_v approached -0.3.

(2) For a change in Y_v from 0 to -0.3, optimum control sensitivity increased. This was because larger, more rapid changes in roll angle were required to control the larger gust-induced position disturbances as the drag increased.

b. Pilot Rating

The effects of the speed-stability parameter, L_{v_g}, and the drag parameter on pilot rating of handling qualities are summarized in Fig. 8. As for the longitudinal results, contours of constant Cooper pilot rating were derived by crossplotting the data for 16 combinations of L_{v_g} and Y_v (Table A-III). Again the contours are presented on four plots of L_p versus L_{v_g} where each plot has a separate value of Y_v (0, -0.1, -0.2, -0.3).

The effects of the lateral speed-stability and drag parameters on PR were similar to those of the corresponding longitudinal parameters. However, a comparison shows that the effects were not as pronounced. For all values of Y_v, the results show a continuous deterioration in pilot rating (PR) with increasing L_{v_g} at a given level of roll rate damping, L_p. Y_v shows little effect on pilot rating except at Y_v of -0.3 where generally poorer ratings were assigned at given values of L_{v_g} and L_p. Based on pilot comments, the primary reasons for these effects were:

(1) Increasing lateral speed stability increased roll gust disturbances, and of lesser importance, decreased the damping of the roll dynamics at a given level of L_p.

(2) The adverse effects of the increase in position disturbances for changes in Y_v from 0 to -0.2 were compensated by the beneficial effects of improved translational damping for maneuvering. Therefore, there was little change in pilot rating. At Y_v of -0.3 the large position disturbances dominated pilot opinion and accounted for the poorer values of PR.

B. Rate Damping Stability Augmentation

1. Pitch Rate Damping

a. Control Sensitivity

The data show that for the range $-1 \geq M_q \geq -4$, there was a nearly linear relationship between the control sensitivities selected by the pilots and the level of pitch rate damping. Typical results are shown in Fig. 3 on plots of

M_q versus M_{δ_e}. The effect of M_q on M_{δ_e} is best summarized by the average slope of the optimum lines fit to data for the 16 combinations of X_u and M_ug (procedure described in Section II). The average slope of the lines was $\partial M_q/\partial M_{\delta_e} = -32.3$. This slope was essentially independent of the drag and speed-stability parameters and the level of turbulence, even though the intercepts of the optimum lines with the zero-damping axis varied over a wide range.

In Section VI this average slope is shown to be in good agreement with flight test data for the Princeton HUP-1 and flight simulator data for the X-22A (also with X-14A as shown in Ref. 7). An analysis is presented in Section VII that describes a possible reason for this relationship between M_q and M_{δ_e}. It shows that M_{δ_e} must increase nearly linearly with M_q to develop a given change in pitch attitude at a specified time following a unit control input.

b. Pilot Rating

The data show that for a given configuration (X_u and M_ug combination), pilot rating improved with the addition of pitch rate damping. The pilot ratings presented in Fig. 3 exhibit this effect. A summary of the data for all configurations is shown in Fig. 5 as lines of constant PR on plots of M_q versus M_ug. These results show that initially PR improved rapidly with M_q, and then for larger values of M_q (depending on the value of M_ug), there was little change in PR. The contours for PR = 3.5 have been replotted in Fig. 9(a) to show the rate damping stability augmentation required for satisfactory handling qualities. It can be seen that the rate damping required for PR = 3.5 at least doubled, depending on X_u, for an increase in M_ug from 0 to 1.0. The primary reasons for the effects are:

(1) Rate damping stabilizes and reduces the frequency of the open-loop pitch dynamics (Fig. 10(a)). In doing so, it reduces the lead compensation required of the pilot (discussed in Ref. 5 and shown quantitatively in Section V).

(2) Rate damping is effective in reducing the attitude response to gust disturbances. An example of this can be seen by comparing the damping required for satisfactory handling qualities for $X_u = -0.05$, $M_ug = 1.0$ and no turbulence with the damping required for a similar configuration and turbulence (Fig. 9(a)). Therefore, at values of M_ug near 1.0 under conditions of moderate turbulence, the damping required for satisfactory handling qualities is higher than would be expected on the basis of stability considerations alone.

(3) While rate damping does not directly reduce gust-induced disturbances in the position-loop ($X_u \cdot u_g$), it does compensate for the adverse effects of higher drag by providing the pilot with improved attitude control.

2. Roll Rate Damping

a. Control Sensitivity

The effects of rate damping on lateral optimum control sensitivity were similar to the longitudinal effects of M_q on M_{δ_e}. For the range $-1 \geq L_p \geq -4$, pilots selected control sensitivities that increased approximately linearly with L_p. Typical results are shown in Fig. 6 on plots of L_p versus L_{δ_a}. The average slope of the lines fit to the data for 16 combinations of L_{v_g} and Y_v (Cases R1 to R64, Table A-III) is $\partial L_p / \partial L_{\delta_a} = -21.5$. Again, this slope was essentially independent of the drag and speed-stability parameters and the level of turbulence.

As with longitudinal control, for a given configuration and turbulence level, the pilot needs higher control sensitivity at higher levels of damping to offset the slower response to a given control moment. As shown in Section VII, there is less agreement among the slopes of the lateral optimum control sensitivities from several studies than there is for longitudinal control. The slope from this study (-21.5) agrees well with that from simulation studies of the X-22A (about -19) presented in Ref. 12. However, it is somewhat less than that for Tapscott's studies with the S-61 helicopter (-37) reported in Ref. 13.

b. Pilot Rating

The beneficial effects of L_p on handling qualities were similar to the effects of M_q. Pilot ratings are shown in Fig. 6 for seven different combinations of L_{v_g} and Y_v at four levels of L_p. The contours of constant PR on plots of L_p versus L_{v_g} in Fig. 8 summarize the effects of rate damping on PR for the range of Y_v and L_{v_g} investigated. Again, PR initially improved rapidly with L_p, then improved slowly as the attitude characteristics became well damped. With good attitude control, pilot rating was dominated by the position characteristics which accounts for the slower rate of improvement in PR for large magnitudes of L_p. The level of L_p required for satisfactory handling qualities increased with L_{v_g} (Fig. 9(b)) and, except for magnitudes of Y_v greater than 0.2, was relatively unaffected by Y_v. Pilot comments indicate that satisfactory roll-control characteristics were actually obtained at lower levels of L_p than indicated for Y_v of -0.3. Unsatisfactory ratings were assigned at these levels because pilot rating was dominated by the gust induced disturbances in position. For example, results of studies with L_{v_g} of -1.0 and no turbulence show that the L_p required for satisfactory handling qualities (PR = 3.5) was -1.7 for Y_v = -0.05 (Cases R81 to R84,

Table A-III), but only -1.2 for Y_v = -0.25 (Cases R113 to R116). The comments listed in Paragraphs B.1.b. for the effects of M_q on PR applying equally well to L_p.

C. Attitude Stability Augmentation

The flight simulator studies of the effects of attitude stabilization on handling qualities were conducted for four combinations of $M_u g$ (0.33, 1.0) and X_u (-0.05, -0.2) and four combinations of $L_v g$ (-0.33, -1.0) and Y_v (-0.05, -0.2). The longitudinal and lateral configurations evaluated are listed in Tables II and III, respectively. For each of the lateral and longitudinal configurations, the handling qualities were evaluated for two values of rate damping (M_q, L_p) and four or five levels of attitude stabilization (M_θ, L_ϕ). Figure 10 shows the effect of M_θ and L_ϕ on the root locations of the longitudinal and lateral characteristic equations in hover for one configuration.

The longitudinal studies of attitude stability augmentation were planned to determine the effect of M_θ on the handling qualities of configurations which had unsatisfactory handling qualities with rate stabilization alone. Consequently, the two values of M_q investigated for each configuration were relatively low. The effect of M_θ on the open-loop dynamics for all the configurations was similar to that shown in Fig. 10(a). That is, increasing M_θ stabilized the aircraft (more positive $\zeta\omega_n$) but, because of the low values of M_q, monotonically increased the frequency of oscillation, ω_d.

Subsequently, the two values of L_p for the lateral studies were selected to produce the effects on dynamics shown in Fig. 10(b). For the smaller magnitude of L_p, the effect of making L_ϕ more negative was similar to that found for increasing the magnitude of M_θ in the longitudinal studies (ω_d increased continuously as L_ϕ became more negative). The larger magnitude value of L_p was selected, however, so that with more negative L_ϕ the frequency ω_d decreased until all three of the open-loop roots became real. As shown in Fig. 10(b), making L_ϕ more negative resulted in two of the roots again becoming oscillatory. At these more negative values of L_ϕ, the damping ratio, ζ, of the oscillatory roots was relatively large.

1. Pitch Attitude Stabilization

a. Control Sensitivity

The results listed in Table II show that M_θ had a relatively small effect on optimum control sensitivity. For the range of M_θ from 0 to -4, the total change in M_{δ_e} was less than 10% except for one configuration ($M_u g$ = 0.33, X_u = -0.05, M_q = -1) where it was about 20%. In comparison, a change in M_q from 0 to -4 generally results in an increase in M_{δ_e} of more than 40%. This difference can be seen by comparing the two lower plots of Fig. 11 where

TABLE II

RESULTS FOR LONGITUDINAL ATTITUDE STABILIZATION EXPERIMENTS

$L_v g = -0.1$ $\quad Y_v = -0.1$ $\quad L_p = -3$ $\quad L_{\delta_a} = 0.301$ $\quad \sigma_{v_g} = 1.3$ $\quad \sigma_{u_g} = 5.1$

$N_v = 0.002$ $\quad N_r = -1$ $\quad N_{\delta_r} = 0.2$

Case*	Pilot	$M_u g$	X_u	M_q	M_θ	Real Roots			Complex Roots $-\zeta\omega_n \pm j\omega_d$	$M_{\delta_e}\|_{OPT}$	PR
						RR (1)	RR (2)	RR (3)			
P93	A	0.33	-0.05	-0.5	0	-0.918			0.184 ± j 0.574	0.243	4.75
P94	↓	↓	↓	↓	-1	-0.397			-0.076 ± j 0.979	0.253	4.0
P95	↓	↓	↓	↓	-2	-0.222			-0.164 ± j 1.390	0.256	3.25
P96	↓	↓	↓	↓	-3	-0.163			-0.193 ± j 1.710	0.269	3.5
P97	↓	↓	↓	↓	-4	-0.134			-0.208 ± j 1.981	0.268	3.75
P98	A	0.33	-0.05	-1.0	0	-1.23			0.090 ± j 0.513	0.261	4.25
P99	↓	↓	↓	↓	-2	-0.23			-0.409 ± j 1.301	0.287	3.5
P100	↓	↓	↓	↓	-3	-0.166			-0.442 ± j 1.646	0.301	3.0
P101	↓	↓	↓	↓	-4	-0.136			-0.457 ± j 1.930	0.312	3.5
P102	A	0.33	-0.05	0	-2	-0.213			0.081 ± j 1.424	0.262	4.25
P103	↓	↓	↓	-0.5	↓	-0.222			-0.164 ± j 1.390	0.282	3.75
P104	↓	↓	↓	-1	↓	-0.233			-0.409 ± j 1.301	0.288	2.75
P105	↓	↓	↓	-2	↓	-0.267			-0.892 ± j 0.911	0.321	2.25
P106	↓	↓	↓	-3	↓	-0.386	-0.524	-2.140		0.341	2.25
P107	A	1.00	-0.05	-1	0	-1.480			0.213 ± j 0.795	0.412	4.75
P108	↓	↓	↓	↓	-1	-1.030			-0.013 ± j 1.010	0.417	4.5
P109	↓	↓	↓	↓	-2	-0.619			-0.217 ± j 1.318	0.422	4.0
P110	↓	↓	↓	↓	-3	-0.413			-0.319 ± j 1.640	0.421	3.75
P111	↓	↓	↓	↓	-4	-0.314			-0.368 ± j 1.920	0.430	4.0
P112	A	1.00	-0.05	-2	0	-2.210			0.080 ± j 0.668	0.439	4.25
P113	↓	↓	↓	↓	-2	-1.050			-0.501 ± j 0.894	0.470	4.0
P114	↓	↓	↓	↓	-3	-0.491			-0.778 ± j 1.310	0.472	3.75
P115	↓	↓	↓	↓	-4	-0.340			-0.854 ± j 1.670	0.461	3.75
P116	↓	↓	↓	-5	0	-5.042			-0.005 ± j 0.445	0.538	2.75
P117	B	0.33	-0.2	-0.5	0	-0.958			0.129 ± j 0.575	0.250	5.0
P118	↓	↓	↓	↓	-1	-0.528			-0.086 ± j 1.000	0.251	4.0
P119	↓	↓	↓	↓	-2	-0.371			-0.164 ± j 1.400	0.260	3.75
P120	↓	↓	↓	↓	-3	-0.313			-0.193 ± j 1.720	0.265	4.25
P121	↓	↓	↓	↓	-4	-0.285			-0.208 ± j 1.980	0.275	4.5
P122	B	0.33	-0.2	-1.0	0	-1.250			0.026 ± j 0.515	0.267	4.25
P123	↓	↓	↓	↓	-1	-0.636			-0.283 ± j 0.872	0.266	3.75
P124	↓	↓	↓	↓	-2	-0.389			-0.406 ± j 1.311	0.263	4.0
P125	↓	↓	↓	↓	-3	-0.320			-0.440 ± j 1.650	0.266	4.25
P126	↓	↓	↓	↓	-4	-0.288			-0.456 ± j 1.930	0.278	4.5
P127	B	1.00	-0.2	-1	0	-1.510			0.154 ± j 0.800	0.443	5.0
P128	↓	↓	↓	↓	-2	-0.751			-0.224 ± j 1.346	0.462	4.75
P129	↓	↓	↓	↓	-3	-0.563			-0.318 ± j 1.655	0.462	4.0
P130	↓	↓	↓	↓	-4	-0.467			-0.367 ± j 1.930	0.458	4.5
P131	A	↓	↓	↓	-5	-0.410			-0.395 ± j 2.173	0.456	4.25
P132	B	1.00	-0.2	-2	0	-2.220			0.011 ± j 0.671	0.429	4.0
P133	↓	↓	↓	↓	-2	-1.170			-0.514 ± j 0.965	0.427	4.25
P134	↓	↓	↓	↓	-3	-0.675			-0.762 ± j 1.338	0.435	3.75
P135	↓	↓	↓	↓	-4	-0.508			-0.846 ± j 1.681	0.438	4.25
P136	↓	↓	↓	-0.5	-3	-0.531			-0.084 ± j 1.730	0.378	4.75

* Pilot comments listed in Table A-II for each case.

M_{δ_e} is plotted versus M_θ on the left (M_q constant) and versus M_q on the right (M_θ constant) for one combination of M_{ug} (0.33) and X_u (-0.05). The small increase in M_{δ_e} with M_θ is probably due to (1) trim requirements when maneuvering and (2) the need for rapid control inputs to stabilize a commanded attitude change when maneuvering (because of the higher-frequency, springy response).

b. Pilot Rating

Pilot opinion of handling qualities improved overall with the addition of pitch attitude stabilization for all configurations (Table II). Results for one configuration are plotted in Fig. 11. The data show that generally:

(1) The improvement in pilot rating was small. For low M_q, the maximum improvement in PR was not greater than about 1.25 units.

(2) Most configurations exhibited an optimum level of M_θ; that is, after improving, PR deteriorated at high values of M_θ.

(3) Best pilot ratings resulted from combinations of moderate M_θ (-2 to -3) and a level of M_q high enough to provide satisfactory handling qualities without the M_θ.

Probable reasons for these results are:

(1) The initial improvement in PR with M_θ was due to improved open-loop stability. This allowed the pilot to divert his attention from attitude control without the aircraft being upset.

(2) The deterioration in PR at high levels of M_θ with low M_q was due to the high frequency and low damping ratio of the open-loop pitch dynamics.

2. Roll Attitude Stabilization

a. Control Sensitivity

As for M_θ, the results in Table III show that L_ϕ had a relatively small effect on optimum control sensitivity. For the range $0 \geq L_\phi \geq -4$, the total change in L_{δ_a} was less than 11% except for Cases R132 and R156 which had a change of about 19%. Again for comparison, a change in L_p from 0 to -4 generally resulted in an increase in L_{δ_a} of more than 50%. This difference can be seen by comparing the two lower plots of Fig. 12. For all configurations, including the one shown in Fig. 12, L_{δ_a} increased with L_ϕ even though ω_d decreased with L_ϕ for the high value of L_p (Fig. 10). The fact that L_{δ_a}

TABLE III

RESULTS FOR LATERAL ATTITUDE STABILIZATION EXPERIMENTS

$M_u g = 0.67$ $X_u = -0.1$ $M_q = -3$ $M_{\delta_e} = 0.431$ $\sigma_{u_g} = 1.3$ $\sigma_{v_g} = 5.1$

$N_v = 0.002$ $N_r = -1$ $N_{\delta_r} = 0.2$

Case*	Pilot	$L_v g$	Y_v	L_p	L_ϕ	Real Roots			Complex Roots $-\zeta\omega_n \pm j\omega_d$	$L_{\delta_a}\|_{OPT}$	PR
						RR (1)	RR (2)	RR (3)			
R129	A	-0.33	-0.05	-1	0	-1.230			0.090 ± j 0.513	0.254	4.0
R130	↓	↓	↓	↓	-1	-0.494			-0.278 ± j 0.835	0.268	3.0
R131	↓	↓	↓	↓	-2	-0.233			-0.409 ± j 1.301	0.264	3.5
R132	↓	↓	↓	↓	-4	-0.136			-0.457 ± j 1.928	0.302	4.0
R133	A	-0.33	-0.05	-3	0	-3.037			-0.007 ± j 0.331	0.366	2.5
R134	↓	↓	↓	↓	-1	-2.673			-0.188 ± j 0.328	0.383	2.5
R135	↓	↓	↓	↓	-2	-2.140	-0.524	-0.386		0.392	2.25
R136	↓	↓	↓	↓	-4			-0.143	-1.454 ± j 1.274	0.403	2.0
R137	A	-1.0	-0.05	-2	0	-2.210			-0.080 ± j 0.668	0.433	4.5
R138	↓	↓	↓	↓	-1	-1.764			-0.143 ± j 0.758	0.448	4.0
R139	↓	↓	↓	↓	-2	-1.048			-0.501 ± j 0.894	0.468	3.0
R140	↓	↓	↓	↓	-4	-0.341			-0.854 ± j 1.669	0.465	3.25
R141	A	-1.0	-0.05	-5	0	-5.040			-0.005 ± j 0.445	0.533	2.75
R142	↓	↓	↓	↓	-2	-4.614			-0.218 ± j 0.437	0.555	2.5
R143	↓	↓	↓	↓	-4	-4.081			-0.485 ± j 0.243	0.570	2.0
R144	↓	↓	↓	↓	-6	-1.540	-0.260	-3.250		0.592	2.0
R145	B	-0.33	-0.2	-1	0	-1.252			0.026 ± j 0.515	0.275	5.0
R146	↓	↓	↓	↓	-1	-0.634			-0.283 ± j 0.872	0.264	3.5
R147	↓	↓	↓	↓	-2	-0.389			-0.406 ± j 1.312	0.283	4.0
R148	↓	↓	↓	↓	-4	-0.288			-0.456 ± j 1.931	0.281	4.5
R149	B	-0.33	-0.2	-4	0	-4.022			-0.089 ± j 0.274	0.392	3.5
R150	↓	↓	↓	↓	-1	-3.759			-0.221 ± j 0.305	0.423	3.0
R151	↓	↓	↓	↓	-3	-3.057	-0.425	-0.719		0.424	3.0
R152	↓	↓	↓	↓	-5			-0.284	-1.96 ± j 0.924	0.413	3.0
R153	B	-1.0	-0.2	-2	0	-2.222			-0.011 ± j 0.671	0.352	6.0
R154	↓	↓	↓	↓	-1	-1.792			-0.204 ± j 0.792	0.398	5.0
R155	↓	↓	↓	↓	-2	-1.171			-0.514 ± j 0.965	0.419	4.0
R156	↓	↓	↓	↓	-4	-0.508			-0.846 ± j 1.681	0.377	4.5
R157	B	-1.0	-0.2	-5	0	-5.041			-0.080 ± j 0.438	0.552	3.5
R158	↓	↓	↓	↓	-1	-4.838			-0.181 ± j 0.464	0.613	3.0
R159	↓	↓	↓	↓	-3	-4.368			-0.416 ± j 0.440	0.590	3.0
R160	↓	↓	↓	↓	-6	-0.454	-3.260	-1.486		0.613	3.0

* Pilot comments listed in Table A-III for each case.

increased for both high and low L_p (even though there was a contrast in ω_d behavior) would seem to indicate that the small effect of L_ϕ on L_{δ_a} is due mainly to trim considerations when maneuvering and not to frequency effects.

b. Pilot Rating

As mentioned previously, the two basic values of L_p for each configuration were selected so that ω_d increased as the magnitude of L_ϕ increased for the smaller value of L_p and ω_d decreased with more negative L_ϕ for the larger value of L_p (see example on Fig. 10). The results listed in Table III show that generally for cases with small magnitude of L_p, PR initially improved as L_ϕ became more negative, then deteriorated at the larger magnitudes of L_ϕ. For the cases having the larger magnitude of L_p, PR generally continued to improve as L_ϕ became more negative. These effects are shown in Fig. 12. In fact, as illustrated by the results in Fig. 12, the PR assigned for combinations of L_ϕ and L_p having large magnitudes were better than those assigned to purely rate-stabilized configurations. Probable reasons for these effects are:

(1) Improved open-loop stability accounted for the initial improvement in PR as L_ϕ became more negative for all values of L_p.

(2) Pilot rating deteriorated at large magnitudes of L_ϕ when the magnitude of L_p was small because (a) the high frequency of oscillation made it difficult to command and hold an attitude change and (b) the configuration was still sensitive to short-period gusts.

(3) Pilot rating was good for combinations of L_p and L_ϕ having large magnitudes because the open-loop dynamics were well damped. The trim effects caused by L_ϕ apparently did not adversely affect PR.

D. RMS Turbulence Level

The effects of the longitudinal and lateral components of rms turbulence level on handling qualities were evaluated in separate experiments. For the longitudinal studies, the rms level of the lateral component of turbulence was 25% as large as the longitudinal component. The selection of this ratio of lateral to longitudinal turbulence was somewhat arbitrary. It was felt that this ratio would force the pilot to pay some attention to lateral control while not affecting significantly his evaluation of the aircraft longitudinal control characteristics. The converse was used for the lateral studies. The configurations examined are listed in Table A-I and the data, including pilot comments, are listed in Tables A-II and A-III. The simulated turbulence was generated by passing the output of a random noise generator having a

relatively uniform low-frequency power spectrum through a first-order filter with a break frequency of 0.314 rad/sec (described in Section II).

1. Longitudinal Component

a. Control Sensitivity

The data show that optimum control sensitivity increased rapidly with rms turbulence level σ_{u_g}, especially for large magnitudes of M_{u_g} or X_u. Typical results are shown in Fig. 13(a) for one configuration evaluated with 4 levels of σ_{u_g} (0, 2.6, 5.1, and 7.7 ft/sec). These results show that M_{δ_e} nearly doubled for an increase in σ_{u_g} from 0 to 7.7. A summary of the effects of σ_{u_g} on M_{δ_e} for the four configurations investigated is presented in Fig. 14 in terms of the intercepts of the fitted optimum lines with the zero-damping axis. For small X_u (-0.05) and low M_{u_g} (0.33), σ_{u_g} has little effect on M_{δ_e} selected by the pilot. This was because the control sensitivity required for good attitude response while maneuvering was adequate for controlling the small gust disturbances. However, the basic control sensitivity required for maneuvering was not adequate for controlling gust disturbances with large X_u (-0.25) or high M_{u_g} (1.0). For this reason there was a steady increase in M_{δ_e} with σ_{u_g} at all levels of rate damping.

b. Pilot Rating

The rms turbulence level generally had a deleterious effect on pilot opinion of longitudinal handling qualities. Results for one configuration presented in Fig. 13 show the deterioration in PR with turbulence level at constant M_q. The pilot ratings for all configurations are plotted in Fig. 15. These results show:

(1) Both $X_u \cdot \sigma_{u_g}$ and $M_{u_g} \cdot \sigma_{u_g}$ are important factors in determining handling qualities. This is shown by the high rate of deterioration of PR with σ_{u_g} for large magnitudes of X_u and/or high M_{u_g} while the effect of σ_{u_g} on PR is relatively small for low magnitudes of X_u and low M_{u_g}.

(2) Rate stabilization is effective in suppressing gust disturbances in the inner loop. Results have shown that for small σ_{u_g}, PR remains unchanged with increasing σ_{u_g}, provided the magnitude of M_q is increased appropriately. For large σ_{u_g}, the position-loop disturbances resulting from $X_u \cdot \sigma_{u_g}$ cause a deterioration in PR regardless of the level of M_q.

2. Lateral Component

a. Control Sensitivity

A general increase is evident in control sensitivity selected by the pilots with rms turbulence level. Some typical results are shown in Fig. 13(b) for one configuration evaluated with four levels of σ_{u_g} (0, 2.6, 5.1 and 7.7 ft/sec). For this configuration the intercept of the optimum lines with the zero-damping axis L_{δ_o} increased about 70% with a change in σ_{u_g} from 0 to 7.7 ft/sec. A comparison of Fig. 13(b) with (a) shows that the lateral control sensitivity was less affected by rms turbulence level than was longitudinal control sensitivity. The results in Fig. 14 show that this is generally true for all four configurations. The reason for this difference is not fully understood. It may be related to differences in the physiology of arm motions for longitudinal and lateral control inputs and differences in pitch and roll attitude cues. These factors probably also relate to the differences in the slopes of the longitudinal and lateral optimum control sensitivity lines with rate damping. Again, because of differences in the magnitude of disturbance levels, control sensitivity is influenced more by σ_{v_g} for large magnitudes of Y_v and/or L_{v_g} than at small Y_v and L_{v_g}.

b. Pilot Rating

Pilot opinion rating of lateral handling qualities deteriorated with increasing rms turbulence level. This can be seen for the results of one configuration in Fig. 13(b). The pilot ratings for all of the lateral configurations are plotted in Fig. 16. The effects of rms turbulence level on PR of lateral handling qualities are similar to those discussed previously for longitudinal handling qualities. The results in Fig. 16 show that (1) both $Y_v \cdot \sigma_{v_g}$ and $L_{v_g} \cdot \sigma_{v_g}$ are important factors in determining the sensitivity of PR to turbulence level and (2) roll rate damping, L_p, is effective in offsetting some of the adverse effects of turbulence by suppressing the attitude disturbances and improving attitude control.

E. Additional Factors that Influence Handling Qualities

Limited flight simulator studies were conducted to evaluate several additional factors that are known to influence handling qualities in hovering and low-speed flight. The factors investigated included stick force gradient, control moment lag (first-order time constant), control backlash, and authority of the rate stabilization system. The experiments were not intended to be a comprehensive evaluation of these factors. The purpose was to determine the limit of these factors for which handling qualities are not degraded. This would then provide an estimate of the range of these parameters for which the results of the linearized simulations used in this study would be valid. For this reason, only one configuration ($M_{u_g} = 0.67$, $X_u = -0.1$, and $M_q = -3$) was evaluated and, except for control force gradient, only the longitudinal handling

qualities were assessed. The lateral and directional parameters were the same as those listed for Case P1 in Table A-I.

1. Stick Force Gradient

Pilot ratings and control sensitivities selected by the pilot are shown for one configuration in Fig. 17. Results obtained with and without a stick force gradient (SFG) are presented. Only one value of longitudinal and lateral SFG (1.5 lb/in.) was evaluated. The optimum control sensitivity lines and pilot ratings predicted from the contours of M_{δ_o}, L_{δ_o} and PR (Figs. 4, 5, 7, and 8) are also shown. These contours are based on data obtained without an SFG and an rms turbulence level of 5.1 ft/sec.

a. Control Sensitivity

The addition of an SFG of 1.5 lb/in. had little effect on optimum control sensitivity. The data for longitudinal sensitivity (Fig. 17(a)) show some small differences between those with an SFG and those without. Also, both sets are slightly higher than those predicted from the contours. The lateral control sensitivities with an SFG are all higher than both the data and the contour predictions for no SFG. The significance of the effect of SFG on lateral and longitudinal control sensitivities was difficult to assess. Since only one value of SFG was available in the simulator, it could not be established that those changes in sensitivity were indicative of a trend with SFG. It should be noted, however, that the pilots thought the SFG was disagreeably large for lateral control. A pilot may desire higher control sensitivity when the SFG is too high so that he can control the aircraft with smaller control displacements.

b. Pilot Rating

An examination of the pilot ratings in Fig. 17 indicates that only small variations in PR resulted from the addition of an SFG. Comments for these cases are listed in Tables A-II (P137 to P140) and A-III (R171-to R174). For the longitudinal evaluation with an M_q of -1, Pilot A thought that the addition of an SFG reduced the likelihood of inadvertently introducing unwanted control inputs. This factor could be especially important under conditions of severe aircraft motion. For this low-damped configuration with acceleration-type attitude response, Pilot B felt that adding an SFG made it more difficult to control attitude with precision because displacement of the control stick could not be controlled as accurately. This may indicate a need to match the control "feel" characteristics to the aircraft dynamics. With high rate damping the pilots liked the addition of both the longitudinal and lateral control force gradients.

2. Longitudinal Control Lag

Flight simulator data listed in Table IV show the effect of a longitudinal control lag on optimum control sensitivity, pilot rating and pilot comments. The control lag was simulated by a first-order time constant, τ_c. The time constant, τ_c, is the time for the effective control displacement (or the pitching moment) to reach 63% of its final value following a step input of the control.

a. Control Sensitivity

Table IV shows that control lag, τ_c, had little effect on pilot selection of control sensitivity. The addition of a first-order lag slows the attitude

TABLE IV

EFFECT OF LONGITUDINAL CONTROL LAG ON HANDLING QUALITIES

$M_u g = 0.67$ $\quad M_q = -3$

$X_u = -0.1$ $\quad \sigma_{u_g} = 5.1$

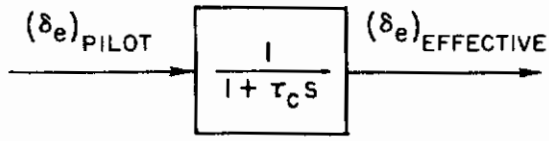

Control Lag, τ_c	$M_{\delta_{e/OPT}}$	PR	Summary of Pilot Comments
0	0.432	3.0	Very controllable, predictable attitude response. Can concentrate on position control.
0.05	0.433	3.5	Notice some oscillation in pitch response. Some overshoot on θ commands. Not difficult to control, but irritating.
0.1	0.433	4.0	Periods when pitch becomes oscillatory. Some trouble in controlling position.
0.2	0.406	5.0	Pitch response unpredictable. Must watch attitude closely and follow up on control inputs. Had to relax attitude control.
0.5	0.405	6.0	Impossible to control attitude precisely. Requires high level of attention and rapid control follow up. Must relax control and tolerate position errors.

response to a control input. Therefore, it might be expected that the pilot would desire higher control sensitivity with increasing lag, τ_c. This did not occur; in fact, the values of M_{δ_e} selected for $\tau_c > 0.1$ were slightly smaller than those for the control with no lag. With increasing τ_c, the pilot found that he was forced to relax his control and accept slower than desired attitude response in order to maintain stable closed-loop control. These results are important since they indicate that a criterion for control sensitivity will have to specify more than aircraft attitude response to a unit control input. To satisfy such a criterion, control sensitivity would have to increase rapidly with control lag. The resulting control sensitivities may be unacceptably high for the pilot.

b. Pilot Rating

Pilot rating for a satisfactory configuration with no control lag became unsatisfactory for a value of τ_c of 0.1 sec. The pilot commented that with τ_c of 0.05 sec, he noticed some oscillation in pitch attitude but it was not difficult to control. For τ_c of 0.1 sec he had some difficulty in controlling hovering position. For this configuration and rms turbulence level, the maximum lag that was acceptable to the pilot was between 0.05 and 0.1 sec. Results for the simulation of the XV-4B to be discussed in Section VI show that lags up to 0.2 sec were acceptable. The XV-4B has much lower values of M_{ug} (0.15) and X_u (-0.02), hence the gust-induced disturbances were smaller for it. This indicates that the disturbance level may be important in determining the acceptable limit of control lag. The acceptable limit of control lag may also be lower for lightly damped aircraft since the aircraft is difficult to control even with no lags.

3. Control Backlash

The data for the flight simulator studies of backlash are shown in Table V. With backlash, control moment (or $\delta_{e_{effective}}$) increases in proportion to control displacement. However, when the pilot reverses the direction of control displacement, there is no change in moment in the opposite direction until after δ_e has gone through a displacement equal to the width of the backlash, b. Backlash was simulated only for pitch attitude control

a. Control Sensitivity

The results in Table V show that the pilot made no change in M_{δ_e} for backlash $b \leq 0.6$ in. For $b \leq 0.4$, the pilot continued to use a proportional-type control technique so that higher values of M_{δ_e} would have made pitch attitude too responsive to control inputs. For the higher values of b (0.6 and 0.9 in.), the pilot tended to adopt a high frequency, bang-bang type of control technique. With this type of control technique, higher control sensitivity was desirable and was selected for b = 0.9. As with control lag, these results suggest that a control-sensitivity criterion based solely on attitude response to a 1 in. control input may result in inappropriate sensitivities. For example, this criterion

TABLE V

EFFECT OF LONGITUDINAL CONTROL BACKLASH ON HANDLING QUALITIES

$M_u g = 0.67$ $M_q = -3$

$X_u = -0.1$ $\sigma_{u_g} = 5.1$

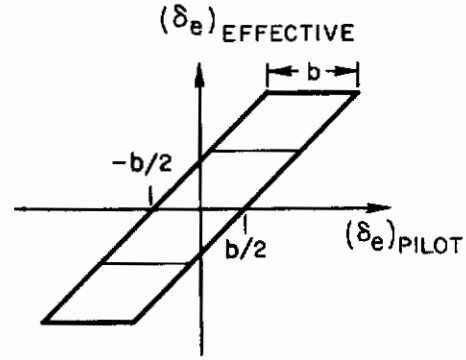

Backlash b, in.	$M_{\delta_e/OPT}$	PR	Summary of Pilot Comments
0	0.417	3.0	Good attitude control. Not too difficult to hover. Maneuver characteristics good.
0.1	0.412	3.0	Very predictable response to stick inputs. Can hover precisely and maneuver well.
0.2	0.412	3.5	Slight oscillations in hover. Possibly a slight dead-band effect in control. Pitch quite controllable.
0.4	0.412	4.0	Difficult to control pitch with precision. Attitude in constant motion. Tend to oscillate in position.
0.6	0.412	4.5	Must watch pitch very closely. Have to adopt bang-bang type motion of control stick. Can perform task.
0.9	0.478	5.5	Very difficult to maneuver and hover. Attitude motion very unpredictable. Must use rapid, bang-bang control motions.

would result in longitudinal control sensitivities which are too high for control systems that contain moderate values of backlash (i.e., less than that which forces the pilot to adopt a bang-bang control technique). It is believed that the open-loop dynamics and the gust sensitivity of the aircraft are also important in determining the acceptable limit of backlash in a control system.

b. Pilot Rating

The results in Table V show that the addition of control backlash did not produce unsatisfactory handling qualities until it reached a value of 0.4 in.

For the case with b of 0.2 in., the pilot commented that there seemed to be a control dead band present. For b of 0.4 in., he found that both attitude and hovering position were difficult to control.

4. Rate Stabilization System Authority

Results of the studies to determine the effect on handling qualities when the authority of the pitch rate stabilization system is limited are presented in Table VI. The authority M_{RA} is the maximum control moment that can be

TABLE VI

EFFECT OF PITCH RATE STABILIZATION AUTHORITY ON HANDLING QUALITIES

$M_u g = 0.67$ $\quad M_q = -3$

$X_u = -0.1$ $\quad \sigma_{u_g} = 5.1$

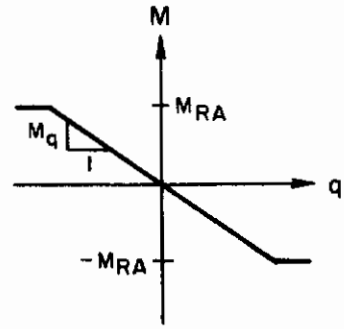

Rate SAS Authority M_{RA}, rad/sec^2	$M_{\delta_e/OPT}$	PR	Summary of Pilot Comments
Unlimited	0.441	3.0	Well damped. Predictable attitude response to control inputs.
0.15	0.432	3.0	Seems well damped. Several times noticed rather rapid response to large gust. Easy to control pitch.
0.1	0.352	4.0	Difficult to evaluate. Sometimes when maneuvering noticed rapid pitch motion. Frequently had overshoots in response to commands.
0.06	0.301	4.5	Pitch control requires attention. Must avoid abrupt control inputs. Needs damping.
0.03	0.253	5.5	Pitch quite difficult to control. Inadvertently develop large pitch angles when maneuvering. Gusts quite annoying.
0	0.272	6.0	Very unstable, oscillatory. Difficult to select suitable control sensitivity. Probably could land it but mission accomplishment doubtful.

commanded by the rate stability augmentation system (SAS). Some VTOL aircraft have been designed so that the SAS authority is limited to values between 10 and 50% of the maximum total control moment available. This insures that adequate control moment is available to overcome "hardover" failures of SAS systems. The purpose of these limited experiments was to determine for one configuration the limit to which the SAS authority could be reduced without seriously degrading handling qualities.

a. Control Sensitivity

The results show a steady decrease in control sensitivity as the SAS authority was reduced. This would be expected, since limiting the SAS authority appeared to the pilot as a reduction in the effective pitch rate damping of the configuration. These control sensitivities are similar to those shown in Fig. 17 which resulted for the same basic configuration when M_q was reduced.

b. Pilot Rating

For rate SAS authority M_{RA} of 0.1 rad/sec^2 and smaller, the results show that pilot opinion of handling qualities deteriorated. This is to be expected because the total SAS moment which can be commanded is not adequate to effectively damp the aircraft's response to turbulence or stick commands. For this turbulence level and configuration, a SAS authority of about 0.15 rad/sec^2 was required for satisfactory handling qualities. Since the value of M_q was -3, this means that the stability augmentation system saturated for a pitch rate of $\pm$0.05 rad/sec. The results of the precision hovering experiments in Table A-VI (Case PH11) show that this was also approximately the rms pitch rate for this configuration. It is expected that for less gust-sensitive configurations, smaller SAS authority would be acceptable since the average pitch rates are lower.

SECTION IV

RESULTS FOR THE PRECISION HOVERING TASK

Data obtained in the flight simulator for the longitudinal precision hovering task are discussed in this section. These data consist of pilot ratings and measured rms values of pitch rate, pitch attitude, hovering position error, longitudinal velocity and control stick activity. The effect on these quantities of speed-stability and drag parameters, rate damping and attitude stabilization, and turbulence level are discussed. Limited results showing the effect of stick force gradient are also presented. All variations in stability derivatives discussed in this section were made about a common configuration of $M_{ug} = 0.67$, $X_u = -0.1$, $M_q = -3$, $M_\theta = 0$, $\sigma_{u_g} = 5.1$ and SFG = 0. A guide to the configurations investigated is contained in Table A-V. Detailed tabulations of these longitudinal data are presented in Table A-VI.

A. Speed-Stability and Drag Parameters

1. Longitudinal Speed Stability

The speed-stability parameter, M_{ug}, caused significant variations in aircraft dynamics and pitch-attitude disturbance level. However, for the range of M_{ug} investigated, increasing M_{ug} had little effect on hovering accuracy, although it did cause variations in pilot rating.

The speed-stability parameter affects both the pitch disturbance level and open-loop VTOL aircraft dynamics. Turbulence causes pitching moments through M_u according to the product $M_u \cdot u_g$. RMS turbulence level, σ_{u_g}, was constant for this study so the disturbance level was proportional to M_{ug}. As shown in Sketch IV-A, increasing M_{ug} increased the natural frequency, ω_n, and decreased the damping ratio, ζ, of the oscillatory portion of the open-loop pitch-attitude dynamics (Table A-VII). However, the first-order pole location, $1/T_{sp}$, did not change significantly with M_{ug}.

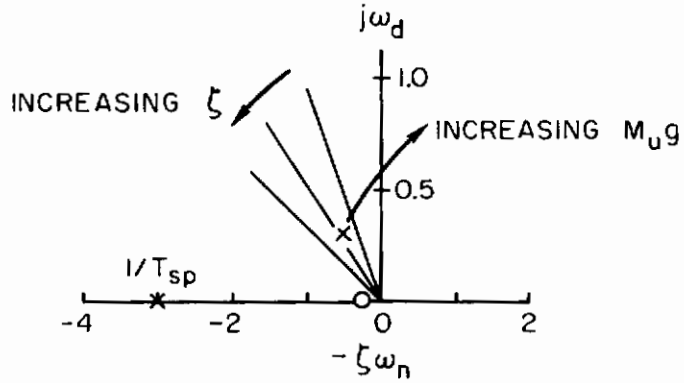

SKETCH IV-A Effect of M_{ug} on Open-Loop Pitch Dynamics

The effects of $M_u g$ on pilot rating and rms measurements of pitch rate (σ_q), pitch attitude (σ_θ), longitudinal velocity (σ_u), hovering position error (σ_x), and control stick activity (σ_{δ_e}), are shown in Fig. 18. These results and all others discussed in this section are presented for two pilots. Both σ_q and σ_θ increased with increasing $M_u g$. However, rms pitch rate increased more rapidly than rms pitch attitude. As pitch attitude disturbances became greater with larger $M_u g$, the pilots had to change pitch attitude more rapidly to attenuate the disturbances and maintain hovering position accuracy. The measured values of σ_x and σ_u exhibited some random variations, but there was no systematic change with $M_u g$. Control stick activity increased steadily with $M_u g$ due to the larger pitch disturbances which had to be controlled. As might be expected, there are differences in the measured results between pilots. These differences can be attributed to differences in pilot capabilities, control technique, and motivation.

Pilot opinion of the precision hovering task changed no more than one rating point as $M_u g$ was increased. There were two reasons for the small initial improvement in pilot rating. First, there was a very slight increase in longitudinal velocity damping, and second, the pilot was able to predict, to a limited extent, position disturbances resulting from turbulence acting on the drag parameter ($X_u \cdot u_g$). Pitch attitude responds faster to turbulence than hovering position. Hence, when the pilot can see pitch attitude respond to turbulence he can anticipate a position disturbance. As $M_u g$ increased still further, pitch attitude disturbances became more difficult to control, however. At $M_u g = 1.0$, pilot opinion was unsatisfactory because of the effort necessary to control pitch attitude. Note that pilot ratings do not correlate well with any of the measured rms functions. The trend towards an unsatisfactory pilot rating for large $M_u g$ is reflected in the increased σ_q and σ_{δ_e}, however.

2. Longitudinal Drag Parameter

Unlike $M_u g$, the longitudinal drag parameter, X_u, had a significant effect on hovering accuracy (Fig. 19). Results indicate that the product $X_u \cdot u_g$ is the primary factor determining hovering position errors. Pilot rating also deteriorated when X_u became more negative.

The longitudinal drag parameter is similar to $M_u g$ in that it also affects the magnitude of an input disturbance. Turbulence causes displacement from the hovering position by acting through X_u. The drag parameter, X_u, of course, also had a small effect on the aircraft dynamics. Specifically, an increase in the magnitude of X_u (1) increased slightly the damping ratio of the open-loop pitch-attitude oscillatory dynamics, (2) had little effect on the natural frequency, (3) did not change the location of the first-order pole, and (4) drove the first-order zero away from the origin by making it more negative (Table A-VII and Sketch IV-B). Increasing the magnitude of X_u also increased the longitudinal velocity damping of the configuration.

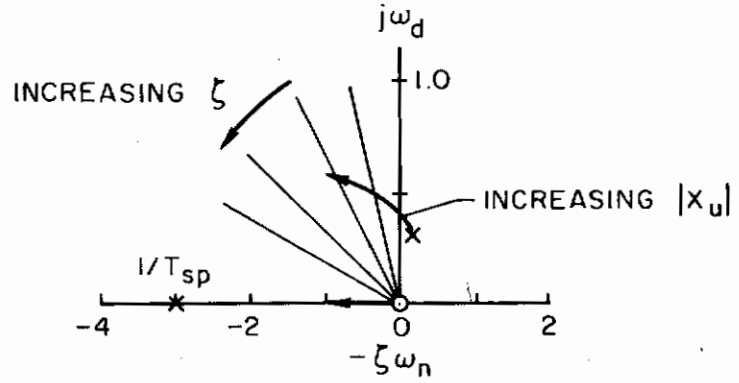

SKETCH IV-B. Effect of X_u on Open-Loop Pitch Dynamics

The effects of X_u on pilot opinion and rms performance are shown in Fig. 19. These results make it clear that for the values of $M_u g$ and X_u considered (representative of those to be expected in VTOL aircraft), hovering accuracy in turbulent air is more dependent on X_u than $M_u g$. RMS hovering position error increased proportionately as X_u became more negative, as did rms position rate. It is apparent that the increase in the damping of longitudinal velocity when X_u became more negative was overshadowed by the increase in position disturbances induced through X_u. RMS pitch attitude and rms pitch rate also increased with the magnitude of X_u. This reflects the larger, more rapid changes in thrust vector orientation which were required to attenuate position disturbances. Note that σ_q and σ_θ did not increase proportionately with X_u for magnitudes of $X_u \geq 0.1$ and that the rate of change of σ_x with X_u increased for X_u more negative than -0.1. This is because at larger magnitudes of X_u the pilots used smaller pitch angles and rates than were required to maintain the better hovering accuracy that was achieved at smaller magnitudes of X_u. The pilots were not willing to use higher angles and rates because they considered them unrealistic (dangerous in actual flight operations). The increase in control stick activity with the magnitude of X_u also reflected the increased pilot effort required to maintain position control. Pilot opinion deteriorated rapidly when X_u became more negative because of the pilot concentration and effort required to control position.

There is, obviously, a marked difference in the pilot's ability to suppress pitch and position-loop disturbances. The pilot can observe and correct for inner-loop disturbances before their effect is integrated into any significant hovering position error. On the other hand, the pilot generally cannot correct for position disturbances until after he has observed them, i.e., until after an error in hovering position has resulted. This inherent difficulty is complicated by the large lag between control inputs and hovering position response (four integrations are involved in converting δ_e to x).

B. Rate Damping Stability Augmentation

Pilots adapted to the changes in aircraft dynamics and attitude disturbances caused by M_q in such a way that hovering position accuracy was unaffected (Fig. 20). This result is similar to that for $M_u g$. Both of these parameters affected primarily pitch attitude control characteristics. Although hovering performance was unaffected by M_q, pilot rating varied.

Rate damping produces a restoring moment to null pitch rates and, thereby, attenuates pitch response to turbulence. Rate damping also decreased the frequency of the open-loop pitch oscillatory response, increased its damping ratio, and moved the first-order pole away (more negative) from the origin (Table A-VII and Fig. 10).

The effects of M_q on pilot rating and rms measurements are shown in Fig. 20. As pitch rate damping increased, σ_q decreased, while σ_θ, σ_x and σ_u remained nearly constant. Increasing the magnitude of M_q reduced pitch rate response to turbulence and also reduced the pitch transient response to stick inputs, providing a more predictable pitch response to stick commands. Control stick activity decreased as the magnitude of M_q was increased. This, combined with the more predictable attitude response characteristics and the reduced pitch disturbances, resulted in improved pilot opinion. However, there is no further improvement in opinion as M_q changed from -3 to -5. Pilot comments indicate that opinion didn't improve because pitch response is so heavily damped at $M_q = -5$ that the pilot can no longer observe pitch response to turbulence. Although he does not have to attenuate pitch disturbances, the pilot cannot predict position response to turbulence by observing pitch disturbances. Thus, it becomes slightly more difficult to control position disturbances. Again, as for $M_u g$, the decrease in σ_q and σ_{δ_e} with increased damping correlates with the general improvement in pilot opinion.

C. Attitude Stability Augmentation

The results for M_θ are similar to those for $M_u g$ and M_q. Changes in M_θ affected primarily pitch attitude control and, as for the $M_u g$ and M_q studies, the pilot hovering performance was unaffected by M_θ. Pilot rating did change with M_θ, however, as shown in Fig. 2.

Attitude stabilization produces a restoring moment that tends to drive pitch attitude angle to zero. The addition of M_θ, then, results in a decrease in the amplitude of pitch response to low frequency gust disturbances produced through $M_u g$. However, the use of M_θ can amplify high-frequency pitch disturbances when used with low levels of rate damping (Ref. 8). For the configurations evaluated, changing M_θ to -3 increased both the damping ratio of the open-loop pitch oscillatory dynamics and the natural frequency. Increasing

the magnitude of M_θ further to 5 continued to increase the natural frequency but the damping ratio decreased (Fig. 10). The first-order pole in the pitch dynamics moved towards the origin (became less stable) as M_θ became more negative.

The effects of M_θ on pilot rating and the measured rms functions are presented in Fig. 21. As M_θ became more negative, σ_q and σ_θ decreased. This would be expected since pitch response to turbulence decreased. Again σ_x and σ_u did not vary with M_θ. This result is similar to those obtained for the previous studies of M_{u_g} and M_q. Control stick activity did not change significantly as the magnitude of M_θ increased.

Pilot opinion improved as the magnitude of M_θ was increased from 0 to 3. This is probably a reflection of the increased attitude damping ratio and the decrease in low-frequency pitch response to turbulence. When M_θ was changed to -5, low-frequency pitch response to turbulence decreased further. Pilot A apparently felt this was beneficial enough to offset the attendant decrease in damping ratio and slight increase in high-frequency pitch disturbances as his rating continued to improve. Pilot B did not care for these side effects, however, and his rating deteriorated. Note that the constant σ_{δ_e} does not correlate with the overall improvement in pilot rating as M_θ becomes more negative; however, the decrease in σ_q does.

D. RMS Turbulence Level

Pilot hovering accuracy deteriorated with increasing rms turbulence intensity level (Fig. 22). The results for changes in σ_{u_g} are similar to those obtained for X_u. Pilot rating deteriorated with increasing σ_{u_g}.

Increasing σ_{u_g} increased both pitch attitude disturbances and position disturbances through M_{u_g} and X_u. There was, of course, no change in VTOL aircraft dynamic characteristics as σ_{u_g} was increased. All of the rms functions increased with σ_{u_g}. These results are similar to those for increasing the longitudinal drag parameter. The pilots seemed to be able to control the increased pitch attitude disturbances caused by $M_{u_g} \cdot u_g$. However, they could not attenuate the position disturbances resulting from $X_u \cdot u_g$ sufficiently well to maintain hovering accuracy. The reason the pilot could not control the increased position rates is similar in some respects to that outlined in the discussion of the X_u results. However, pitch disturbances increased as well as position disturbances when σ_{u_g} was made larger. Thus, the pilot should have been better able to predict position disturbance here than when only $|X_u|$ was made larger. Consequently, the increase in σ_x with σ_{u_g} was probably due largely to the pilot's unwillingness to destabilize pitch attitude control to the extent necessary for suppression of the increased position disturbances.

E. Stick Force Gradient

Limited results on the effects of stick force gradient indicate that it caused no significant change in pilot hovering performance or opinion.

The addition of a stick force gradient (SFG) increased the pilot physical effort required to make control inputs. It also provided a centering force (and, therefore, a null reference) which reduced inadvertent pilot inputs. Results from the SFG study for Pilot A are tabulated in the following listing (see Table A-VI for Pilot B results).

SFG	σ_q	σ_θ	σ_u	σ_x	σ_{δ_e}	PR
0	0.047	0.033	0.93	1.46	0.57	3.0
1.5	0.045	0.035	0.97	1.53	0.49	3.25

There appeared to be no significant effects of SFG evident in the rms and pilot rating results of this limited study. The pitch dynamics for which rms data were measured in the SFG study were well damped ($M_q = -3$). The addition of SFG generally results in the pilot using more abrupt input commands. Consequently, if these measurements had been made for poorly damped dynamics, SFG might have affected hovering performance.

F. Summary of Precision Hovering Results

The precision hovering results can be summarized as follows:

(1) Variations in the pitch dynamic characteristics and pitch response to turbulence had little effect on rms hovering position for the configurations evaluated. Pilot opinion was affected by these parameters, however, because they determined the level of pilot effort necessary to maintain hovering accuracy. Position error was unaffected because pilots could observe and correct for pitch error before it was integrated into a position error and also because the lag between stick command and attitude response was small.

(2) Increasing the level of position disturbances by making X_u more negative or increasing σ_{u_g} resulted in a proportional increase in hovering position error and a significant deterioration in pilot rating. This was primarily the result of the large lag which exists between stick command and position response.

(3) For the dynamics considered, the addition of an SFG has no noticeable effect on pilot performance of the precision hovering task.

The effects of $M_u g \cdot \sigma_{u_g}$ and $X_u \cdot \sigma_{u_g}$ on hovering performance, discussed in (1) and (2) above, are illustrated in Fig. 23. The hovering position error is plotted versus the rms values of the disturbance forcing functions $M_u \cdot \sigma_{u_g}$ and $X_u \cdot \sigma_{u_g}$. The plot for pitch disturbances shows results from the $M_u g$ investigation and also one case from a series of special hovering tests which will be discussed in detail in Section V. The position disturbance function is constant for all of these points ($|X_u \cdot \sigma_{u_g}| = 0.51$). The plot for position disturbance level presents results from both the X_u and rms turbulence level studies. Results (1) and (2) discussed above are confirmed by Fig. 23. That is, rms hovering position error was unaffected by changes in pitch disturbance level when position disturbance level was held constant, but rms hovering position error was strongly affected by changes in position disturbance level when pitch disturbance level was held constant. Also, the data point for $|X_u \cdot \sigma_{u_g}| = 0.77$ is from the studies where rms turbulence level was a variable; therefore, the value of $M_u \cdot \sigma_{u_g}$ is higher than for the results from the studies where X_u was a variable. However, the point agrees well with the overall trend, indicating that increased pitch disturbances were not a significant source for hovering error even when position control became more difficult.

SECTION V

CLOSED-LOOP MODEL ANALYSIS OF THE HOVERING TASK

The results of an analysis based on a closed-loop representation for the longitudinal precision hovering task are presented in this Section. The objective of the analysis was to develop a limited number of generalized parameters which correlate with pilot opinion for a wide range of VTOL aircraft. Such parameters could provide the understanding necessary for the formulation of handling qualities specifications. It was felt that pilot-model adaptable parameters which describe human pilot dynamic behavior might correlate with opinion. These adaptable parameters were computed from the rms hovering performance results presented in Section IV. Trends in the parameters with pilot opinion and optimum control sensitivity are presented and reasons for pilot adaptation of these parameters are discussed.

The effects of speed-stability and drag parameters, rate damping and attitude stabilization, turbulence level, and stick force gradient are examined in this analysis. The effects of the locations of the roots for the characteristic equations of the pitch and position open-loop dynamics are also considered. Results of the study are discussed in this Section and a detailed tabulation of the pilot adapted parameters and other pertinent data are contained in Table A-VII.

A. The Hovering Task Model

1. Assumed Loop-Closure Structure

The model used to represent the two-degree-of-freedom hovering task is presented in Fig. 24. It was developed under the assumption that the pilot closes the pitch (inner) loop and position (outer) loop in series. That is, the series-loop closure assumes that the pilot observes his hovering position error and mentally generates a pitch attitude command angle, θ_x. The attitude command angle is that which is needed to tilt the thrust vector and develop the longitudinal acceleration for reducing position error. This attitude angle represents a command which is routed to the pitch loop. There the pilot generates control inputs, δ_e, to null the error between the commanded attitude angle and the actual pitch attitude.

The series-loop closure for the hovering task model is predicated upon observed pilot behavior. It was selected after first considering a parallel-loop-type model. The basic form of the series model was first brought to the attention of UARL by R. L. Stapleford of Systems Technology, Inc. An identical model has been developed independently at MIT for a helicopter longitudinal two-degree-of-freedom hovering task (Ref. 15).

2. Human Pilot Model

The models selected to represent the human pilot dynamics (Fig. 24) were fundamentally linear, but included a pure time delay or transport lag. These quasi-linear models have been found to be realistic approximations for pilot dynamic behavior in one-degree-of-freedom compensatory tracking tasks (Refs. 16 and 17). The hovering task is also, basically, a compensatory tracking task. It is reasonable to assume, then, that quasi-linear pilot models can be used here as well.

The form of the quasi-linear pilot model used in this study is given in Laplace transform notation by

$$Y_{P_\theta} = \frac{K_{P_\theta}\left(T_{L_\theta}s + 1\right)e^{-\tau_\theta s}}{T_N s + 1} \qquad (10)$$

Equation (10) represents the quasi-linear pilot model used for the pitch loop. Pilot gain, K_{P_θ}, represents the pilot's stick response to an error in the magnitude of a controlled variable. The lead term, $(T_{L_\theta}s + 1)$, is an indication of the pilot's stick response to the rate of change in error of the controlled element variable. The parameters K_{P_θ} and T_{L_θ} are adaptive. When the aircraft dynamics and/or turbulence characteristics change, the pilot can adapt his gain and lead to the new conditions. Through this adaptation the pilot can generally maintain stable control and achieve desirable system response characteristics. Pilots can also supply an adaptive lag, $1/(T_I s+1)$. However, it does not appear that adapting lag would improve the pilot's hover control capability. This term, consequently, was not included in the pilot models used in this analysis. The model factors $1/(T_N s+1)$ and $e^{-\tau_\theta s}$ define inherent pilot lags. The constant transport lag, $e^{-\tau_\theta s}$, represents an accumulation of delays involved in the transmission of information and decision making. The term $1/(T_N s+1)$, where T_N is another constant, is an approximation to the neuromuscular lag involved in the response of the arm to a commanded motion. The neuromuscular lag term is only present in the pitch-loop pilot model. This is because the series loop hovering task model assumes that arm activity is restricted to the pilot's control of the pitch loop. These lags and the limitations in the assumption that they are constant are discussed in more detail in Appendix B.2 and Ref. 14. The values used in this study for these constants were $\tau_\theta = 0.09$ sec and $T_N = 0.35$ sec. These values were chosen from the results in Ref. 16. Their choice is also discussed in more detail in Appendix B.2.

B. Computation of Pilot Adapted Parameters

Previous studies concerned with the development of pilot quasi-linear models (Refs. 16, 17 and 18) have involved the computation of random-excitation describing functions to represent pilot dynamic behavior. Such describing functions permit an evaluation of the pilot's adaptation to

different test characteristics, the extent to which he is a linear operator, and the effects of his inherent nonlinearities. However, the procedures necessary to compute them are complex and costly.

Since the objectives of the UARL study were limited to determining trends in pilot adapted parameters with various factors, a method different from the describing function technique was developed to provide the necessary data. This method involves iterating the pilot-model adapted parameters until the computed rms performance of the closed-loop hovering model matches the measured rms hovering performance of Section IV. The measured rms hovering performance was obtained in the flight simulator with a human pilot. Details of the computational method, its verification, and the hovering task model equations used are contained in Appendix B. In addition, Appendix B contains a discussion of the effects of pilot nonlinearities on the computed parameters and how these effects can be reduced by judicious selection of the rms performance functions to be measured. The interpretation of adapted position-loop lead is also discussed.

C. Results of the Model Analysis

Pilot-model adapted parameters for the different handling qualities studies are presented and discussed in this subsection. These parameters represent the pilot's quasi-linear control characteristics. The pilots adapted their control characteristics to compensate for the effects of VTOL aircraft dynamics and obtain the loop closures necessary for good hovering performance. Tight, well-damped closures result in small values of the rms hovering performance functions. The loop-closure characteristics are given in the frequency domain by the crossover frequencies (ω_c) and phase margins (PM). For example, as aircraft response to turbulence increases the pilot must tighten the loop closure to suppress the increased disturbances. Tightening the loop while maintaining the same degree of stability results in an increase in ω_c and no change in PM.

To achieve the loop closures, the pilot must adapt his control characteristics -- i.e., supply gain and/or lead -- to compensate for the effects of the VTOL aircraft dynamics. Increasing gain will generally extend ω_c (increase closed-loop response) and supplying lead will increase PM (provide a greater degree of closed-loop stability). Pilot opinion and optimum control sensitivity are affected by the adaptation required of the pilot. The crossover frequency, ω_c, is that frequency at which the frequency-dependent magnitude of the product of the pilot model (e.g., Y_{P_θ}) and open-loop dynamics (e.g., θ/δ_e) is equal to 1. Generally, larger values of ω_c indicate more rapid closed-loop response. Phase margin is computed using the phase angle (also a function of frequency) measured between a sine wave input to a transfer function and its output. Phase margin is then the difference between the combined phase angle contributed by the pilot model and open-loop dynamics at ω_c and a constant equal to -180°, i.e., PM = Phase (ω_c) - (-180°). Phase

margin is an indicator of closed-loop stability. Generally, a larger PM implies a more heavily damped closed-loop system.

Detailed listings of the configurations studied, the roots of the characteristic equations for the open-loop pitch and position dynamics of these configurations, pilot adapted parameters and loop-closure characteristics are contained in Table A-VII.

1. Speed-Stability and Drag Parameters

a. Longitudinal Speed Stability

The computed pilot-adapted parameters for the longitudinal speed-stability study are presented in Fig. 25. These parameters were computed from the rms hovering performance results for four configurations (cases PH6-PH9, Tables A-VI and A-VII) shown previously in Fig. 18. Pitch-loop lead, T_{L_θ}, increased steadily with $M_u g$, while position-loop lead, T_{L_x}, generally decreased. Pitch-loop gain, K_{P_θ}, did not exhibit a consistent trend with $M_u g$ but appeared to be relatively constant. However, position-loop gain, K_{P_x}, increased steadily with $M_u g$. Note that pilot opinion was relatively insensitive to $M_u g$ variations for the precision hovering task.

The computed loop-closure characteristics for the $M_u g$ values were as follows:

$M_u g$, per sec^3	ω_{c_θ}, rad/sec		PM_θ, deg		ω_{c_x}, rad/sec		PM_x, deg	
	A*	B*	A	B	A	B	A	B
0	---	2.2	---	7	---	0.86	---	19
0.33	2.2	2.7	14	7	0.84	0.88	24	18
0.67	2.7	3.0	10	9	0.86	0.96	20	19
1.00	2.6	3.2	24	10	0.99	0.99	31	21

*refers to pilot

Pitch-loop crossover frequency (ω_{c_θ}) increased with $M_u g$ and pitch-loop phase margin (PM_θ) increased slightly. This is a reflection of the pilot's desire to suppress the increase in pitch disturbances with $M_u g$, resulting from turbulence. Position-loop crossover frequency (ω_{c_x}) also increased slightly. Apparently, the pilots tightened position-loop control to account for a small increase in position disturbances induced by the pilot's inability to completely suppress the pitch disturbances with $M_u g$. The fact that the position-loop phase margins increased slightly indicates that the pilot was able to maintain closed-loop stability as he increased his crossover frequencies.

The pitch and position open-loop dynamics (θ/δ_e and $x/\theta_x|_{\theta \to \delta_e}$ given in Appendix B.1) affected the pilot adaptation required to achieve the above loop closure results. The open-loop pitch dynamics changed little with $M_u g$ (Table A-VII, Δ_1 for Cases PH6-PH9). The damping of the oscillatory roots decreased slightly and the natural frequency increased. As a result, it can be shown that the gain and phase lag of the open-loop dynamics in the region of crossover frequency both increased somewhat. The roots of the open-loop position dynamics -- factors of Δ_2 in Table A-VII -- changed in such a way that the phase lag near crossover frequency was unaffected by $M_u g$. The effect of these roots on gain was such that it varied little with $M_u g$ near crossover.

The pitch-loop gain results have interesting implications on possible criteria for pilot selection of optimum control sensitivity. The values of M_{δ_e} used by both pilots were obtained from the UARL contours for optimum control sensitivity and are shown in the following list.

$M_u g$, per sec^3	M_{δ_e}, $rad/sec^2/in.$	K_{P_θ}, in./rad	
		A*	B*
0	0.300	26.6	32.6
0.33	0.360	28.2	38.6
0.67	0.431	31.4	37.7
1.00	0.481	23.7	36.7

*refers to pilot

The pilots desired to increase pitch open-loop gain by increasing M_{δ_e} rather than K_{P_θ}. Hence, for variations in $M_u g$ it appears that the pilots' criterion for selection of optimum M_{δ_e} was to keep K_{P_θ} constant.

Correlation does exist between the trends in certain of the adapted parameters and pilot opinion. Because pitch disturbances were very small at low $M_u g$, pilot opinion was largely dependent on the position-loop control characteristics. The effective-position-loop lead (as discussed in Appendix B.4, this is a first-order lead term whose phase contribution is equal to the phase contribution from both T_{L_θ} and T_{L_x}) was relatively large -- about 0.8 sec; however, the pilots commented that the position-loop disturbances were small and that the handling qualities were satisfactory. As $M_u g$ increased to values greater than 0.33, the pitch attitude disturbances increased; at $M_u g = 1.0$, they were the principal factor which caused the deterioration in pilot opinion. The lead requirements in pitch were relatively low, $T_{L_\theta} \lesssim 0.2$ sec, and according to the pilots the increase in pitch disturbances did not change pilot opinion a great deal until considerable pilot effort was necessary to suppress them. A small general improvement in average pilot opinion results at $M_u g = 0.33$ because pilots could predict position disturbances to a limited extent. This made position control easier, and

since pitch disturbances were still small, opinion improved. These results indicate that the major trends in pilot opinion may be dependent on the interaction between the disturbance levels, pitch-loop lead, and effective-position-loop lead.

b. Longitudinal Drag Parameter

The pilot adapted parameters for changes in the longitudinal drag parameter, X_u, are shown in Fig. 26. They were computed using the rms results presented in Fig. 19 for five configurations (Cases PH1-PH5, Tables A-VI and A-VII). Pitch-loop lead, T_{L_θ}, was nearly constant as X_u changed and remained at a relatively small value. Position-loop lead, T_{L_x}, was large at $X_u = 0$ and then decreased with X_u up to $X_u = -0.1$. It then remained relatively constant for pilot B as X_u was made more negative but increased for pilot A. This divergence in trends for the two pilots is also evident in the variation of pitch-loop gain, K_{P_θ}, with X_u while position-loop gain, K_{P_x}, was nearly constant. Pilot opinion deteriorated from a good rating at $X_u = 0$ to unsatisfactory ratings at $X_u = -0.2$ and -0.3. The divergence in the trends of K_{P_θ} and T_{L_x} for the two pilots as the magnitude of X_u increased indicates that their control behavior was not as similar as it was for the $M_u g$ study. These differences and the reasons for variations in the other adapted parameters will be considered in succeeding paragraphs.

The computed loop-closure characteristics are presented in the following listing.

X_u, per sec	ω_{c_θ}, rad/sec		PM_θ, deg.		ω_{c_x}, rad/sec		PM_x, deg	
	A*	B*	A	B	A	B	A	B
0	2.7	2.6	17	27	0.78	0.73	22	24
-0.05	2.7	2.6	18	22	0.92	0.95	23	28
-0.1	3.0	3.2	8	7	0.86	1.00	19	15
-0.2	2.5	3.1	13	6	0.85	0.92	30	20
-0.3	2.4	3.8	16	3	0.76	0.83	43	24

*refers to pilot

Since position-loop crossover frequency, ω_{c_x}, increased, it appears that the pilots made an attempt to maintain hovering accuracy (Fig. 19) when X_u changed from 0 to -0.1. Hovering position error increased, however, despite the pilots' tightened loop closure. Phase margin, PM_x, varied, but appeared to be a minimum at $X_u = -0.1$. As position disturbance became even greater, requiring large rapid control motions, the pilots closed the position loop less tightly. Crossover frequency, ω_{c_x}, decreased and PM_x became larger as the pilots adapted a more stable, less responsive form of loop closures. The trends in pitch-loop closure characteristics for pilot A are similar to the

trends exhibited by his position-loop closures. However, this is not the case for pilot B. Pilot B continually increased ω_{c_θ} when X_u was made more negative.

The effect of X_u on the open-loop dynamics influences the adaptable parameters and the loop-closure characteristics. The open-loop pitch dynamics (θ/δ_e) did not change greatly with X_u (PH1-PH5, Δ_1 in Table A-VII). The damping for the oscillatory roots of the characteristic equation increased slightly and, in the complex frequency domain, the numerator zero moved away from the origin. As a result of these variations, neither the gain nor the phase lag of the open-loop pitch dynamics changed significantly with X_u in the region of crossover frequency. The roots of the open-loop position transfer function ($x/\theta_x|_{\theta\rightarrow\delta_e}$, Δ_2 in Table A-VII) changed such that its phase lag near crossover frequency decreased. This was the most significant change in the open-loop position dynamics.

The pitch-loop gain results for variations in X_u exhibit similarities with those from the $M_u g$ study in that they also indicate a tendency for the pilot to maintain constant K_{P_θ} when selecting M_{δ_e}. This is shown in the following list.

X_u, per sec	M_{δ_e}, rad/sec^2/in.		K_{P_θ}, in./rad	
	A*	B*	A	B
0	0.282	0.287	46.4	39.5
-0.05	0.412	0.420	30.9	28.5
-0.1	0.356	0.385	38.5	42.0
-0.2	0.465	0.469	26.5	46.1
-0.3	0.506	0.516	22.0	37.7

*refers to pilot

The pitch-loop gain results for pilot B changed little with X_u, indicating again that his criterion for selecting optimum control sensitivity may have been to keep K_{P_θ} constant. The results for pilot A are variable, but the trend seems to be a decrease in K_{P_θ} with a more negative value of X_u.

For the X_u studies, there also appears to be correlation between the computed adaptable parameters and pilot opinion. Note in Fig. 26 that pilot opinion deteriorates rapidly with X_u. For X_u = 0 and -0.05, where position disturbances were quite small, pilot opinion was good even though the pilot was supplying 1.5 sec of effective-position-loop lead. Then, as position disturbances became larger, opinion deteriorated rapidly and the pilot could not extend ω_{c_x} sufficiently to maintain hovering accuracy. Finally for X_u = -0.2 and -0.3, the pilot put more emphasis on maintaining stable control than on attempting to hover accurately. This regression in loop closure at the large

magnitudes of X_u is the result of the pilot's inability to supply large position-loop lead (to account for the large lags between stick input and position response), when position disturbances became large. Neither pilot was able to supply large T_{L_x} and also keep position-loop crossover frequency at a large value. Pilot A supplied large position-loop lead in the presence of large disturbances by reducing his response to them. That is, pilot A could supply the large T_{L_x} only when his ω_{c_x} had again regressed to a smaller value.

In summary, the adaptable parameter and opinion results for the X_u studies indicate that pilot opinion may be primarily dependent on the lead requirements placed on the pilot and also the magnitude of the disturbances the pilot must try to suppress. These conclusions are similar to those for the M_{ug} study.

2. Rate Damping Stability Augmentation

The pilot adapted parameters for variations in the level of rate stabilization, M_q, are shown in Fig. 27. These parameters were computed for three configurations (Cases PH10-PH12, Tables A-VI and A-VII) from the hovering performance data shown in Fig. 20. Pitch-loop lead, T_{L_θ}, decreased rapidly with M_q while T_{L_x} was higher for M_q of -5 than for M_q of -3 and -1. There was a continuous increase in adapted pitch gain, K_{P_θ}, while K_{P_x} decreased with M_q. The trends in parameters are quite similar for both pilots.

The computed loop-closure characteristics which resulted from matching the series-model performance to measured rms hovering performance are as follows:

M_q, per sec	ω_{c_θ}, rad/sec		PM_θ, deg		ω_{c_x}, rad/sec		PM_x, deg	
	A*	B*	A	B	A	B	A	B
-1	3.0	3.4	7	8	0.93	1.05	20	21
-3	2.7	3.1	5	8	0.89	1.00	16	15
-5	2.6	2.8	11	10	0.89	0.97	22	19

*refers to pilot

Pitch response to turbulence is, of course, largest for the lowest level of pitch rate damping, i.e., $M_q = -1$. Consequently, ω_{c_θ} is largest at $M_q = -1$ because the pilots had to respond rapidly to disturbances. As the magnitude of M_q increased, pitch response to turbulence decreased and, as expected, so did ω_{c_θ}. Pitch closed-loop stability was essentially unchanged since PM_θ was nearly constant. Position-loop crossover frequency decreased only slightly

with M_q. However, in general, the position-loop-closure characteristics changed little because the position-loop disturbances were essentially unchanged with M_q.

The pilot adaptation required to achieve the desired loop-closure characteristics was affected by the change in VTOL aircraft dynamics as M_q changed. Increased rate damping moved the location, in the complex frequency domain, of the first-order pole in the pitch open-loop dynamics (Δ_1 for Cases PH10-PH12, Table A-VII) away from the origin. It also increased the damping and decreased the natural frequency of the oscillatory roots. The gain of the open-loop pitch dynamics near the crossover frequencies decreased as M_q became more negative, because of the changes in dynamics, as did the phase lag. The changes in the open-loop position dynamics (pitch loop closed) near the crossover frequencies consisted of a decrease in phase lag and a slight increase in gain.

Pitch-loop gain, K_{P_θ}, did not remain constant with M_q. Instead, it increased as M_q became more negative. Pitch-loop gain and control sensitivity are shown in the following table.

M_q, per sec	M_{δ_e}, rad/sec^2/in.	K_{P_θ}, in./rad	
		A*	B*
-1	0.369**	23.6	25.6
-3	0.431	34.2	39.7
-5	0.493	38.7	43.8

*refers to pilots

**control sensitivity, M_{δ_e}, used by both pilots was taken from the UARL optimum sensitivity contours. Both pilots assured themselves that it was near-optimum for the hovering task.

Constant K_{P_θ} would appear not to have been the criterion for pilot selection of optimum control sensitivity for variations in M_q as it may have been for variations in M_{ug} and X_u.

The adaptable parameter results for the M_q study show good correlation with pilot opinion (Fig. 27). The improvement in rating correlated with the marked reduction in T_{L_θ}. An additional contributing factor was that pitch attitude response to turbulence also decreased with the addition of M_q. When M_q was changed to -5, the pitch-loop lead requirements were further reduced as were the pitch disturbances, but pilot opinion did not improve. This was because the pitch response to turbulence was suppressed to such an extent that the pilot could not use pitch disturbances to predict position disturbances. Generally, control of the position loop was not regarded as difficult because the position-loop disturbances were relatively small.

3. Attitude Stability Augmentation

The pilot adaptable parameters for changes in pitch attitude stabilization, M_θ, are presented in Fig. 28. Three configurations (Cases PH17, PH19, PH21, Tables A-VI and A-VII) were evaluated using rms results already discussed in Section IV (Fig. 21). The adapted lead terms, T_{L_θ} and T_{L_x}, for the two pilots remained relatively unchanged as M_θ was changed from 0 to -5. Pitch-loop gain, K_{P_θ}, also remained relatively constant for pilot B, but K_{P_θ} for pilot A decreased slightly. Position-loop gain, K_{P_x}, increased for both pilots when M_θ became more negative. Pilot opinion increased as M_θ changed from 0 to -3 and then changed little as M_θ was changed to -5.

The computed loop-closure characteristics were as follows:

M_θ, per sec^2	ω_{c_θ}, rad/sec		PM_θ, deg		ω_{c_x}, rad/sec		PM_x, deg	
	A*	B*	A	B	A	B	A	B
0	3.2	3.2	10	11	0.98	1.20	18	17
-3	2.9	3.4	9	6	0.93	1.10	26	21
-5	3.3	3.8	18	10	1.10	1.00	23	18

*refers to pilot

There was a rather small general increase in ω_{c_θ} when M_θ was made more negative. For $M_\theta = 0$, the configuration (PH17) was lightly damped and responsive to turbulence. The computed ω_{c_θ} is relatively large and reflects the pilot's need for rapid response to suppress the pitch disturbances. As the magnitude of M_θ increased, the low-frequency pitch response to turbulence was reduced, but smaller, high-frequency pitch disturbances were still present. The large ω_{c_θ} indicates that the pilots responded to them, especially pilot B. The other loop-closure characteristics, PM_θ, ω_{c_x} and PM_x, did not exhibit a consistent increase or decrease with M_θ.

The effect of M_θ on the open-loop dynamics was somewhat different than the effect of the other factors investigated. As M_θ was made more negative, the location, in the complex frequency domain, of the first-order pole in the open-loop pitch dynamics moved towards the origin. The damping and natural frequency of the oscillatory roots increased with M_θ. The open-loop gain of the pitch dynamics in the region of crossover frequency also increased as M_θ was made more negative. This was because the effects of the increase in natural frequency of the oscillatory roots were not completely offset by the movement of the first-order pole towards the origin. The open-loop position dynamics (pitch loop closed) changed slightly with M_θ. The gain of these dynamics in the region of crossover frequency decreased but the phase lag was not affected significantly by M_θ.

The control sensitivity and pitch-loop gain results indicate that for the M_θ studies the pilots' criterion for selecting optimum control sensitivity again was to keep K_{P_θ} relatively constant. This is shown in the following listing.

M_θ, per sec^2	M_{δ_e}, rad/sec^2/in.		K_{P_θ}, in./rad	
	A*	B*	A	B
0	0.429	0.403	19.2	20.0
-3	0.385	0.352	15.1	23.7
-5	0.359	0.327	15.1	21.0

*refers to pilots

As indicated above, K_{P_θ} for pilot B changed little while M_{δ_e} decreased. For pilot A, M_{δ_e} also decreased but, in addition, K_{P_θ} decreased between M_θ = 0 and -3. However, it did not change when M_θ was changed to -5.

Pilot opinion improved initially with M_θ primarily because of improved open-loop stability and also because the low-frequency pitch response to turbulence was reduced. As the magnitude of M_θ was increased to 5, the requirements for T_{L_θ} remained relatively large. Pilot comments indicate that there was a smaller, additional reduction in low-frequency gust disturbances but the small-amplitude, high-frequency disturbances increased. Pilot A, whose hovering position errors were larger, apparently derived more benefit from the reduction in lower-frequency disturbances and his opinion improved. Pilot B generally hovered more accurately and was, therefore, bothered more by the high-frequency oscillatory pitch characteristics. As a result, his opinion deteriorated. These changes in pilot opinion were not dependent on position-loop control characteristics. Position disturbances were small and, even though effective-position-loop lead was relatively large, position-loop control characteristics were not disagreeable.

4. RMS Turbulence Level

Figure 29 shows the adaptable parameters computed for each pilot for various rms turbulence levels, σ_{u_g} (Cases PH13, PH15 and PH16, Tables A-VI and A-VII). The hovering performance data used to compute the parameters are shown in Fig. 22. The adapted pitch-loop lead did not vary with σ_{u_g}; however, position-loop lead decreased rapidly with increasing σ_{u_g}. Pitch-loop gain increased with σ_{u_g} for both pilots as did position-loop gain. Since the configuration was the same for all three levels of turbulence, the pilots did not have to account for changes in aircraft dynamics.

The computed loop-closure characteristics for the σ_{u_g} study are as follows:

σ_{u_g}, ft/sec	ω_{c_θ}, rad/sec		PM_θ, deg		ω_{c_x}, rad/sec		PM_x, deg	
	A*	B*	A	B	A	B	A	B
2.6	1.7	2.1	39	23	1.03	0.95	33	29
5.1	2.5	3.0	18	9	0.87	0.96	26	19
7.7	3.0	3.5	10	4	0.86	1.03	22	12

*refers to pilot

Both pilots extended pitch-loop crossover frequency, ω_{c_θ}, with increasing σ_{u_g} in an effort to suppress the increased pitch disturbances. As indicated by the decrease in pitch-loop phase margin, PM_θ, this was done at the expense of closed-loop stability. Position-loop crossover frequency, ω_{c_x}, did not change consistently with σ_{u_g}; however, since PM_x decreased, the position loop became less stable with σ_{u_g}.

The optimum control sensitivity selected by the pilots is listed in the following tabulation.

σ_{u_g}, ft/sec	M_{δ_e}, rad/sec^2/in.		K_{P_θ}, in./rad	
	A*	B*	A*	B*
2.6	0.396	0.396	15.5	21.6
5.1	0.424	0.431	24.1	37.4
7.7	0.476	0.477	33.4	45.1

*refers to pilots

As for the variations in M_q, the pilot did not keep K_{P_θ} constant. It would seem that, for variations in σ_{u_g}, constant K_{P_θ} was not the pilot's criterion for selecting optimum control sensitivity.

The implications of the adapted parameter results and their correlation with opinion for the σ_{u_g} study are very similar to those observed in the M_{u_g} and X_u studies. The pilots increased ω_{c_θ} to suppress pitch disturbances that increased with σ_{u_g} (as for M_{u_g}). They apparently were able to increase ω_{c_θ} because large T_{L_θ} was not required to do so. However, neither pilot increased ω_{c_x} significantly with σ_{u_g} even though this would have been necessary to maintain constant hovering accuracy. Extending ω_{c_x} and maintaining system stability would have required adapting a large lead term. These results are similar to those observed for the X_u studies. In those studies, as position disturbances increased because of large magnitudes of X_u, the pilots were not able to adapt large lead terms and also extend ω_{c_x}.

These results are another indication of the apparent interaction between lead requirements and opinion. When disturbances due to turbulence are small,

larger lead terms can be adapted, if they are required, and pilot opinion is not necessarily degraded. When disturbances increase, the adaptation of lead becomes more difficult and opinion deteriorates. Of course, opinion can deteriorate for large disturbances even if large lead is not required (e.g., the M_{ug} studies). However, pilot opinion changes much more rapidly with disturbances when large lead is necessary for closed-loop stability.

5. Stick Force Gradient

Sufficient data were not obtained to permit an evaluation of stick force gradient on pilot adapted parameters.

6. Additional Experiments

The hovering task model results discussed in previous subsections resulted in preliminary conclusions regarding pilot adaptation of lead, the correlation of pilot model parameters with opinion, and pilot selection of optimum control sensitivity. Additional information was desired concerning the validity of these conclusions. Consequently, several experiments were designed to examine the effects on pilot opinion and adapted parameters of open-loop pole location in the complex frequency domain of both the pitch and position loops and the interaction between pitch-loop lead requirements and disturbance (turbulence) levels. The test configurations, turbulence intensities, open-loop roots, pilot ratings and pilot adapted parameters (computed from measured rms hovering performance) are shown in Table VII. These results and also the loop-closure characteristics and M_{δ_e} are listed in Table A-VII.

The first configuration (PH28) shown in Table VII was selected so that the effect on pitch-loop lead of the relative frequency domain location of the first-order pole and the complex pair could be examined. For this configuration the first-order pole was very near the origin (-0.19) and the complex pair was heavily damped ($\zeta = 0.90$) and had a high natural frequency ($\omega_n = 2.7$). The pitch-loop lead (T_{L_θ}) adapted by the pilot for this configuration was small and pilot opinion of the configuration was good. Previous results for the variable M_q showed that moving the first-order pole away from the origin (negatively) reduced T_{L_θ} and resulted in improved pilot opinion. One might have been led to believe that the location of this pole was critical in determining good handling qualities. The results from configuration PH28 show that the complex pair of roots can cancel the adverse effects of the near-origin location of the first-order pole. The significant factor in determining T_{L_θ} and pilot opinion is apparently the combined effect of the poles and the first-order numerator term on phase lag near the pilot's crossover frequency. Thus, low T_{L_θ} requirements and good pilot opinion can result for transfer functions having either a large negative real pole and a lightly damped, low-frequency complex pair of roots or a small negative real pole and a heavily damped, high-frequency complex pair.

TABLE VII

EFFECT OF CRITICAL DYNAMIC CHARACTERISTICS ON PILOT OPINION AND PILOT ADAPTED PARAMETERS FOR HOVER

$$\frac{\theta}{\delta_e} = \frac{M_{\delta_e}(s - X_u)}{\Delta_1}$$

$$\frac{x}{\theta_x}\bigg|_{\theta \to \delta_e} = \frac{-K_{P_\theta} \cdot M_{\delta_e} \cdot g\,(T_{L_\theta} s + 1)(-\frac{\tau_\theta}{2} s + 1)}{\Delta_2}$$

Case	X_u	$M_u g$	M_θ	M_q	σ_{u_g}	$\frac{\text{Factors of } \Delta_1}{\text{Factors of } \Delta_2}$	PR	Pilot Model Parameters			
								K_{P_θ}	T_{L_θ}	K_{P_x}	T_{L_x}
PH28	-0.05	1.00	-8	-5	5.1	$\frac{s + 0.191\ ,\ s^2 + 4.86\ s + 7.32}{s + 0.766,\ s + 6.82,\ s + 22.5,\ s^2 + 7.23\ s + 15.4}$	2.0	49.8	0.07	-0.0238	0.61
PH29	-0.05	0.33	0	-3	10.3	$\frac{s + 3.04,\ s^2 + 0.0133\ s + 0.110}{s + 0.0667,\ s + 4.50,\ s + 23.2,\ s^2 + 0.392\ s + 12.1}$	4.0	50.5	0.19	-0.0214	0.42
PH30	-0.20	1.33	0	-3	2.6	$\frac{s + 3.14,\ s^2 + 0.0560\ s + 0.424}{s + 0.268,\ s + 4.45,\ s + 23.1,\ s^2 + 0.410\ s + 11.8}$	3.5	43.6	0.20	-0.0227	0.31
PH31	-0.10	0.33	0	-1	5.1	$\frac{s + 1.24,\ s^2 - 0.137\ s + 0.269}{s + 0.139,\ s + 2.29,\ s + 23.3,\ s^2 + 0.484\ s + 10.4}$	3.5	31.7	0.46	-0.0186	0.51
PH32	-0.025	0.33	0	-1	20.6	$\frac{s + 1.23,\ s^2 - 0.201\ s + 0.272}{s + 0.0600,\ s + 1.73,\ s + 23.7,\ s^2 + 0.597\ s + 14.9}$	6.5	21.8	0.60	-0.0260	0.44
PH33	-0.10	0.33	0	-3	5.1	$\frac{s + 3.04,\ s^2 - 0.0626\ s + 0.110}{s + 0.125,\ s + 5.03,\ s + 22.6,\ s^2 + 0.448\ s + 7.41}$	3.0	38.8	0.13	-0.0165	0.60
PH34	-0.025	0.33	0	-3	20.6	$\frac{s + 3.04,\ s^2 - 0.0114\ s + 0.110}{s + 0.0428,\ s + 3.89,\ s + 23.4,\ s^2 + 0.772\ s + 13.0}$	5.0	39.0	0.25	-0.0241	0.51
PH35	-0.09	0.20	0	-1	8.6	$\frac{s + 1.16,\ s^2 - 0.0709\ s + 0.172}{s + 0.111,\ s + 2.57,\ s + 23.2,\ s^2 + 0.281\ s + 10.2}$	5.0	31.4	0.40	-0.0204	0.34
PH36	-0.36	0.80	0	-1	2.1	$\frac{s + 1.48,\ s^2 - 0.121\ s + 0.540}{s + 0.429,\ s + 2.44,\ s + 23.5,\ s^2 + 0.0896\ s + 12.9}$	3.5	42.1	0.42	-0.0224	0.08

Configurations PH29 and PH30 in Table VII were selected to evaluate the effects of the natural frequency of the pitch-loop dynamics on pilot opinion and pilot-adapted parameters. The rms value of the disturbance forcing function for the pitch loop ($M_{u_g} \cdot \sigma_{u_g}$) was kept the same for both configurations. However, M_{u_g} for configuration PH30 was four times the value it had in configuration PH29. Since σ_{u_g} had to be changed to keep $M_{u_g} \cdot \sigma_{u_g}$ constant, the value of X_u for configuration PH30 was also changed to keep the position forcing function ($X_u \cdot \sigma_{u_g}$) constant. As a result of these stability-derivative variations, the first-order pole location was virtually unchanged (-3.14 vs -3.04). The damping ratio of the complex pair doubled but still remained quite small (0.04 vs 0.02). However, the frequency of the complex pair also doubled from a small to a moderately large value (0.332 vs 0.652). Pilot opinion of the pitch control characteristics was the same for both configurations. Pilot rating was better for configuration PH30, however, because of the increased outer-loop damping resulting from the larger X_u and M_{u_g}. Pilot-adapted pitch-loop parameters (K_{P_θ}, T_{L_θ}) were relatively unchanged between the two configurations. Pilot outer-loop lead (T_{L_x}) decreased slightly for configuration PH30 reflecting the increased outer-loop damping. In summary, then, these results indicate that, for the range of parameters investigated, the natural frequency of the pitch dynamics is less significant in determining pilot opinion and parameter adaptation than pitch attitude disturbance level.

Configurations PH31, PH32, PH33 and PH34 were selected to evaluate the interaction between T_{L_θ} and the effort the pilot must expend in controlling attitude-loop disturbances. Previous results for changes in M_{u_g}, X_u and M_q indicated that pilot opinion was a function of both lead and pitch disturbance level. Configurations PH31 and PH32 both require relatively large T_{L_θ}. For configuration PH32, M_{u_g} was the same as for configuration PH31 but σ_{u_g} was increased by a factor of four. The product of $X_u \cdot \sigma_{u_g}$ was kept constant for both configurations by varying X_u. Configurations PH33 and PH34 require significantly less T_{L_θ}. Again, for configuration PH34, σ_{u_g} was increased by a factor of four over that for configuration PH33. The drag parameter, X_u, was decreased to keep $X_u \cdot \sigma_{u_g}$ constant. If T_{L_θ} and pilot effort are significant in determining opinion, one would expect a deterioration in opinion from configuration PH31 to PH32 and from configuration PH33 to PH34 because of the increase in pilot effort required to hover accurately. One would also expect that the average ratings for configurations PH31 and PH32 would be poorer than for PH33 and PH34 because the lead requirements are higher for PH31 and PH32. The data in Table VII show these expected results. It is interesting to note also that the decrement in pilot rating resulting from the increase in turbulence is greater for the configurations requiring large T_{L_θ} (PH31 and PH32) than for those requiring small T_{L_θ} (PH33 and PH34).

Configurations PH35 and PH36 (Table VII) were selected to study the effects of the outer-loop damping on pilot opinion and pilot-adapted parameters. The inner-loop disturbances were kept small for these configurations to allow outer-loop effects to predominate in the formation of pilot opinion.

Configuration PH35 has low outer-loop damping since X_u and $M_u g$ are small. For configuration PH36 the values of X_u and $M_u g$ were increased by a factor of four. The turbulence intensity for configuration PH36 was reduced to one-quarter the value it had for configuration PH35 to keep the products $M_u g \cdot \sigma_{u_g}$ and $X_u \cdot \sigma_{u_g}$ constant for both configurations. The most significant outer-loop effect resulting from increasing $|X_u|$ and $M_u g$, then, was to drive the first-order pole which is located closest to the origin away from the origin. This results in reduced phase lag at the crossover frequency and the pilot, therefore, does not have to adapt as much outer-loop lead (T_{L_x}) for configuration PH36 as for PH35. This decrease in T_{L_x} required for configuration PH36 correlates with an improvement in pilot opinion (T_{L_θ} remained nearly constant).

D. Summary of Closed-Loop Model Analysis Results

The results from the closed-loop model analysis of the precision hovering task can be summarized as follows:

(1) Trends in pilot opinion correlate with changes in computed pilot-adapted lead; that is, opinion deteriorates as the lead requirements become greater. Opinion also deteriorates as the pilot effort required to suppress turbulence-induced disturbances increases.

(2) The deterioration in pilot opinion with disturbance level is much more rapid when large lead is required than when the lead requirements are small.

(3) The pilot's ability to supply relatively large amounts of lead decreases as the disturbances he is required to attenuate increase. This can cause the pilot to revert to a less responsive, more stable form of control while he allows hovering position errors to increase.

(4) Pilot-adapted lead appears to be dependent on the phase lag near crossover frequency contributed by all the poles and zeros in the VTOL aircraft dynamics. The location of any particular pole or zero is not necessarily significant in determining pilot-adapted lead or opinion.

(5) There is some indication that under certain conditions the pilot's criterion for selecting optimum control sensitivity is to maintain internal pitch-loop gain (K_{P_θ}) constant. Additional studies should be undertaken to determine more conclusively the generality of this criterion.

SECTION VI

SIMULATION STUDIES OF XC-142 AND XV-4B AIRCRAFT

The results of the simulation studies of the XC-142 and XV-4B V/STOL aircraft are presented in this section. The XC-142 is a tilt-wing type aircraft in the 37,000-lb gross-weight class built by Ling-Temco-Vought (LTV). The XV-4B is a direct-lift type research aircraft in the 12,000-lb gross-weight class built by the Lockheed-Georgia Company. These aircraft were simulated using stability derivatives for hovering flight and their handling qualities in hovering and low-speed flight evaluated. The purpose of these studies was to assess the applicability of the generalized results of Section III to cases in which coupling derivatives, control power limitations, nonlinear control effects, and the vertical degree of freedom are present. Results from the XC-142 simulation are also compared with flight test data. Results of the XV-4B simulation should be applicable to the planning of the flight test program for the aircraft. Also in this section, results from the generalized studies (Section III) are compared with Princeton flight test data for the HUP-1 helicopter and with Bell flight simulator data for the X-22A research V/STOL aircraft.

A. XC-142 Aircraft Simulation Studies

1. Stability Derivatives

The stability and control derivatives used in the simulation of the XC-142 aircraft are listed in Tables A-VIII and A-IX. Several other parameters that were used in the simulation such as control power and moments of inertia are also listed. The stick force gradient (1.5 lb/in.) is not that used in the flight vehicle; it is the SFG used in the simulation since only one value is available in the UARL simulator. The hovering stability derivatives for the basic aircraft without stability augmentation were obtained from Ref. 19; the stability augmentation parameters and the corresponding control sensitivities were obtained from Ref. 20. The stability derivatives are based on estimates by LTV instead of those obtained in the Princeton Long Track Facility. It was stated in Ref. 20 that the derivatives estimated by LTV were considered to be more representative of the full-scale vehicle.

As is typical of VTOL aircraft in hover without stability augmentation, the unaugmented XC-142 has very low damping about all axes (the magnitudes of M_q, L_p and N_r are all less than 0.3). The vertical damping is also quite low ($Z_w = -0.17$). The longitudinal and lateral speed-stability parameters are relatively small ($M_u g = 0.31$ and $L_v g = -0.24$). The lateral drag parameter is negligible while the longitudinal drag parameter is higher than for most VTOL aircraft ($X_u = -0.15$). Tables A-VIII and A-IX show that high levels of rate and attitude stabilization and vertical damping are provided by the stability augmentation system.

2. Simulation Results

The optimum control sensitivities and pilot ratings obtained in the simulation of the XC-142 are summarized in Table VIII and Fig. 30. These data

TABLE VIII

SUMMARY OF SIMULATION RESULTS FOR XC-142 AIRCRAFT

$M_u g = 0.308 \quad X_u = -0.15 \quad L_v g = -0.236 \quad Y_v = 0$

Data Source	SAS	Longitudinal		Lateral		PR for Entire Configuration*
		M_{δ_e}	PR	L_{δ_a}	PR	
XC-142 Simulation	OFF[1]	0.251	4.5	0.266	5.5	6.0
UARL Contours		0.231	5.0	0.180	5.5	-
Flight Test		0.200	-	0.333	-	6.0
XC-142 Simulation	ON[2]	0.423	3.0	0.403	2.5	3.0
UARL Contours		0.371	-	0.348	-	-
Flight Test		0.395	-	0.680	-	2.0

1 SAS OFF: $M_q = -0.20$, $L_p = -0.22$, $M_\theta = 0$, $L_\phi = 0$, $Z_w = -0.16$, $N_r = -0.11$

2 SAS ON: $M_q = -4.7$, $L_p = -3.8$, $M_\theta = -2.4$, $L_\phi = -3.8$, $Z_w = -1.4$, $N_r = -4.7$

This is the SAS installed in the flight vehicle (Ref. 20).

* Longitudinal, lateral and entire configuration evaluations were all conducted with six degrees of freedom simulated. However, pilot ratings were assigned both for control of individual axes and the entire configurations.

are also compared with predicted optimum control sensitivity lines and pilot ratings from the generalized contours of Section III. The comparison is shown even though the predicted quantities are based on data for rate-stabilized configurations having a zero stick force gradient. The pilot comments for these configurations are summarized in Table IX.

TABLE IX

SUMMARY OF PILOT COMMENTS FROM THE XC-142 SIMULATION

SAS	Summary of Pilot Comments		
	Longitudinal	Lateral	Other
OFF	Not difficult to control, but requires attention. Position loop fairly well damped, but get blown off hover point occasionally. Adequate control power. PR=4.5	Difficult to control position when maneuvering due to low drag. Roll dynamics require attention to control. Gust effects minimal. Adequate roll control power. PR=5.5	Need damping in yaw and vertical motion. Requires a lot of effort to control with all axes poorly damped.
ON[1]	Level of effort and concentration reduced. $M\delta_e$ selected to control position disturbances in hover. Control power adequate, but notice limitations periodically. PR=3.0	Good roll control. More drag would aid position control. Roll control power adequate. PR=2.5	Yaw and height control vastly improved. Little higher yaw control power desirable for rapid turning. Pleasant to fly.

Note 1: See Table VIII for SAS parameters.

The results show a significant improvement in both the longitudinal and lateral handling qualities with the addition of the rate and attitude stabilization. The pilot comments indicate that the addition of yaw and height damping also contributed to this improvement. Figure 30 shows that the ratings and control sensitivities agree fairly well with those predicted by contours of Section III for rate-stabilized configurations. The generally higher control sensitivities are probably due in part to the presence of the control force gradient and attitude stabilization in the simulation which is not included in the results from the contours.

Data from the XC-142 flight vehicle are also shown. The control sensitivities of the aircraft are compared with the UARL data in Fig. 30. Good agreement is shown for longitudinal control, but the lateral control sensitivities of the flight vehicle are considerably higher than the optimum control sensitivities of this study. The high lateral control sensitivity

(L_{δ_a} = 0.68) of the stability augmented configuration was also examined on the flight simulator. This sensitivity was found to be acceptable with a control force gradient, but highly unsatisfactory with a free stick. With a force gradient, the pilot tended to use a pulse-type lateral control motion rather than proportional-type control.

The pilot ratings for the entire configuration are compared in Table VIII with those for the flight vehicle (Ref. 21). The ratings for the unaugmented vehicles are the same (6.0) but the augmented configuration was rated 1 unit better in flight than on the flight simulator (PR = 2.0 versus 3.0). The flight evaluations were made under relatively calm atmospheric conditions. Simulated turbulence was included in the flight simulator evaluations which made the piloting task more difficult and probably accounts for some of the difference.

Root-mean-square hovering performance data for the simulated XC-142 and the adapted pilot-model parameters recovered from these data for the closed-loop hovering model are listed in Tables A-VI and A-VII, respectively. The unaugmented configuration is designated as PH24 and the augmented configuration as PH25. The rms data show no significant differences except that, with SAS, the rms control stick activity was about 10% lower. These results provide another example where there was no change in rms hovering performance even though there was a large change in both pitch-loop dynamics and pilot opinion rating. The rms value of the total moment applied by the pitch control jets ($M_q q + M_{\delta_e}\delta_e + M_\theta\theta$) decreased from 0.208 to 0.158 rad/sec^2 with the addition of SAS. This indicates that the control power required of the pitch-control system with SAS would be lower than for the unaugmented aircraft.

While rms performance did not correlate with pilot opinion, the pilot model pitch-loop lead derived from the rms data did.

Case	SAS	M_{δ_e}	PR	σ_x	T_{L_θ}	T_{L_x}
PH24	OFF	0.251	4.5	1.68	0.62	0.22
PH25	ON	0.423	3.0	1.60	-0.04	0.43

With the addition of SAS, T_{L_θ} decreased (the small negative lead is equivalent in phase, though not in magnitude, to a small first-order lag). Position-loop lead showed a small increase, but since T_{L_θ} decreased, the effective lead that the pilot was supplying in the position loop changed little.

B. XV-4B Aircraft Simulation Studies

1. Stability Derivatives

The stability and control derivatives used in the simulation of the XV-4B aircraft are listed in Tables A-VIII and A-IX. These tables also include

values for control power and several physical characteristics of the aircraft. Again, the value for stick force gradient (1.5 lb/in.) was that available in the UARL simulation and not that installed in the aircraft. As part of this study, the stability derivatives were derived from aerodynamic and propulsive data contained in Ref. 22. The contribution to the derivatives of external aerodynamic effects is small. The derivatives result almost entirely from propulsion forces and interference effects of the inlet and exhaust flows of the engines with the fuselage and wings. The rate coupling derivatives (L_q, etc.) are due primarily to the gyroscopic moments resulting from the angular momentum of the six engines (four mounted with their axes longitudinally, two vertically). The notations $Z_{|\delta_e|}$ and $Z_{|\delta_a|}$ mean that a net upward force results from the deflection of the pilot's control stick, regardless of direction. This results because all attitude control jets are directed downward.

As shown in Tables A-VIII and A-IX, the pitch and roll rate damping of the unaugmented XV-4B are negligible. The variable stability system (VSS) being developed for the XV-4B will, however, allow simulation of a wide range of rate damping. The longitudinal drag and speed-stability parameters are rather small (X_u = -0.02 and $M_u g$ = 0.15). In contrast, the corresponding lateral parameters are much larger (Y_v = -0.13 and $L_v g$ = -1.1). Thus a significant difference between the longitudinal and lateral control characteristics of the XV-4B aircraft can be expected.

2. Simulation Results

The optimum control sensitivities and pilot ratings obtained from the simulation of the XV-4B are summarized in Table X and Fig. 31. Data for the rate-stabilized configurations are compared with the optimum control sensitivity lines and pilot ratings from the generalized contours of Section III. Handling qualities of the simulated XV-4B with a combination of rate and attitude stabilization were also evaluated even though the initial variable stability system of the XV-4B flight vehicle will not include provision for attitude stabilization. The pilot comments for all of the XV-4B configurations evaluated are summarized in Table XI.

The results show that the longitudinal handling qualities were acceptable even without stability augmentation (PR = 4.0). Adding rate damping resulted in only a small improvement in rating (PR = 3.0). The pilot comments indicate that further improvement in PR was somewhat limited by the low longitudinal drag which made it difficult to maneuver with precision. Addition of attitude stabilization (SAS-3 case) had little influence on either pilot comments or ratings. Lateral control without stability augmentation was extremely difficult (PR = 6.5) because the high lateral speed stability ($L_v g$ = -1.1) made the dynamics unstable and very sensitive to gust disturbances. The poor lateral control combined with the lightly damped height control made the overall configuration almost impossible to control (PR = 8.0).

TABLE X

SUMMARY OF SIMULATION RESULTS FOR THE XV-4B AIRCRAFT

$M_u g = 0.146$ $X_u = -0.02$ $L_v g = -1.11$ $Y_v = -0.13$

Data Source	SAS	Longitudinal		Lateral		PR for Entire Configuration**
		M_{δ_e}	PR	L_{δ_a}	PR	
XV-4B Simulation	OFF[1]	0.180	4.0	0.212	6.5	8.0
UARL Contours		0.231	4.0	0.250	5.5	
Flight Vehicle		0.289	-	0.800	-	
XV-4B Simulation	SAS-1 ON[2]	0.274	3.0	0.354	4.5	5.0
UARL Contours		0.297	3.25	0.342	4.5	
XV-4B Simulation	SAS-2 ON[3]	0.420	3.0	0.510	3.0	4.0
UARL Contours		0.354	3.0	0.432	3.0	
XV-4B Simulation	SAS-3 ON[4]	0.442	2.0	0.476	3.0	4.0
UARL Contours*		0.354	2.5	0.432	3.5	

1 SAS OFF: $M_q = -0.006$, $L_p = 0$, $M_\theta = 0$, $L_\phi = 0$, $Z_w = -0.02$

2 SAS-1 ON: $M_q = -2.0$, $L_p = -2.0$, $M_\theta = 0$, $L_\phi = 0$, $Z_w = -1.35$, $N_r = -4.70$

3 SAS-2 ON: $M_q = -4.0$, $L_p = -4.0$, $M_\theta = 0$, $L_\phi = 0$, $Z_w = -1.35$, $N_r = -4.70$

4 SAS-3 ON: $M_q = -4.0$, $L_p = -4.0$, $M_\theta = -2.0$, $L_\phi = -2.0$, $Z_w = -1.35$, $N_r = -4.70$

* Contours developed from configurations having rate damping only.

** Longitudinal, lateral and entire configuration evaluations were all conducted with six degrees of freedom simulated. However, pilot ratings were assigned both for control of individual axes and the entire configuration.

TABLE XI

SUMMARY OF PILOT COMMENTS FROM XV-4B SIMULATION

SAS	Summary of Pilot Comments		
	Longitudinal	Lateral	Other
OFF	Pitch lightly damped, requires attention. Gust disturbances low so control not difficult. PR=4.0	Extremely difficult to control. Inadvertently develop large roll rates. Gusts annoying. PR=6.5	Height control difficult, needs damping. Difficult to arrest yaw rates. Lateral-directional coupling annoying.
SAS-1 ON[1]	Adequate damping. Good, predictable attitude response. Gust effects minimal. Would like more drag for maneuvering. PR=3.0	Control moderately difficult. Gusts occasionally upset roll. Large roll angles required to hover. PR=4.5	Yaw and height control adequately damped. Desire more yaw control power for rapid turning.
SAS-2 ON[1]	Well damped. Gusts unnoticeable. Better PR limited by low drag. PR=3.0	Adequate damping. Excellent maneuvering characteristics. Position disturbances a little annoying in hover. PR=3.0	Overall, aircraft is not difficult to control. No coupling problems. Lateral position disturbances require attention.
SAS-3 ON[1]	Good control. Gusts unnoticeable. Easy to control. PR=2.0	Good roll control. Concentration and effort required to control lateral position disturbances. PR=3.0	Good height and yaw control. No undesirable coupling. Adequate control power provided.

Note 1: See Table X for SAS parameters.

Figure 31 shows a comparison between the flight simulator results and the optimum control sensitivity lines and pilot ratings derived from the generalized contours of Section III. In general, there is good agreement between them. The control sensitivities for the XV-4B flight vehicle are also shown. The longitudinal control sensitivity of the flight vehicle is about the same as the optimum values determined in this study; however, the lateral control sensitivity is considerably higher. The flight simulations indicate that this sensitivity is too high for the lightly damped, unstable lateral dynamics of the unaugmented aircraft. Control sensitivity will be a parameter of the

variable stability system of the flight vehicle, so the pilot will be able to select the value he desires.

Root-mean-square hovering performance data and the closed-loop pilot model parameters derived from the data are listed in Tables A-VI and A-VII as Cases PH26 and PH27. The XV-4B stability augmented configuration for which rms data were measured is SAS-3. It had both rate and attitude stabilization. The addition of the SAS had no effect on the measured rms hovering position error, but did reduce rms pitch rate and pitch attitude (about 40% and 20%, respectively). The rms control motion was also much smaller with SAS (0.14 in. versus 0.41 in.). As with the XC-142, the rms value of the total pitch control moment ($M_q q + M_{\delta_e}\delta_e + M_\theta\theta$) decreased following the addition of the SAS (0.074 to 0.045 rad/sec^2).

Again, the improvement in pilot rating with the addition of the SAS was not accompanied by any improvement in rms hovering position error. There was,

Case	SAS	M_{δ_e}	PR	σ_x	T_{L_θ}	T_{L_x}
PH26	OFF	0.180	4.0	0.73	0.76	0.41
PH27	SAS-3	0.442	2.0	0.72	-0.09	0.83

however, a significant change in the computed pilot-model adaptive parameters. With the addition of the SAS, the inner-loop lead T_{L_θ} decreased and the outer-loop lead T_{L_x} increased. The improvement in pilot rating is consistent with the decrease in T_{L_θ}. As discussed in Appendix B, the increase in T_{L_x} is necessary to compensate for the reduction in phase margin contribution by T_{L_θ} so the effective position-loop lead supplied by the pilot was not changed greatly.

Results of studies of pitch rate stabilization authority (maximum moment that can be commanded by the SAS) and control backlash were discussed in Section III. Limited flight simulator studies were also conducted in which these factors were examined for one XV-4B configuration (SAS-2). Figure 32 shows results for the effect of rate stabilization authority (M_{RA}) on handling qualities for both the XV-4B and the "basic" configuration ($M_u g = 0.67$, $X_u = -0.1$ and $M_q = -3$) used in precision hovering studies of Section IV. Reducing the authority decreases the effective rate damping. For this reason, pilot rating and control sensitivity approached the values for the XV-4B without the SAS (shown in Table X) as M_{RA} approached zero. The effect of M_{RA} is more pronounced on the "basic" configuration because it is much more gust sensitive ($M_u g = 0.67$, $X_u = -0.1$) than the XV-4B ($M_u g = 0.15$, $X_u = -0.02$).

Figure 33 shows the effects of control lag (first-order time constant, τ_c) on handling qualities. A significant deterioration in pilot opinion rating occurred for values of τ_c greater than 0.2 sec, but there was no

significant change in optimum control sensitivity. Again, the acceptable limit of longitudinal control lag is higher for the XV-4B than for the "basic" configuration because of the differences in gust sensitivity.

3. Results Applicable to the Flight Test Program

The following results from the flight simulator studies are pertinent to the planning of the hovering and low-speed maneuvering flight test program of the XV-4B aircraft:

(1) Because of small longitudinal speed-stability and drag parameters, the longitudinal handling qualities showed little sensitivity to the level of pitch rate damping augmentation. Values of M_q greater than 2.0 did not significantly improve handling qualities.

(2) The large lateral speed-stability and drag parameters produced very poor, nearly uncontrollable, lateral control characteristics for the unaugmented aircraft. For this reason, in moderate turbulence, the lateral handling qualities continue to improve as the magnitude of L_p is increased (to L_p magnitudes of 4 or 5).

(3) Limiting the authority of the pitch rate stabilization had little effect on longitudinal handling qualities because of the relatively small influence of rate damping. Because of the need for high levels of roll rate damping, however, the lateral handling qualities would be expected to be more sensitive to the rate damping authority. Values lower than 0.5 rad/sec^2 may result in a deterioration in pilot opinion.

(4) The longitudinal handling qualities were not degraded by control lags, τ_c, smaller than about 0.2 sec. The aircraft was flyable with a lag of 0.5 sec, but the resulting handling qualities were unacceptable for normal operation. Because lateral control is more difficult, lateral control lags as low as 0.05 to 0.1 sec may be unacceptable and the aircraft may be unflyable with lags as large as 0.5 sec.

C. Comparison with Data for the HUP-1 and X-22A Aircraft

1. HUP-1 Tandem Rotor Helicopter

Hovering and low-speed maneuvering flight tests were conducted by Princeton University with a variable-stability, tandem-rotor HUP-1 helicopter (Ref. 1). The flight task consisted of precision hovering and low-speed maneuvering around a closed course. The principal parameters investigated were the longitudinal speed-stability parameter, M_ug, pitch rate damping, M_q, and the rms level of turbulence, σ_{ug}. The estimated basic values of the stability derivatives of the HUP-1 are $M_ug = 1.13$ and $X_u = -0.02$.

Flight test data for the HUP-1 are compared with the UARL data in Fig. VI-5. The optimum control sensitivity line and pilot ratings of the UARL data are from the generalized contours of Figs. 4 and 5. As shown at the top of Fig. 34, the values of σ_{u_g} and $M_u g$ for the UARL data are slightly lower than for the Princeton data. The experimental conditions of the two studies were very similar, however, especially the frequency content of the simulated turbulence and the type of flight task. Comparison of the results shows good agreement between the optimum control sensitivity lines and the level of damping required for satisfactory handling qualities (PR = 3.5). The differences in ratings within the range of unsatisfactory handling qualities are probably due to the lack of motion cues in the UARL studies.

Also shown in Fig. 34 are data from studies conducted by Grumman (Ref. 23) with a moving-base simulator (motion in pitch and roll). The effects of drag and speed-stability parameters, rate damping, and rms turbulence level on hovering and low-speed flight were also investigated in these studies. The primary purpose, however, was to determine control power requirements as a function of these variables. The low control sensitivities shown in Fig. 34 result from the use of a constant effective control travel (6.4 in.) in combination with relatively low levels of control power (maximum value 0.7 rad/sec^2). In comparison, the Princeton and UARL data are unaffected by limitations in control power. Plotted against control sensitivity, the Grumman data are in good agreement with the pilot rating boundaries of the Princeton studies. These results indicate that to perform studies of control power, it is necessary to provide the pilot with near optimum control sensitivities and then set control power level by varying the effective travel of the control stick.

2. X-22A Ducted Propeller Aircraft

The X-22A is a dual tandem-ducted propeller V/STOL research aircraft in the 15,000-lb gross-weight class. Results of longitudinal and lateral handling qualities studies conducted by Bell (Ref. 12) are presented in Fig. 35. A fixed-base simulator with a detailed analog and digital computer simulation of the aircraft was used for these studies. Random turbulence was not simulated, but the hovering and maneuvering task was performed with a simulated 20-knot steady wind.

In Fig. 35, the pilot rating boundaries of the Bell study are compared with the optimum lines and pilot ratings obtained from the contours of Section III. The stability derivatives for the X-22A were obtained from Ref. 19. Good correlation is shown in the upper plot for the longitudinal handling qualities. For the speed stability ($M_u g = 0.5$) of the X-22A, turbulence did not have a major effect on the UARL data. In the lower plot, the predicted optimum line compares well with the Bell pilot rating boundaries. Because of large lateral speed stability ($L_v g = -1.03$), however, the UARL results indicate that the damping for satisfactory handling qualities (PR = 3.5) is twice that found in the Bell study. The importance of turbulence for aircraft with

large L_{vg} is indicated by results for a similar configuration, Case R113 of Table A-III ($L_{vg} = -1.0$, $Y_v = -0.25$, $\sigma_{ug} = 0$). For this case, the value of L_p required for satisfactory handling qualities is between -1 and -2. This agrees more closely with the Bell results.

SECTION VII

SUMMARY OF RESULTS

This section contains a summary of the results of the handling qualities study. In Part A, the effects on handling qualities of the various factors which were investigated are summarized. In Part B, the results are compared with existing or suggested handling qualities criteria (MIL-H-8501A, etc.). Finally, in Part C, suggested criteria for dynamic characteristics and minimum control response characteristics are presented.

A. Summary of Effects of Various Factors

The results pertaining to the effects of various factors on optimum control sensitivity and pilot rating are described in Section III. Comments on the rms hovering performance data and the pilot model adapted parameters are from Sections IV and V, respectively. Unless stated otherwise, all comments apply to handling qualities in the presence of a moderate level of turbulence ($\sigma_{u_g} \sim 5$ ft/sec). Results listed under "pilot model parameters" apply specifically to the precision hovering task, and do not include the effects of maneuvering.

1. Speed-Stability and Drag Parameters

(1) Optimum control sensitivity. In general, the effect of the speed-stability parameters ($M_u g$ and $L_v g$) on optimum control sensitivity was relatively small for parameter values less than about 0.4. For larger values, optimum control sensitivity tended to increase with the parameters due to gust disturbances on attitude. The effect of the drag parameters (X_u, Y_v) was relatively small, except that optimum control sensitivity was high for drag parameters near -0.3 (the largest magnitude considered) because large, rapid attitude changes were required to control the large gust-induced position disturbances.

(2) Pilot Rating (PR). PR initially deteriorated slowly with increasing $M_u g$ and $|L_v g|$, then more rapidly for values greater than 0.5 due to gust disturbances. Arresting velocities while maneuvering was somewhat difficult for X_u and Y_v near zero. Maneuvering precision improved with increased drag, but position gust disturbances were annoying for X_u and Y_v near -0.3.

(3) RMS hovering performance. Changes in $M_u g$ had no effect on rms hovering position error, σ_x. However, σ_x increased rapidly with increasing magnitudes of X_u primarily because of the large lag in hovering position response to control inputs.

(4) Pilot model parameters. Pitch-loop lead (T_{L_θ}) increased slightly with $M_u g$ while position-loop lead (T_{L_x}) remained essentially unchanged. As a result, PR was nearly constant. For magnitudes of $X_u < 0.1$, T_{L_x} was large but seemed to have no adverse effect on PR. For magnitudes of $X_u \geq 0.2$, PR was poor because large, rapid control motion was required and pilots could not supply the large position-loop lead required to suppress position disturbances. Pitch-loop lead, T_{L_θ}, was unaffected by X_u.

2. Rate Damping Stabilization

(1) Optimum control sensitivity. For the range of magnitudes of M_q and L_p useful for VTOL aircraft (greater than about 1.0), optimum control sensitivity increased nearly linearly with rate damping. This linear increase can be approximated by $\partial M\delta_e/\partial M_q = (-32.3)^{-1}$ and $\partial L\delta_a/\partial L_p = (-21.5)^{-1}$.

(2) Pilot rating (PR). PR initially improved rapidly with increasing magnitudes of M_q and L_p (up to 1.0 to 2.0) due to improved stability and decreased frequency of the open-loop dynamics. Additional damping was also beneficial at high levels of speed stability for suppressing attitude gust disturbances.

(3) RMS hovering performance. For a change in M_q from -1 to -5, there was no significant change in rms hovering performance even though there was a relatively large change in PR. RMS pitch rate decreased for more negative M_q.

(4) Pilot model parameters. For a change in M_q from -1 to -5, the improvement in PR was accompanied by a large reduction in T_{L_θ} ($T_{L_\theta} \approx -1/M_q$). Position-loop lead requirements were essentially unaffected.

3. Attitude Stabilization

(1) Optimum control sensitivity. Optimum control sensitivity increased slightly with the addition of attitude stabilization. For a change in M_θ and L_ϕ from 0 to -4, the increase in optimum control sensitivity was generally less than 10 to 15%.

(2) Pilot rating (PR). Pilot rating improved initially with increasing magnitudes of L_ϕ and M_θ due to improved stability. When M_θ and L_ϕ were used with low damping such that damped frequency, ω_d, increased with more negative M_θ and L_ϕ, PR deteriorated at values of M_θ and L_ϕ more negative than about -2 due to high frequency and low damping of the open-loop dynamics. When

used with high damping such that ω_d decreased with M_θ and L_ϕ, PR improved still further. Attitude stabilization was also beneficial because it gave the pilot a fixed relation between aircraft attitude and stick position which it was felt would be useful in IFR flight.

(3) RMS hovering performance. Like rate damping, the addition of M_θ had little effect on rms hovering position performance even though there was some improvement in PR. RMS pitch attitude and pitch rate decreased slightly when M_θ was increased in magnitude.

(4) Pilot model parameters. Attitude stabilization had little effect on pilot-model lead. For a change in M_θ from 0 to -5, both T_{L_x} and T_{L_θ} were essentially unchanged even though $1/T_{sp}$ decreased from 1.48 to 0.31 sec^{-1} (in contrast, for changes in M_q, $T_{L_\theta} \approx T_{sp}$).

4. RMS Turbulence Level

(1) Optimum control sensitivity. For combinations of small magnitudes of X_u and M_{ug} (less than about 0.1 and 0.3, respectively), rms turbulence level, σ_{ug}, had little effect on optimum control sensitivity. For large magnitudes of X_u ($|X_u| \gtrsim 0.2$) and/or large M_{ug} ($M_{ug} \gtrsim 0.5$), optimum control sensitivity increased rapidly with σ_{ug}. Similar results were found for the lateral parameters.

(2) Pilot rating (PR). For cases with large magnitude X_u and/or large M_{ug} ($|X_u| \gtrsim 0.2$ and $M_{ug} \gtrsim 0.5$), an increase in σ_{ug} was generally accompanied by a significant deterioration in PR. Increased rate damping was required to maintain satisfactory handling qualities with increasing turbulence level. However, when position-loop disturbances predominated, rate damping was ineffective in offsetting the adverse effects of turbulence.

(3) RMS hovering performance. RMS hovering position error increased rapidly with turbulence level due to increased disturbances in the position loop. For the gust-sensitive configuration investigated, the rapid deterioration in PR was accompanied by an increase in rms pitch attitude and rate and rms control stick activity.

(4) Pilot model parameters. For increasing σ_{ug} (which was accompanied by a rapid deterioration in PR), T_{L_θ} remained small while T_{L_x} decreased significantly. The pilot was unable to supply

large T_{L_x} when the position-loop disturbances increased because of the large, rapid attitude changes that would have been required.

5. Additional Factors

(1) Stick force gradient (SFG). SFG had little effect on optimum control sensitivity, but higher values of sensitivity were acceptable with SFG than without. The SFG investigated (1.5 lb/in.) was generally too high for lightly damped dynamics, indicating that there may be a need to match the control feel characteristics to the dynamics. The SFG has no effect on PR, rms hovering performance, or the pilot model parameters.

(2) Control lag (τ_c). Optimum control sensitivity remained unchanged with τ_c even though the rate of aircraft response to a unit control input decreased. The limit of acceptable lag decreased with increasing pitch disturbance level.

(3) Control backlash (b). Optimum control sensitivity was unchanged with backlash except that it increased for large backlash when the pilot adopted a rapid bang-bang control technique. Hovering and maneuvering task performance and PR deteriorated at high values of backlash.

(4) Rate stabilization system authority (M_{RA}). Limiting the authority of the rate stabilization system appeared to the pilot as a reduction in the effective pitch rate damping. With decreasing M_{RA}, optimum control sensitivity decreased and PR deteriorated, but hovering performance remained essentially unchanged. Greater authority was required for gust-sensitive configurations than for relatively insensitive configurations.

B. Comparison of Results with Existing Criteria

1. Dynamic Stability

The results presented in Section III show how various factors influence the stability augmentation requirements for satisfactory handling qualities. These results from the hovering and low-speed maneuvering experiments, for rate-stabilized systems, are compared in Fig. 36 with the dynamic stability criteria of MIL-H-8501A for helicopters (Ref. 24). This complex-plane type plot shows damped frequency ($j\omega_d$) versus the damping parameter $-\zeta\omega_n$. Roots of the hovering characteristic equation located in the left half-plane indicate stable aircraft dynamics (open loop), and roots in the right half-plane indicate unstable aircraft dynamics.

The UARL results are shown in Fig. 36 as two intersecting sets of lines. One set has constant values of $M_u g$, the other constant values of X_u. The short-period frequency and damping at a given combination of X_u and $M_u g$ are those that result when M_q is at the value which resulted in a pilot rating of 3.5. These values of M_q are given in Fig. 9. The dynamic stability criterion of MIL-H-8501A (Item 3.6.1.2) is shown by the shaded boundary. This criterion requires that the roots of the hovering characteristic equation be located to the left of the boundary. The open-loop dynamics must be stable, except that slightly unstable open-loop dynamics are permitted for oscillations having periods greater than 20 seconds ($\omega_d \leq 0.314$).

The flight simulator results shown in Fig. 36 do not correlate well with the criterion of MIL-H-8501A. The results indicate that there is probably no simple frequency-damping criterion that will insure satisfactory handling qualities without making the specification overly stringent for some types of configurations or inadequate for others. For example, a boundary near $-\zeta\omega_n = 0.04$ might result in large magnitude X_u, small $M_u g$ configurations having unsatisfactory handling qualities since they would not have sufficient M_q. On the other hand, a criterion with a boundary near $-\zeta\omega_n = -0.06$ would require vehicles with low magnitude X_u to have more damping than necessary for PR = 3.5. It can be concluded from these results that handling qualities criteria for V/STOL aircraft expressed in terms of frequency-domain parameters should specify more than the short-period damping ratio and frequency conditions.

Results of the studies of lateral handling qualities are presented in Fig. 37 in the format just used for the longitudinal results. The locations of the lines having constant values of $L_v g$ and Y_v are very similar to those for the corresponding values of $M_u g$ and X_u. Again, there doesn't seem to be a simple damping-frequency criterion that is adequate for these data.

The suggested criteria of Curry and Matthews (USAAML TR 65-45 -- Ref. 25) for longitudinal dynamic stability of V/STOL aircraft are presented in Fig. 38. The suggested criteria are expressed as lines labeled "target," "normal minimum acceptable," and "single failure limit line." The UARL data for combinations of X_u, $M_u g$ and M_q corresponding to minimum satisfactory handling qualities (PR = 3.5) are shown as lines of constant X_u with the direction of increasing $M_u g$ indicated. Again, the results of this study show little correlation with damping ratio and frequency and the suggested criteria of Curry and Matthews seem unsuited for these data.

2. Rate Damping Augmentation

It is not possible to make a general comparison of the required damping for satisfactory handling qualities obtained in this study with the requirements of existing criteria. This is because these criteria either do not specify damping requirements or specify them in terms of moments of inertia.

The damping requirements determined in this study are presented in Fig. 9 on plots of pitch and roll damping versus the speed-stability parameters. The suggested requirements of Curry and Matthews do not specify the minimum damping levels. Minimum damping levels are specified by MIL-H-8501A (Ref. 24) and AGARD 408 (Ref. 26) in terms of aircraft moments of inertia as:

	MIL-H-8501A		AGARD 408
	VFR	IFR	
M_q	$8(I_y)^{-0.3}$	$15(I_y)^{-0.3}$	$15(I_y)^{-0.3}$
L_p	$18(I_x)^{-0.3}$	$25(I_x)^{-0.3}$	$25(I_x)^{-0.3}$

The suggested AGARD 408 requirements for V/STOL aircraft are the same as for the IFR requirements of MIL-H-8501A.

The above criteria can be compared with the flight simulator results for the XC-142, XV-4B, HUP-1 and X-22A aircraft using the moments of inertia for these aircraft. This has been done in Figs. 30, 31, 34 and 35, respectively. For convenience, the suggested requirements from AGARD 408 and the results for PR = 3.5 from the generalized contours of Section III are listed below:

AIRCRAFT	MINIMUM M_q		MINIMUM L_p	
	AGARD	UARL	AGARD	UARL
XC-142	-0.44	-1.8	-0.65	-1.8
XV-4B	-0.90	-1.6	-2.37	-3.7
HUP-1	-0.94	-4.7	-----	----
X-22A	-0.36	-2.2	-1.01	-4.0

The UARL results show that for satisfactory handling qualities, considerably more damping is required than the minimum specified by AGARD 408. This deficiency has been found in other studies, too. For example, in a flight test simulation of the CL-84 (Ref. 14) the damping required to achieve satisfactory handling qualities was four to five times the AGARD minimum. The best agreement is shown for the XV-4B aircraft. This is because the AGARD requirements for M_q and L_p are relatively high for this aircraft due to low moments of inertia (especially in roll) and the UARL requirement for M_q is low due to the small longitudinal speed-stability parameter ($M_{u}g = 0.15$).

The MIL-H-8501A and AGARD criteria require increased damping with decreasing aircraft size (proportional to $I_y^{-0.3}$ and $I_x^{-0.3}$). Two reasons have been given as the basis for this scaling. First, with increasing aircraft size, the pilot will tend to be located further away from the center of

gravity. Therefore, the linear accelerations of the pilot due to aircraft angular accelerations increase with aircraft size. With the improved motion cues, it is believed the pilot will accept lower levels of rate damping (Ref. 27). Second, the gust sensitivity of V/STOL aircraft decreases with increasing size since, on the basis of dimensional analysis, M_ug is inversely proportional to a characteristic length of the aircraft (Ref. 28). Therefore, for classes of aircraft to which this relationship applies, lower damping will be required with increasing aircraft size (Ref. 29). The damping requirements should decrease with improved motion cues and lower gust sensitivity; however, these characteristics do not necessarily correlate with the postulated scaling law. For example, pilot position from the center of gravity is not always proportional to aircraft size, especially vertical or lateral position. Generally, the pilot sits near the roll axis regardless of aircraft size. Also, as shown by the following tabulation, there is little correlation of the parameters that determine attitude gust sensitivity (M_ug and L_vg) with aircraft size.

Aircraft	Weight	I_y	I_x	M_ug	L_vg
X-14	2,960	1,671	1,139	0	-
HUP-1	5,430	-	-	1.13	-1.03
XV-4B	12,500	11,950	2,590	0.15	-1.10
X-22A	15,000	32,300	14,553	0.50	-1.03
XC-142	37,400	126,000	191,700	0.31	-0.24

Aside from the effects of motion cues and gust sensitivity, it is possible that a pilot may desire more damping with larger aircraft because improved control may be necessary to avoid having the extremities of the aircraft strike the ground when hovering. Since this is also contrary to the assumed scaling law, it would appear that improved criteria for minimum damping are required.

3. Control Response

The suggested requirements of AGARD 408 specify minimum aircraft response to a control input in terms of the angular displacement that must be developed within 1 sec following a 1-in. control input. The required pitch angle in radians is given as

$$\theta_R = \frac{75/57.3}{\sqrt[3]{W + 1000}} \tag{11}$$

and the required roll angle as

$$\phi_R = \frac{100/57.3}{\sqrt[3]{W + 1000}} \tag{12}$$

For a control system without lags or nonlinearities, the minimum control sensitivity can then be expressed by

$$M_{\delta_e}\Big|_{min} = \frac{\left(\theta_R\Big|_{t = 1\ sec}\right) M_q^2}{e^{M_q} - M_q - 1} \tag{13}$$

and

$$L_{\delta_a}\Big|_{min} = \frac{\left(\phi_R\Big|_{t = 1\ sec}\right) L_p^2}{e^{L_p} - L_p - 1} \tag{14}$$

These criteria are compared with the predicted optimum control sensitivity lines for the XC-142, XV-4B, HUP-1 and the X-22A aircraft in Figs. 30, 31, 34 and 35, respectively. In all cases, the optimum control sensitivity lines from this study indicate higher control sensitivity than the AGARD 408 minimum lines. Since minimum acceptable control sensitivity was not investigated in this study, no general conclusions regarding the adequacy of the AGARD criteria can be drawn. However, as shown in Figs. 4 and 6, the results of this study indicate that the optimum control sensitivity is dependent primarily on the speed-stability parameters and the level of damping (especially for magnitudes of X_u and Y_v less than 0.15). Therefore, it is possible that the minimum acceptable control sensitivity in reality is also dependent primarily on the speed-stability and damping parameters. Since there seems to be no consistent correlation of speed stability with aircraft weight, it may not be realistic to base the response criteria on aircraft weight.

C. Possible Handling Qualities Criteria Based on Flight Simulator Results

1. Dynamic Stability and Minimum Damping

Results of this study have shown that the stability augmentation needed for satisfactory handling qualities is determined by requirements for suppression of disturbances due to turbulence and for obtaining some degree of dynamic stability. The relative importance of any one of the factors is dependent on the type of configuration. At least two methods or formats, based on the results of this study, can be used to summarize these stability augmentation requirements. One method is based on the stability derivatives of the aircraft and the other on open-loop dynamic features of the aircraft. While both methods may provide adequate handling qualities criteria, they are not in a form that can be easily applied to flight test measurements. However,

these criteria are useful as a basis for formulating the time-domain criteria that are needed for a handling qualities specification.

a. Stability Derivatives

Handling qualities criteria can be expressed in terms of generalized contours of stability derivatives required for optimum control sensitivity and pilot rating, as presented in Section III. For a given configuration, applying the criteria involves the following steps:

(1) Estimate the drag (X_u, Y_v) and speed-stability ($M_u g$, $L_v g$) parameters of the aircraft.

(2) Obtain the minimum level of damping (M_q, L_p) for "normal operation" from the contours of PR = 3.5 in Figs. 5 and 8.

(3) Obtain the intercepts of the optimum control sensitivity lines with the zero-damping axis ($M\delta_o$, $L\delta_o$) from Figs. 4 and 7. The desired control sensitivity at a given level of damping can then be computed from

$$M_{\delta_e} = M_{\delta_o} - \frac{1}{32.3} M_q \tag{15}$$

$$L_{\delta_a} = L_{\delta_o} - \frac{1}{21.5} L_p \tag{16}$$

(4) If attitude stabilization (M_θ, L_ϕ) is provided, the level of rate damping stabilization must be maintained at the level given by (3) or greater.

b. Open-Loop Dynamic Features

Possible handling qualities criteria expressed in terms of open-loop dynamic features (Ref. 30) have been suggested by Systems Technology, Inc. (STI). These criteria express necessary conditions to provide pilot ratings for handling qualities in the range of $3 \leq PR \leq 4$. Several of these which are pertinent to rate-stabilized systems are:

(1) Damped frequency of oscillation, $\omega_d \leq 0.5$ rad/sec

(2) Damping ratio of oscillatory roots, $\zeta \geq 0$ (stable)

(3) Aperiodic pole location, $1/T_{sp} \geq 1.0$ sec^{-1}

The minimum rate damping required by each of these conditions is shown in Fig. 39. The shaded boundary shows the minimum level (i.e., minimum absolute value) of rate damping required by these criteria as a function of the speed-stability parameters. The levels of M_q and L_p for satisfactory handling

qualities obtained from the flight simulator experiments of this study (Fig. 9) are compared with these criteria in the upper and lower plots, respectively. Taking the least restrictive of the STI criteria, the agreement with M_q is especially good. Fairly good agreement is also shown for lateral handling qualities, although there is a noticeable difference for small values of L_{vg}. In this region, PR is relatively insensitive to L_p since PR is primarily determined by outer-loop characteristics (e.g., for $L_{vg} = 0$ and $L_p = -1$, average PR = 4.0). In general, then, these suggested criteria would seem adequate to specify the longitudinal and lateral stability augmentation requirements for rate-stabilized aircraft under moderately turbulent conditions and with X_u and Y_v near -0.1 . Modification may be required for systems having attitude stabilization since the results in Tables II and III show that satisfactory pilot ratings were obtained for values of the aperiodic pole, $1/T_{sp}$, as low as 0.2 sec^{-1} and also for values of ω_d up to 1.5 rad/sec.

2. Minimum Control Response Criteria

As mentioned previously, the results of this study are not directly applicable to criteria for minimum aircraft response to control inputs. However, since pilots will generally accept a bandwidth of control sensitivities about an "optimum" value, it might be reasonable to assume that the minimum acceptable control sensitivity would be proportional to the optimum value. On this assumption, the results of this study can be used to develop formats for possible attitude response criteria. The usefulness of the concept and the actual constants of proportionality involved would have to be determined from flight test data. The important point is that these criteria would relate the minimum attitude response of the aircraft to the gust sensitivity of the aircraft rather than the weight of the aircraft as is suggested in the AGARD 408 requirements. Two possible formats are suggested: the first is expressed in terms of the aircraft speed-stability and rate-damping derivatives, the second relates the required angular response of the aircraft to its speed-stability derivatives.

a. Speed-Stability and Rate-Damping Derivatives

One possible criterion for minimum control response would make use of empirical relations, based on the flight simulator data, to express the optimum control sensitivity in terms of the speed-stability and rate-damping derivatives. It is assumed that most VTOL aircraft will have drag parameters (X_u, Y_v) around -0.1. Then, using the data of Figs. 4 and 7, the intercepts of the optimum control sensitivity lines with the zero damping axes can be approximated by

$$M_{\delta_o} = 0.18 + 0.23\, M_{ug} \tag{17}$$

$$L_{\delta_o} = 0.15 - 0.10\, L_{vg} \tag{18}$$

Assuming that the intercept of the minimum control sensitivity line with the zero-damping axis is some fraction of the intercept of the optimum control sensitivity line, minimum control response criteria can be developed. These criteria, which use the average slopes of the longitudinal and lateral optimum control sensitivity lines from this study, could be expressed as

$$M_{\delta e}\Big|_{min} = K_e\,(0.18 + 0.23\,M_u g) - \frac{1}{32.3}\,M_q \qquad (19)$$

and

$$L_{\delta a}\Big|_{min} = K_a\,(0.15 - 0.10\,L_v g) - \frac{1}{21.5}\,L_p \qquad (20)$$

The results in Fig. 35 indicate that it is reasonable to assume that the minimum acceptable sensitivity line is parallel to the optimum sensitivity line. When sufficient damping is supplied ($|M_q| \geq 4$), Fig. 35 indicates that a satisfactory pilot rating is dependent on control sensitivity. For example, the PR = 3.5 boundary line indicates that reducing M_{δ_e} below a certain value results in an unsatisfactory rating for sufficient levels of M_q. Examination of the 3.5 boundary for low sensitivities shows that this boundary is approximately parallel to the optimum sensitivity line. Thus the variation in the minimum sensitivity line with M_q for a satisfactory pilot rating can be approximated as a line parallel to that for optimum sensitivity. Equations (19) and (20) describe minimum control sensitivity lines that are parallel to the optimum control sensitivity lines determined in this study. With minimum control sensitivity lines of this form drawn tangent to the PR = 3.5 boundaries of the Bell data for the X-22A (Fig. 35), K_e and K_a would both have values of about 0.50. Whether or not these values would be applicable to a wide range of aircraft parameters must be determined in flight tests.

b. Angular Response

An alternate criterion for minimum control response would specify, in terms of the gust sensitivity of the aircraft, the minimum change in attitude of the aircraft within one second after a one-inch control input. These criteria would be similar to the AGARD 408 criteria discussed earlier, except the minimum pitch and roll angle responses would be expressed in terms of the speed-stability parameters rather than the weight of the aircraft.

Using Eqs. (13) and (14) for the minimum control sensitivity in terms of the required angular responses, θ_R and ϕ_R, the minimum control sensitivities for zero pitch and roll rate damping are

$$M_{\delta e}\Big|_{min} = 2\theta_R \qquad (M_q = 0) \qquad (21)$$

and

$$L_{\delta_a}\Big|_{min} = 2\phi_R \quad (L_p = 0) \tag{22}$$

These are the intercepts of the AGARD-type minimum control sensitivity lines (Fig. 35) with the zero-damping axes. Again, assuming that the intercepts of the minimum control sensitivity lines are some fraction of the intercepts of the optimum lines, and combining Eqs. (21) and (22) with Eqs. (17) and (18), the required angles can be expressed as

$$\theta_R = 0.5\, K_e'(0.18 + 0.23\, M_u g) \tag{23}$$

and

$$\phi_R = 0.5\, K_a'(0.15 + 0.23\, L_v g) \tag{24}$$

where K_e' and K_a' are the ratios of the intercepts of the minimum control sensitivity lines (given by Eqs. (13) and (14)) with the zero-damping axes to the intercepts of the optimum control sensitivity lines. As an example, fitting these lines tangent to the PR = 3.5 boundaries of the Bell X-22A data (Fig. 35) would result in $K_e' \approx 0.25$ and $K_a' \approx 0.35$. Again, whether or not these values would be applicable to a wide range of aircraft parameters would have to be determined in flight tests.

The advantage of this second form of response criteria over the first is that the aircraft angular response is specified. Therefore, whether or not a particular aircraft complies with the criteria could be determined from flight test measurements. It would seem better than the AGARD requirements because it relates minimum control response to the aircraft gust sensitivity rather than weight. The disadvantages, however, are that the speed-stability parameters must be computed for the aircraft and that, as noted in Paragraph III.E.2, control system nonlinearities can make the response to a one-inch stick deflection less meaningful.

SECTION VIII

CONCLUSIONS AND RECOMMENDATIONS

A. Results and Conclusions

(1) For a hovering and low-speed maneuvering task, rate damping augmentation must increase with speed stability to provide necessary aircraft control characteristics and to suppress gust disturbances. Rate damping is effective in offsetting position disturbances only insofar as it improves attitude control.

(2) Attitude stabilization is somewhat ineffective in suppressing short-period gust disturbances, but is beneficial in that it provides open-loop stability. It should be used with a level of damping that is high enough so that, with increasing attitude stability, the oscillatory damped frequency decreases.

(3) For configurations having low gust sensitivity, optimum control sensitivity is determined by attitude response requirements for maneuvering. Optimum control sensitivity increases rapidly with turbulence level for configurations having high gust sensitivity. With a high stick force gradient, higher control sensitivities are more acceptable than for a stick with light control forces, but the higher sensitivities are not necessary.

(4) Hovering performance is directly related to the level of position-loop disturbances. However, performance may be unaffected by changes in attitude-loop dynamics and disturbance level that are large enough to cause significant changes in pilot opinion of handling qualities.

(5) The results of this study do not agree well with criteria that specify minimum damping for VTOL aircraft in terms of moments of inertia, primarily because speed stability does not correlate with aircraft size for representative aircraft.

(6) Criteria expressed solely in terms of the damping ratio and frequency of the oscillatory portion of VTOL hover dynamics are not adequate to specify stability augmentation requirements for a wide range of VTOL configurations. The data of this study indicate that additional restrictions must be placed on the magnitude of the first-order pole of the open-loop dynamics and other factors.

(7) Closed-loop pilot-model analyses of rms hovering data show that pilot rating is dependent on both the requirements for pilot lead and the effective disturbance level that must be controlled.

B. Recommendations

To obtain fundamental information needed in the development of handling qualities specifications for VTOL aircraft, it is recommended that research be conducted in the following areas:

(1) Development of practical specifications for aircraft dynamic characteristics and minimum attitude response to control inputs. These specifications should be in such a form that aircraft compliance with the specifications can be established conveniently from flight tests. It would seem that the information relative to VTOL handling qualities contained in this report would be pertinent to this effort.

(2) The evaluation of minimum acceptable levels of control power for basic hovering and low-speed maneuvering tasks in the presence of turbulence. These studies need to be conducted for conditions in which near-optimum control sensitivities are provided the pilot.

(3) Pilot control techniques and necessary aircraft stability limits following failure of the stability augmentation system. This research should be performed with ground simulators that produce accurate motion cues or with in-flight simulators. This information is important to any attempt at specifying the redundancy required in stability augmentation systems.

(4) Determination of acceptable limits for control lags and nonlinearities and the effect of stability augmentation on such limits. These control problems can be especially acute for large aircraft because of their long, complicated control linkages and power-boost controls.

REFERENCES

1. Seckel, E., J. J. Traybar, and G. E. Miller: Longitudinal Handling Qualities for Hovering. Princeton University Report No. 594, December 1961.

2. McGregor, D. M.: The Influence of Aircraft Size on Control Power and Control Sensitivity Requirements. A Comparison of Results from Two Variable Stability Helicopters. NRC-NAE Aero. Report LR-459, July 1966.

3. Garren, J. F., Jr., J. R. Kelly, and J. P. Reeder: A Visual Flight Investigation of Hovering and Low-Speed VTOL Control Requirements. NASA Technical Note D-2788, May 1965.

4. Rolls, L. S. and F. J. Drinkwater, III: A Flight Determination of Attitude Control Power and Damping Requirements for a Visual Hovering Task in the Variable Stability and Control X-14A Research Vehicle. NASA TN D-1328, May 1962.

5. Stapleford, R. L., et al: An Analytical Study of V/STOL Handling Qualities in Hover and Transition. AFFDL-TR-65-73, October 1965.

6. Vinje, E. W. and D. P. Miller: "Interpretation of Pilot Opinion by Application of Multiloop Models to a VTOL Flight Simulator Task." USC-NASA Conference on Manual Control, Los Angeles, March 1967.

7. Miller, D. P. and J. W. Clark: "Research on VTOL Aircraft Handling Qualities Criteria." Journal of Aircraft, Vol. 2, No. 3, May 1965.

8. Miller, D. P. and E. W. Vinje: Flight Simulator Studies of Some Factors Which Influence VTOL Handling Qualities. United Aircraft Research Laboratories Report E-110129-1, October 1966.

9. Clark, J. W., D. P. Miller, and R. A. Gallant: Investigation of Control and Stability Augmentation Requirements for Tandem Tilting Ducted Propeller VTOL Transports. United Aircraft Research Laboratories Report R-1624-5, July 1963 (prepared under Bureau of Naval Weapons Contract NOw 61-0848-d).

10. Clark, J. W. and D. P. Miller: "Research on Factors Influencing Handling Qualities for Precision Hovering and Gun Platform Tasks." Proceedings of the Twenty-First Annual National Forum of the American Helicopter Society, May 1965.

11. Wolkovitch, J. and R. P. Walton: VTOL and Helicopter Approximate Transfer Functions and Closed-Loop Handling Qualities. Systems Technology, Inc. TR No. 128-1, June 1965.

REFERENCES (Cont'd.)

12. Gaul, J. W.: Application of Pilot-Controller Integration Techniques to a Representative V/STOL Aircraft. AFFDL-TR-65-200, October 1965.

13. Tapscott, R. J. and S. Salmirs: The Effects of Various Combinations of Damping and Control Power on Helicopter Handling Qualities During Both Instrument and Visual Flight. NASA TN D-58, October 1959.

14. McGregor, D. M.: Simulation of the Canadair CL-84 Tilt-Wing Aircraft Using an Airborne V/STOL Simulator. NRC-NAE Aero. Report LR-435, July 1965.

15. Friedman, G. R.: Helicopter Control: A Multi-Loop Manual Control System. MIT, Man-Vehicle Control Laboratory, Report No. MVT-67-2, June 1967.

16. McRuer, D. T., D. Graham, E. S. Krendell, and W. Reisener: Human Pilot Dynamics in Compensatory Systems. AFFDL-TR-65-16, July 1965.

17. Lollar, T. E. and J. Matous: "Observed Pilot-Vehicle Loop-Closure Characteristics for Hovering Aircraft Control." IEEE Transactions, Vol. HFE-4, No. 1, September 1963.

18. Elkind, J. I.: Characteristics of Simple Manual Control Systems. MIT, Lincoln Laboratory, TR-11, April 1956.

19. Walton, R. P.: Transfer Function Description of XC-142 and X-22A VTOL Configurations in Transition Flight. Systems Technology, Inc. TM No. 135-I-1, April 1964.

20. Shields, M. E.: Estimated Flying Qualities XC-142A V/STOL Assault Transport. Ling-Temco-Vought, Vought Aeronautics Division Report No. 2-53310/4R939, May 1964.

21. Shepard, T. W.: "The XC-142A Flight Test Program." Proceedings of the First National V/STOL Aircraft Symposium, Wright-Patterson AFB, November 1965.

22. Anon.: XV-4B Control Equations. North American Aviation, Inc., 1967.

23. Bruel, H. T.: A Simulator Study of Low-Speed VTOL Handling Qualities in Turbulence. Grumman Aircraft Engineering Corp. RE238, NOw 65-0518, February 1966.

24. Anon.: Military Specification - General Requirements for Helicopter Flying and Ground Handling Qualities. MIL-H-8501A, September 7, 1961.

REFERENCES (Cont'd.)

25. Curry, P. R. and J. T. Matthews, Jr.: Suggested Requirements for V/STOL Flying Qualities. U. S. Army Aviation Material Laboratories Technical Report 65-45, June 1965.

26. Anon.: Recommendations for V/STOL Handling Qualities. AGARD Report No. 408, October 1962.

27. Anon.: Comments on AGARD Report 408 by the V/STOL Handling Qualities Technical Assistance Panel, N64-18505, January 1964.

28. Anderson, S. B.: "Considerations for Revision of V/STOL Handling Qualities Criteria." Proceedings of NASA Conference on V/STOL and STOL Aircraft, NASA SP-116, April 1966.

29. Johnston, J., I. H. Culver, and C. F. Friend: Study of Size Effects on VTOL Handling Qualities Criteria. USAAML TR 65-24, September 1965.

30. Craig, S. J. and W. P. Walton: Analysis of VTOL Handling Qualities Requirements, Longitudinal Hovering and Transition and Lateral Approach. Systems Technology Inc., TR No. 171-1, October 1967 and to be published as AFFDL-TR-67-179.

31. Stapleford, R. L.: Multiloop Data Reduction. Systems Technology, Inc. Working Paper No. 128-1, October 1966.

32. Newton, G. C., Jr., L. G. Gould and J. F. Kaiser: Analytical Design of Linear Feedback Controls. John Wiley and Sons, Inc., New York, 1957.

Figure 1. Photograph of Interior of V/STOL Aircraft Flight Simulator

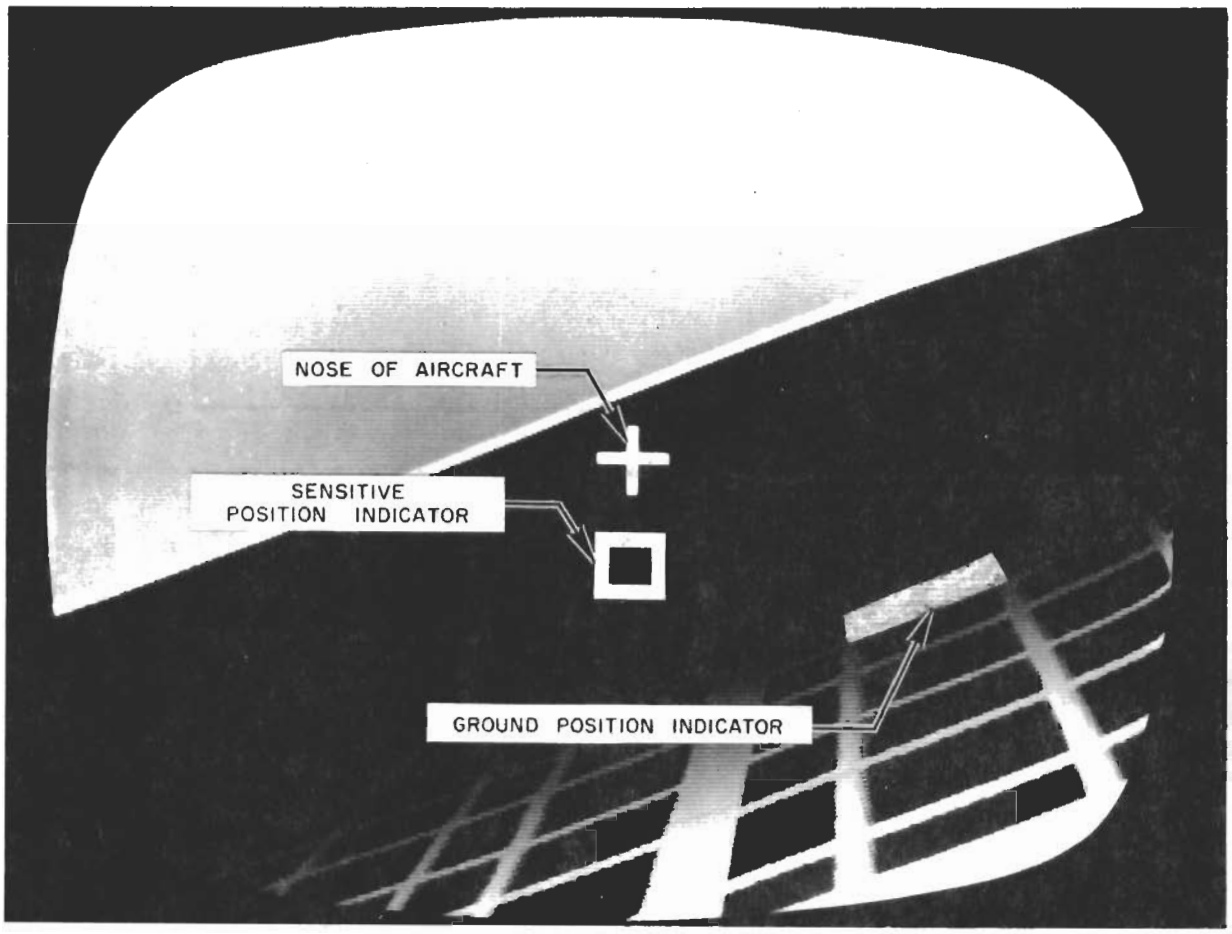

Figure 2. Contact Analog Display for Hovering and Low-Speed Maneuvering Task

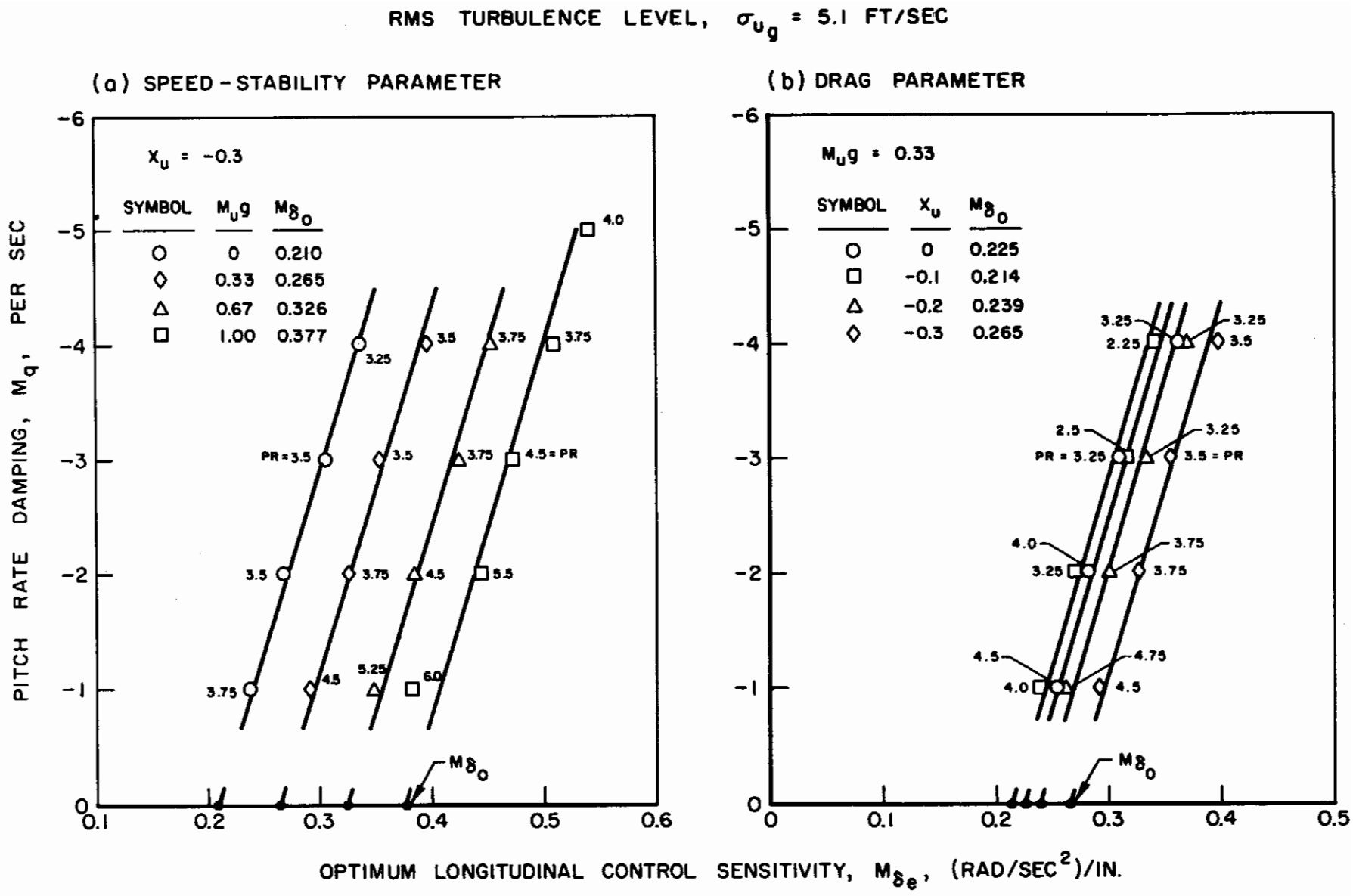

Figure 3. Effect of the Longitudinal Speed-Stability and Drag Parameters on Handling Qualities

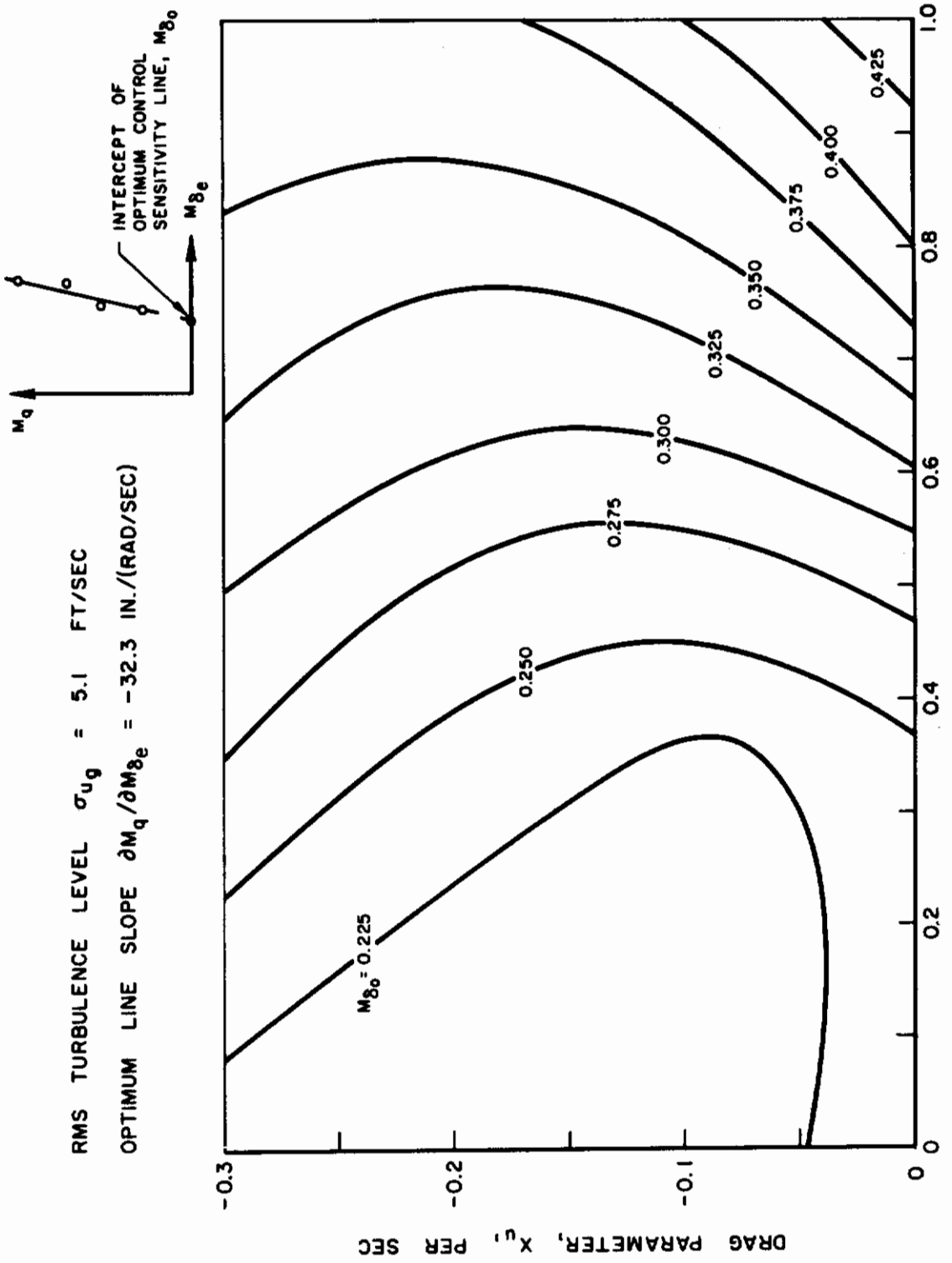

Figure 4. Contours of Intercept of the Optimum Longitudinal Control Sensitivity Line with the Zero-Damping Axis

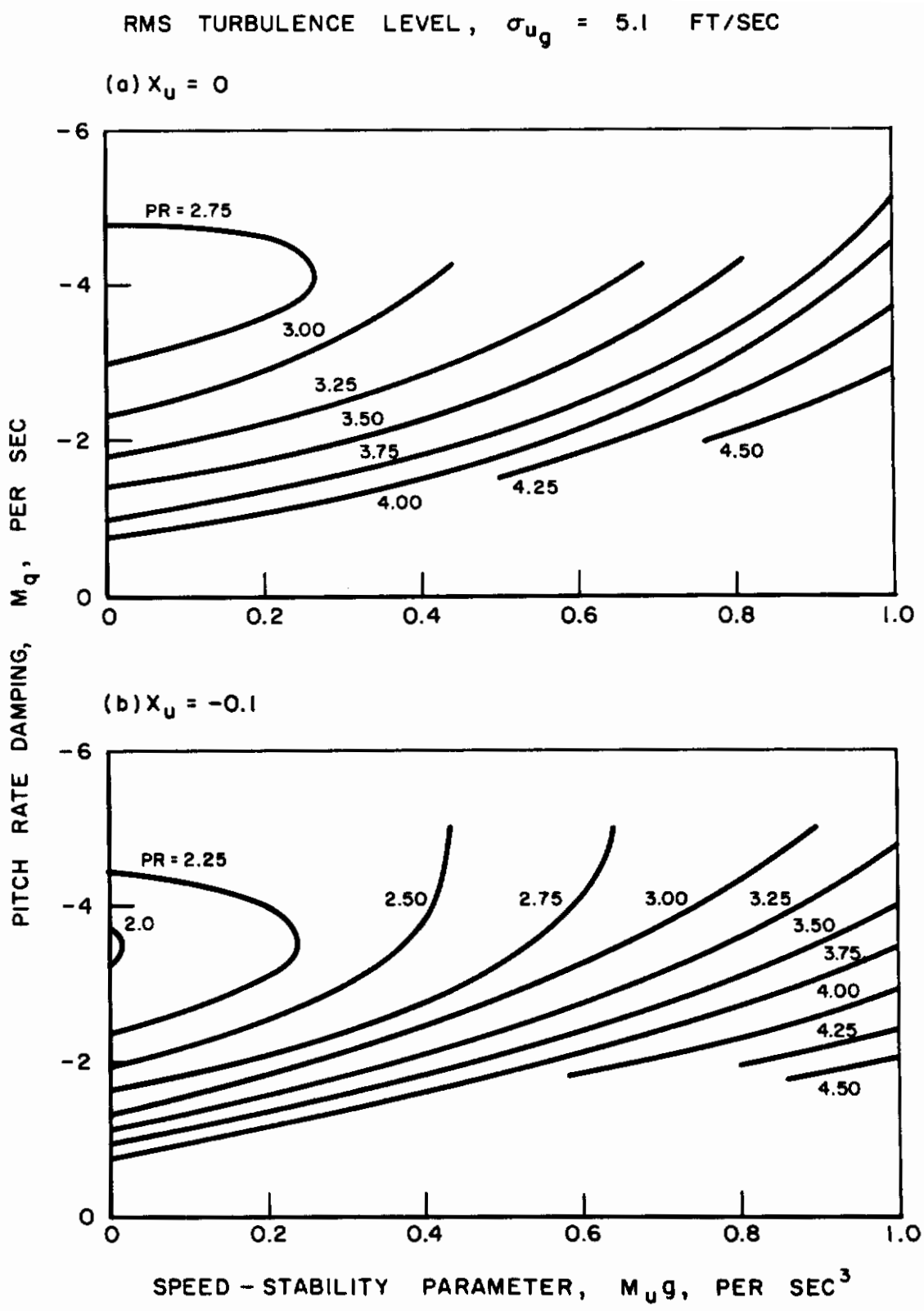

Figure 5. Contours of Average Pilot Ratings for Longitudinal Handling Qualities

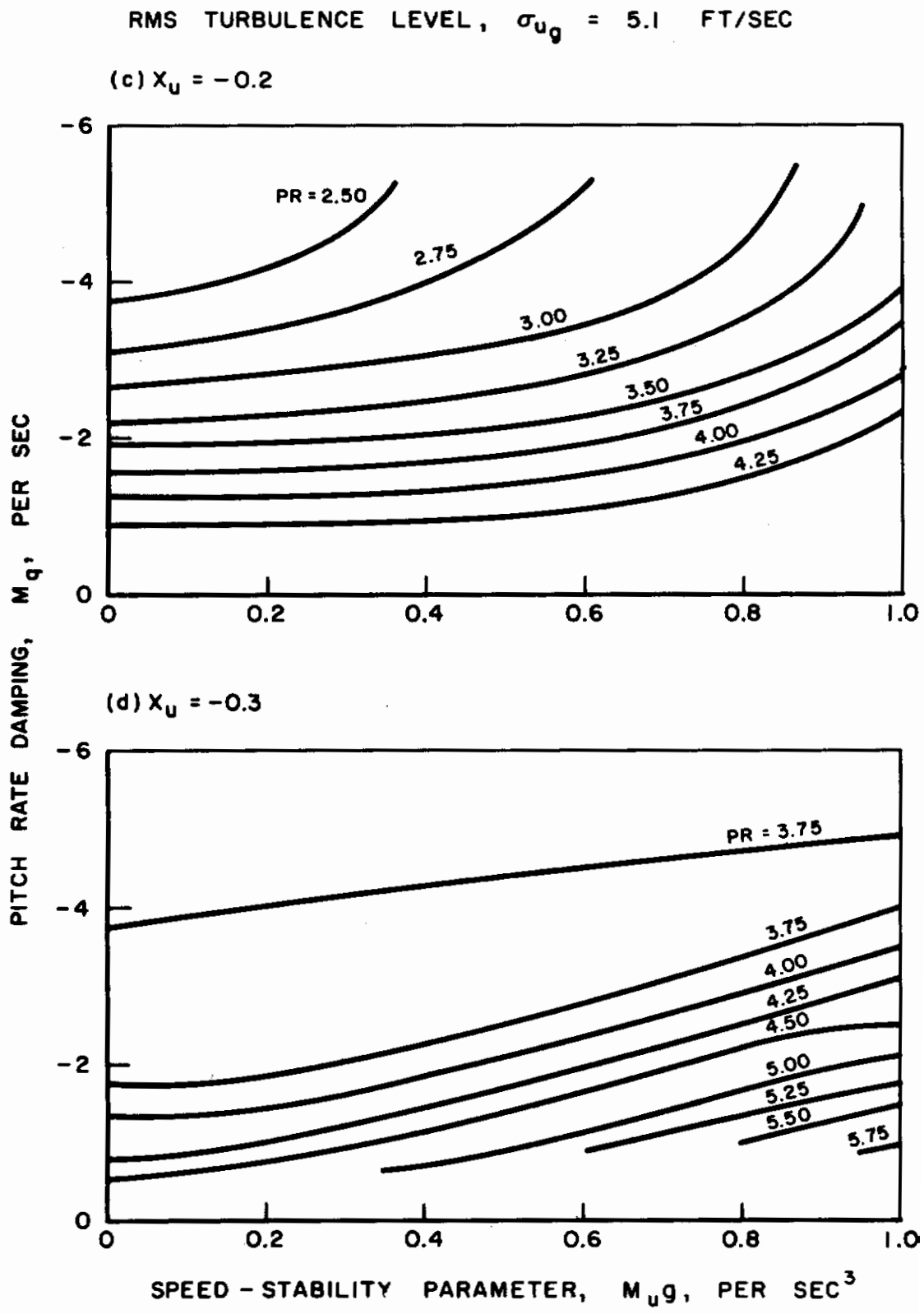

Figure 5. (Concluded)

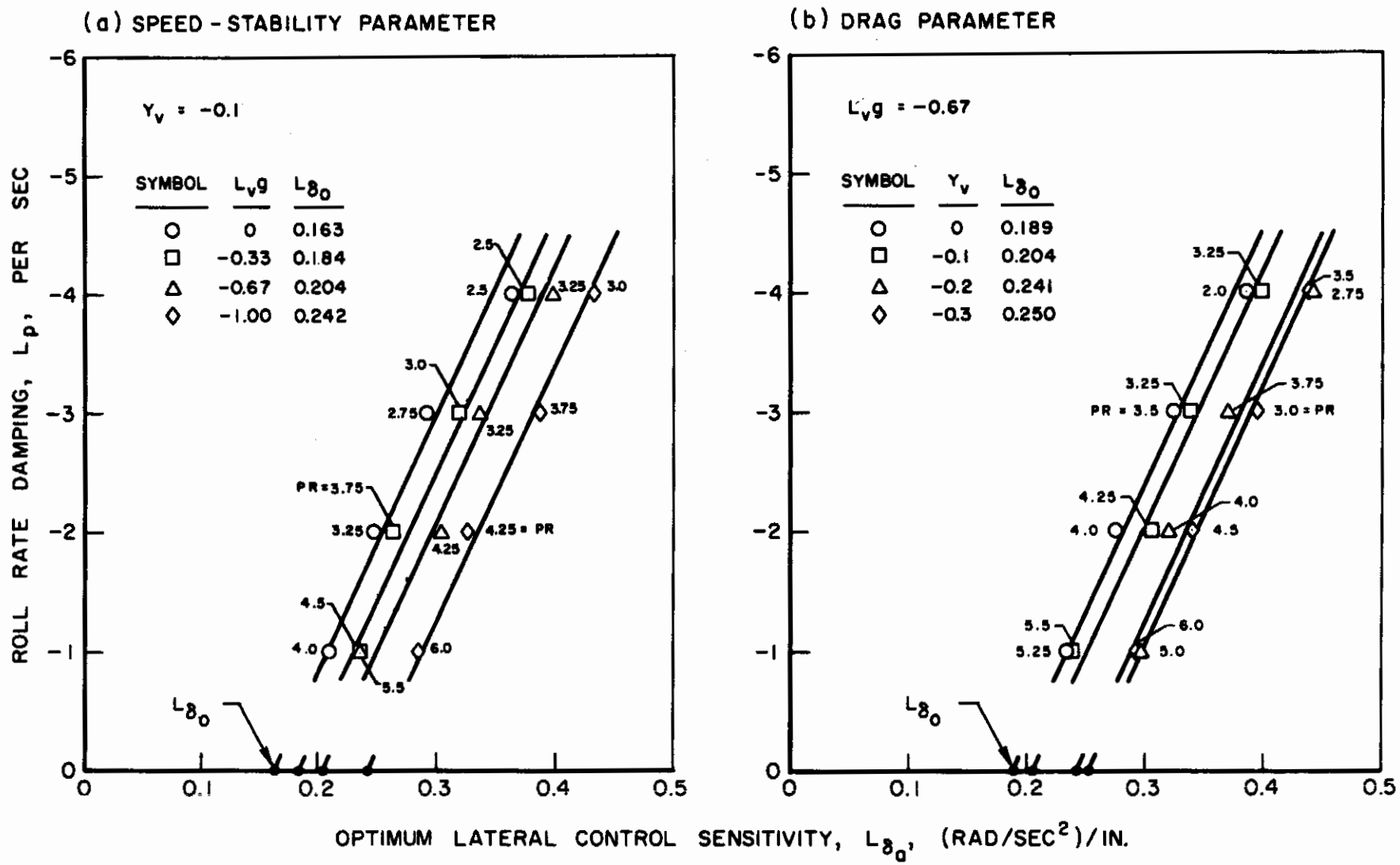

Figure 6. Effect of the Lateral Speed-Stability and Drag Parameters on Handling Qualities

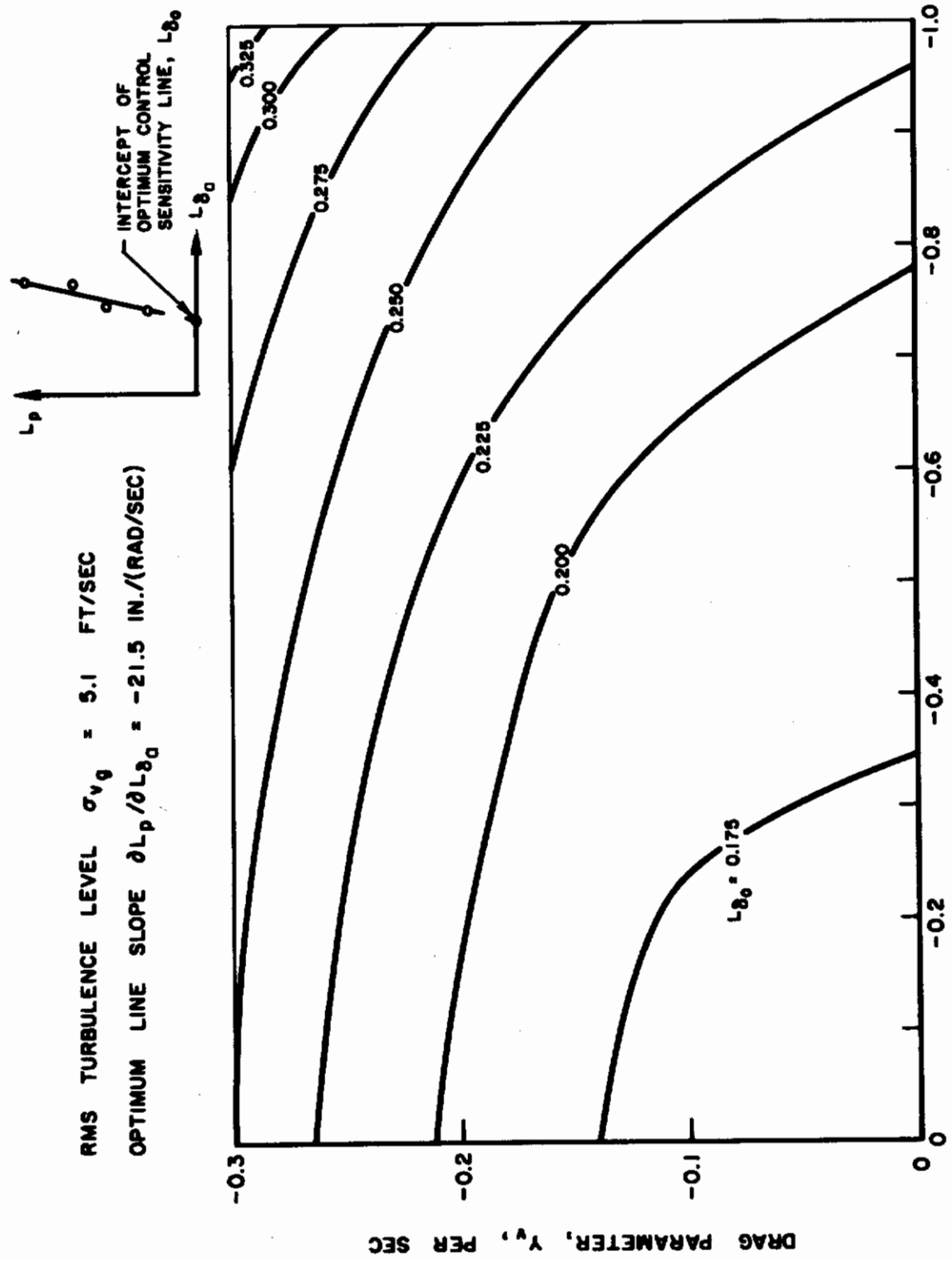

Figure 7. Contours of Intercept of the Lateral Optimum Control Sensitivity Lines with the Zero-Damping Axis

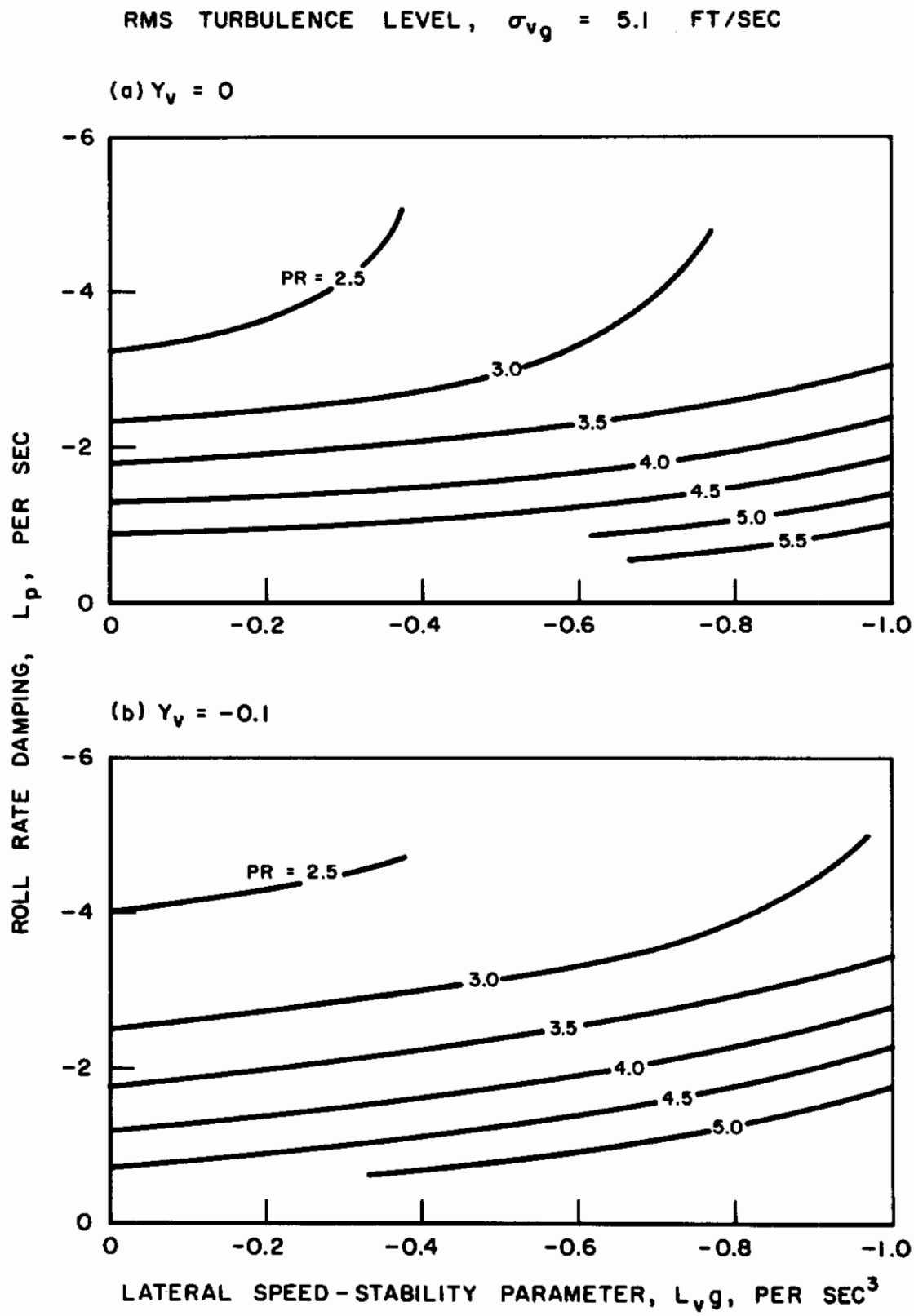

Figure 8. Contours of Average Pilot Ratings for Lateral Handling Qualities

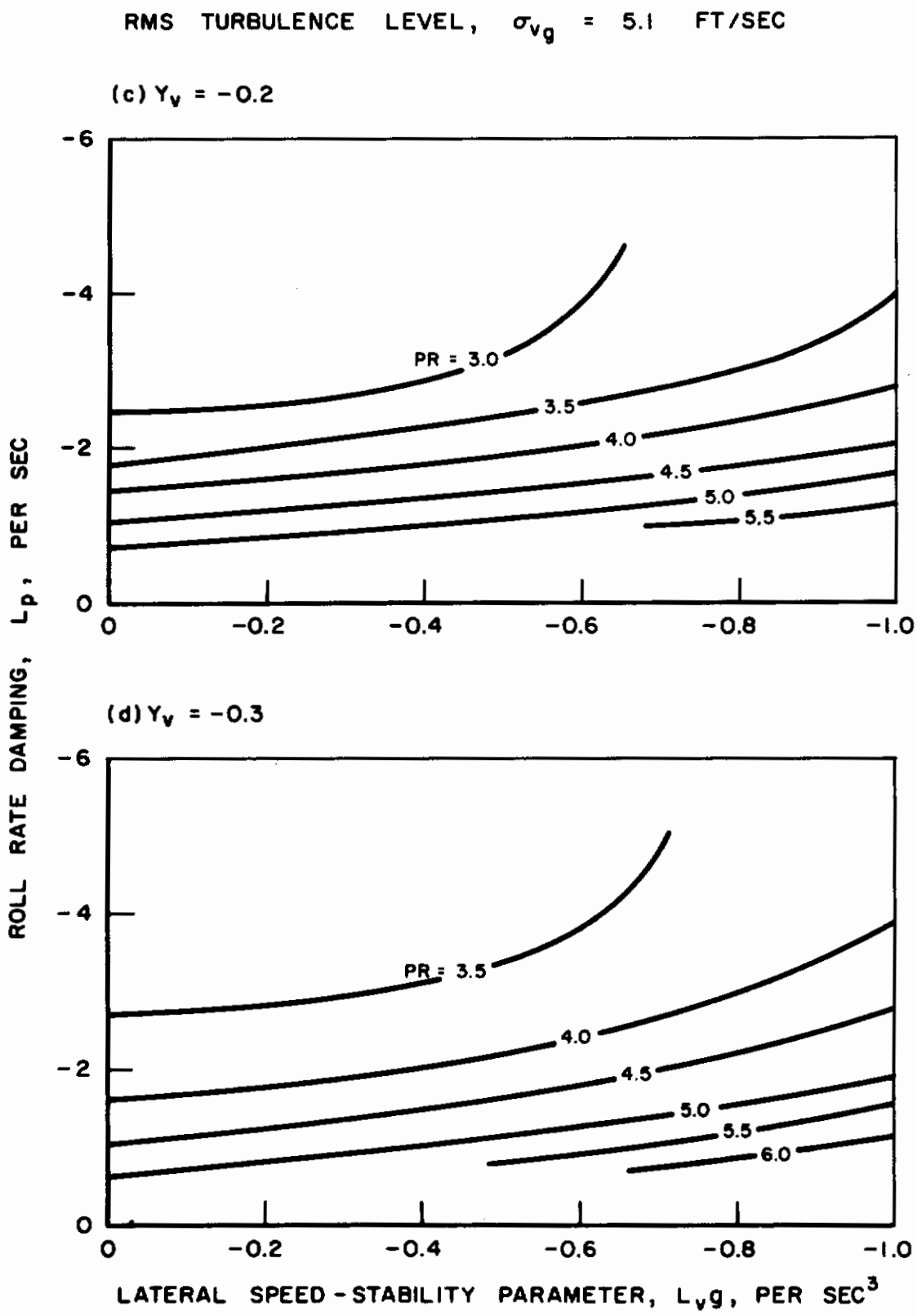

Figure 8. (Concluded)

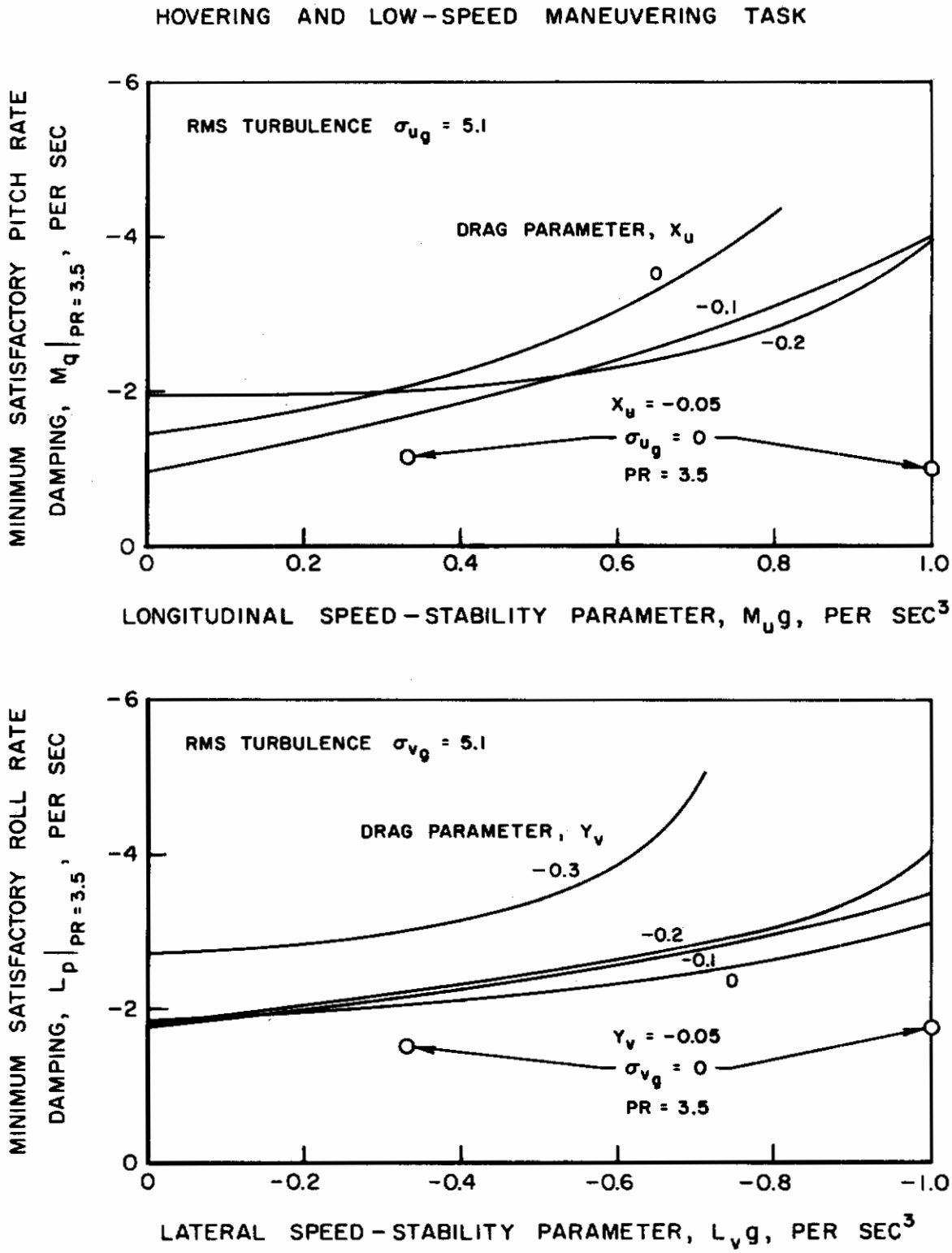

Figure 9. Rate Damping Required for Satisfactory Handling Qualities

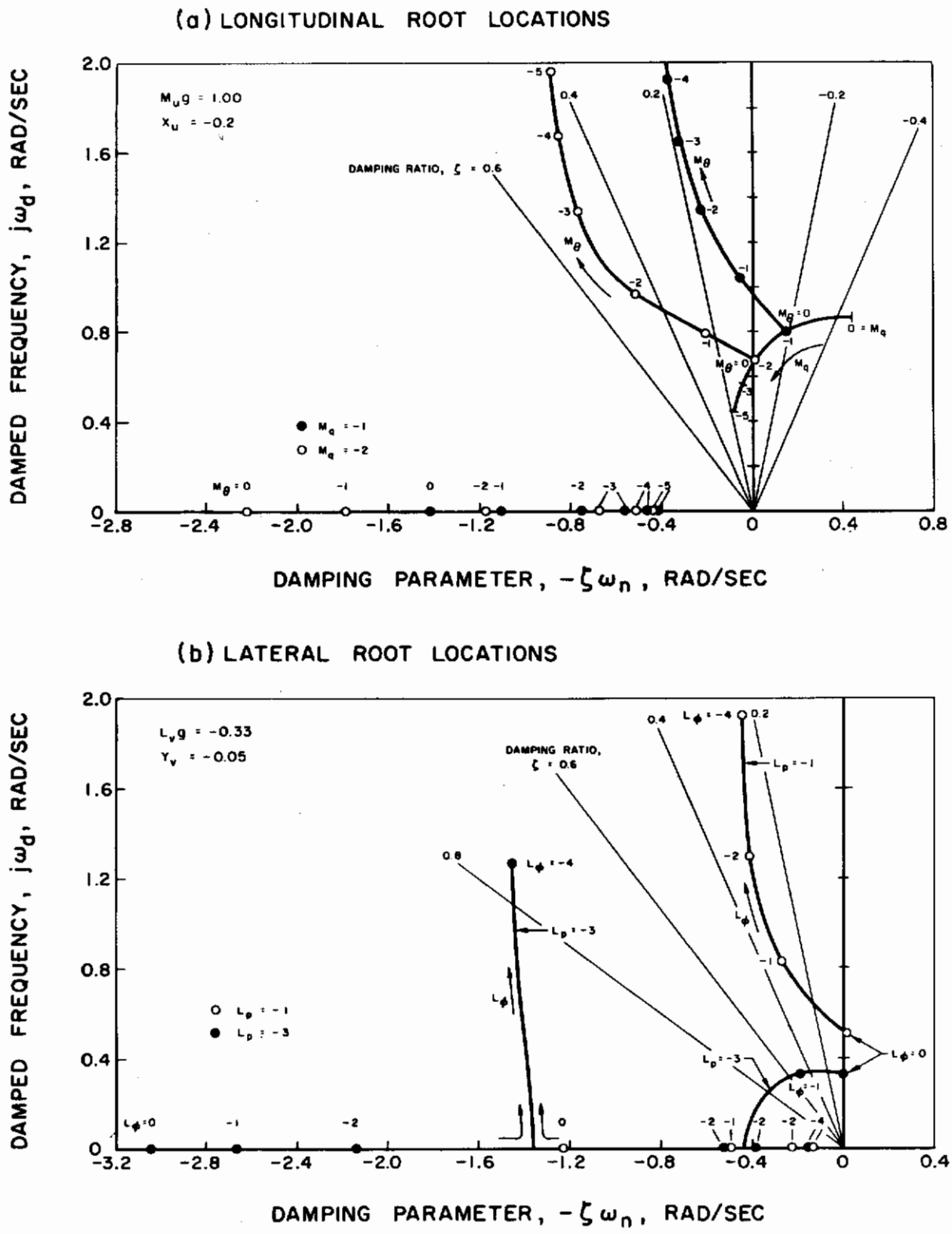

Figure 10. Effect of Attitude Stabilization on Roots of Hovering Characteristic Equation

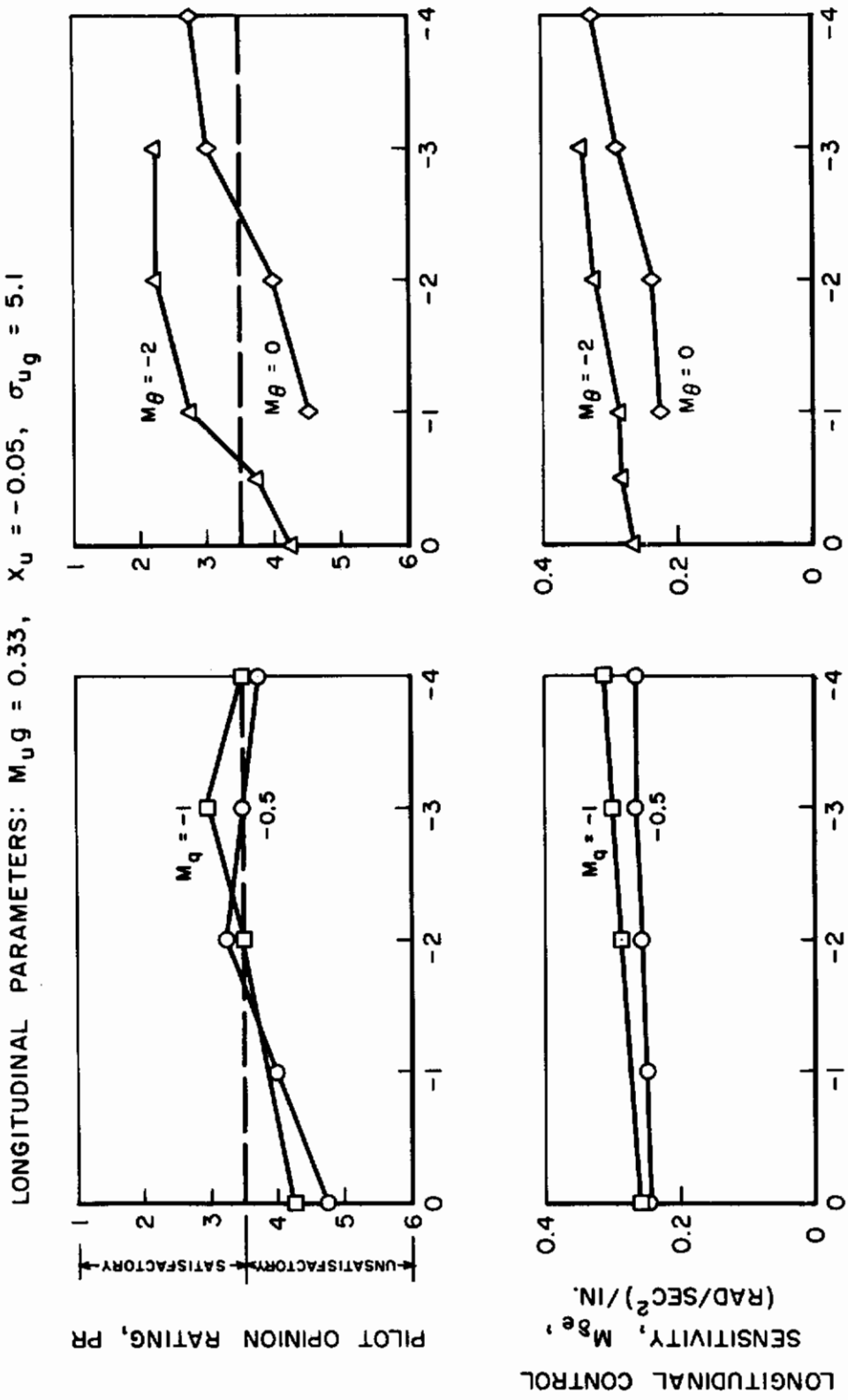

Figure 11. Effect of Pitch Attitude Stabilization and Pitch Rate Damping on Pilot Rating and Optimum Control Sensitivity

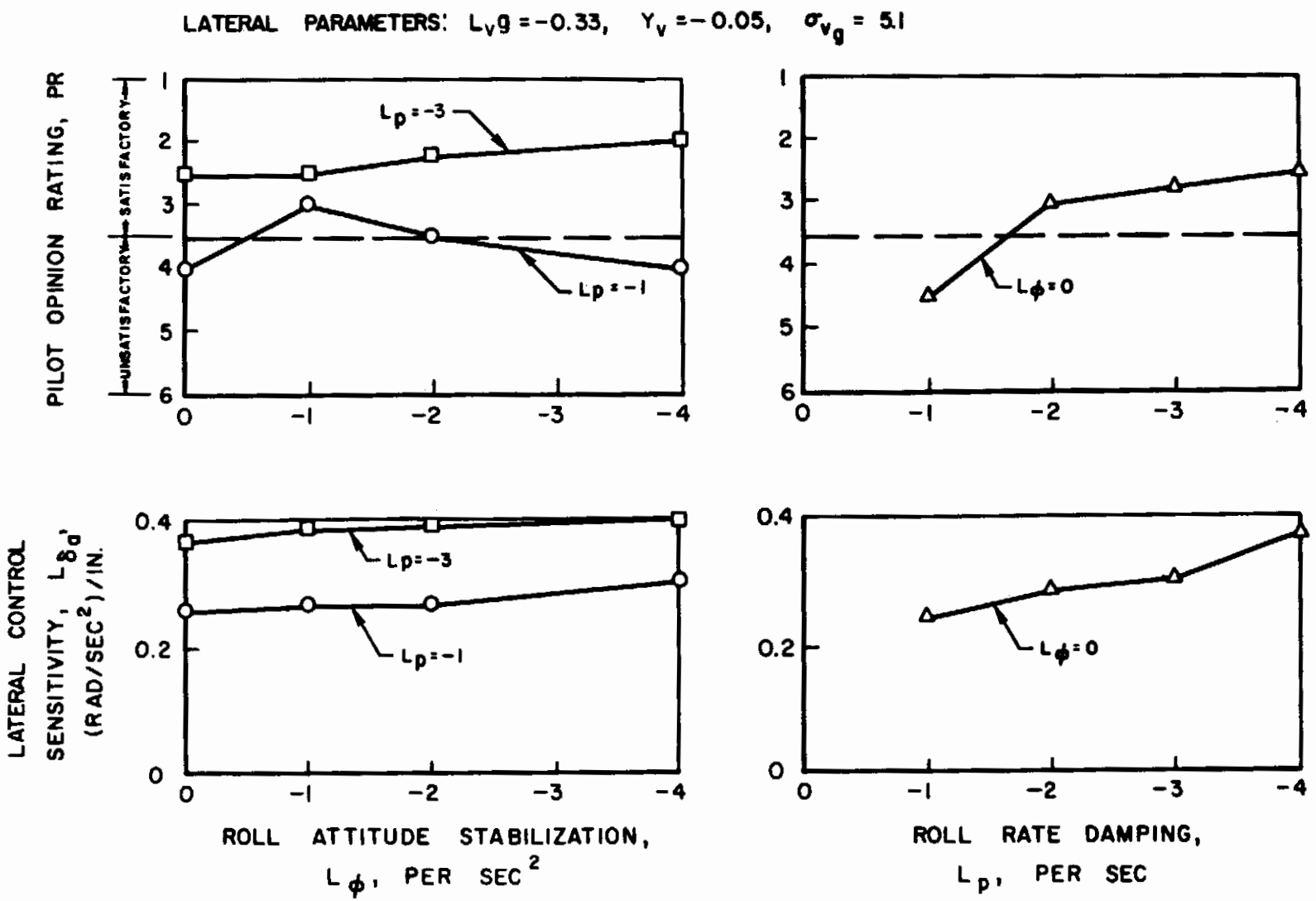

Figure 12. Effect of Roll Attitude Stabilization and Roll Rate Damping on Pilot Rating and Optimum Control Sensitivity

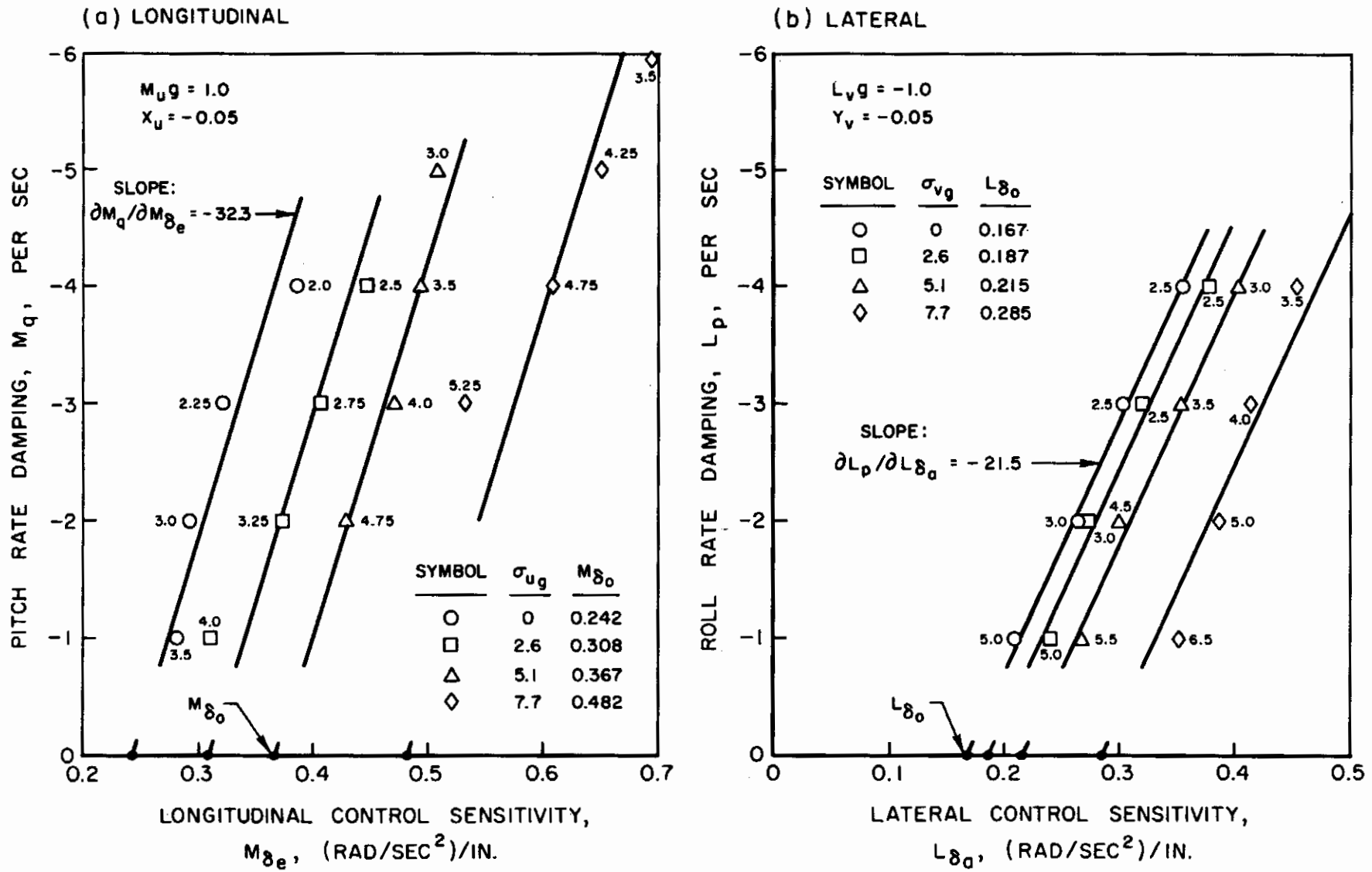

Figure 13. Effect of RMS Turbulence Level on Longitudinal and Lateral Handling Qualities

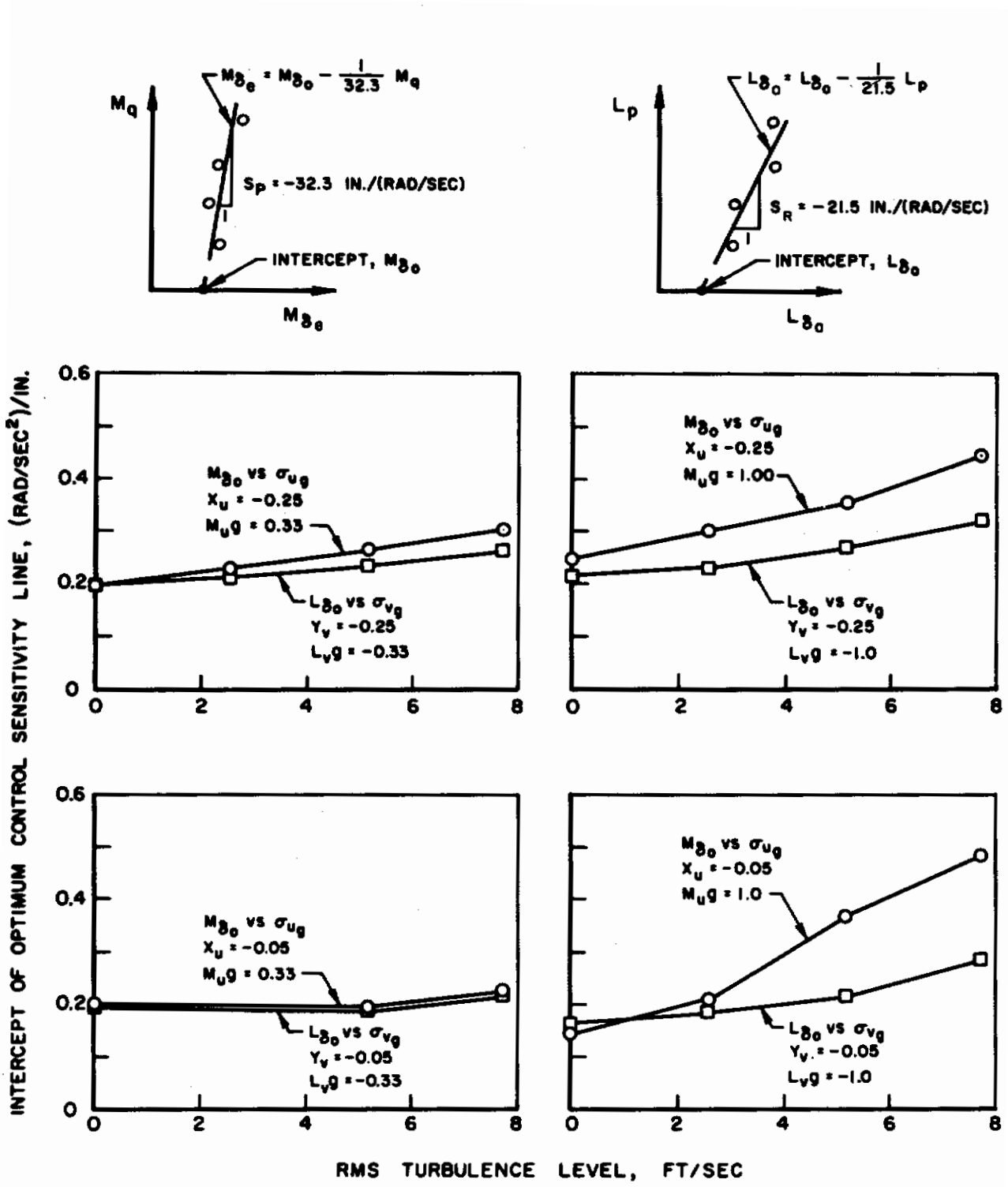

Figure 14. Effect of RMS Turbulence Level on Longitudinal and Lateral Optimum Control Sensitivity

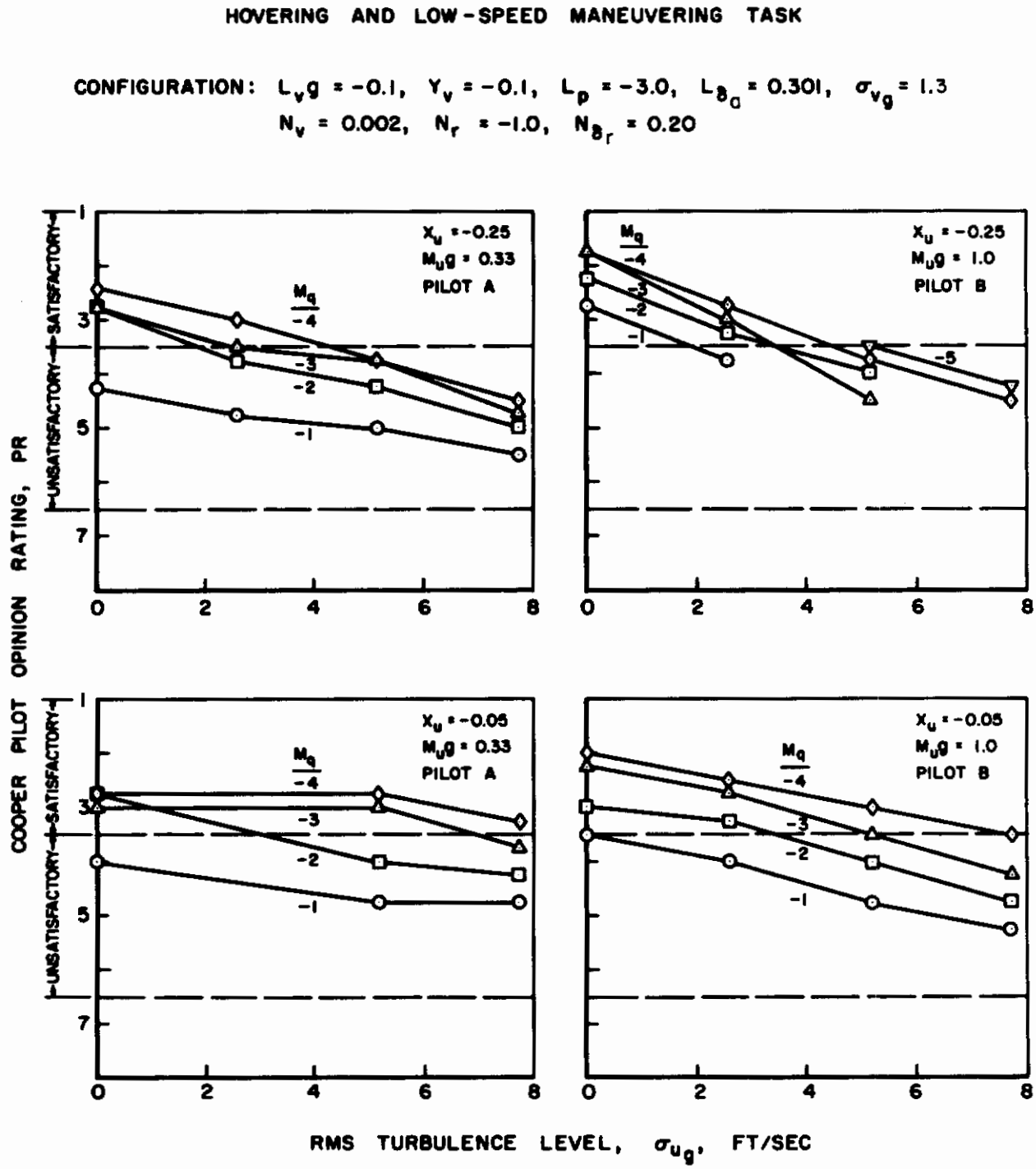

Figure 15. Effect of RMS Turbulence Level on Pilot Opinion Rating of Longitudinal Handling Qualities

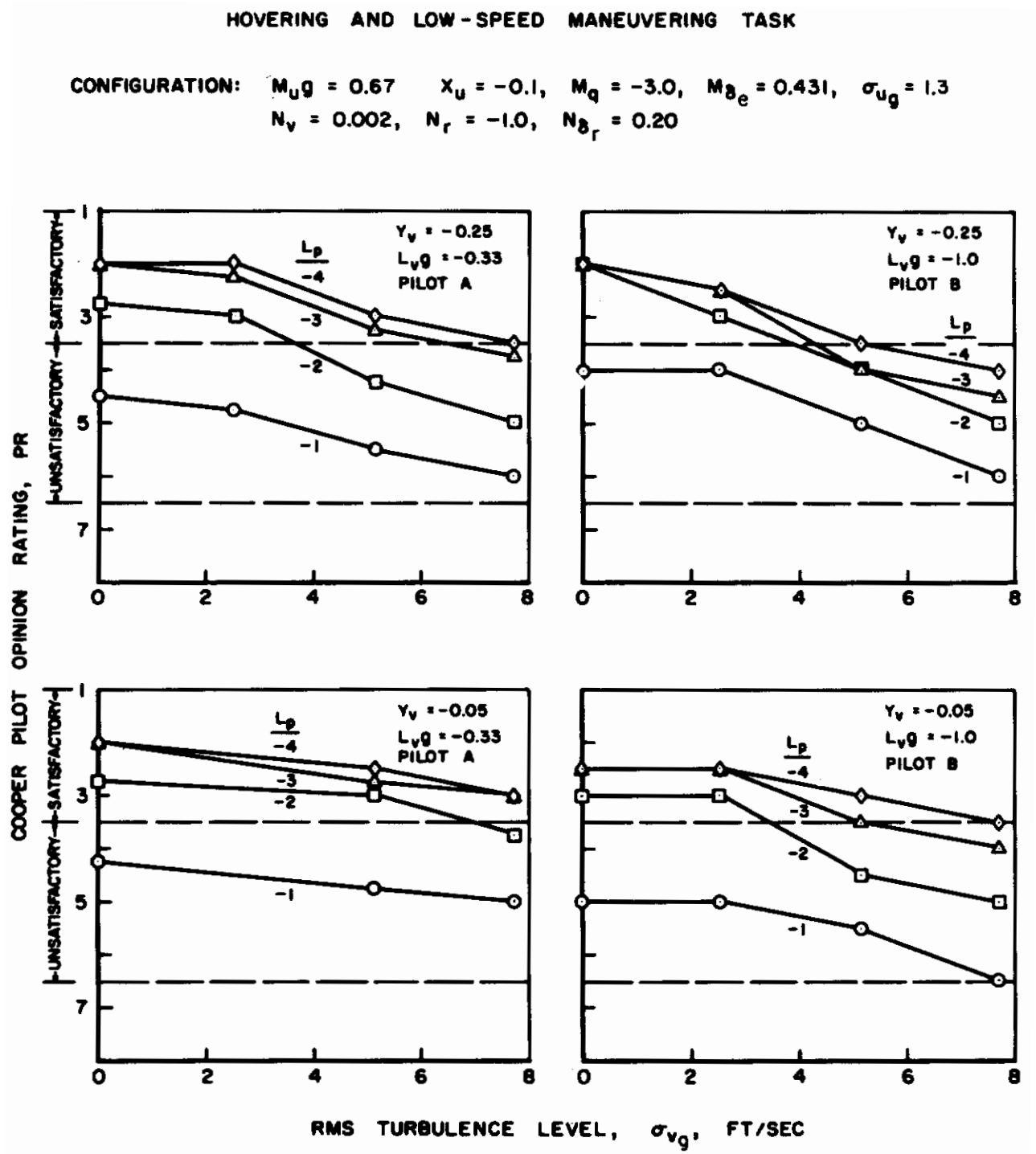

Figure 16. Effect of RMS Turbulence Level on Pilot Opinion Rating of Lateral Handling Qualities

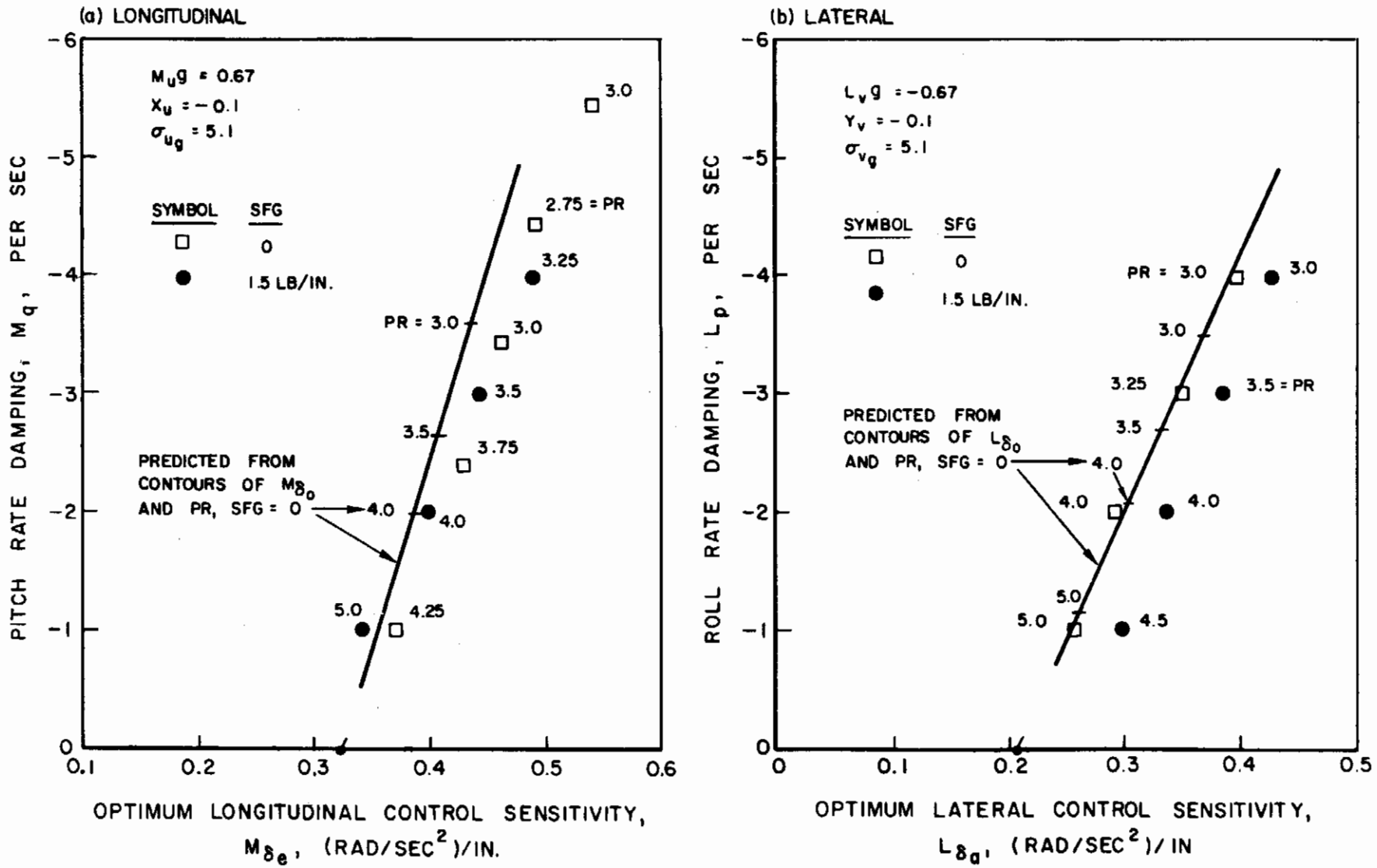

Figure 17. Effect of Stick Force Gradient on Handling Qualities

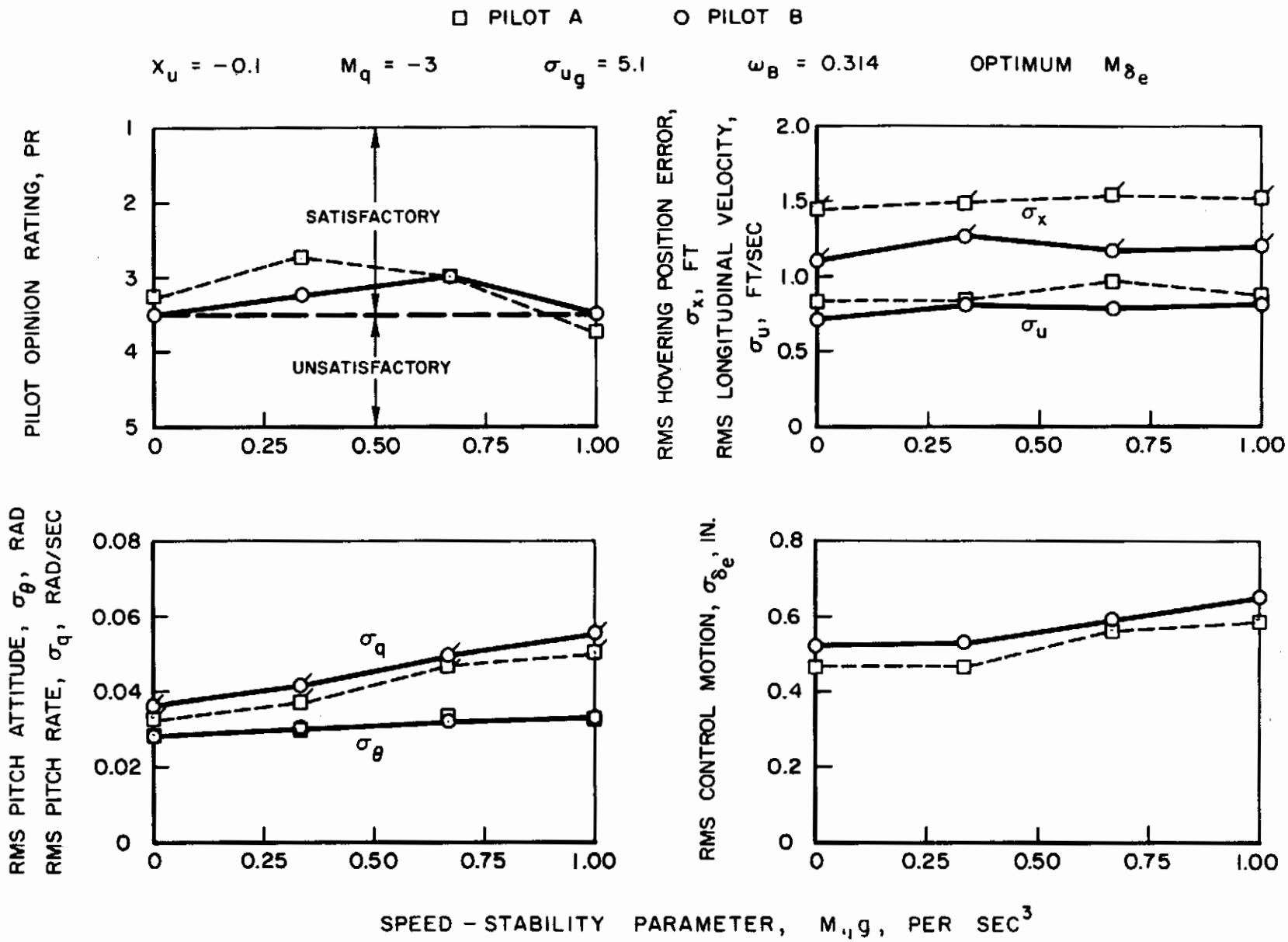

Figure 18. Effect of Longitudinal Speed-Stability Parameter on RMS Hovering Performance

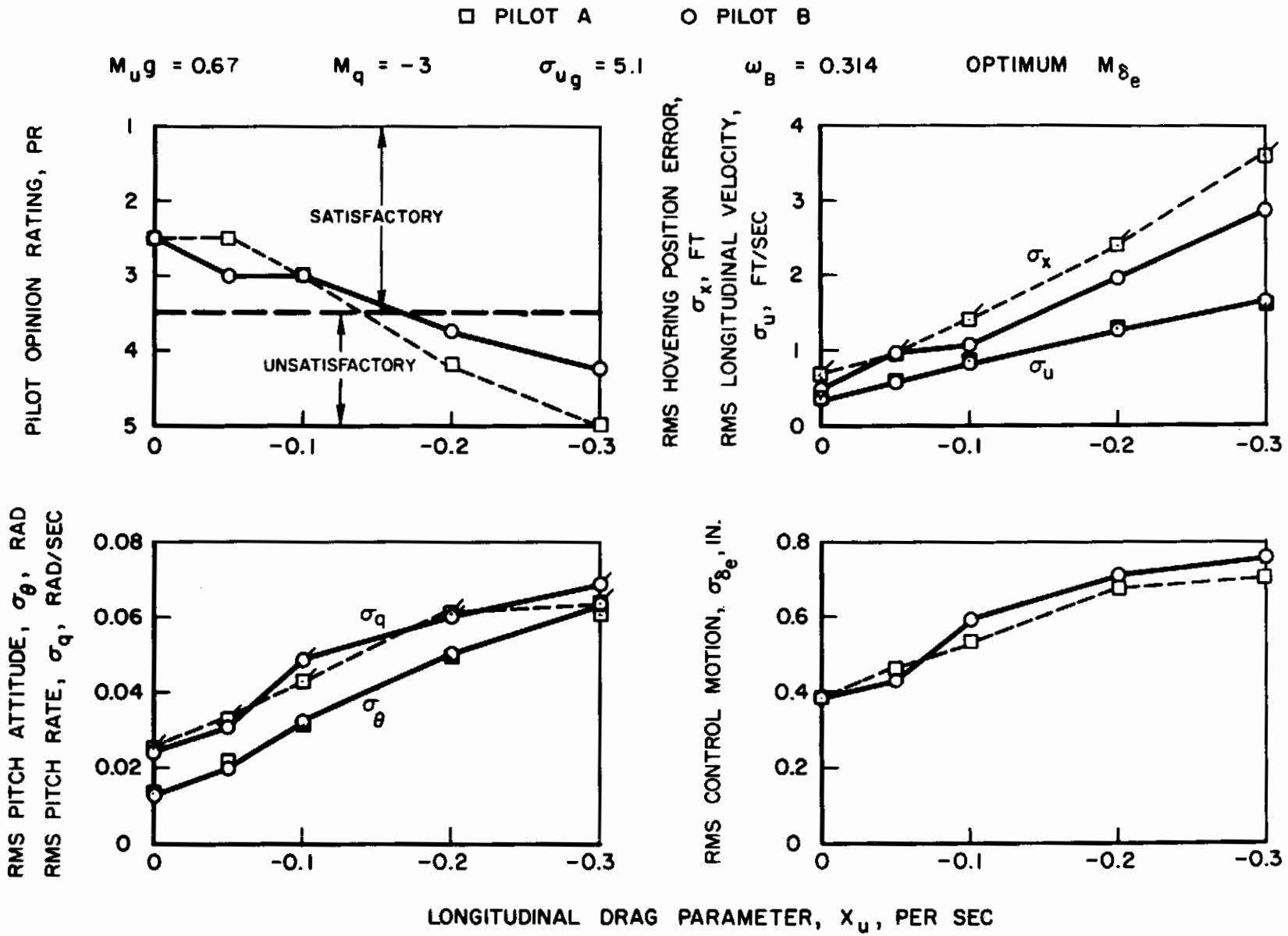

Figure 19. Effect of Longitudinal Drag Parameter on RMS Hovering Performance

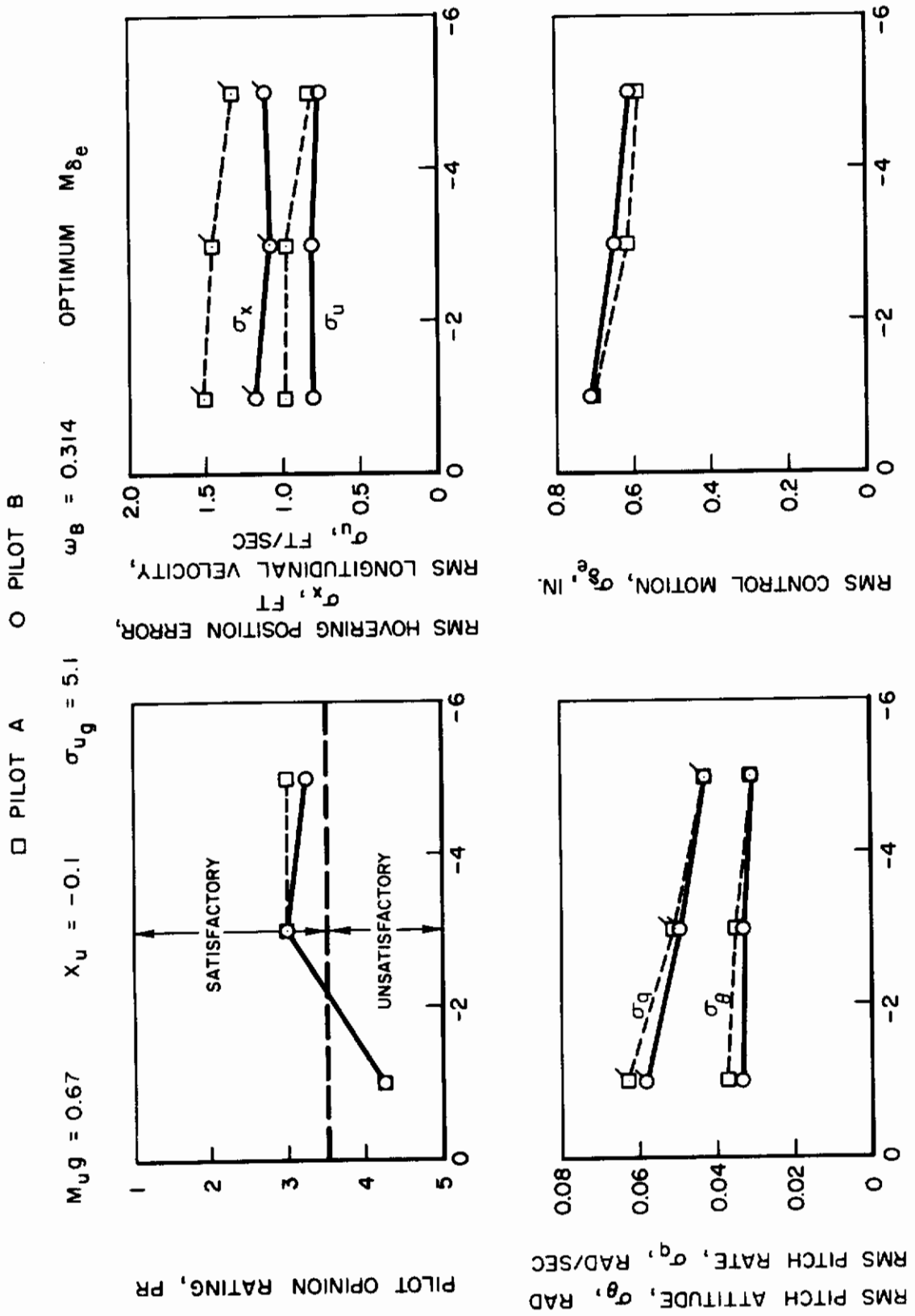

Figure 20. Effect of Pitch Rate Damping on RMS Hovering Performance

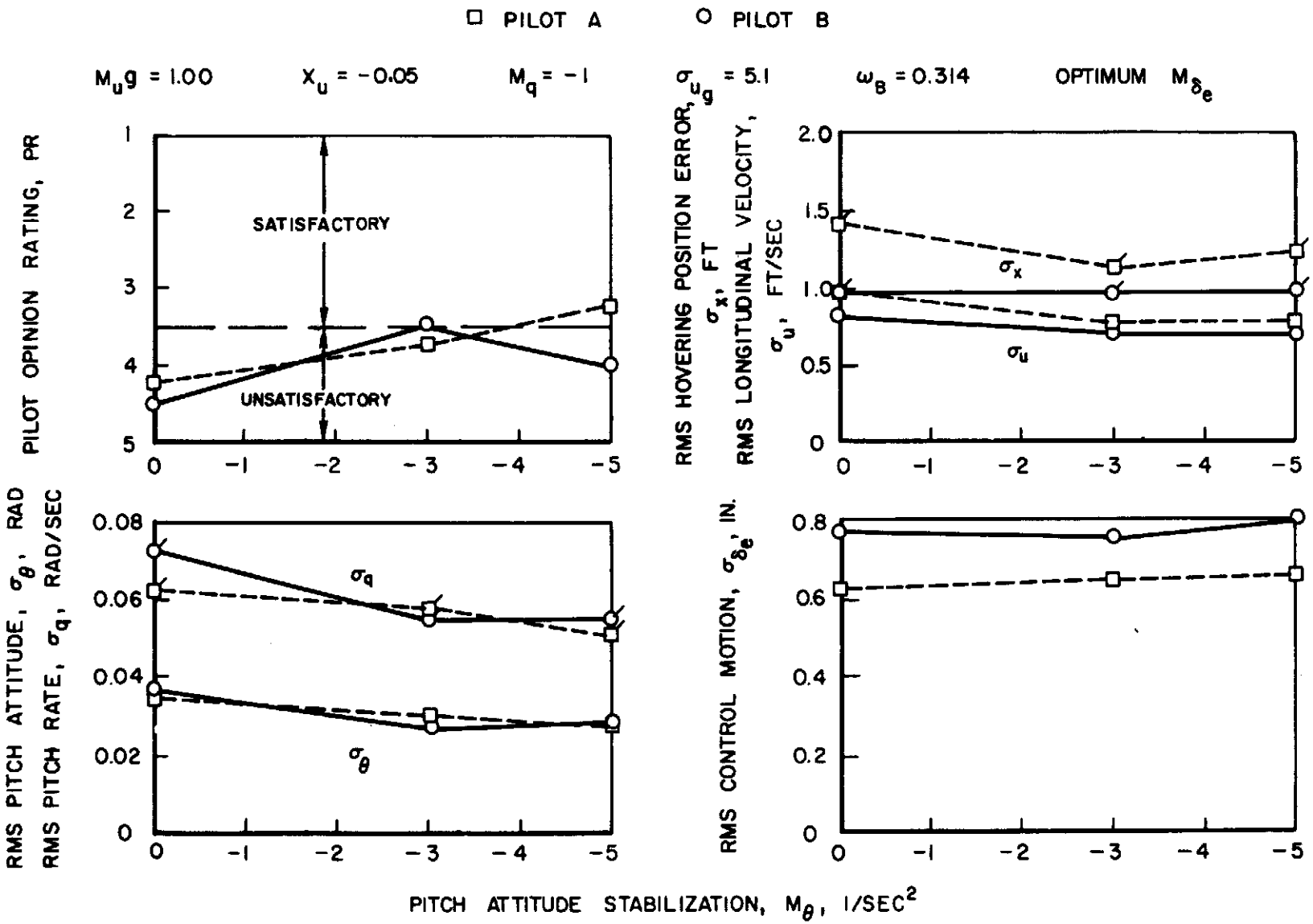

Figure 21. Effect of Pitch Attitude Stabilization on RMS Hovering Performance

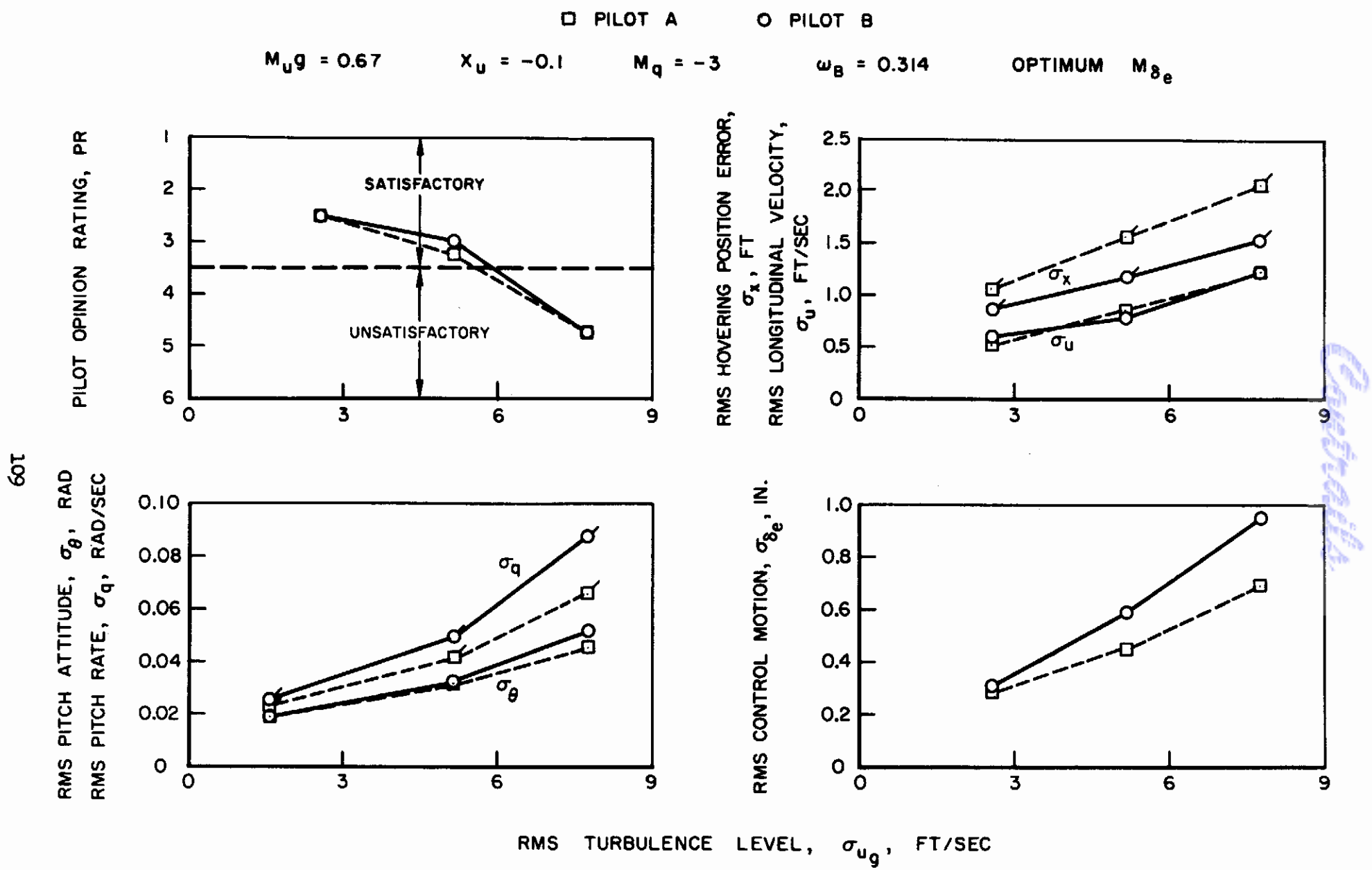

Figure 22. Effect of Turbulence Level on RMS Hovering Performance

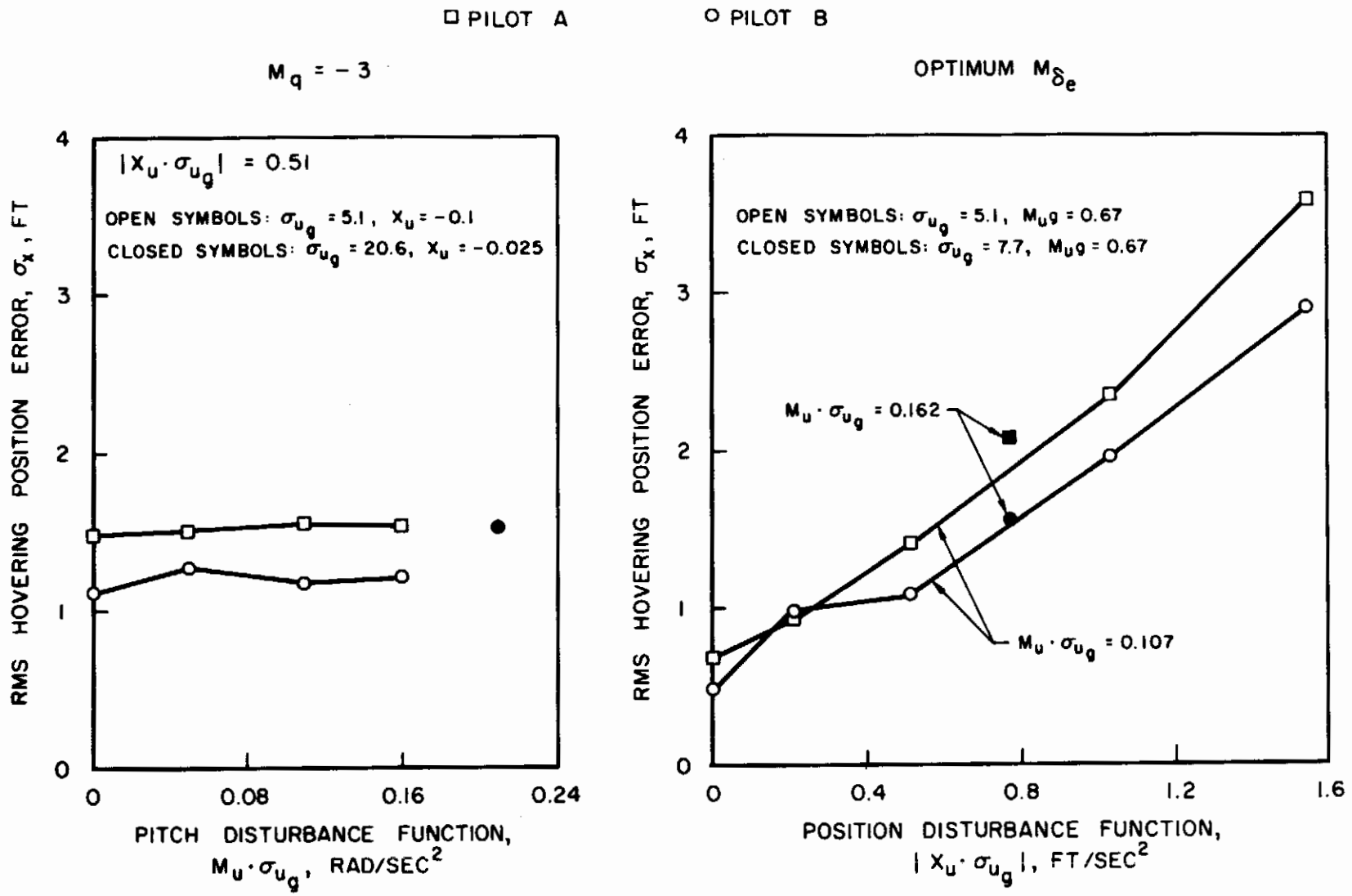

Figure 23. Effect of Pitch and Position Disturbance Functions on RMS Longitudinal Hovering Position

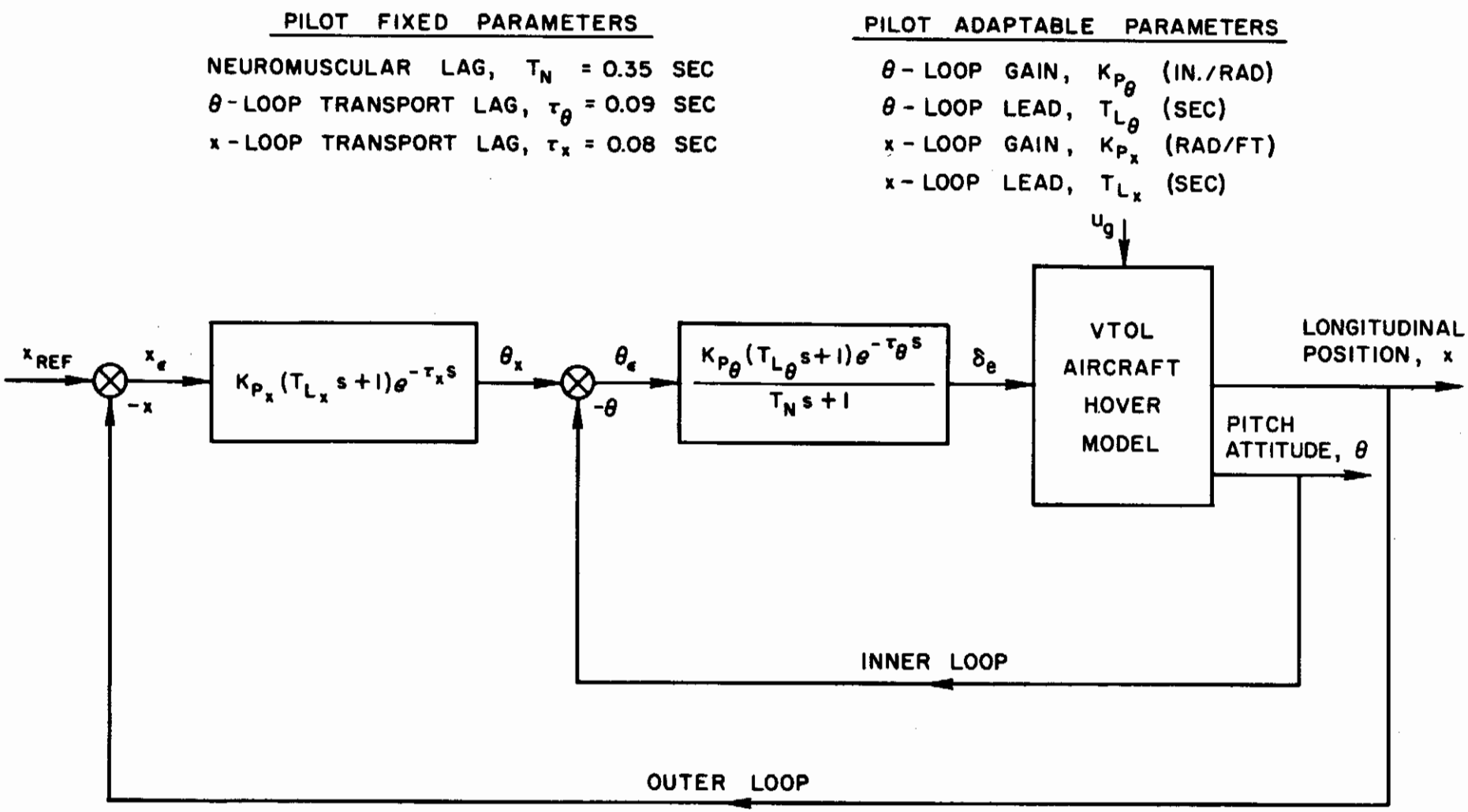

Figure 24. Series-Loop Model for Pilot Control in Hover

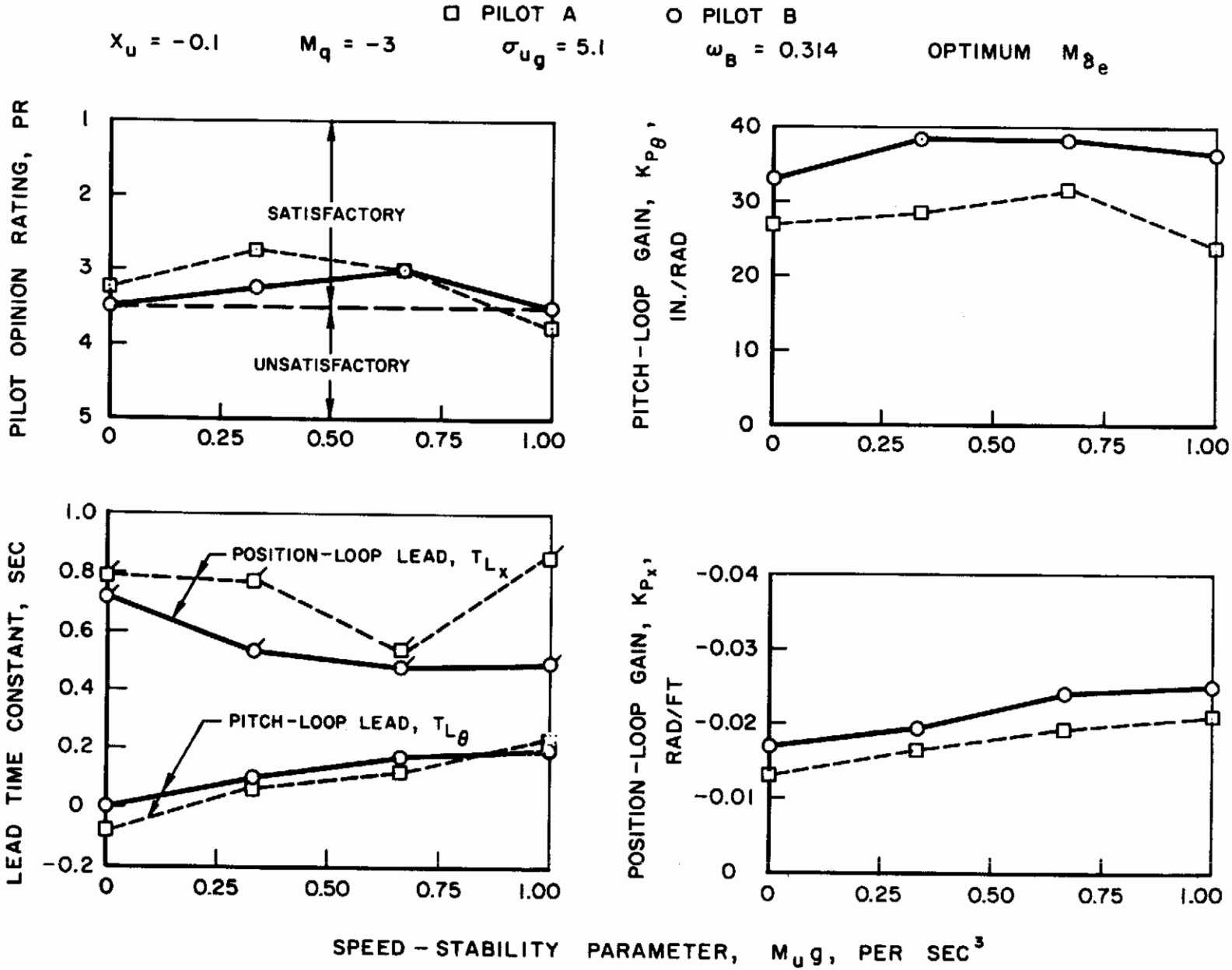

Figure 25. Effect of Longitudinal Speed-Stability on Pilot Adapted Parameters for Hover

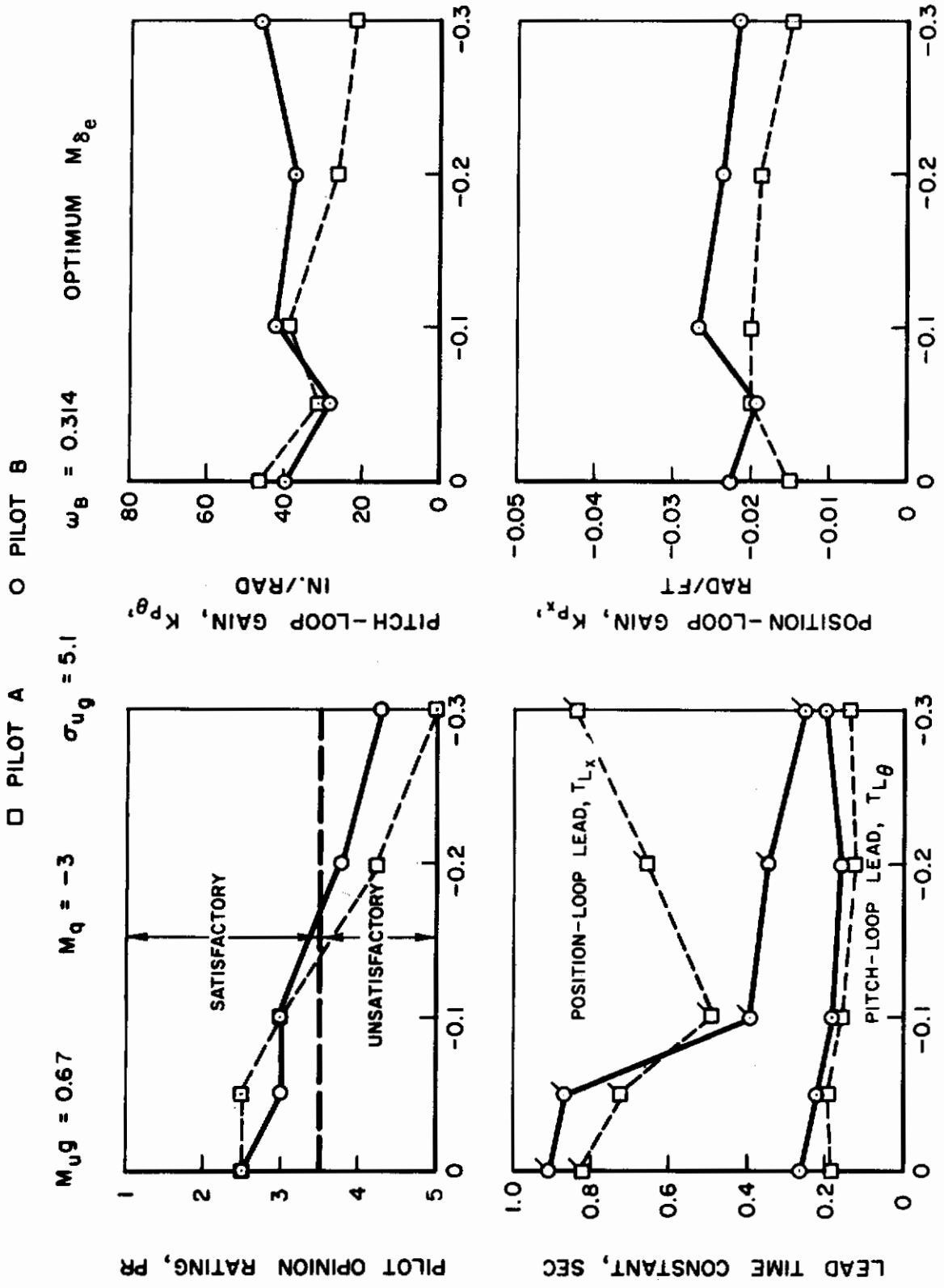

Figure 26. Effect of Longitudinal Drag on Pilot Adapted Parameters for Hover

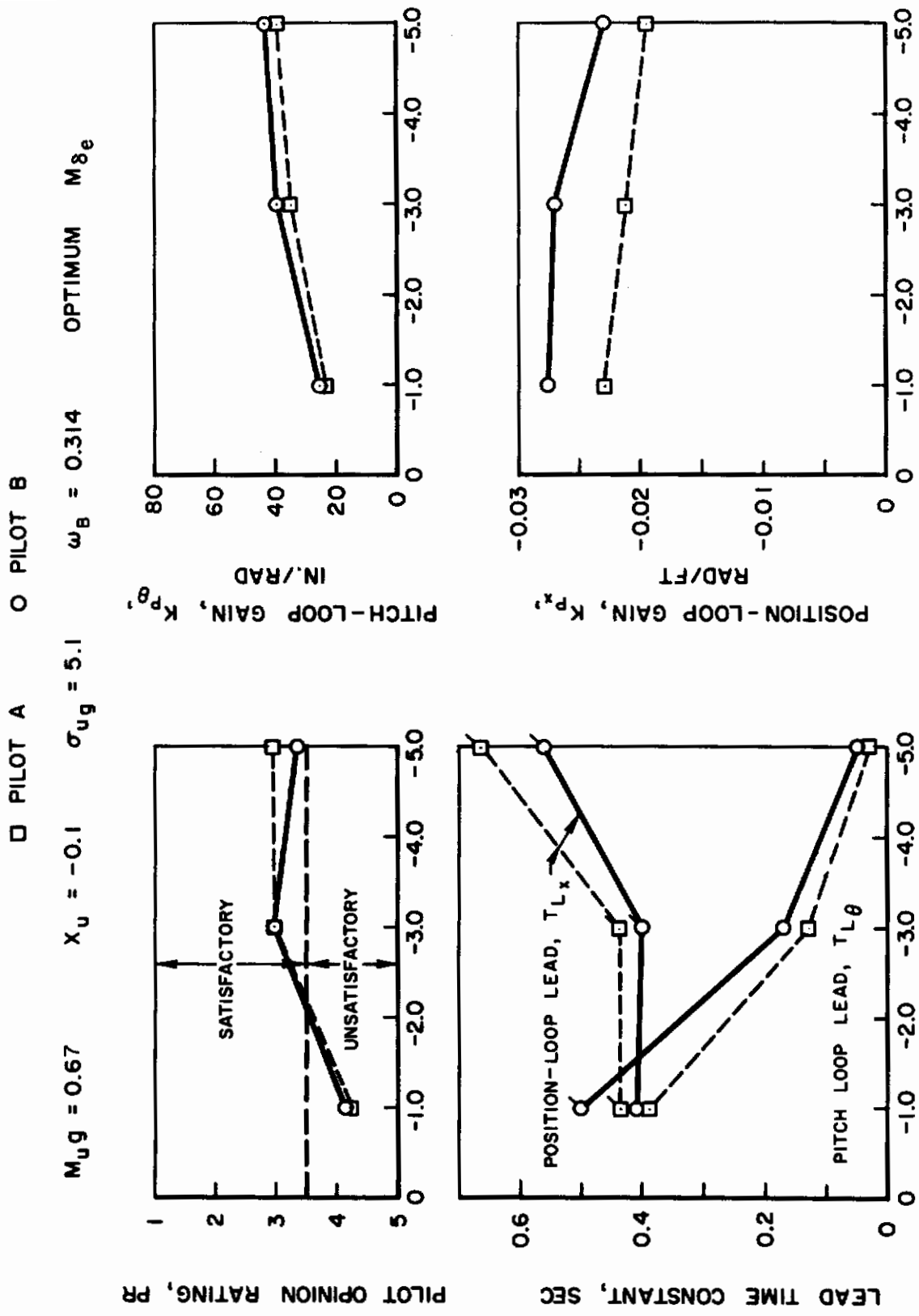

Figure 27. Effect of Pitch Rate Damping on Pilot Adapted Parameters for Hover

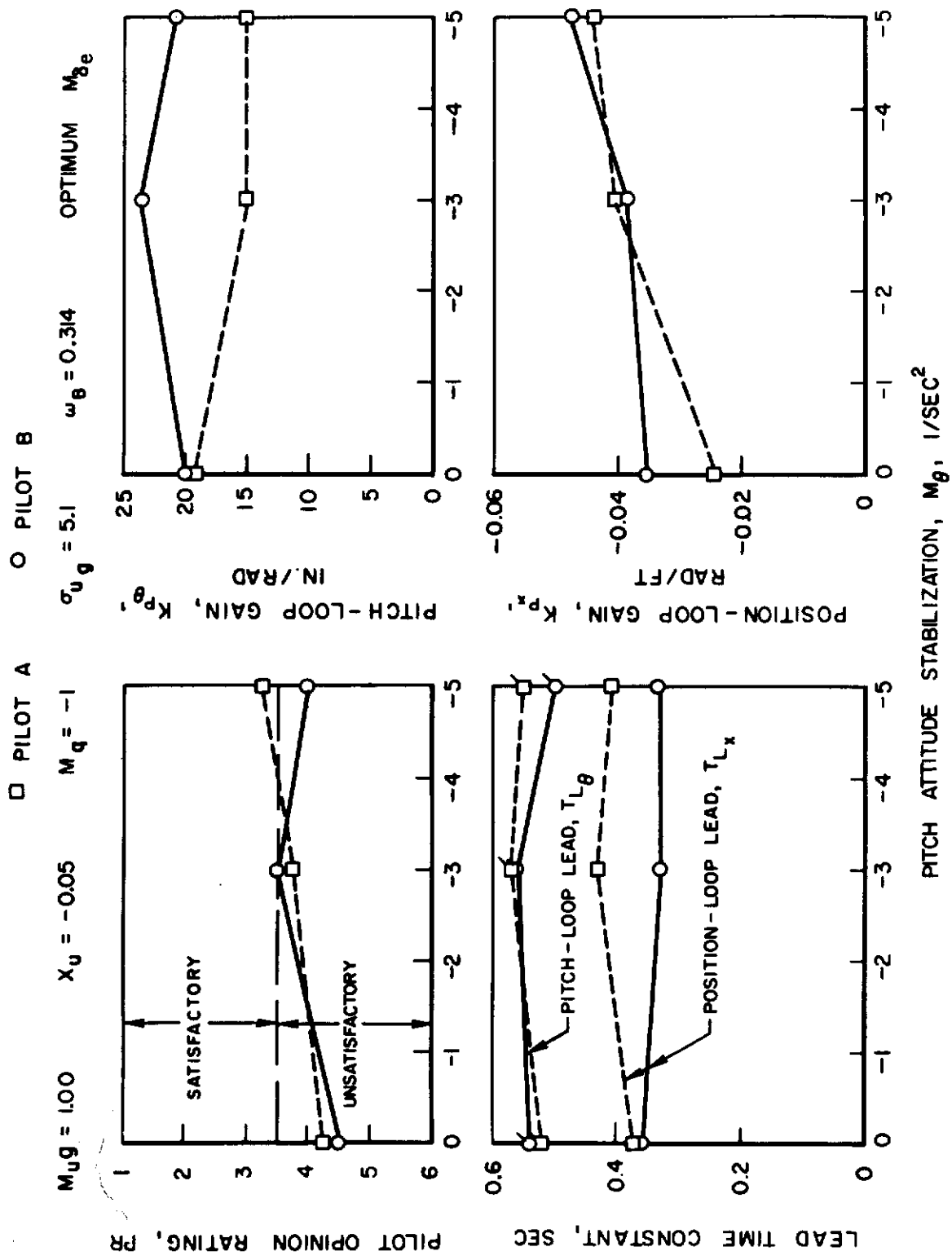

Figure 28. Effect of Pitch Attitude Stabilization on Pilot Adapted Parameters for Hover

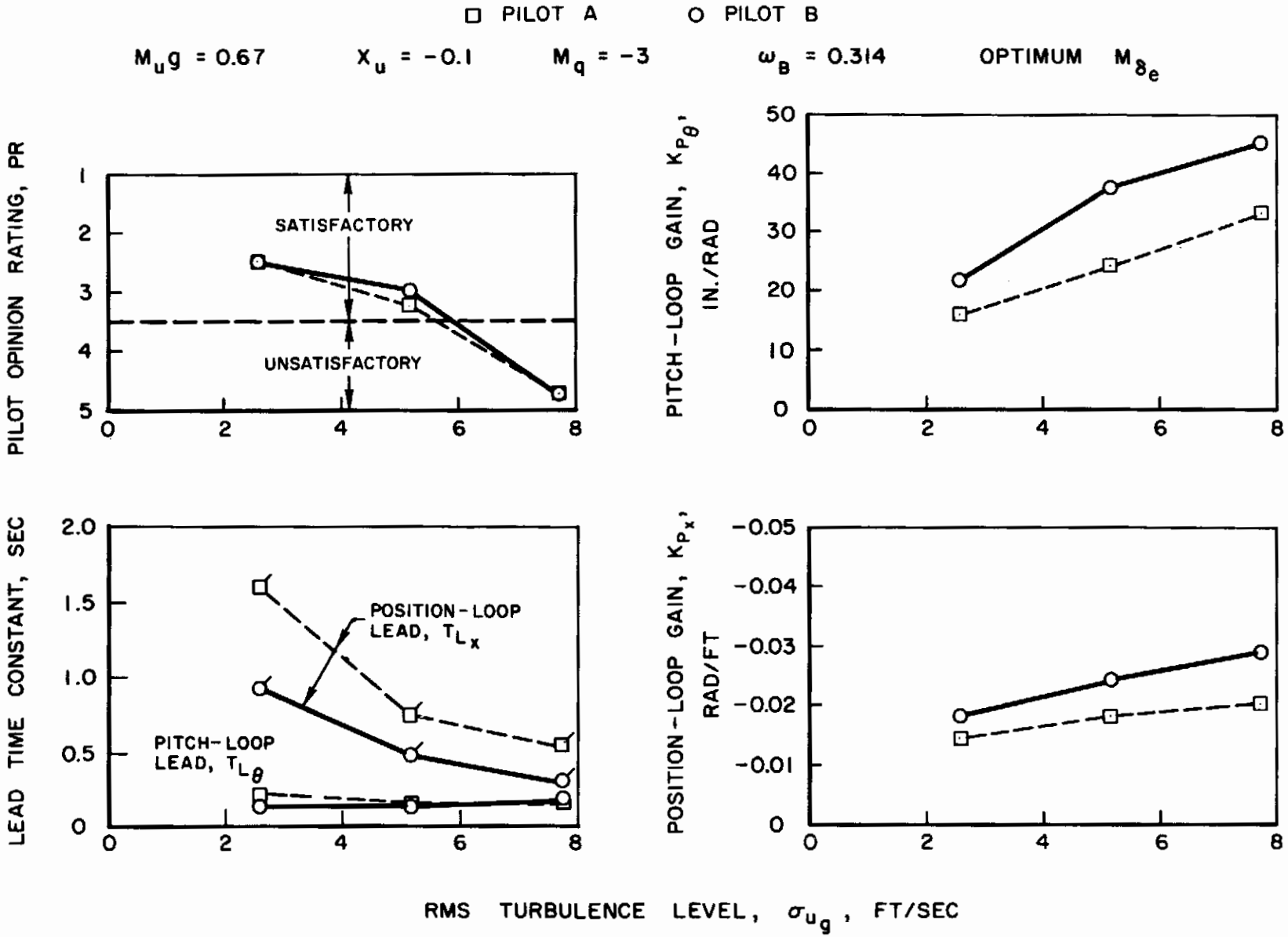

Figure 29. Effect of RMS Turbulence Level on Pilot Adapted Parameters for Hover

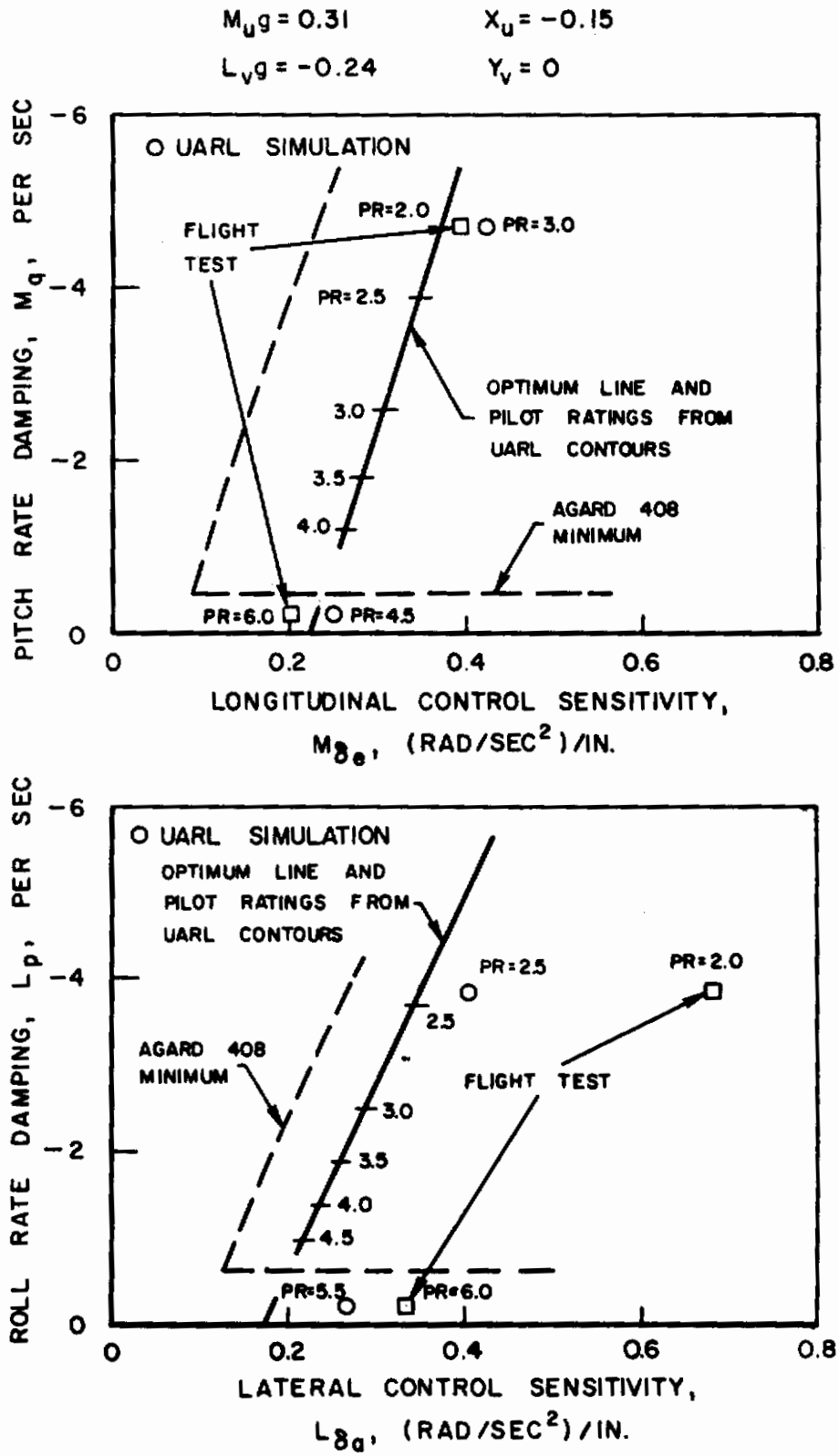

Figure 30. Flight Simulator Results for XC-142 Aircraft

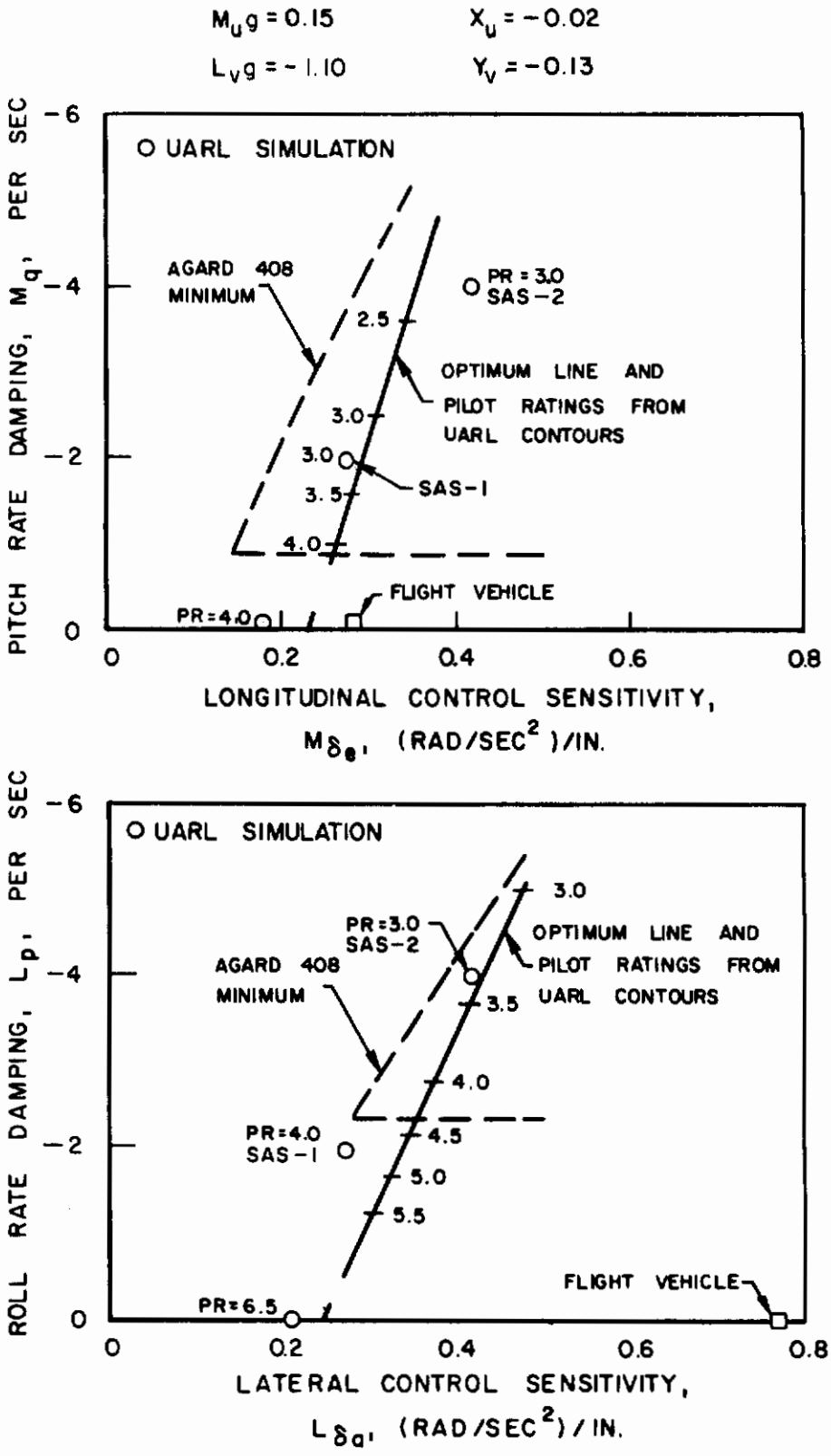

Figure 31. Flight Simulator Results for XV-4B Aircraft

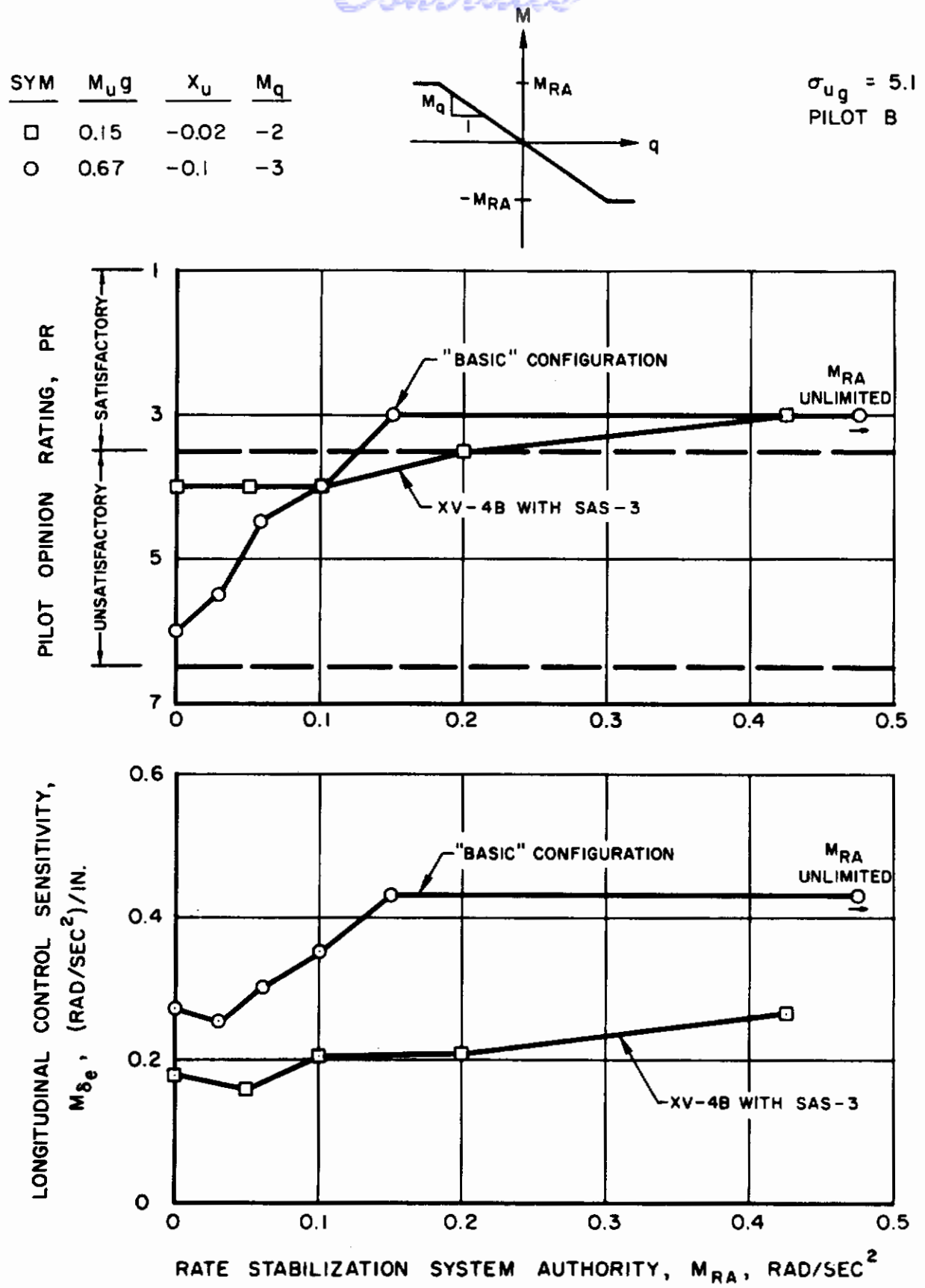

Figure 32. Effect of Rate Stabilization Authority on Handling Qualities of XV-4B Aircraft

SYM	$M_u g$	X_u	M_q
□	0.15	-0.02	-2
○	0.67	-0.1	-3

$(\delta_e)_{PILOT}$ → $\frac{1}{1+\tau_c s}$ → $(\delta_e)_{EFFECTIVE}$

σ_{ug} = 5.1
PILOT B

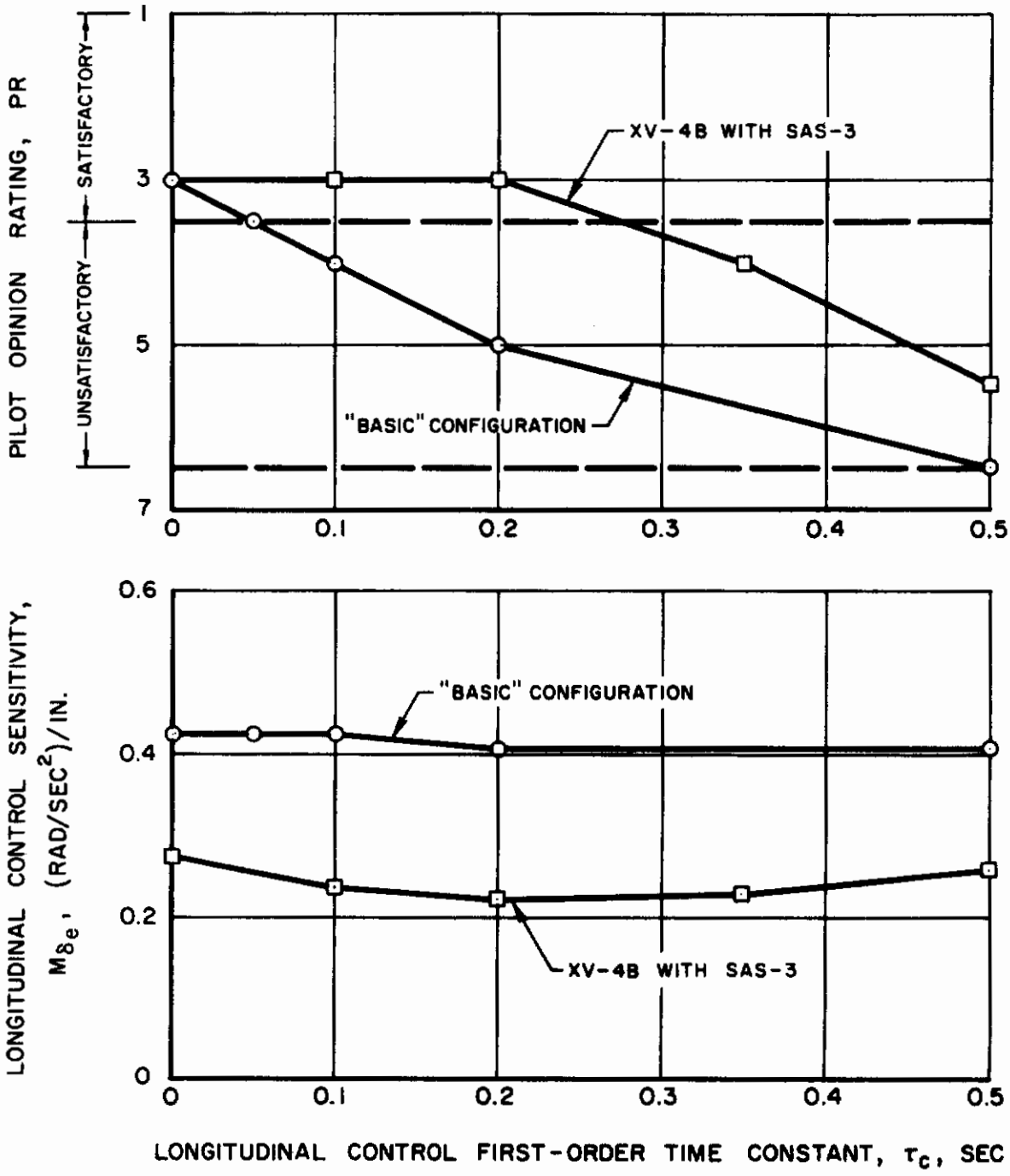

Figure 33. Effect of Longitudinal Control Lag on Handling Qualities of XV-4B Aircraft

	PRINCETON	GRUMMAN	UARL
$M_u g$	1.13	1.0	1.0
X_u	-0.02	-0.10	-0.05
σ_{ug}	6.3	6.0	5.14

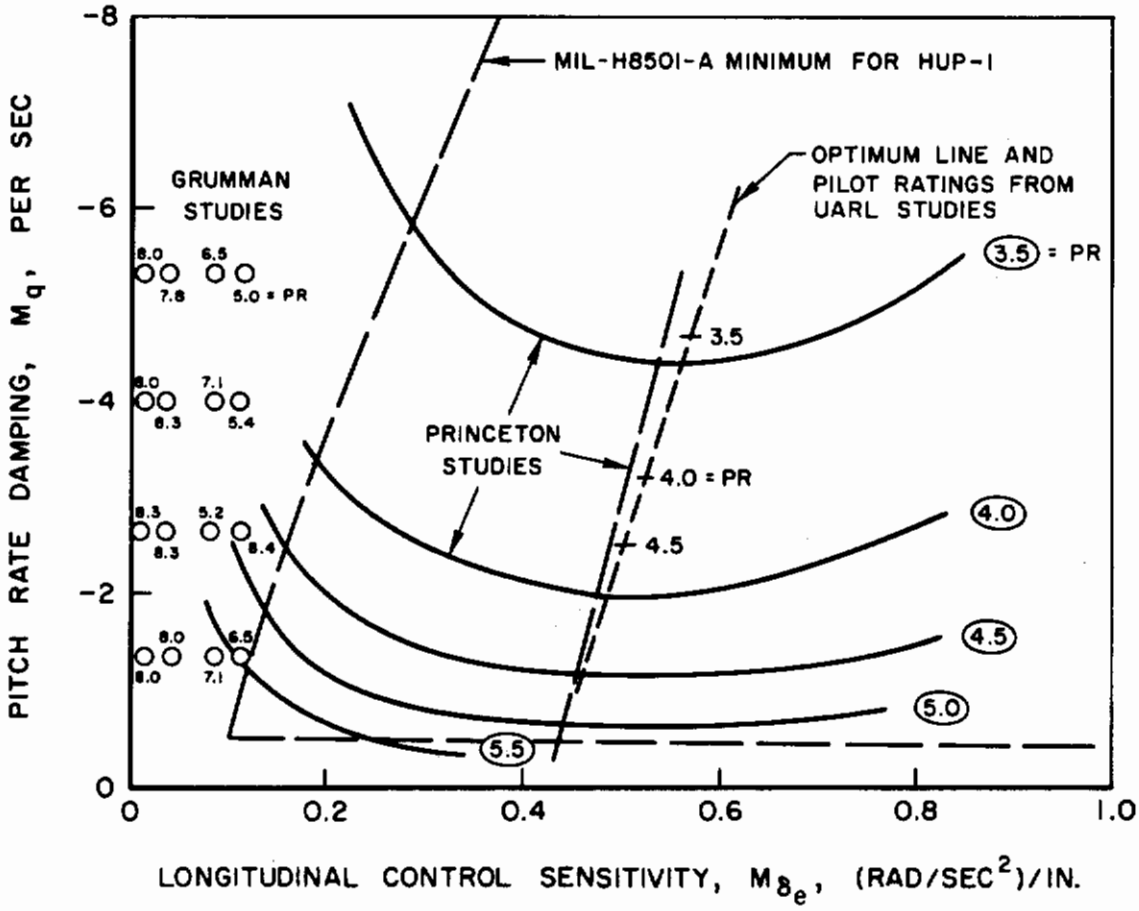

Figure 34. Flight Simulator Results for HUP-1 Tandem-Rotor Helicopter

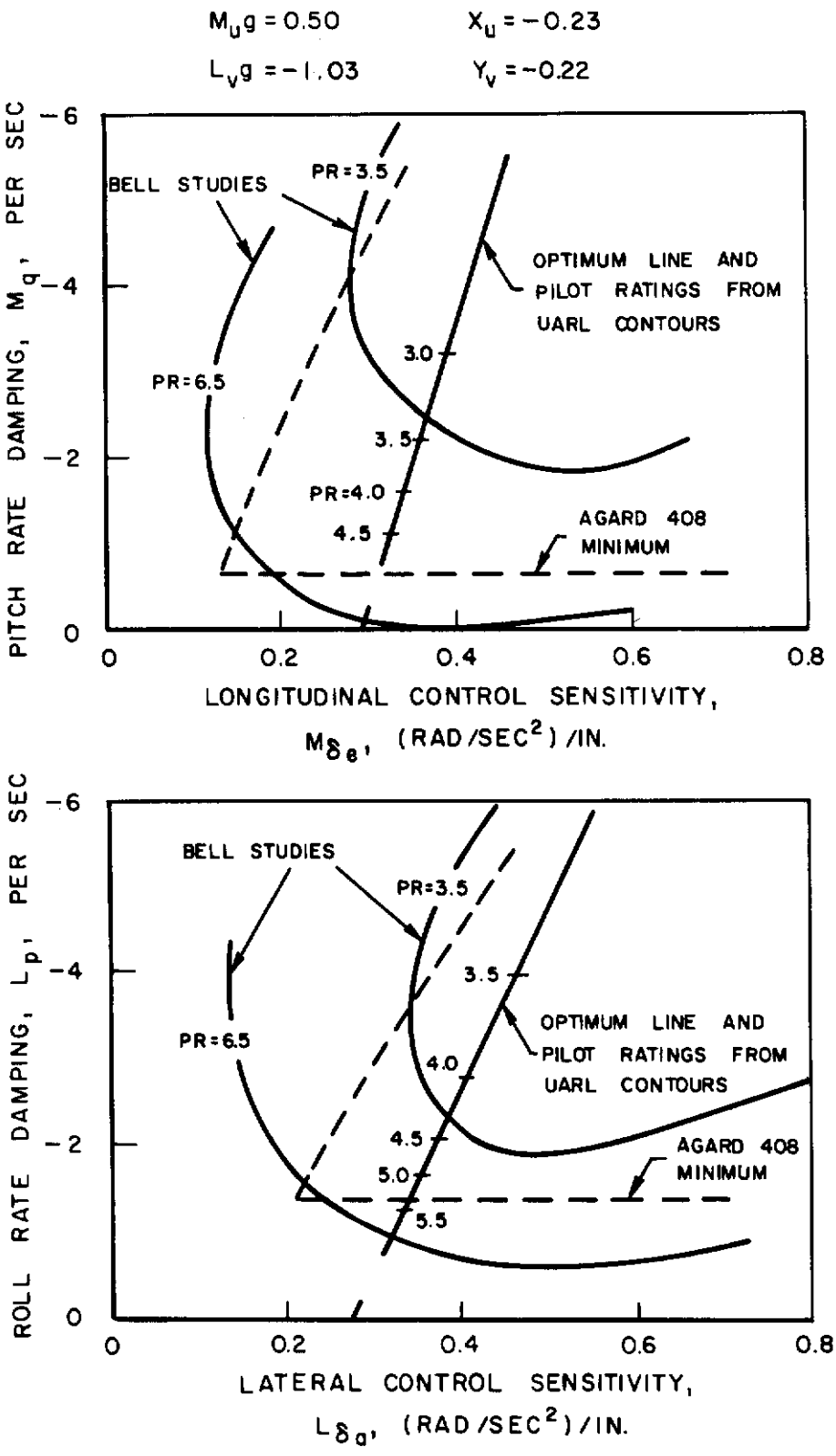

Figure 35. Flight Simulator Results for X-22A Aircraft

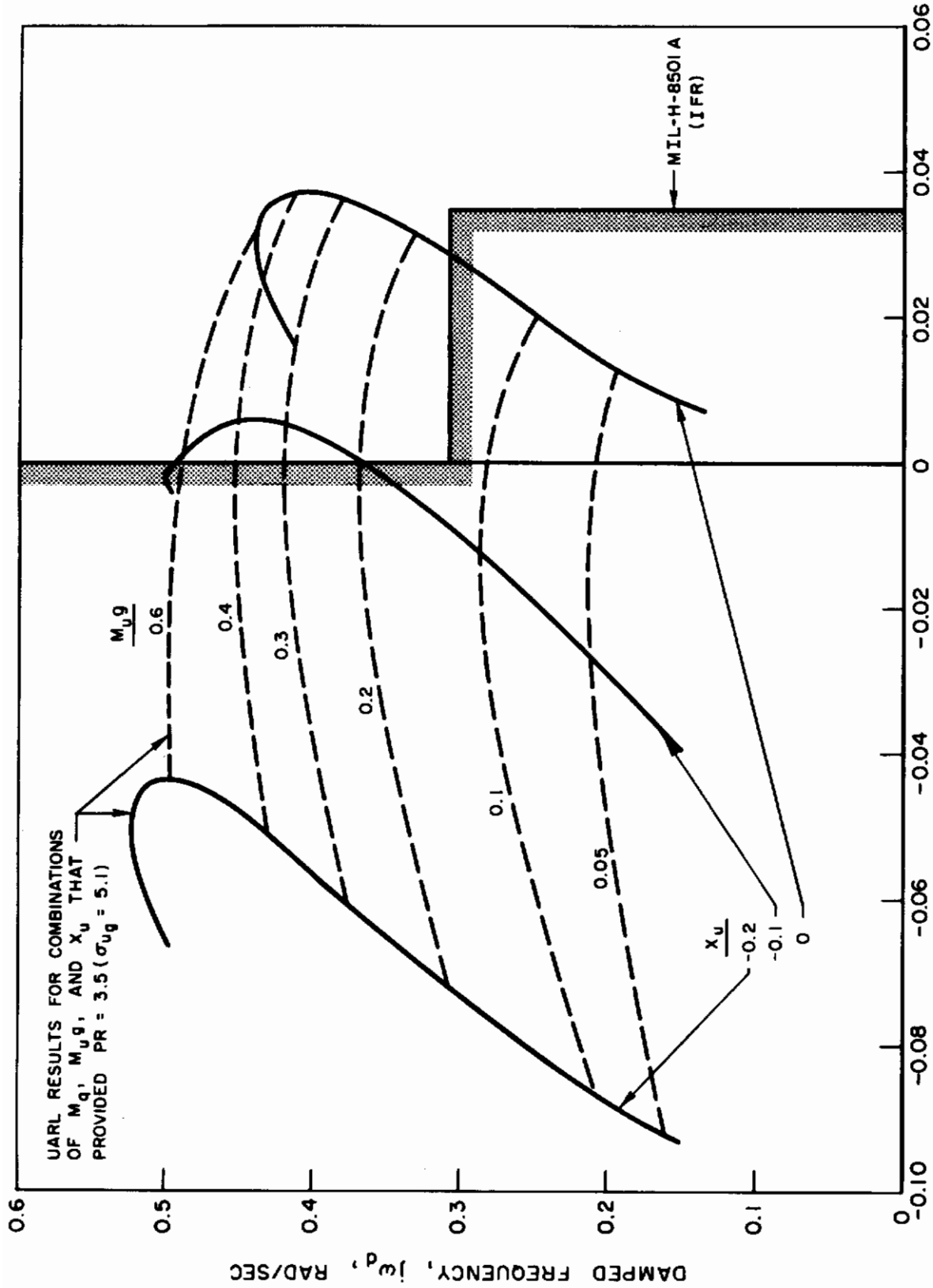

Figure 36. Comparison of UARL Results for Minimum Satisfactory Longitudinal Handling Qualities with MIL-H-8501A Requirements

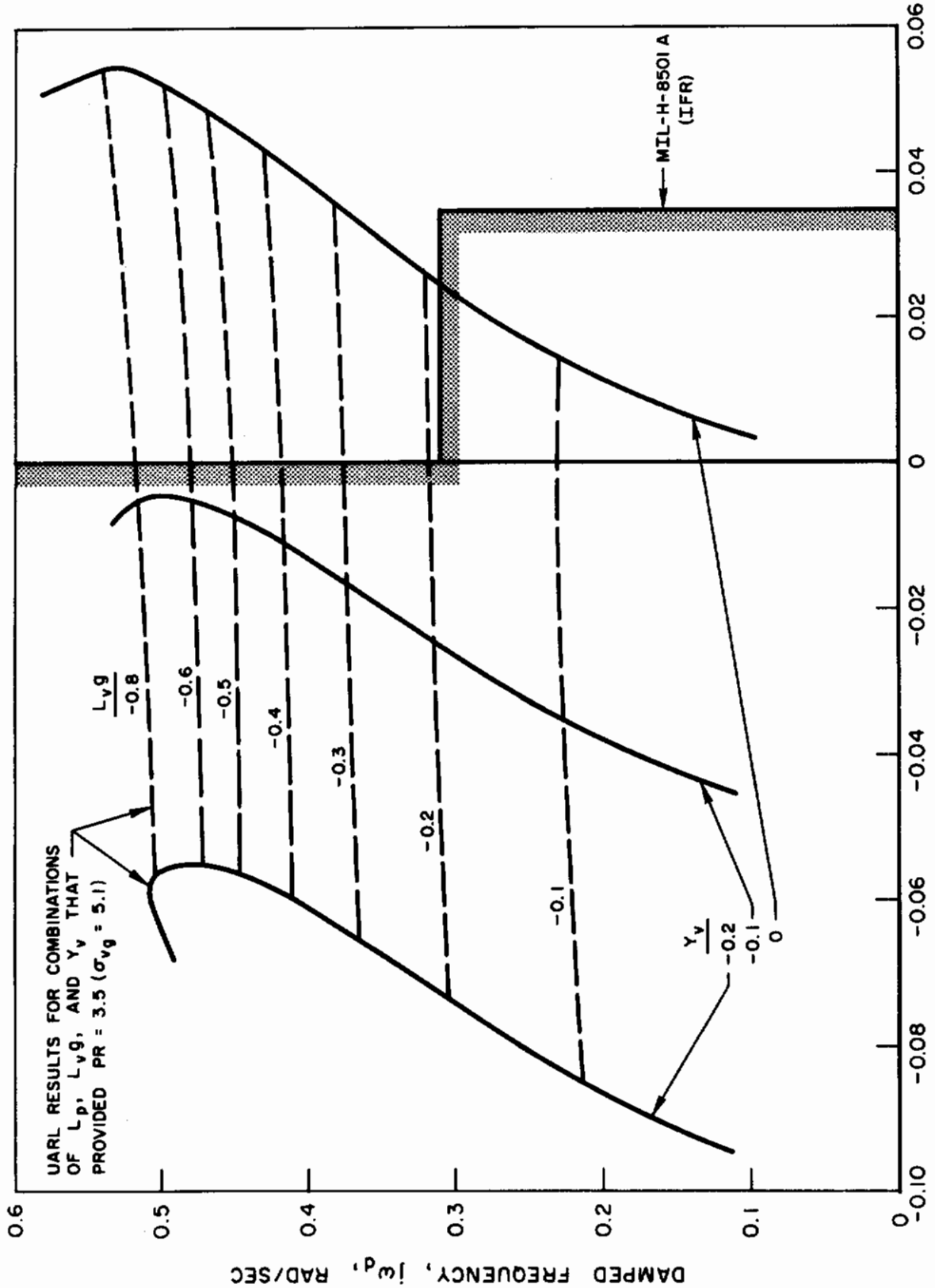

Figure 37. Comparison of UARL Results for Minimum Satisfactory Lateral Handling Qualities with MIL-H-8501A Requirements

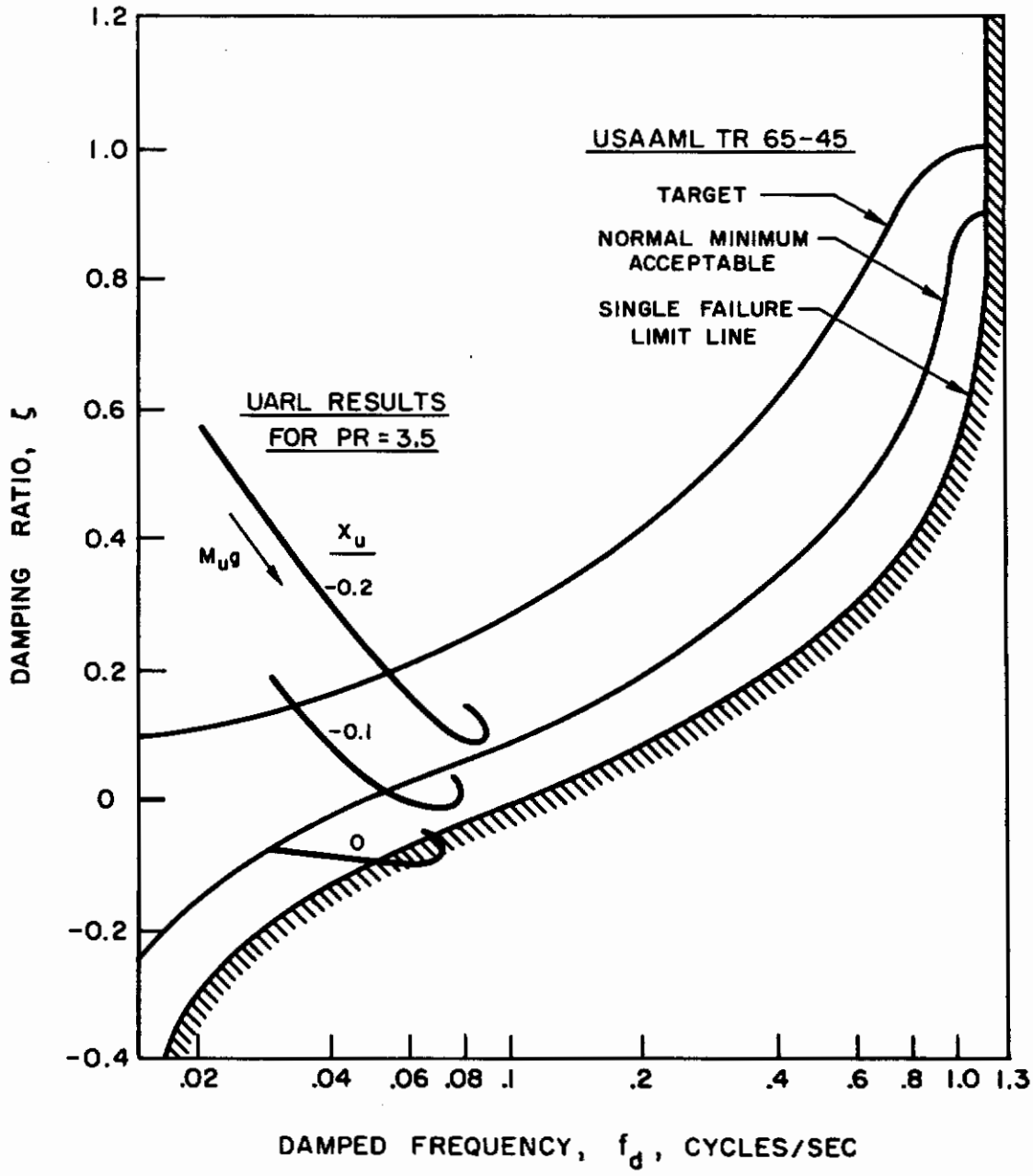

Figure 38. Comparison of UARL Results for Minimum Satisfactory Longitudinal Handling Qualities with USAAML TR 65-45 Requirements

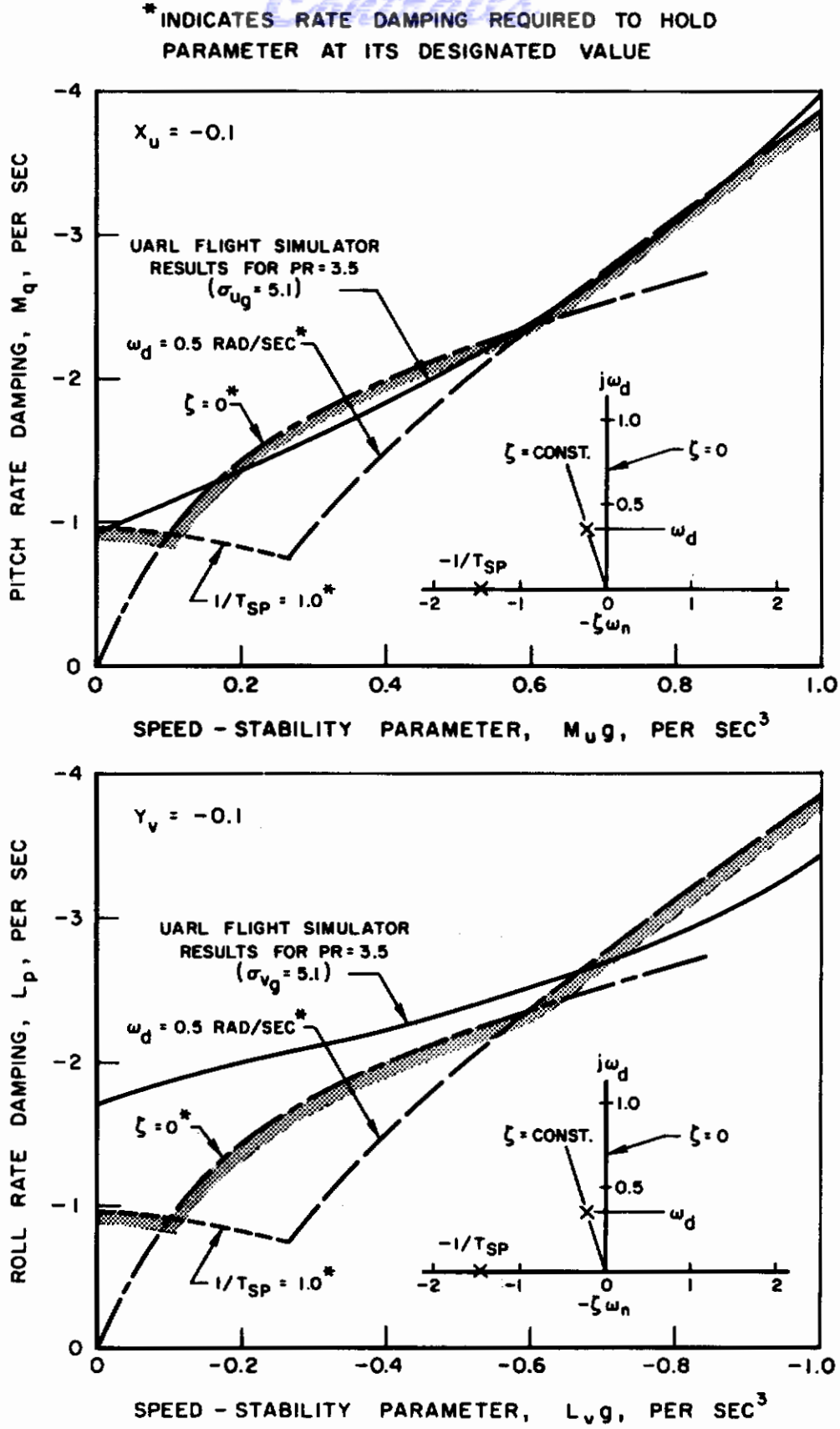

Figure 39. Comparison of UARL Results with Criteria for Open-Loop Frequency and Damping Parameters

APPENDIX A

DATA FOR HOVERING AND MANEUVERING TASK, PRECISION HOVERING (RMS) TASK AND COMPUTED PILOT MODEL PARAMETERS

This Appendix contains a detailed listing of the data for the study. Table A-I provides a key to the configurations investigated for the hovering and low-speed maneuvering task. Optimum control sensitivities and pilot ratings and comments for these studies are presented in Tables A-II and A-III for the longitudinal and lateral evaluations, respectively. In Table A-IV, the handling qualities comments of the CAL and UARL pilots are compared. The configurations studied in the precision hovering experiments are listed in Table A-V. The rms hovering performance data for these configurations are contained in Table A-VI and the pilot model parameters and loop-closure characteristics computed from these data are presented in Table A-VII. Finally, the stability derivatives for the XC-142 and XV-4B aircraft are listed in Tables A-VIII and A-IX.

TABLE A-I

CONFIGURATIONS EVALUATED IN HOVERING AND LOW-SPEED MANEUVERING TASK

Directional Parameters: $N_v = 0.002$ $N_r = -1$ $N_{\delta_r} = 0.2$

P: Indicates Parameter Varied Within Group S: Control Sensitivity Selected by Pilot

Principal Parameters	Cases	Longitudinal							Lateral							Table[2]
		$M_u g$	X_u	M_q	M_θ	M_{δ_e}	σ_{u_g}	SFG[1]	$L_v g$	Y_v	L_p	L_ϕ	L_{δ_a}	σ_{v_g}	SFG[1]	
$M_u g$, X_u	P1 to P16	0.33	P	P	0	S	5.1	0	-0.1	-0.1	-3	0	0.301	1.3	0	A-II
	P17 to P28	P	-0.3	P	↓	↓	↓	↓	↓	↓	↓	↓	↓	↓	↓	
σ_{u_g}	P29 to P44	0.33	-0.05	P	0	S	P	0	-0.1	-0.1	-3	0	0.301	P	0	
	P45 to P60	1.00	-0.05	↓	↓	↓	↓	↓	↓	↓	↓	↓	↓	↓	↓	
	P61 to P76	0.33	-0.25													
	P77 to P92	1.00	-0.25													
M_θ	P93 to P106	0.33	-0.05	P	P	S	5.1	0	-0.1	-0.1	-3	0	0.301	1.3	0	
	P107 to P116	1.00	-0.05	↓	↓	↓	↓	↓	↓	↓	↓	↓	↓	↓	↓	
	P117 to P126	0.33	-0.2													
	P127 to P136	1.00	-0.2													
SFG	P137 to P140					S	5.1	1.5	-0.1	-0.1	-3	0	0.301	1.3	1.5	
$L_v g$, Y_v	R1 to R16	0.67	-0.1	-3	0	0.431	1.3	0	P	0	P	0	S	5.1	0	A-III
	R17 to R32	↓	↓	↓	↓	↓	↓	↓	↓	-0.1	↓	↓	↓	↓	↓	
	R33 to R48									-0.2						
	R49 to R64									-0.3						
σ_{v_g}	R65 to R80	0.67	-0.1	-3	0	0.431	P	0	-0.33	-0.05	P	0	S	P	0	
	R81 to R96	↓	↓	↓	↓	↓	↓	↓	-1.00	-0.05	↓	↓	↓	↓	↓	
	R97 to R112								-0.33	-0.25						
	R113 to R128								-1.00	-0.25						
L_ϕ	R129 to R136	0.67	-0.1	-3	0	0.431	1.3	0	-0.33	-0.05	P	P	S	5.1	0	
	R137 to R144	↓	↓	↓	↓	↓	↓	↓	-1.00	-0.05	↓	↓	↓	↓	↓	
	R145 to R152								-0.33	-0.2						
	R153 to R160								-1.00	-0.2						
	R161 to R170[3]			P	P	P			-0.67	-0.1						
SFG	R171 to R174	0.67	-0.1	-3	0	0.431	1.3	1.5	-0.67	-0.1	P	0	S	5.1	1.5	

Notes:

1. SFG: Stick force gradient, lb/in.
2. Indicates Table listing corresponding pilot ratings, optimum control sensitivities, and pilot comments.
3. R167 to R170: Six degrees of freedom simulated. $M_q = L_p$, $M_\theta = L_\phi$, $Z_w = -1.0$, $Z_{\delta_c} = -3.2$

TABLE A-II

LONGITUDINAL HANDLING QUALITIES RESULTS FROM HOVERING AND LOW-SPEED MANEUVERING TASK

Note: Lateral and directional parameters given in Table A-I

Case	$M_u g$	X_u	M_q	M_θ	σ_{u_g}	SFG	Real Roots RR (1)	RR (2)	RR (3)	Complex Roots $-\zeta\omega_n \pm j\omega_d$	Pilot	M_{δ_e}	PR	Summary of Pilot Comments
P1	0.33	0	-1	0	5.1	0	-1.22			0.111 ± j 0.510	A	0.254	4.5	Unstable. Too responsive to gusts. Requires rapid
											B	0.269	4.25	reversal in control to arrest pitch rate.
P2			-2				-2.08			0.039 ± j 0.398	A	0.280	4.0	Adequate damping. Gust effects minimal. Good hovering
											B	0.286	3.5	performance by tightening up on attitude loop.
P3			-3				-3.04			0.018 ± j 0.331	A	0.311	3.25	Good pitch control. Easy to hover. Must anticipate desired
											B	0.323	3.25	hovering point when maneuvering.
P4			-4				-4.02			0.010 ± j 0.288	A	0.363	3.25	Seems slightly unstable but has good control. Tend to slide
											B	0.386	3.25	by hovering point when maneuvering.
P5	0.33	-0.10	-1	0	5.1	0	-1.24			0.068 ± j 0.514	A	0.238	4.0	Pitch is oscillatory and responsive to gusts. Experience
											B	0.240	4.25	overshoots on attitude commands. Unstable, but easily controllable.
P6			-2				-2.08			-0.010 ± j 0.400	A	0.270	3.25	Fairly good attitude and position control. Gust effects
											B	0.286	3.0	require a little attention.
P7			-3				-3.04			-0.031 ± j 0.330	A	0.316	2.5	Easy to hover and maneuver. Seems stable. No gust effects
											B	0.313	2.75	on attitude.
P8			-4				-4.02			-0.039 ± j 0.285	A	0.341	2.25	Gust effects minimal. Good task performance. Little effort
											B	0.332	2.75	required.
P9	0.33	-0.20	-1	0	5.1	0	-1.25			-0.026 ± j 0.515	A	0.261	4.75	Difficult to command and hold desired attitude. Too oscil-
											B	0.248	4.50	latory. Position disturbances are somewhat of a problem.
P10			-2				-2.08			-0.058 ± j 0.395	A	0.300	3.75	Fairly good attitude control. Bothered by position disturb-
											B	0.281	3.25	ances.
P11			-3				-3.04			-0.081 ± j 0.321	A	0.334	3.25	Adequate damping. Position disturbances limit PR. Fairly
											B	0.338	3.0	good task performance.
P12			-4				-4.02			-0.089 ± j 0.274	A	0.369	3.25	Heavily damped, but good response. Notice gusts only on
											B	0.363	3.0	position. Position disturbances limit PR.
P13	0.33	-0.30	-1	0	5.1	0	-1.27			-0.015 ± j 0.512	A	0.291	4.5	Lightly damped, very oscillatory. Unstable, but not too
											B	0.284	4.5	difficult to control.
P14			-2				-2.09			-0.105 ± j 0.385	A	0.327	3.75	Position disturbances require large attitude changes.
											B	0.332	4.0	Difficult to develop translational velocity.
P15			-3				-3.04			-0.130 ± j 0.304	A	0.355	3.5	Good attitude control (could rate 2.0) hovering performance
											B	0.378	4.0	relatively poor. Maneuvers slowly.
P16			-4				-4.02			-0.139 ± j 0.252	A	0.398	3.5	Well damped. Control effort high due to position disturb-
											B	0.432	4.25	ances.

TABLE A-II (Continued)

Case	M_{u_g}	X_u	M_q	M_θ	σ_{u_g}	SFG	Real Roots RR (1)	Real Roots RR (2)	Real Roots RR (3)	Complex Roots $-\zeta\omega_n \pm j\omega_d$	Pilot	M_{δ_e}	PR	Summary of Pilot Comments
P17	0	-0.30	-1	0	5.1	0	-1.00	-0.30	0.0		A	0.239	3.75	No gust or trim effects on attitude. Maneuvers slowly.
											B	0.236	4.5	Poor hovering performance due to position disturbances.
P18			-2				-2.00	-0.30	0.0		A	0.269	3.5	Good attitude control. Large θ changes required to hover.
											B	0.253	4.25	Maneuvering fairly good, but slow.
P19			-3				-3.00	-0.30	0.0		A	0.306	3.5	Attitude has relatively long period response. Neutral
											B	0.283	4.25	stability. PR depends on importance of hovering performance.
P20			-4				-4.00	-0.30	0.0		A	0.337	3.25	Good attitude control. Position-loop disturbances limit PR.
											B	0.324	4.25	
P21	0.67	-0.30	-1	0	5.1	0	-1.42			0.060 ± j 0.683	A	0.349	5.25	Attitude oscillations large. Very oscillatory. Very
											B	0.326	5.5	difficult to accomplish task.
P22			-2				-2.16			-0.067 ± j 0.551	A	0.384	4.5	Needs more damping. A lot of effort and concentration
											B	0.394	4.5	required.
P23			-3				-3.08			-0.111 ± j 0.452	A	0.426	3.75	Fairly good attitude control. Large attitude changes
											B	0.418	3.75	required to control position disturbances.
P24			-4				-4.04			-0.128 ± j 0.385	A	0.454	3.75	Good attitude control. Work load high due to position
											B	0.470	4.0	disturbances. With effort get fair task performance.
P25	1.00	-0.30	-1	0	5.1	0	-1.53			0.115 ± j 0.800	A	0.383	6.0	Attitude is unstable and very oscillatory. Gust sensitivity
											B	0.387	5.5	high. Task accomplishment in doubt.
P26			-2				-2.23			-0.034 ± j 0.668	A	0.444	5.5	Gust disturbances large. Difficult to hover accurately.
											B	0.441	4.75	Use attitude disturbances to anticipate position disturbances.
P27			-3				-3.11			-0.093 ± j 0.559	A	0.482	4.5	Seems well damped, but difficult to hover accurately.
											B	0.458	4.25	Control effort high.
P28			-4				-4.06			-0.117 ± j 0.482	A	0.510	3.75	Well damped, seems stable. Attitude disturbances minimal.
											B	0.512	3.75	Slow maneuvering. Effort required relatively high.
P29	0.33	-0.05	-1	0	0	0	-1.23			0.090 ± j 0.513	A	0.215	4.0	Lightly damped, oscillatory. Experience overshoot on attitude commands.
P30			-2				-2.08			0.014 ± j 0.400	A	0.269	2.75	No gust effects. Good θ control. Good task performance.
P31			-3				-3.04			-0.007 ± j 0.331	A	0.285	3.0	Good performance. Would like a little more drag to aid maneuvering.
P32			-4				-4.02			-0.014 ± j 0.287	A	0.325	2.75	Get constant pitch rate per unit control deflection. May be more damping then necessary.

TABLE A-II (Continued)

Case	$M_u g$	X_u	M_q	M_g	σ_{u_g}	SFG	Real Roots RR (1)	Real Roots RR (2)	Real Roots RR (3)	Complex Roots $-\zeta\omega_n \pm j\omega_d$	Pilot	M_{δ_e}	PR	Summary of Pilot Comments
P33	0.33	-0.05	-1	0	5.1	0	-1.23			0.090 ± j 0.513	A	0.224	4.5	Annoyed by gusts on attitude. Requires a lot of attention. Lightly damped.
P34			-2				-2.08			0.014 ± j 0.400	A	0.238	4.0	Requires a lot of attention on θ. Needs more damping.
P35			-3				-3.04			-0.007 ± j 0.331	A	0.289	3.0	Good control. Gust effects minimal. Maneuvering set M_{δ_e}. Easy to hover.
P36			-4				-4.02			-0.014 ± j 0.287	A	0.333	2.75	Can hover well. A little more drag desirable for maneuvering. Well damped.
P37	0.33	-0.05	-1	0	7.7	0	-1.23			0.090 ± j 0.513	A	0.268	4.75	Gust disturbances on θ large. Requires a lot of attention and effort.
P38			-2				-2.08			0.014 ± j 0.400	A	0.269	4.25	Requires more damping. Unsatisfactory.
P39			-3				-3.04			-0.007 ± j 0.331	A	0.299	3.75	Effort to hover because of gusts on θ. Would like more drag to maneuver.
P40			-4				-4.02			-0.014 ± j 0.287	A	0.328	3.25	Good level of damping. PR limited by gust effects on θ plus low drag.
P41	0.33	-0.05	-1	0	10.3	0	-1.23			0.090 ± j 0.513	A	0.270	5.5	Task performance doubtful. Requires full attention to control. Needs damping.
P42			-2				-2.08			0.014 ± j 0.400	A	0.275	4.75	Unacceptable because of work load to control θ. Task performance acceptable.
P43			-3				-3.04			-0.007 ± j 0.331	A	0.325	3.75	Gust effects on θ require attention, but performance not impaired.
P44			-4				-4.02			-0.014 ± j 0.287	A	0.343	3.5	Well damped. Gust effects on position a little annoying.
P45	1.00	-0.05	-1	0	0	0	-1.48			0.213 ± j 0.795	B	0.281	3.5	Would like more damping. Overshoots on θ commands. Need M_{δ_e} to overcome speed stability.
P46			-2				-2.21			0.078 ± j 0.668	B	0.292	3.0	Prefer more damping. Some overshoot on θ commands when maneuvering.
P47			-3				-3.11			0.028 ± j 0.567	B	0.321	2.25	Well damped. Easy to fly. Good maneuvering performance.
P48			-4				-4.06			0.006 ± j 0.496	B	0.386	2.0	Excellent. Easy to maneuver. Speed stability no problem.

TABLE A-II (Continued)

Case	$M_u g$	X_u	M_q	M_θ	σ_{u_g}	SPG	Real Roots RR (1)	RR (2)	RR (3)	Complex Roots $-\zeta\omega_n \pm j\omega_d$	Pilot	M_{δ_e}	PR	Summary of Pilot Comments
P49	1.00	-0.05	-1	0	2.6	0	-1.48			0.213 ± j 0.795	B	0.311	4.0	Needs more damping. Overshoots in θ when maneuvering. Can hover reasonably well.
P50			-2				-2.21			0.078 ± j 0.668	B	0.374	3.25	Combination of gusts and speed stability sets M_{δ_e}. Desire a little more damping.
P51			-3				-3.11			0.028 ± j 0.567	B	0.407	2.75	Adequate damping. Task easy to perform. Gusts noticeable.
P52			-4				-4.06			0.006 ± j 0.496	B	0.448	2.5	Good attitude control. Gusts noticeable only when maneuvering.
P53	1.00	-0.05	-2	0	5.1	0	-2.21			0.078 ± j 0.668	B	0.429	4.75	Attitude very oscillatory. Difficult to control regardless of M_{δ_e}. Fair task performance.
P54			-3				-3.11			0.028 ± j 0.567	B	0.471	4.0	Oscillatory. Would like more damping. Noticeable gust effects on θ when maneuvering.
P55			-4				-4.06			0.006 ± j 0.496	B	0.494	3.5	Sufficient damping. Gust effects minimal.
P56			-5				-5.04			-0.005 ± j 0.445	B	0.508	3.0	Can maneuver and hover quite well. M_{δ_e} set by gusts on attitude.
P57	1.00	-0.05	-3	0	7.7	0	-3.11			0.028 ± j 0.567	B	0.532	5.25	Requires considerable attention and effort. Hovering accuracy fairly good. Difficult to maneuver.
P58			-4				-4.06			0.006 ± j 0.496	B	0.608	4.75	Needs more damping. A lot of effort to hover. Oscillatory.
P59			-5				-5.04			-0.005 ± j 0.445	B	0.650	4.25	Requires constant attention and careful control to maneuver accurately.
P60			-6				-6.03			-0.011 ± j 0.407	B	0.697	3.5	Desire a little more damping. Occasionally get upset by gusts. Requires attention.
P61	0.33	-0.25	-1	0	0	0	-1.26			0.005 ± j 0.512	A	0.241	4.25	Lightly damped. Overshoot on θ commands. No gusts.
P62			-2				-2.09			-0.082 ± j 0.389	A	0.267	2.75	Responsive to control inputs. Stable. Maneuvers slowly.
P63			-3				-3.04			-0.106 ± j 0.312	A	0.278	2.75	A little overshoot in θ commands. No gusts evident. Easy to stop when maneuvering.
P64			-4				-4.02			-0.114 ± j 0.263	A	0.328	2.5	Well damped. Rate dynamics. High drag requires large attitudes to maneuver.

TABLE A-II (Continued)

Case	$M_u g$	X_u	M_q	M_θ	σ_{u_g}	SFG	Real Roots RR (1)	RR (2)	RR (3)	Complex Roots $-\zeta\omega_n \pm j\omega_d$	Pilot	M_{δ_e}	PR	Summary of Pilot Comments
P65	0.33	-0.25	-1	0	2.6	0	-1.26			0.005 ± j 0.512	A	0.268	4.75	Requires rapid control reversal to stabilize. Notice position disturbances.
P66			-2				-2.09			-0.082 ± j 0.389	A	0.278	3.75	Fairly good attitude control. Position disturbances a factor on PR.
P67			-3				-3.04			-0.106 ± j 0.312	A	0.309	3.5	Good attitude control. Accurate hovering requires a lot of stick motion.
P68			-4				-4.02			-0.114 ± j 0.263	A	0.350	3.0	Well damped. Some attention required to hover. Maneuvers slowly.
P69	0.33	-0.25	-1	0	5.1	0	-1.26			0.005 ± j 0.512	A	0.294	5.0	Very oscillatory. Hovering performance poor. Mission doubtful.
P70			-2				-2.09			-0.082 ± j 0.389	A	0.326	4.25	Principal problem is position control. More damping desirable.
P71			-3				-3.04			-0.106 ± j 0.312	A	0.348	3.75	Good attitude control. Poor hovering performance. PR limited by position disturbances.
P72			-4				-4.02			-0.114 ± j 0.263	A	0.403	3.75	Well damped. Large attitude disturbances required to hover. Speed control difficult when maneuvering.
P73	0.33	-0.25	-1	0	7.7	0	-1.26			0.005 ± j 0.512	A	0.339	5.5	Very lightly damped. Seem to have θ disturbances in addition to large position disturbances.
P74			-2				-2.09			-0.082 ± j 0.389	A	0.362	5.0	Need more damping. Large θ changes required to hold position.
P75			-3				-3.04			-0.106 ± j 0.312	A	0.391	4.75	Fairly well damped. Hovering and maneuvering difficult.
P76			-4				-4.02			-0.114 ± j 0.263	A	0.422	4.5	Well damped. A lot of work just to hover. PR limited by position disturbances.
P77	1.00	-0.25	-1	0	0	0	-1.52			0.134 ± j 0.800	B	0.264	2.75	Oscillatory. Difficult to develop maneuvering velocity.
P78			-2				-2.23			-0.011 ± j 0.670	B	0.292	2.25	A little oscillatory. Easy to maneuver. M_{δ_e} set to offset speed stability when maneuvering.
P79			-3				-3.11			-0.069 ± j 0.563	B	0.363	1.75	Well damped. Like high drag. Can stop with precision.
P80			-4				-4.06			-0.093 ± j 0.487	B	0.384	1.75	M_{δ_e} set to overcome damping. Easy to maneuver.

TABLE A-II (Continued)

Case	$M_u g$	X_u	M_q	M_θ	σ_{u_g}	SFG	Real Roots RR (1)	Real Roots RR (2)	Real Roots RR (3)	Complex Roots $-\zeta\omega_n \pm j\omega_d$	Pilot	M_{δ_e}	PR	Summary of Pilot Comments
P81	1.00	-0.25	-1	0	2.6	0	-1.52			0.134 ± j 0.800	B	0.316	3.75	Attitude quite oscillatory. Good task performance. Some overshoot on θ commands.
P82	↓	↓	-2	↓	↓	↓	-2.23			-0.011 ± j 0.670	B	0.357	3.25	M_{δ_e} set to overcome drag and speed stability when maneuvering.
P83	↓	↓	-3	↓	↓	↓	-3.11			-0.069 ± j 0.563	B	0.403	3.0	Well damped. Appears a little oscillatory. Can hover accurately.
P84	↓	↓	-4	↓	↓	↓	-4.06			-0.093 ± j 0.487	B	0.437	2.75	Attitude not too active. M_{δ_e} set to overcome position disturbances in hover.
P85	1.00	-0.25	-2	0	5.1	0	-2.23			-0.011 ± j 0.670	B	0.399	4.5	Considerable effort required. Gust disturbances on attitude and position. Can perform task.
P86	↓	↓	-3	↓	↓	↓	-3.11			-0.069 ± j 0.563	B	0.454	4.0	Oscillatory in pitch. Desire a little more damping. Continuously disturbed in position.
P87	↓	↓	-4	↓	↓	↓	-4.06			-0.093 ± j 0.487	B	0.487	3.75	Maneuvering not too difficult. Hovering requires large θ changes.
P88	↓	↓	-5	↓	↓	↓	-5.04			-0.104 ± j 0.433	B	0.517	3.5	Good pitch dynamics. Maneuvers quite well. A lot of concentration required to hover.
P89	1.00	-0.25	-3	0	7.7	0	-3.11			-0.069 ± j 0.563	B	0.539	4.5	Bothered by pitch oscillations when maneuvering. Work load high.
P90	↓	↓	-4	↓	↓	↓	-4.06			-0.093 ± j 0.487	B	0.581	4.5	Fairly good pitch dynamics. M_{δ_e} set to overcome damping when large θ changes required.
P91	↓	↓	-5	↓	↓	↓	-5.04			-0.104 ± j 0.433	B	0.600	4.25	Position disturbances overshadow everything else. Hovering performance poor.
P92	↓	↓	-6	↓	↓	↓	-6.03			-0.111 ± j 0.392	B	0.627	4.25	Good attitude characteristics. Position disturbances limit PR.
P93	0.33	-0.05	-0.5	0	5.1	0	-0.92			-0.184 ± j 0.574	A	0.243	4.75	Difficult to command and hold attitude when maneuvering. Very unstable.
P94	↓	↓	↓	-1	↓	↓	-0.40			-0.076 ± j 0.979	A	0.253	4.0	Unstable. Not too difficult to control θ. No gust effects. Requires attention to stabilize.
P95	↓	↓	↓	-2	↓	↓	-0.22			-0.164 ± j 1.388	A	0.256	3.25	A little too high in frequency. Springy. Doesn't diverge, but difficult to hold attitude.
P96	↓	↓	↓	-3	↓	↓	-0.16			-0.193 ± j 1.710	A	0.269	3.5	Too oscillatory. Easy to hover, but difficult to command attitude when maneuvering.
P97	↓	↓	↓	-4	↓	↓	-0.13			-0.208 ± j 1.981	A	0.268	3.75	Too much attitude stability. High frequency oscillation. Stable, but lightly damped.

TABLE A-II (Continued)

Case	$M_u g$	X_u	M_q	M_θ	σ_{u_g}	SFG	Real Roots RR (1)	RR (2)	RR (3)	Complex Roots $-\zeta\omega_n \pm j\omega_d$	Pilot	M_{δ_e}	PR	Summary of Pilot Comments
P98	0.33	-0.05	-1.0	0	5.1	0	-1.23			0.090 ± j 0.513	A	0.261	4.25	Gust effects minimal. Difficult to command attitude. Rapid control reversal required to stabilize.
P99				-2			-0.23			-0.408 ± j 1.301	A	0.287	3.5	Stable, but difficult to hold attitude. Easy to hover. Low drag makes it difficult to maneuver accurately.
P100				-3			-0.17			-0.442 ± j 1.646	A	0.301	3.0	Stable, not too oscillatory. No problems with trim changes. Gusts evident on θ, but not problem.
P101	↓	↓	↓	-4	↓	↓	-0.14			-0.457 ± j 1.928	A	0.312	3.5	Very stable. Notice gusts on attitude. Difficult to control θ with precision. Desire more drag.
P102	0.33	-0.05	0	-2	5.1	0	-0.21			0.081 ± j 1.424	A	0.262	4.25	Performance fairly good, but slightly unstable and gusts disturb pitch. A little too oscillatory.
P103			-0.5				-0.22			-0.164 ± j 1.388	A	0.282	3.75	Needs damping. Gusts somewhat annoying on pitch. Have some overshoot on θ commands.
P104			-1.0				-0.23			-0.408 ± j 1.301	A	0.288	2.75	Good attitude stability. Very little overshoot on θ commands. Gust effects minimal.
P105			-2.0				-0.27			-0.892 ± j 0.911	A	0.321	2.25	Maneuvering determines M_{δ_e}. Good performance. Would like a little more drag for maneuvering.
P106	↓	↓	-3.0	↓	↓	↓	-2.14	-0.52	-0.39		A	0.341	2.25	Very good. Attitude command response. Very stable. Gusts not evident. A little more drag desirable.
P107	1.00	-0.05	-1	0	5.1	0	-1.48			0.213 ± j 0.795	A B	0.412 0.389	4.75 4.5	Very oscillatory and unstable. Large gust attitude disturbances. Large attitude overshoots.
P108				-1			-1.03			-0.012 ± j 1.012	A B	0.417 0.427	4.5 4.5	Needs damping. Very oscillatory. Difficult to select satisfactory M_{δ_e}. Poor maneuvering performance.
P109				-2			-0.62			-0.217 ± j 1.318	A B	0.422 0.425	4.0 3.5	Can maneuver quite well. M_{δ_e} set by trim and response characteristics while maneuvering.
P110				-3			-0.41			-0.319 ± j 1.639	A B	0.421 0.484	3.75 4.0	Somewhat oscillatory. M_{δ_e} needed for trim effects makes attitude too sensitive to control inputs.
P111	↓	↓	↓	-4	↓	↓	-0.31			-0.368 ± j 1.919	A B	0.430 0.449	4.0 4.0	Very oscillatory but stable. Difficult to hold attitude when maneuvering. Too sensitive to control inputs.

TABLE A-II (Continued)

Case	$M_u g$	X_u	M_q	M_θ	σ_{u_g}	SPG	Real Roots RR (1)	RR (2)	RR (3)	Complex Roots $-\zeta\omega_n \pm j\omega_d$	Pilot	M_{δ_e}	PR	Summary of Pilot Comments
P112	1.00	-0.05	-2	0	5.1	0	-2.21			-0.080 ± j 0.668	A	0.439	4.25	Seems unstable. Lightly damped. Attitude gust disturbances big annoyance, but can be controlled.
P113				-2			-1.05			-0.501 ± j 0.894	A	0.470	4.0	Attitude stable, but still bothered by gusts on attitude. Very oscillatory.
P114				-3			-0.49			-0.778 ± j 1.314	A	0.472	3.75	Too much attitude activity. A lot of attention required to hold in hover.
P115				-4			-0.34			-0.854 ± j 1.669	A	0.461	3.75	Gusts disturb attitude. Springy response to control inputs. Difficult to command θ while maneuvering.
P116			-5	0			-5.04			-0.005 ± j 0.445	A	0.538	2.75	Low attitude activity. Seems well damped. Control effort is low, relaxed.
P117	0.33	-0.20	-0.5	0	5.1	0	-0.96			0.129 ± j 0.575	B	0.250	5.0	Poorly damped. Large overshoots to control inputs. Large attitude motions present.
P118				-1			-0.53			-0.086 ± j 1.001	B	0.251	4.0	Lightly damped. M_{δ_e} set by hovering requirements. Large position disturbances.
P119				-2			-0.37			-0.165 ± j 1.397	B	0.260	3.75	Can control attitude quite well. Stable.
P120				-3			-0.31			-0.193 ± j 1.715	B	0.265	4.25	Attitude stability too high. Must follow up pitch commands with stick. Springy response.
P121				-4			-0.28			-0.208 ± j 1.985	B	0.275	4.5	Too much attitude feedback. Don't experience large upsets even when attention diverted.
P122	0.33	-0.20	-1	0	5.1	0	-1.25			0.026 ± j 0.515	B	0.267	4.25	Good pitch response. Position loop requires a lot of attention to control disturbances.
P123				-1			-0.63			-0.283 ± j 0.872	B	0.266	3.75	Like attitude control. PR limited by position disturbances.
P124				-2			-0.39			-0.406 ± j 1.311	B	0.263	4.0	Position-loop performance dominates PR. Stable.
P125				-3			-0.32			-0.440 ± j 1.651	B	0.266	4.25	Somewhat oscillatory. Requires concentration to maneuver.
P126				-4			-0.29			-0.456 ± j 1.931	B	0.278	4.5	Get high frequency, low amplitude response to control inputs. Too oscillatory.

TABLE A-II (Concluded)

Case	$M_u g$	X_u	M_q	M_θ	σ_{u_g}	SFG	Real Roots RR (1)	Real Roots RR (2)	Real Roots RR (3)	Complex Roots $-\zeta\omega_n \pm j\omega_d$	Pilot	M_{δ_e}	PR	Summary of Pilot Comments
P127	1.00	-0.2	-1	0	5.1	0	-1.51			0.154 ± j 0.800	A B	0.427 0.443	4.75 5.0	Unstable. Gusts annoying in attitude and position. Cannot divert attention from attitude.
P128			-2				-0.75			-0.224 ± j 1.346	A B	0.430 0.461	4.5 4.75	Attitude very active. Requires attention. Maneuvers at very slow speed.
P129			-3				-0.56			-0.318 ± j 1.655	A B	0.411 0.462	4.5 4.5	Rapid θ response but overshoots desired attitude. Large θ changes required to hover and maneuver.
P130			-4				-0.47			-0.367 ± j 1.930	A B	0.438 0.458	4.0 4.0	Gusts major problem. Attitude stability helpful in stabilizing aircraft.
P131				-5			-0.41			-0.395 ± j 2.173	A	0.456	4.25	Very oscillatory. Springy. Difficult to command and hold attitude changes required to maneuver.
P132	1.00	-0.2	-2	0	5.1	0	-2.22			0.011 ± j 0.671	B	0.429	4.0	Desire more damping. Large θ changes required when hovering to offset position distrubances.
P133			-2				-1.17			-0.514 ± j 0.965	B	0.427	4.25	Oscillatory, but not too difficult to control. High drag helpful when maneuvering.
P134			-3				-0.67			-0.762 ± j 1.338	B	0.435	3.75	Good maneuvering case. Hover not too difficult. PR limited by position disturbances.
P135				-4			-0.51			-0.846 ± j 1.681	B	0.438	4.25	Very oscillatory. M_{δ_e} needed for maneuvering too high for hover. Difficult to command attitude.
P136			-0.5	-3			-0.53			-0.084 ± j 1.733	B	0.378	4.75	Very responsive and oscillatory but doesn't diverge. Controllable but more damping desirable.
P137	0.67	-0.1	-1	0	5.1	1.5	-1.38			0.139 ± j 0.682	A B	0.317 0.339	4.75 5.0	Gusts and unstable dynamics require a lot of attention. A: SFG reduces inadvertent stick inputs. B: Don't like SFG with sensitive (acceleration) attitude response.
P138			-2				-2.15			0.026 ± j 0.556	A B	0.354 0.397	3.75 4.0	Fairly good attitude dynamics. Some gust disturbances. A: Like SFG. B: No comment on SFG.
P139			-3				-3.07			-0.014 ± j 0.466	A B	0.408 0.443	3.25 3.5	Good attitude control. Good performance but requires effort. B: Lateral SFG too high, longitudinal SFG acceptable.
P140			-4				-4.04			-0.029 ± j 0.405	A B	0.448 0.488	2.75 3.25	Easy to control. SFG gradient desirable with rate dynamics. Can hover accurately with little effort.

TABLE A-III

LATERAL HANDLING QUALITIES RESULTS FROM HOVERING AND LOW-SPEED MANEUVERING TASK

Note: Longitudinal and directional parameters given in Table A-I

Case	L_{v_g}	Y_v	L_p	L_ϕ	σ_{v_g}	SFG	Real Roots RR (1)	Real Roots RR (2)	Real Roots RR (3)	Complex Roots $-\zeta\omega_n \pm j\omega_d$	Pilot	L_{δ_a}	PR	Summary of Pilot Comments
R1	0	0	-1	0	5.1	0	-1.00	0.0	0.0		A B	0.217 0.230	4.25 4.5	Roll PIO tendencies. Requires attention. Needs damping.
R2			-2				-2.00	0.0	0.0		A B	0.247 0.254	3.5 3.0	Rapid roll response. Some overshoot on ϕ commands. No gust disturbances evident.
R3			-3				-3.00	0.0	0.0		A B	0.301 0.295	2.75 2.25	Good roll rate control. Response to control very predictable. Pleasant to hover.
R4			-4				-4.00	0.0	0.0		A B	0.359 0.358	2.75 2.25	Excellent roll control. No gusts evident. Somewhat difficult to stop with precision when maneuvering.
R5	-0.33	0	-1	0	5.1	0	-1.22			0.111 ± j 0.510	A B	0.222 0.233	4.5 4.5	Must anticipate roll response. PIO tendencies. Notice gusts in roll. Needs damping.
R6			-2				-2.08			0.038 ± j 0.398	A B	0.251 0.263	3.75 3.25	Fairly good roll control. L_{δ_a} set by maneuvering requirements. Difficult to arrest position velocity.
R7			-3				-3.04			0.018 ± j 0.331	A B	0.307 0.313	3.0 2.5	Good roll control. No gusts evident.
R8			-4				-4.02			0.010 ± j 0.288	A B	0.373 0.363	2.75 2.5	Excellent roll control. Rate response to δ_a. L_{δ_a} set by maneuvering.
R9	-0.67	0	-1	0	5.1	0	-1.36			0.180 ± j 0.677	A B	0.236 0.261	5.25 4.5	Difficult to control ϕ when maneuvering. Speed stability a minor annoyance. Difficult to maneuver accurately.
R10			-2				-2.14			0.072 ± j 0.553	A B	0.274 0.285	4.0 3.5	Needs a little more damping for good roll control.
R11			-3				-3.07			0.035 ± j 0.465	A B	0.324 0.320	3.5 3.0	Good roll control. Must anticipate hovering position when maneuvering.
R12			-4				-4.04			0.020 ± j 0.406	A B	0.385 0.313	3.0 2.75	Easy to hover. Gusts not evident. Need drag to improve maneuvering.
R13	-1.0	0	-1	0	5.1	0	-1.46			0.233 ± j 0.792	A B	0.294 0.274	6.0 5.0	PIO in roll a problem. Annoyed by gusts in hover. Needs damping.
R14			-2				-2.20			0.103 ± j 0.665	A B	0.320 0.305	4.5 4.25	L_{δ_a} set by gust effects on roll. Needs more damping to be satisfactory.
R15			-3				-3.10			0.052 ± j 0.565	A B	0.374 0.354	3.75 3.25	Fairly good roll control, but gust effects require effort.
R16			-4				-4.06			0.030 ± j 0.495	A B	0.415 0.413	3.50 3.0	Good roll control. Gusts on ϕ noticeable, but no problem. Needs drag and lower speed stability for maneuvering.

TABLE A-III (Continued)

Case	L_{v_g}	Y_v	L_p	L_ϕ	σ_{v_g}	SFG	Real Roots RR (1)	Real Roots RR (2)	Real Roots RR (3)	Complex Roots $-\zeta\omega_n \pm j\omega_d$	Pilot	L_{δ_a}	PR	Summary of Pilot Comments
R17	0	-0.1	-1	0	5.1	0	-1.00	-0.10	0.0		A B	0.210 0.220	4.0 4.25	Some PIO tendencies in hover. Needs damping. Notice position disturbances.
R18			-2				-2.00	-0.10	0.0		A B	0.248 0.238	3.25 3.25	Adequate damping. Good maneuvering case.
R19			-3				-3.00	-0.10	0.0		A B	0.294 0.295	2.75 2.75	Easy to hover and maneuver. Little effort required.
R20			-4				-4.00	-0.10	0.0		A B	0.363 0.349	2.5 2.5	Maneuvering determines L_{δ_a} level. Notice gusts on position in hover.
R21	-0.33	-0.1	-1	0	5.1	0	-1.24			0.068 ± j 0.514	A B	0.237 0.246	4.5 4.5	Requires constant effort to stabilize and recover from small gust disturbances.
R22			-2				-2.08			-0.010 ± j 0.400	A B	0.265 0.267	3.75 3.5	Hover fairly accurately with moderate effort. Fairly good ϕ control.
R23			-3				-3.04			-0.031 ± j 0.330	A B	0.321 0.308	3.0 3.0	Adequate damping. Gust disturbances small. Good maneuvering capability.
R24			-4				-4.02			-0.039 ± j 0.285	A B	0.378 0.377	2.5 2.75	Good roll control. Little effort required. Notice hovering position disturbances.
R25	-0.67	-0.1	-1	0	5.1	0	-1.38			0.139 ± j 0.682	A B	0.238 0.253	5.5 5.0	Difficult to control ϕ accurately. Gust disturbances on ϕ annoying.
R26			-2				-2.15			0.026 ± j 0.556	A B	0.306 0.289	4.25 4.0	Some overshoot on ϕ commands. Hovering accuracy unimpaired.
R27			-3				-3.07			-0.013 ± j 0.466	A B	0.338 0.348	3.25 3.25	Slightly annoyed by speed stability and gusts. Good roll control.
R28			-4				-4.04			-0.029 ± j 0.405	A B	0.399 0.396	3.25 3.0	Good maneuvering case. Gusts on hovering position require continuous effort.
R29	-1.0	-0.1	-1	0	5.1	0	-1.48			0.193 ± j 0.797	A B	0.285 0.291	6.0 5.5	Very difficult to stabilize. Gusts add to problem. Needs damping.
R30			-2				-2.21			0.057 ± j 0.670	A B	0.326 0.313	4.25 4.5	Requires effort to command and hold ϕ. Inadvertently introduce large ϕ when maneuvering.
R31			-3				-3.11			0.004 ± j 0.567	A B	0.388 0.389	3.75 3.75	Gusts on ϕ make more damping desirable, but not necessary for good task performance.
R32			-4				-4.06			-0.019 ± j 0.496	A B	0.434 0.434	3.0 3.25	Good roll control, but speed stability annoying when maneuvering. Gusts still disturb ϕ.

TABLE A-III (Continued)

Case	L_{v_g}	Y_v	L_p	L_ϕ	σ_{v_g}	SFG	Real Roots RR (1)	Real Roots RR (2)	Real Roots RR (3)	Complex Roots $-\zeta\omega_n \pm j\omega_d$	Pilot	L_{δ_a}	PR	Summary of Pilot Comments
R33	0	-0.2	-1	0	5.1	0	-1.00	-0.20	0.0		A B	0.257 0.239	4.25 4.5	Position gust disturbances fairly large. Introduce large roll transients when hovering and maneuvering.
R34			-2				-2.00	-0.20	0.0		A B	0.289 0.275	3.0 3.5	A little overshoot on ϕ commands, but good hovering and maneuvering performance.
R35			-3				-3.00	-0.20	0.0		A B	0.321 0.341	2.5 3.25	Good roll control. Lateral position disturbances require continuous control activity to hover accurately.
R36			-4				-4.00	-0.20	0.0		A B	0.390 0.380	2.5 3.0	Good maneuvering capability. Position disturbances a little annoying.
R37	-0.33	-0.2	-1	0	5.1	0	-1.25			0.026 ± j 0.515	A B	0.246 0.253	4.75 5.0	Requires effort to stabilize. Difficult to command and hold roll angles.
R38			-2				-2.08			-0.058 ± j 0.396	A B	0.303 0.293	3.5 3.75	Roll control fairly good, but requires some attention. Gusts not much of a problem.
R39			-3				-3.04			-0.081 ± j 0.321	A B	0.341 0.367	2.5 3.25	Good roll control. Position control difficult when hovering and maneuvering due to gust disturbances.
R40			-4				-4.02			-0.089 ± j 0.274	A B	0.388 0.388	2.5 3.25	Rating limited by position-loop control problems due to gusts.
R41	-0.67	-0.2	-1	0	5.1	0	-1.40			0.099 ± j 0.684	A B	0.297 0.287	5.0 6.0	Difficult to stabilize roll. Poor task performance. Difficult to select a satisfactory L_{δ_a}.
R42			-2				-2.16			-0.021 ± j 0.556	A B	0.321 0.309	4.0 4.25	Some overshoot on ϕ commands. Needs more damping. Gusts annoying on both ϕ and y.
R43			-3				-3.08			-0.062 ± j 0.462	A B	0.370 0.383	3.0 3.5	Adequate roll damping. Good maneuvering performance.
R44			-4				-4.04			-0.078 ± j 0.398	A B	0.441 0.401	2.75 3.5	Only problem is controlling hovering position accurately.
R45	-1.0	-0.2	-1	0	5.1	0	-1.51			0.154 ± j 0.800	A B	0.320 0.289	5.5 6.5	Very difficult to stabilize. Get upset by gust disturbances.
R46			-2				-2.22			0.011 ± j 0.671	A B	0.387 0.348	4.25 4.5	Considerable effort to get acceptable performance. Difficult to maintain constant lateral velocity.
R47			-3				-3.11			-0.045 ± j 0.565	A B	0.411 0.411	3.5 4.0	A little too oscillatory. Gusts annoying on ϕ and y.
R48			-4				-4.06			-0.068 ± j 0.491	A B	0.471 0.448	3.25 3.75	Good roll control and maneuvering characteristics. Position disturbances limit PR.

TABLE A-III (Continued)

Case	L_{v_g}	Y_v	L_p	L_ϕ	σ_{v_g}	SFG	Real Roots RR (1)	RR (2)	RR (3)	Complex Roots $-\zeta\omega_n \pm j\omega_d$	Pilot	L_{δ_a}	PR	Summary of Pilot Comments
R49	0	-0.3	-1	0	5.1	0	-1.00	-0.30	0.0		A B	0.236 0.347	4.5 4.5	Needs more roll damping. Task performance satisfactory. Position disturbances large.
R50			-2				-2.00	-0.30	0.0		A B	0.284 0.374	3.75 3.75	Probably adequate damping. Difficult to hold position.
R51			-3				-3.00	-0.30	0.0		A B	0.371 0.417	3.25 3.5	Very good roll control. Gust disturbance on ϕ might help position control.
R52			-4				-4.00	-0.30	0.0		A B	0.387 0.476	3.0 3.5	Hovering accuracy requires effort. PR limited by position disturbances.
R53	-0.33	-0.3	-1	0	5.1	0	-1.27			-0.015 ± j 0.512	A B	0.270 0.345	5.0 5.0	Attempts to tighten up on position control results in PIO's. Requires attention to stabilize.
R54			-2				-2.09			-0.105 ± j 0.385	A B	0.301 0.378	4.0 3.75	Would like a little more damping. With effort task performance satisfactory.
R55			-3				-3.04			-0.130 ± j 0.304	A B	0.358 0.392	3.5 3.5	Adequate damping. Position disturbances limit better PR.
R56			-4				-4.02			-0.139 ± j 0.252	A B	0.391 0.489	3.0 3.5	Very good roll control, but position disturbances large.
R57	-0.67	-0.3	-1	0	5.1	0	-1.42			0.060 ± j 0.683	A B	0.290 0.372	6.0 5.0	Large overshoots in roll control. Task performance poor.
R58			-2				-2.16			-0.067 ± j 0.551	A B	0.340 0.409	4.5 4.5	Requires attention to avoid overshoots in roll. Gusts annoying in roll and position.
R59			-3				-3.08			-0.111 ± j 0.452	A B	0.395 0.432	3.75 4.0	Adequate damping. Must hold large roll angle to sustain lateral velocity.
R60			-4				-4.04			-0.128 ± j 0.385	A B	0.438 0.498	3.5 3.75	Good roll control. A lot of stick activity required to hover.
R61	-1.0	-0.3	-1	0	5.1	0	-1.53			0.115 ± j 0.800	A B	0.352 0.402	7.0 5.5	Very difficult to control roll. Large upsets due to gusts.
R62			-2				-2.23			-0.034 ± j 0.668	A B	0.424 0.446	5.0 4.75	Difficult to hover. Gusts on both ϕ and y annoying. Needs more damping.
R63			-3				-3.11			-0.093 ± j 0.559	A B	0.468 0.506	4.25 4.0	Fairly good roll control. High speed-stability annoying when maneuvering.
R64			-4				-4.06			-0.117 ± j 0.482	A B	0.484 0.573	3.75 4.0	No gust effects on ϕ noticed. Speed-stability and drag too high for maneuvering.

TABLE A-III (Continued)

Case	$L_v g$	Y_v	L_p	L_ϕ	σ_{v_g}	SFG	Real Roots RR (1)	RR (2)	RR (3)	Complex Roots $-\zeta\omega_n \pm j\omega_d$	Pilot	L_{δ_a}	PR	Summary of Pilot Comments
R65	-0.33	-0.05	-1	0	0	0	-1.23			0.090 ± j 0.513	A	0.228	4.25	Unstable, requires attention. With effort get satisfactory task performance.
R66			-2				-2.08			0.014 ± j 0.400	A	0.261	2.75	No apparent disturbances. Fairly good roll control.
R67			-3				-3.04			-0.007 ± j 0.331	A	0.354	2.0	Pleasant to fly. Very good ϕ control. L_{δ_a} set by maneuvering.
R68			-4				-4.02			-0.014 ± j 0.287	A	0.393	2.0	Easy to hover. Good maneuvering performance.
R69	-0.33	-0.05	-1	0	5.1	0	-1.23			0.090 ± j 0.513	A	0.247	4.5	Hovering requires some effort. Needs damping. Task requires effort.
R70			-2				-2.08			0.014 ± j 0.400	A	0.284	3.0	Notice gusts on ϕ. L_{δ_a} set by hovering. Like level of speed stability.
R71			-3				-3.04			-0.007 ± j 0.331	A	0.305	2.75	Control effort low. Adequate damping.
R72			-4				-4.02			-0.014 ± j 0.287	A	0.376	2.5	Uncertain if gusts present. Low drag requires anticipating hovering point when maneuvering.
R73	-0.33	-0.05	-1	0	7.7	0	-1.23			0.090 ± j 0.513	A	0.254	5.0	Lightly damped. Gusts pose a problem. Have PIO tendencies.
R74			-2				-2.08			0.014 ± j 0.400	A	0.306	3.75	Gusts on ϕ a little annoying. Roll control fairly good.
R75			-3				-3.04			-0.007 ± j 0.331	A	0.372	3.0	Adequate damping. Gust effects minimal. Good ϕ control.
R76			-4				-4.02			-0.014 ± j 0.287	A	0.383	3.0	Gusts no problem. Maneuvering performance good since easy to command and hold ϕ.
R77	-0.33	-0.05	-1	0	10.3	0	-1.23			0.090 ± j 0.513	A	0.296	6.0	Gust disturbances in roll large. Hovering task performance poor. High control effort required.
R78			-2				-2.08			0.014 ± j 0.400	A	0.349	4.5	Needs more damping. Gust effects on ϕ annoying. Considerable effort required to perform task.
R79			-3				-3.04			-0.007 ± j 0.331	A	0.387	3.5	Task performance fairly good although some effort required. Disturbances on ϕ most annoying.
R80			-4				-4.02			-0.014 ± j 0.287	A	0.421	3.25	Gust disturbances on ϕ rather small. Good roll control. Good maneuvering performance.

TABLE A-III (Continued)

Case	L_{v_g}	Y_v	L_p	L_ϕ	σ_{v_g}	SFG	Real Roots RR (1)	RR (2)	RR (3)	Complex Roots $-\zeta\omega_n \pm j\omega_d$	Pilot	L_{δ_a}	PR	Summary of Pilot Comments
R81	-1.00	-0.05	-1	0	0	0	-1.48			0.213 ± j 0.795	B	0.210	5.0	Difficult to stabilize. Tend to induce overshoots and oscillations when hovering a. i maneuvering.
R82			-2				-2.21			0.080 ± j 0.668	B	0.264	3.0	Almost adequate damping. Some tendency to induce too large roll angles when maneuvering.
R83			-3				-3.10			0.028 ± j 0.567	B	0.302	2.5	Easy to hover and maneuver. No disturbances. L_{δ_a} set to overcome speed stability when maneuvering.
R84			-4				-4.06			0.006 ± j 0.496	B	0.354	2.5	Good roll control. No trim problems when maneuvering. No disturbances noticeable.
R85	-1.00	-0.05	-1	0	2.6	0	-1.48			0.213 ± j 0.795	B	0.240	5.0	Very oscillatory. Difficult to command and hold roll angle. Notice turbulence effects on ϕ.
R86			-2				-2.21			0.080 ± j 0.668	B	0.275	3.0	Prefer a little more damping. No PIO problems. Some tendency to slide by desired hovering position.
R87			-3				-3.10			0.028 ± j 0.567	B	0.321	2.5	Well damped. Noticed gusts on roll, but no problem. Pleasant.
R88			-4				-4.06			0.006 ± j 0.496	B	0.376	2.5	Easy to fly. Gusts minimal. Would like a little more drag to improve maneuvering.
R89	-1.00	-0.05	-1	0	5.1	0	-1.48			0.213 ± j 0.795	B	0.268	5.5	Quite difficult to control. Roll very responsive to gusts and control inputs. Too much effort required.
R90			-2				-2.21			0.080 ± j 0.668	B	0.300	4.5	Needs more damping. Upset by gusts in hovering and maneuvering.
R91			-3				-3.10			0.028 ± j 0.567	B	0.352	3.5	Concentration required to control gust effects. Large effort to hover accurately. L_{δ_a} set by hovering requirements.
R92			-4				-4.06			0.006 ± j 0.496	B	0.402	3.0	Adequate damping, but controlling gusts requires some effort. Task performance satisfactory.
R93	-1.00	-0.05	-1	0	7.7	0	-1.48			0.213 ± j 0.795	B	0.351	6.5	Exhausting just to stabilize. Roll in constant motion. Violent control motions required.
R94			-2				-2.21			0.080 ± j 0.668	B	0.387	5.0	Difficult to control. Gust disturbances large. Response to control inputs is predictable.
R95			-3				-3.10			0.028 ± j 0.567	B	0.413	4.0	Concentration required to hover accurately. Gusts disturbing in roll.
R96			-4				-4.06			0.006 ± j 0.496	B	0.452	3.5	Gust disturbances enough to make control difficult. Fairly good roll control, but effort high.

TABLE A-III (Continued)

Case	$L_v g$	Y_v	L_p	L_ϕ	σ_{v_g}	SFG	Real Roots RR (1)	Real Roots RR (2)	Real Roots RR (3)	Complex Roots $-\zeta\omega_n \pm j\omega_d$	Pilot	L_{δ_a}	PR	Summary of Pilot Comments
R97	-0.33	-0.25	-1	0	0	0	-1.26			0.005 ± j 0.512	A	0.265	4.5	Needs a little more damping to improve roll control. High drag. Fairly good maneuvering performance.
R98			-2				-2.09			-0.082 ± j 0.389	A	0.300	2.75	Seems stable. Good roll control. No disturbances. Little effort to hover.
R99			-3				-3.04			-0.105 ± j 0.312	A	0.335	2.0	Control effort low. Good task performance. No disturbances evident.
R100			-4				-4.02			-0.114 ± j 0.262	A	0.358	2.0	Good. Rate dynamics in roll. Precision performance in hovering and maneuvering.
R101	-0.33	-0.25	-1	0	2.6	0	-1.26			0.005 ± j 0.512	A	0.279	4.75	Lightly damped. PIO tendencies at times. Gusts very annoying. Wouldn't want another loop like this.
R102			-2				-2.09			-0.082 ± j 0.389	A	0.298	3.0	Notice gusts on roll and position while hovering. Effort fairly high. L_{δ_a} set by maneuvering.
R103			-3				-3.04			-0.105 ± j 0.312	A	0.340	2.25	Very good roll control. Notice gusts on position.
R104			-4				-4.02			-0.114 ± j 0.262	A	0.382	2.0	Very easy to fly. Task performance good.
R105	-0.33	-0.25	-1	0	5.1	0	-1.26			0.005 ± j 0.512	A	0.290	5.5	Work load high. Gust disturbances make it difficult to control. Task performance poor.
R106			-2				-2.09			-0.082 ± j 0.389	A	0.305	4.25	Need more damping to improve roll control so position disturbances can be controlled. Control activity high.
R107			-3				-3.04			-0.105 ± j 0.312	A	0.378	3.25	Task performance not too bad. Requires effort to control position.
R108			-4				-4.02			-0.114 ± j 0.262	A	0.419	3.0	Effort rather high. More damping may improve PR. Good maneuvering performance.
R109	-0.33	-0.25	-1	0	7.7	0	-1.26			0.005 ± j 0.512	A	0.313	6.0	Task performance in doubt. Landing would be difficult. Hard to separate effects of gusts on roll from position.
R110			-2				-2.09			-0.082 ± j 0.389	A	0.349	5.0	Most of problem with position, but needs more damping. Large changes in ϕ to hold hovering position.
R111			-3				-3.04			-0.105 ± j 0.312	A	0.403	3.75	Effort to hold hovering position. Good roll control. Position disturbances large.
R112			-4				-4.02			-0.114 ± j 0.262	A	0.451	3.5	No gusts on ϕ, just position. A lot of ϕ and control activity required. Doubt if more damping will help.

TABLE A-III (Continued)

Case	$L_v g$	Y_v	L_p	L_ϕ	σ_{v_g}	SFG	Real Roots RR (1)	Real Roots RR (2)	Real Roots RR (3)	Complex Roots $-\zeta\omega_n \pm j\omega_d$	Pilot	L_{δ_a}	PR	Summary of Pilot Comments
R113	-1.00	-0.25	-1	0	0	0	-1.52			0.134 ± j 0.800	B	0.266	4.0	L_{δ_a} set to overcome oscillations and overshoots in roll angle. Response to control somewhat unpredictable.
R114			-2				-2.23			-0.011 ± j 0.670	B	0.323	2.0	Easy to maneuver with precision. High speed stability noticeable, but no problem. No disturbances.
R115			-3				-3.11			-0.069 ± j 0.563	B	0.356	2.0	Good control. Damping appears to be more than sufficient.
R116			-4				-4.06			-0.093 ± j 0.487	B	0.382	2.0	Very easy to perform task. Seems a little sluggish in roll.
R117	-1.00	-0.25	-1	0	2.6	0	-1.52			0.134 ± j 0.800	B	0.315	4.0	Needs more damping. Oscillations tend to develop when maneuvering. Have gust disturbances on position.
R118			-2				-2.23			-0.011 ± j 0.670	B	0.335	3.0	A little more damping desirable. Effort required to hover with precision.
R119			-3				-3.11			-0.069 ± j 0.563	B	0.338	2.5	Easy to control. Task performance good. Effort rather low.
R120			-4				-4.06			-0.093 ± j 0.487	B	0.396	2.5	Adequate damping. Position disturbances limit PR.
R121	-1.00	-0.25	-1	0	5.1	0	-1.52			0.134 ± j 0.800	B	0.345	5.0	Difficult to control and prevent oscillation. Gust disturbances large both in hovering and maneuvering flight.
R122			-2				-2.23			-0.011 ± j 0.670	B	0.354	4.0	Gust disturbances rather large. A lot of effort required. Needs more damping.
R123			-3				-3.11			-0.069 ± j 0.563	B	0.400	4.0	Roll control fairly good. Side forces due to gusts make maneuvering with precision somewhat difficult.
R124			-4				-4.06			-0.093 ± j 0.487	B	0.442	3.5	Gust effects on roll minimal. Requires effort to perform task with precision.
R125	-1.00	-0.25	-1	0	7.7	0	-1.52			0.134 ± j 0.800	B	0.361	6.0	Very difficult to stabilize. Large roll angles induced by gusts and control. Poor task performance.
R126			-2				-2.23			-0.011 ± j 0.670	B	0.440	5.0	Considerable effort to control. Performance poor. Very large and rapid stick activity required.
R127			-3				-3.11			-0.069 ± j 0.563	B	0.462	4.5	Control response fairly good. Desire more damping. Hovering performance not too bad.
R128			-4				-4.06			-0.093 ± j 0.487	B	0.482	4.0	Roll disturbances damped fairly well. Position disturbances limit PR.

TABLE A-III (Continued)

Case	L_{v_g}	Y_v	L_p	L_ϕ	σ_{v_g}	SFG	Real Roots RR (1)	RR (2)	RR (3)	Complex Roots $-\zeta\omega_n \pm j\omega_d$	Pilot	L_{δ_a}	PR	Summary of Pilot Comments
R129	-0.33	-0.05	-1	0	5.1	0	-1.23			0.090 ± j 0.513	A	0.254	4.0	Lightly damped. Requires attention to stabilize roll. Overshoot on ϕ commands. Gust no real problem.
R130				-1			-0.49			-0.278 ± j 0.835	A	0.268	3.0	Enough stability to allow attention to be diverted from roll control. Gusts noticeable, but no problem.
R131				-2			-0.23			-0.409 ± j 1.301	A	0.264	3.5	Roll is stable. Oscillatory in roll. Difficult to command and hold a given roll angle.
R132				-3			-0.17			-0.442 ± j 1.646	A	0.302	4.0	Roll attitude very stiff, oscillatory. Like stability, but difficult to maneuver because problem holding ϕ.
R133	-0.33	-0.05	-3	0	5.1	0	-3.04			-0.007 ± j 0.331	A	0.366	2.5	Good roll control. Have rate dynamics in roll. No gust effects evident.
R134				-1			-2.67			-0.188 ± j 0.328	A	0.383	2.5	Good, low frequency roll control. Well damped. No trim problems.
R135				-2			-2.14	-0.52	-0.39		A	0.392	2.25	Good control. No gust effects evident. Low frequency response. Notice some attitude stability.
R136				-4			-0.14			-1.454 ± j 1.274	A	0.403	2.0	Very good control. Attitude command system. Roll angle follows control stick position. No trim problems.
R137	-1.00	-0.05	-2	0	5.1	0	-2.21			-0.080 ± j 0.668	A	0.433	4.5	Moderate damping. Gusts on ϕ evident in hover. Low stability, requires attention. Task performance satisfactory.
R138				-1			-1.76			-0.143 ± j 0.758	A	0.448	4.0	Lightly damped. Effort required to control gusts. Somewhat oscillatory in roll.
R139				-2			-1.05			-0.501 ± j 0.894	A	0.468	3.0	No tendency to diverge in roll, but oscillatory. Gust disturbances on roll quite annoying.
R140				-4			-0.34			-0.854 ± j 1.669	A	0.465	3.25	Good stability, but oscillatory. No trim problem when maneuvering. Easy to hover, although annoyed a little by gusts on roll.
R141	-1.00	-0.05	-5	0	5.1	0	-5.04			-0.005 ± j 0.445	A	0.533	2.75	Well damped. Gust effects minimal. Easy to maneuver, hover. Good stability.
R142				-2			-4.61			-0.218 ± j 0.437	A	0.555	2.5	Have some attitude feedback. Low frequency response. Good maneuvering configuration.
R143				-4			-4.08			-0.485 ± j 0.243	A	0.570	2.0	Good control. Little evidence of gusts. No trim problems.
R144				-6			-1.54	-0.26	-3.25		A	0.592	2.0	Looks like an attitude command system. No trim or gust problems. Pleasant to fly.

TABLE A-III (Continued)

Case	L_{v_g}	Y_v	L_p	L_ϕ	σ_{v_g}	SFG	Real Roots RR (1)	Real Roots RR (2)	Real Roots RR (3)	Complex Roots $-\zeta\omega_n \pm j\omega_d$	Pilot	L_{δ_a}	PR	Summary of Pilot Comments
R145	-0.33	-0.2	-1	0	5.1	0	-1.25			0.026 ± j 0.515	B	0.275	5.0	Major problem is reducing gust-induced position errors. Slight overshoot on ϕ commands.
R146				-1			-0.63			-0.283 ± j 0.872	B	0.264	3.5	Easy to control attitude so position disturbances not too annoying. No attitude disturbances evident.
R147				-2			-0.39			-0.406 ± j 1.312	B	0.283	4.0	Easy to control roll, but response somewhat springy. Attitude feedback a little annoying when maneuvering.
R148				-4			-0.29			-0.456 ± j 1.931	B	0.281	4.5	Too springy. Difficult to command and hold a given attitude.
R149	-0.33	-0.2	-4	0	5.1	0	-4.02			-0.089 ± j 0.274	B	0.392	3.5	Good attitude control characteristics. With little effort position disturbance can be controlled.
R150				-1			-3.76			-0.220 ± j 0.305	B	0.423	3.0	Easy to fly. Low frequency. Good stability.
R151				-3			-0.72	-0.42	-3.06		B	0.424	3.0	Displacement of control directly commands roll angle. Stick force gradient may prevent inadvertent control inputs.
R152				-5			-0.28			-1.958 ± j 0.924	B	0.413	3.0	Excellent roll response. Doesn't seem quite as sluggish as case without attitude feedback.
R153	-1.00	-0.20	-2	0	5.1	0	-2.22			-0.011 ± j 0.671	B	0.352	6.0	Difficult to control roll angle. Very responsive to gusts. Response to control inputs unpredictable.
R154				-1			-1.79			-0.204 ± j 0.792	B	0.398	5.0	Gust disturbances moderately high. Roll control needs improvement.
R155				-2			-1.17			-0.514 ± j 0.965	B	0.419	4.0	Roll response fairly springy. Gust effects not too high. No trim problems.
R156				-4			-0.51			-0.846 ± j 1.681	B	0.377	4.5	Oscillatory or springy characteristics objectionable. Noticeable trim changes when maneuvering.
R157	-1.00	-0.20	-5	0	5.1	0	-5.04			-0.080 ± j 0.438	B	0.552	3.5	Gust effects on position require attention. Roll response kind of sluggish.
R158				-1			-4.84			-0.181 ± j 0.464	B	0.613	3.0	Good roll response, but position needs attention.
R159				-3			-4.37			-0.416 ± j 0.440	B	0.590	3.0	Strong coupling between control displacement and roll attitude. Work load due to position disturbances high.
R160				-6			-0.45	-3.26	-1.49		B	0.613	3.0	Good roll control. No trim problems. Position disturbances limit PR.

TABLE A-III (Concluded)

Case	L_{v_g}	Y_v	L_p	L_ϕ	σ_{v_g}	SFG	Real Roots RR (1)	RR (2)	RR (3)	Complex Roots $-\zeta\omega_n \pm j\omega_d$	Pilot	L_{δ_a}	PR	Summary of Pilot Comments
R161	-0.67	-0.1	-1	0	5.1	0	-1.38			0.139 ± j 0.682	B	0.277	6.0	Needs damping. Get into PIO's in hover.
R162				-2			-0.48			-0.309 ± j 1.306	B	0.309	4.5	A little oscillatory, but stable. Gust response lower than Case 161.
R163				-4			-0.28			-0.412 ± j 1.924	B	0.338	5.0	Too oscillatory for accurate roll control. Gusts not a serious problem.
R164			-2	-2			-0.72			-0.691 ± j 0.854	B	0.367	4.0	Well damped. Good frequency characteristics. Have some position gust disturbances.
R165			-3	-2			-2.25			-0.426 ± j 0.452	B	0.367	3.0	Good roll control. Position-loop characteristics determine PR. Stable.
R166			-3	0			-3.07			-0.014 ± j 0.466	B	0.431	3.0	More responsive in roll than R165. Gusts on roll minimal.
R167*	-0.67	-0.1	-3	0	5.1	0	-3.07			-0.014 ± j 0.466	B	0.391	3.5	Can hover accurately. Controlling height doesn't degrade lateral and longitudinal control.
R168*			-1	0			-1.38			0.139 ± j 0.682	B	0.314	5.5	Difficult to fly. Roll very oscillatory. Controllable, but work load high.
R169*			-1	-2			-0.48			-0.309 ± j 1.306	B	0.298	5.0	About as difficult as R168. Seem to have more damping but frequency of oscillation too high.
R170*			-3	-2			-2.25			-0.426 ± j 0.452	B	0.366	3.25	Quite an improvement over R169. Not very oscillatory. Biggest problem is lateral position disturbances.
R171	-0.67	-0.1	-1	0	5.1	1.5	-1.38			0.139 ± j 0.682	B	0.297	4.5	Difficult to control roll. Must follow up roll inputs. Good hovering performance but difficult to maneuver.
R172			-2				-2.15			0.026 ± j 0.556	B	0.335	4.0	Stick in constant motion to hover. SFG little too high. Some problems with yaw when maneuvering.
R173			-3				-3.07			-0.014 ± j 0.466	B	0.384	3.5	SFG too high. Could not control stick position precisely. Good roll response.
R174			-4				-4.04			-0.029 ± j 0.405	B	0.426	3.0	Like SFG with this well-damped case. Have rate dynamics in roll. Gusts no problem.

* 6 degrees of freedom of motion simulated. $M_q = L_p$, $M_\theta = L_\phi$, $Z_w = -1.0$ $Z_{\delta_c} = -3.2$

TABLE A-IV

COMPARISON OF CAL AND UARL PILOT COMMENTS ON HANDLING QUALITIES FOR VTOL PRECISION HOVERING TASK

1. Nonoptimum Control Stick Sensitivity, M_{δ_e} (rad/sec^2/in.)
Configuration: $M_q = 3$, $M_u g = 0.67$, $X_u = -0.1$, $M_\theta = 0$ $\sigma_{u_g} = 5.1$

M_{δ_e}/(Optimum M_{δ_e})	M_{δ_e}	CAL Pilot Comments	UARL Pilot Comments	UARL Cooper Pilot Rating
0.6	0.260	Lower frequency pitch response which is desirable. Noticed a disturbing tendency to lag the aircraft position rates. Cannot control position precisely.	No comments or ratings are available for these particular configurations. The CAL pilot comments reflect those characteristics which have been observed by UARL pilots when selecting optimum M_{δ_e}.	
1.4	0.603	More abrupt pitch response. Dislike the rapid changes in pitch. Significant reduction in hovering error.		

2. Longitudinal Speed Stability, $M_u g$ (1/sec^3)
Configuration: $M_q = -3$, $X_u = -0.1$, $M_\theta = 0$, $\sigma_{u_g} = 5.1$

$M_u g$	M_{δ_e} (Optimum)	CAL Pilot Comments	UARL Pilot Comments	UARL Cooper Pilot Rating
0	0.330	Appears to be a lag present which limits ability to control position. Control inputs lag position rates. Only gust disturbance cue present is position rate. Difficult to shape control response to position rates. Unsatisfactory position control.	Pitch characteristics very pleasant. Increased concentration on position rates required to maintain hovering position. Some tendency to induce position oscillations.	3.5
0.33	0.360	Pitch response very pleasant. Much less difficult to control position. No sustained oscillations in position.	Increase in pitch activity evident. Easy to control pitch. May reduce attention given to position rates because position rate lead information is developed from pitch response.	3.0
0.67	0.431	More pitch activity. No evident decrease in hovering accuracy. Control stick activity is increased.	Increased attention to pitch control required. Larger pitch response to gusts provides increased information on what one can expect the gusts to do to position. Rating reflects balance between this and increased difficulty of pitch control.	3.0
1.33	0.550	Large pitch oscillations. Constant attention to pitch required. Could be dangerous.	No comments or ratings available for this configuration.	

3. Longitudinal Drag Parameter, X_u (1/sec)
Configuration: $M_q = -3$, $M_u g = 0.67$, $M_\theta = 0$, $\sigma_{u_g} = 5.1$

X_u	M_{δ_e} (Optimum)	CAL Pilot Comments	UARL Pilot Comments	UARL Cooper Pilot Rating
0	0.285	Hovering position control is better than for any previous configuration. Appreciable control activity required to control pitch.	Easy to maintain accurate hover position. Pleasant position control characteristics. Moderate attention to pitch control required.	2.5
-0.2	0.467	Unsatisfactory position control characteristics. Cannot keep up with position rates. Large pitch changes required to control position. Dislike making the large attitude changes.	Maintaining hover position is difficult. Constantly being blown off reference by gusts. Large pitch changes required to arrest position rates. Position control characteristics unsatisfactory.	4.0

TABLE A-IV (Concluded)

4. Pitch Rate Damping, M_q (1/sec)
Configuration: $M_{u_g} = 0.67$, $X_u = -0.1$, $M_\theta = 0$, $\sigma_{u_g} = 5.1$

M_q	M_{δ_e} (Optimum)	CAL Pilot Comments	UARL Pilot Comments	UARL Cooper Pilot Rating
-1	0.369	Pitch response is unsatisfactory. Dislike the large pitch response to small control inputs. Tendency to overcontrol the pitch response.	Pitch response is not damped sufficiently. Cannot relax concentration on pitch or large oscillations result. Constant control motion required to control pitch. No apparent increase in hovering error.	4.25
-3	0.431	Precision of pitch control is greatly improved. Pitch damping is adequate.	Pitch response is adequately damped. Able to hover precisely with nominal concentration on position rates. Pitch response to gusts provides information on what is about to happen to position.	3.0
-5	0.493	Pitch response very satisfactory. Marked increase in hovering error. Appears as though an additional lag has been introduced into position control. Fall behind the position rates. Unacceptable because could not land safely.	Pitch response much less sensitive to gusts. Forced to rely more on position rates to maintain hovering precision. Bothered by the required concentration on position rates.	3.25

5. Pitch Attitude Stabilization, M_θ (1/sec^2). Note: Control sensitivity and comments from UARL pilots are for a configuration with $X_u = -0.05$ and $M_{u_g} = 1.0$ ($M_q = -1.0$, etc.). Adding M_θ has similar effects on this configuration as that shown below. The UARL pilot comments and ratings apply reasonably well to the configuration flown by the CAL pilot.

Configuration: $M_q = -1$, $M_{u_g} = 0.67$, $X_u = -0.1$, $\sigma_{u_g} = 5.1$

M_θ	M_{δ_e} (Optimum)	CAL Pilot Comments	UARL Pilot Comments	UARL Cooper Pilot Rating
0	0.429	Unsatisfactory pitch characteristics need more pitch rate damping. Dislike the large pitch angles resulting from small control inputs.	Lightly damped, quite unstable. Large pitch response to small control inputs. Easy to overshoot desired pitch angle. Hovering accuracy not affected.	4.25
-3	0.385	No improvement in pitch response. Must override the M_θ effects to hover accurately. If loss of precision in pitch and position control is tolerated then M_θ effects are more acceptable.	Amplitude of pitch oscillations greatly reduced. Mildly disturbing increase in frequency of pitch motion. Can divert more attention to position control. Must override M_θ at times of control position.	3.5
-5	0.359	M_θ is too large. Takes large control inputs to override M_θ and maintain hovering position. Pitch response is improved somewhat but not satisfactory.	Increase in frequency of pitch response. Must override M_θ when subjected to low frequency, high amplitude gusts. Have passed the optimum level of M_θ.	4.0

6. RMS Turbulence Level, σ_{u_g} (ft/sec)
Configurations: $M_q = -3$, $M_{u_g} = 0.67$, $X_u = -0.1$, $M_\theta = 0$

σ_{u_g}	M_{δ_e} (Optimum)	CAL Pilot Comments	UARL Pilot Comments	UARL Cooper Pilot Rating
0	0.335	Easy to fly. Pleasant characteristics. Little effort required to hover accurately.	Good configuration. Easy to maintain precision hover. Pleasant to fly.	2.0
2.6	0.390	Difficult to hover accurately. Increase in frequency of control stick inputs. Definite increase in hovering error.	Pleasant characteristics. Effects of gusts are evident. Noticeable increase in control stick activity. Configuration remains easy to control.	2.5
5.1	0.431	No further increase in hovering error. Significant increase in pitch motion. Control stick activity must be increased to maintain hovering accuracy.	Significant increase in pitch activity. Pitch control requires attention but is not difficult. Increased attention to gust-induced position rates is required to maintain hovering accuracy.	3.0

TABLE A-V

CONFIGURATIONS EVALUATED IN PRECISION HOVERING TASK

P: Indicates Parameter Varied Within Group S: Control Sensitivity Selected by Pilot

Principal Parameters	Cases	Longitudinal							Lateral							Table
		$M_u g$	X_u	M_q	M_θ	M_{δ_e}	σ_{u_g}	SFG[1]	$L_v g$	Y_v	L_p	L_ϕ	L_{δ_e}	σ_{v_g}	SFG[1]	
$M_u g$, X_u	PH1 to PH5	0.67	P	-3	0	S	5.1	0	-0.1	-0.1	-3	0	0.301	1.3	0	A-VI[2], A-VII[3]
	PH6 to PH9	P	-0.1	↓	↓	↓	↓	↓	↓	↓	↓	↓	↓	↓	↓	↓
M_q	PH10 to PH12	0.67	-0.1	P	0	S	5.1	0	-0.1	-0.1	-3	0	0.0301	1.3	0	
σ_{u_g}	PH13 to PH16	0.67	-0.1	-3	0	S	P	0	-0.1	-0.1	-3	0	0.0301	1.3	0	
M_θ	PH17 to PH22	0.67	-0.1	-3	P	S	5.1	0	-0.1	-0.1	-3	0	0.0301	1.3	0	
SFG	PH23	0.67	-0.1	-3	0	S	5.1	1.5	-0.1	-0.1	-3	0	0.0301	1.3	1.5	
XC-142 Aircraft	PH24	0.31	-0.15	P	P	S	5.1	1.5	-0.24	0	-0.2	0	0.266	1.3	1.5	
M_q, M_θ	PH25	↓	↓	↓	↓	↓	↓	↓	↓	↓	-3.8	-3.8	0.403	↓	↓	
XV-4B Aircraft	PH26	0.15	-0.017	P	P	S	5.1	1.5	-1.11	-0.13	-2	0	0.212	1.3	1.5	
M_q, M_θ	PH27	↓	↓	↓	↓	↓	↓	↓	↓	↓	-4	-2	0.476	↓	↓	
Pitch Loop Dynamics	PH28 to PH30	P	P	P	P	S	P	0	-0.1	-0.1	-3	0	0.0301	1.3	0	
Pitch Loop Lead Disturbance Level	PH31 to PH34	P	P	P	0	S	5.1	0	-0.1	-0.1	-3	0	0.0301	1.3	0	A-VI[2], A-VII[3]
Position Loop Lead	PH35 to PH36	P	P	-3	0	S	5.1	0	-0.1	-0.1	-3	0	0.0301	1.3	0	
Position Loop Lead	PH37 to PH39	1.6	-0.6	P	0	S	5.1	0	-0.1	-0.1	-3	0	0.0301	1.3	0	A-VI[2]

Notes:

1. SFG: Stick force gradient, lb/in.
2. Indicates table listing corresponding measured rms hovering performance for a precision hovering task.
3. Indicates table listing pilot-adapted parameters and loop-closure characteristics for a precision hovering task.

TABLE A-VI

RMS HOVERING PERFORMANCE DATA FOR THE PRECISION HOVERING TASK

Case	$M_u g$	X_u	M_q	M_θ	σ_{u_g}	SFG	Pilot	M_{δ_e}	PR_H	No. Runs	Pitch Attitude σ_θ, rad	Pitch Rate σ_q, rad/sec	Position σ_x, ft	Position Rate σ_u, ft/sec	Control Position σ_{δ_e}, in.	$M_{\xi_e}\delta_e$
PH1	0.67	0	-3	0	5.1	0	A	0.282	2.5	10	0.0128 (0.0014)*	0.0248 (0.0021)*	0.680 (0.119)*	0.386 (0.061)*	0.384 (0.020)*	.108
							B	0.287	2.5		0.0127 (0.0006)	0.0241 (0.0018)	0.470 (0.065)	0.315 (0.031)	0.383 (0.028)	.110
PH2		-0.05					A	0.412	2.5		0.0214 (0.0022)	0.0334 (0.0026)	0.940 (0.149)	0.584 (0.077)	0.461 (0.021)	.190
							B	0.420	3.0		0.0201 (0.0017)	0.0307 (0.0025)	0.960 (0.120)	0.555 (0.068)	0.431 (0.035)	.181
PH3		-0.1					A	0.356	3.0		0.0306 (0.0034)	0.0434 (0.0058)	1.40 (0.123)	0.870 (0.084)	0.528 (0.031)	.188
							B	0.385	3.25		0.0324 (0.0040)	0.0486 (0.0066)	1.08 (0.165)	0.801 (0.13)	0.599 (0.054)	.231
PH4		-0.2					A	0.465	4.25		0.0491 (0.0049)	0.0605 (0.0098)	2.35 (0.301)	1.28 (0.17)	0.672 (0.082)	.312
							B	0.469	3.75		0.0503 (0.0046)	0.0603 (0.0043)	1.97 (0.205)	1.29 (0.12)	0.710 (0.052)	.333
PH5		-0.3					A	0.506	5.0		0.0605 (0.0060)	0.0640 (0.0068)	3.59 (0.736)	1.60 (0.20)	0.702 (0.064)	.355
							B	0.516	4.5		0.0636 (0.0048)	0.0686 (0.0051)	2.88 (0.454)	1.67 (0.20)	0.755 (0.066)	.390
PH6	0.0	-0.1	-3	0	5.1	0	A	0.300	3.25	10	0.0286 (0.0047)	0.0329 (0.0042)	1.46 (0.21)	0.844 (0.12)	0.464 (0.045)	.139
							B	0.300	3.5		0.0284 (0.0038)	0.0363 (0.0037)	1.10 (0.14)	0.718 (0.13)	0.521 (0.036)	.156
PH7	0.33						A	0.360	2.75		0.0298 (0.0047)	0.0366 (0.0043)	1.48 (0.21)	0.843 (0.13)	0.464 (0.040)	.167
							B	0.360	3.25		0.0301 (0.0037)	0.0419 (0.0037)	1.26 (0.19)	0.804 (0.12)	0.533 (0.041)	.192
PH8	0.67						A	0.431	3.0		0.0334 (0.0051)	0.0464 (0.0062)	1.53 (0.14)	0.952 (0.15)	0.562 (0.058)	.242
							B	0.431	3.0		0.0320 (0.0018)	0.0498 (0.0028)	1.16 (0.10)	0.794 (0.093)	0.590 (0.025)	.254
PH9	1.00						A	0.481	3.75		0.0338 (0.0040)	0.0501 (0.0040)	1.50 (0.26)	0.868 (0.12)	0.591 (0.043)	.284
							B	0.481	3.75		0.0332 (0.0052)	0.0562 (0.0060)	1.20 (0.13)	0.806 (0.13)	0.654 (0.068)	.314
PH10	0.67	-0.1	-1	0	5.1	0	A	0.369	4.25	10	0.0373 (0.0081)	0.0630 (0.010)	1.51 (0.21)	0.986 (0.22)	0.704 (0.061)	.260
							B	0.369	4.25		0.0335 (---)	0.0584 (---)	1.17 (---)	0.802 (---)	0.716 (---)	.264
PH11			-3				A	0.431	3.0		0.0353 (0.0039)	0.0515 (0.0051)	1.45 (0.19)	0.976 (0.11)	0.612 (0.043)	.264
							B	0.431	3.0		0.0330 (0.0026)	0.0495 (0.0049)	1.08 (0.14)	0.808 (0.12)	0.625 (0.065)	.269
PH12			-5				A	0.493	3.0		0.0307 (0.0023)	0.0422 (0.0024)	1.32 (0.18)	0.815 (0.070)	0.584 (0.022)	.238
							B	0.493	3.25		0.0304 (0.0033)	0.0426 (0.0036)	1.10 (0.16)	0.753 (0.075)	0.607 (0.048)	.299

* Quantity in brackets indicates standard deviation of rms quantity.

TABLE A-VI (Continued)

Case	$M_u g$	X_u	M_q	M_θ	σ_{u_g}	SFG	Pilot	M_{δ_e}	PR_H	No. Runs	Pitch Attitude σ_θ, rad	Pitch Rate σ_q, rad/sec	Position σ_x, ft	Position Rate σ_u, ft/sec	Control Position σ_{δ_e}, in.	
PH13	0.67	-0.1	-3	0	2.6	0	A	0.396	2.5	10	0.0187 (0.0013)	0.0233 (0.0021)	1.08 (0.092)	0.536 (0.046)	0.287 (0.022)	.114
							B	0.396	2.5		0.0191 (0.0014)	0.0257 (0.0022)	0.860 (0.0097)	0.511 (0.0042)	0.307 (0.024)	.121
PH14					3.9		A	0.394	2.75		0.0216 (0.0037)	0.0312 (0.0034)	1.28 (0.22)	0.680 (0.13)	0.403 (0.036)	.159
							B	0.409	3.25		0.0236 (0.0030)	0.0417 (0.0036)	0.920 (0.077)	0.586 (0.071)	0.519 (0.043)	.212
PH15					5.1		A	0.474	3.25		0.0312 (0.0029)	0.0401 (0.0034)	1.58 (0.28)	0.896 (0.088)	0.450 (0.035)	.213
							B	0.431	3.5		0.0320 (0.0018)	0.0498 (0.0028)	1.16 (0.10)	0.794 (0.093)	0.590 (0.025)	.254
PH16					7.7		A	0.476	4.75		0.0452 (0.0053)	0.0656 (0.010)	2.07 (0.18)	1.21 (0.11)	0.694 (0.080)	.330
							B	0.477	4.75		0.0510 (0.0054)	0.0876 (0.0092)	1.54 (0.22)	1.23 (0.21)	0.950 (0.080)	.413
PH17	1.00	-0.05	-1	0	5.1	0	A	0.429	4.25	10	0.0344 (0.0029)	0.0615 (0.0035)	1.39 (0.14)	0.953 (0.082)	0.623 (0.034)	.267
							B	0.403	4.5		0.0353 (0.0028)	0.0717 (0.0046)	0.970 (0.12)	0.805 (0.081)	0.769 (0.024)	.310
PH18		-0.2					A	0.483	5.0		0.0620 (0.0068)	0.0929 (0.0088)	2.56 (0.34)	1.58 (0.18)	0.717 (0.044)	.346
							B	0.433	5.0		0.0654 (0.0038)	0.0997 (0.0086)	2.35 (0.28)	1.63 (0.12)	0.883 (0.085)	.382
PH19		-0.05		-3			A	0.385	3.75		0.0301 (0.005)	0.0575 (0.0075)	1.12 (0.10)	0.757 (0.12)	0.635 (0.048)	.244
							B	0.352	3.5		0.0272 (0.0018)	0.0548 (0.0026)	0.960 (0.088)	0.693 (0.071)	0.750 (0.040)	.264
PH20		-0.2					A	0.430	4.25		0.0529 (0.0042)	0.0744 (0.0065)	2.57 (0.27)	1.42 (0.18)	0.742 (0.057)	.319
							B	0.405	4.25		0.0626 (0.0078)	0.0935 (0.0100)	2.26 (0.28)	1.53 (0.24)	0.904 (0.075)	.366
PH21		-0.05		-5			A	0.359	3.25		0.0269 (0.0023)	0.0499 (0.0037)	1.21 (0.16)	0.760 (0.094)	0.654 (0.077)	.235
							B	0.327	4.0		0.0276 (0.0018)	0.0551 (0.0035)	0.980 (0.082)	0.706 (0.048)	0.825 (0.055)	.270
PH22		-0.2					A	0.454	3.75		0.0513 (0.0050)	0.0715 (0.0067)	2.52 (0.25)	1.34 (0.090)	0.807 (0.090)	.366
							B	0.436	4.5		0.0638 (0.0041)	0.0933 (0.0069)	2.22 (0.26)	1.54 (0.13)	0.980 (0.070)	.427
PH23	0.67	-0.1	-3	0	5.1	1.5	A	0.465	3.25	10	0.0351 (0.0031)	0.0448 (0.0040)	1.53 (0.17)	0.972 (0.12)	0.490 (0.039)	.228
							B	0.442	3.25		0.0341 (0.0037)	0.0541 (0.0056)	1.10 (0.092	0.789 (0.11)	0.612 (0.084)	.271

TABLE A-VI (Concluded)

Case	M_{u_g}	X_u	M_q	M_θ	σ_{u_g}	SFG	Pilot	M_{δ_e}	PR_H	No. Runs	Pitch Attitude σ_θ, rad	Pitch Rate σ_q, rad/sec	Position σ_x, ft	Position Rate σ_u, ft/sec	Control Position σ_{δ_e}, in.	
PH24	0.31	-0.15	-0.2	0	5.1	1.5	B	0.251	4.5	15	0.0461 (0.0055)	0.0702 (0.0070)	1.68 (0.18)	1.16 (0.18)	0.809 (0.084)	.203
PH25	↓	↓	-4.7	-2.35	↓	↓	↓	0.423	3.0	↓	0.0443 (0.0044)	0.0561 (0.0050)	1.60 (0.17)	1.15 (0.12)	0.736 (0.071)	.311
PH26	0.15	-0.017	-0.006	0	5.1	1.5	B	0.180	4.0	15	0.0109 (0.0008)	0.0207 (0.0022)	0.73 (0.088)	0.396 (0.039)	0.431 (0.065)	.0775
PH27	↓	↓	-4.0	-2.0	↓	↓	↓	0.442	2.0	↓	0.0081 (0.0013)	0.0110 (0.0018)	0.72 (0.087)	0.342 (0.065)	0.144 (0.023)	.0636
PH28	1.00	-0.05	-5.0	-8.0	5.1	0	B	0.585	2.0	15	0.0162 (0.0017)	0.0238 (0.0016)	0.840 (0.13)	0.506 (0.059)	0.442 (0.051)	.259
PH29	0.33	-0.05	-3.0	0	10.3	0	B	0.394	4.0	15	0.0324 (0.0032)	0.0416 (0.0034)	1.42 (0.16)	0.972 (0.12)	0.498 (0.039)	.196
PH30	1.33	-0.2	↓	↓	2.6	↓	↓	0.433	3.5	↓	0.0269 (0.0024)	0.0357 (0.0027)	1.17 (0.15)	0.734 (0.065)	0.415 (0.042)	.180
PH31	0.33	-0.1	-1.0	0	5.1	0	B	0.277	3.5	15	0.0265 (0.0032)	0.0324 (0.0031)	1.40 (0.13)	0.792 (0.11)	0.471 (0.036)	.130
PH32	↓	-0.025	↓	↓	20.6	↓	↓	0.444	6.5	↓	0.0458 (0.0051)	0.0772 (0.0045)	1.85 (0.30)	1.29 (0.19)	0.832 (0.053)	.368
PH33	↓	-0.1	-3.0	↓	5.1	↓	↓	0.340	3.0	↓	0.0268 (0.0025)	0.0283 (0.0029)	1.49 (0.17)	0.843 (0.093)	0.387 (0.031)	.132
PH34	↓	-0.025	↓	↓	20.6	↓	↓	0.480	5.0	↓	0.0378 (0.0035)	0.0555 (0.0039)	1.51 (0.15)	1.06 (0.12)	0.689 (0.13)	.331
PH35	0.20	-0.09	-1.0	0	8.6	0	B	0.305	5.0	15	0.0427 (0.0047)	0.0478 (0.0063)	1.97 (0.15)	1.29 (0.12)	0.464 (0.049)	.142
PH36	0.80	-0.36	↓	↓	2.1	↓	↓	0.279	3.5	↓	0.0339 (0.0036)	0.0395 (0.0044)	1.51 (0.14)	0.900 (0.077)	0.425 (0.035)	.118
PH37	1.60	-0.72	↓	↓	1.1	↓	↓	0.280	2.5	↓	0.0262 (0.0037)	0.0284 (0.0025)	1.27 (0.18)	0.636 (0.053)	0.326 (0.036)	.0912
PH38	1.60	-0.6	-2.0	0	1.3	0	B	0.300	3.0	15	0.0300 (0.0043)	0.0318 (0.0019)	1.31 (0.14)	0.699 (0.061)	0.387 (0.024)	.116
PH39	1.60	-0.6	-7.0	↓	↓	↓	↓	0.489	3.0	↓	0.0281 (0.0042)	0.0256 (0.0027)	1.31 (0.18)	0.623 (0.056)	0.404 (0.044)	.198

TABLE A-VII

PILOT-ADAPTED PARAMETERS AND LOOP-CLOSURE CHARACTERISTICS FOR THE PRECISION HOVERING TASK

$$\frac{\theta}{\delta_e} = \frac{M_{\delta_e}(s - X_u)}{\Delta_1}, \qquad \frac{\theta}{u_g} = \frac{M_u s}{\Delta_1}, \qquad \frac{x}{u_g} = \frac{X_u(s^2 - M_q s) - M_u g}{s\Delta_1}, \qquad \frac{x}{\theta_x}\bigg|_{\theta \to \delta_e} = \frac{-K_{p_\theta} \cdot M_{\delta_e} \cdot g(T_{L_\theta} s + 1)(-\frac{T_\theta}{2}s + 1)}{\Delta_2}$$

Case	$M_u g$	X_u	M_q	M_θ	σ_{u_g}	SFG	Pilot	M_{δ_e}	PR_H	Factors of Δ_1 / Factors of Δ_2*	Model Parameters K_{P_θ}	T_{L_θ}	$-K_{P_x}$	T_{L_x}	Closure Characteristics ω_{c_θ}	PM_θ	ω_{c_x}	PM_x
PH1	0.67	0	-3	0	5.1	0	A	0.282	2.5	$s + 3.07,\ s^2 - 0.070s + 0.217$	46.4	0.18	0.0148	0.82	2.7	17	0.78	22
							B	0.287	2.5	$s + 0.060,\ s + 3.57,\ s + 23.0,\ s^2 + 1.40s + 8.70$	39.5	0.27	0.0225	0.91	2.6	27	0.73	24
PH2		-0.05					A	0.412	2.5	$s + 3.07,\ s^2 - 0.022s + 0.217$	30.9	0.19	0.0203	0.73	2.7	18	0.92	23
							B	0.420	3.0	$s + 0.106,\ s + 4.05,\ s + 22.9,\ s^2 + 1.06s + 8.18$	28.5	0.22	0.0193	0.88	2.6	22	0.95	28
PH3		-0.1					A	0.356	3.0	$s + 3.07,\ s^2 + 0.027s + 0.217$	38.5	0.16	0.0201	0.49	3.0	8	0.86	19
							B	0.385	3.25	$s + 0.136,\ s + 4.69,\ s + 23.0,\ s^2 + 0.370s + 10.7$	42.0	0.18	0.0268	0.39	3.2	7	1.00	15
PH4		-0.2					A	0.465	4.25	$s + 3.08,\ s^2 + 0.125s + 0.217$	26.5	0.13	0.0186	0.66	2.5	13	0.85	30
							B	0.469	3.75	$s + 0.236,\ s + 4.85,\ s + 22.9,\ s^2 + 0.303s + 10.2$	46.1	0.16	0.0238	0.35	3.1	6	0.92	20
PH5	↓	-0.3	↓	↓	↓	↓	A	0.506	5.0	$s + 3.08,\ s^2 + 0.222s + 0.217$	22.0	0.14	0.0154	0.84	2.4	16	0.76	43
							B	0.516	4.5	$s + 0.327,\ s + 4.50,\ s + 23.4,\ s^2 + 0.175s + 14.4$	37.7	0.20	0.0214	0.26	3.8	3	0.83	24

* Factors of Δ_2 were computed using pitch (θ) loop parameters from pilot B.

TABLE A-VII (Continued)

Case	$M_u g$	X_u	M_q	M_θ	σ_{u_g}	SFG	Pilot	M_{δ_e}	PR_H	Factors of Δ_1 / Factors of Δ_2*	Model Parameters K_{P_θ}	T_{L_θ}	$-K_{P_x}$	T_{L_x}	Closure Characteristics ω_{c_θ}	PM_θ	ω_{c_x}	PM_x
PH6	0	-0.1	-3	0	5.1	0	A	0.300**	3.25	s , $s + 3.00$, $s + 0.100$	26.6	-0.072	0.0130	0.79	-	-	-	-
							B	0.300	3.5	$s + 0.103$, $s + 5.75$, $s + 22.1$, $s^2 + 0.232s + 4.90$	32.6	0.006	0.0170	0.72	2.2	7	0.86	19
PH7	0.33						A	0.360**	2.75	$s + 3.04$, $s^2 + 0.063s + 0.110$	28.2	0.08	0.0164	0.78	2.2	14	0.84	24
							B	0.360	3.25	$s + 0.124$, $s + 5.28$, $s + 22.5$, $s^2 + 0.277s + 7.45$	38.6	0.10	0.0200	0.53	2.7	7	0.88	18
PH8	0.67						A	0.431**	3.0	$s + 3.07$, $s^2 + 0.027s + 0.217$	31.4	0.13	0.0193	0.54	2.7	10	0.86	20
							B	0.431	3.0	$s + 0.140$, $s + 4.76$, $s + 22.9$, $s^2 + 0.414s + 9.64$	37.7	0.16	0.0239	0.49	3.0	9	0.96	19
PH9	1.00	↓	↓	↓	↓	↓	A	0.481**	3.75	$s + 3.11$, $s^2 - 0.007s + 0.322$	23.7	0.23	0.0209	0.85	2.6	24	0.99	31
							B	0.481	3.75	$s + 0.156$, $s + 4.38$, $s + 23.1$, $s^2 + 0.534s + 11.1$	36.7	0.20	0.0251	0.50	3.2	10	0.99	21
PH10	0.67	-0.1	-1	0	5.1	0	A	0.369**	4.25	$s + 0.138$, $s^2 - 0.028s + 0.484$	23.6	0.43	0.0229	0.39	3.0	7	0.93	20
							B	0.369	4.25	$s + 0.173$, $s + 2.09$, $s + 23.4$, $s^2 + 0.474s + 12.1$	25.6	0.50	0.0275	0.41	3.4	8	1.05	21
PH11			-3				A	0.431**	3.0	$s + 3.07$, $s^2 + 0.027s + 0.217$	34.2	0.13	0.0211	0.44	2.7	5	0.89	16
							B	0.431	3.0	$s + 0.138$, $s + 4.72$, $s + 22.9$, $s^2 + 0.388s + 10.2$	39.7	0.17	0.0270	0.41	3.1	8	1.00	15
PH12	↓	↓	-5	↓	↓	↓	A	0.493**	3.0	$s + 5.03$, $s^2 + 0.073s + 0.133$	38.7	0.03	0.0194	0.66	2.6	11	0.89	22
							B	0.493	3.25	$s + 0.130$, $s + 7.36$, $s + 22.3$, $s^2 + 0.426s + 8.41$	43.8	0.05	0.0233	0.56	2.8	10	0.97	19
PH13	0.67	-0.1	-3	0	2.6	0	A	0.396	2.5	$s + 3.07$, $s^2 + 0.027s + 0.217$	15.5	0.22	0.0143	1.58	1.7	39	1.03	33
							B	0.396	2.5	$s + 0.178$, $s + 4.67$, $s + 22.5$, $s^2 + 0.851s + 5.18$	21.6	0.14	0.0178	0.94	2.1	23	0.95	29
PH15					5.1		A	0.474	3.25	$s + 3.07$, $s^2 + 0.027s + 0.217$	24.1	0.17	0.0180	0.75	2.5	18	0.87	26
							B	0.431	3.5	$s + 0.141$, $s + 4.78$, $s + 22.8$, $s^2 + 0.414s + 9.45$	37.4	0.16	0.0239	0.49	3.0	9	0.96	19
PH16	↓	↓	↓	↓	7.7	↓	A	0.476	4.75	$s + 3.07$, $s^2 + 0.027s + 0.217$	33.4	0.17	0.0199	0.55	3.0	10	0.86	22
							B	0.477	4.75	$s + 0.130$, $s + 4.68$, $s + 23.2$, $s^2 + 0.203s + 12.7$	45.1	0.18	0.0289	0.31	3.5	4	1.03	12

* Factors of Δ_2 were computed using pitch (θ) loop parameters from pilot B.

** These values of M_{δ_e} were selected from the UARL contours. The pilots assured themselves that these values were satisfactory before proceeding with the precision hovering task.

TABLE A-VII (Continued)

Case	M_{u_g}	X_u	M_q	M_θ	σ_{u_g}	SFG	Pilot	M_{δ_e}	PR_H	Factors of Δ_1 / Factors of Δ_2*	Model Parameters K_{P_θ}	T_{L_θ}	$-K_{P_x}$	T_{L_x}	Closure Characteristics ω_{c_θ}	PM_θ	ω_{c_x}	PM_x
PH17	1.00	-0.05	-1	0	5.1	0	A	0.429	4.25	$s + 1.47,\ s^2 - 0.425s + 0.677$	19.2	0.52	0.0246	0.37	3.2	10	0.98	18
							B	0.403	4.50	$s + 0.179,\ s + 1.179,\ s + 23.4,\ s^2 + 0.665s + 11.1$	20.0	0.54	0.0351	0.36	3.2	11	1.20	17
PH18		-0.2		↓			A	0.483	5.0	$s + 1.51,\ s^2 - 0.307s + 0.662$	15.4	0.44	0.0235	0.34	2.9	9	0.93	26
							B	0.433	5.0	$s + 0.307,\ s + 2.24,\ s + 23.4,\ s^2 + 0.356s + 11.6$	22.3	0.47	0.0305	0.28	3.4	6	1.10	21
PH19		-0.05		-3			A	0.385	3.75	$s + 0.412,\ s^2 + 0.638s + 2.79$	15.1	0.57	0.0408	0.43	3.3	18	1.10	23
							B	0.352	3.5	$s + 0.140,\ s + 2.03,\ s + 23.4,\ s^2 + 0.530s + 14.9$	23.7	0.56	0.0389	0.33	3.8	10	1.00	18
PH20		-0.2		↓			A	0.430	4.25	$s + 0.562,\ s^2 + 0.638s + 2.84$	13.4	0.47	0.0320	0.43	3.1	16	0.88	31
							B	0.405	4.25	$s + 0.310,\ s + 2.69,\ s + 22.9,\ s^2 + 0.426s + 9.43$	15.3	0.39	0.0437	0.34	3.0	12	1.10	24
PH21		-0.05		-5			A	0.359	3.25	$s + 0.258,\ s^2 + 0.792s + 4.85$	15.1	0.55	0.0439	0.41	3.4	20	0.94	23
							B	0.327	4.0	$s + 0.135,\ s + 2.33,\ s + 23.1,\ s^2 + 0.542s + 13.9$	21.0	0.50	0.0476	0.33	3.6	13	1.00	18
PH22	↓	-0.2	↓	↓	↓	↓	A	0.454	3.75	$s + 0.410,\ s^2 + 0.790s + 4.88$	7.9	0.51	0.0503	0.50	2.9	32	0.88	35
							B	0.436	4.5	$s + 0.312,\ s + 2.98,\ s + 22.5,\ s^2 + 0.452s + 8.48$	9.2	0.31	0.0605	0.33	2.8	25	0.99	21
PH23	0.67	-0.1	-3	0	5.1	1.5	A	0.465	3.25	$s + 3.07,\ s^2 + 0.027s + 0.217$	24.0	0.15	0.0201	0.66	2.4	19	0.92	22
							B	0.442	3.25	$s + 0.145,\ s + 4.81,\ s + 22.8,\ s^2 + 0.473s + 8.57$	33.2	0.16	0.0261	0.52	2.8	11	1.04	19
PH24	0.31	-0.15	-0.2	0	5.1	1.5	B	0.251	4.5	$s + 0.800,\ s^2 - 0.444s + 0.386$ / $s + 0.203,\ s + 1.83,\ s + 23.3,\ s^2 + 0.155s + 9.57$	25.7	0.62	0.0241	0.22	3.1	3	0.95	17
PH25	↓	↓	-4.7	-2.35	↓	↓	↓	0.423	3.0	$s + 4.15,\ s^2 + 0.700s + 0.161$ / $s + 0.167,\ s + 8.13,\ s + 21.6,\ s^2 + 0.086s + 7.87$	45.6	-0.04	0.0255	0.43	-	-	-	-
PH26	0.15	-0.02	-0.1	0	5.1	1.5	B	0.180	4.0	$s + 0.535,\ s^2 - 0.511s + 0.273$ / $s + 0.044,\ s + 1.51,\ s + 23.3,\ s^2 + 0.210s + 10.1$	31.4	0.76	0.0134	0.41	3.2	4	0.70	15

* Factors of Δ_2 were computed using pitch (θ) loop parameters from pilot B.

TABLE A-VII (Concluded)

Case	M_{u_g}	X_u	M_q	M_θ	σ_{u_g}	SFG	Pilot	M_{δ_e}	PR_H	Factors of Δ_1 / Factors of Δ_2*	Model Parameters K_{P_θ}	T_{L_θ}	$-K_{P_x}$	T_{L_x}	Closure Characteristics ω_{c_θ}	PM_θ	ω_{c_x}	PM_x
PH27	0.15	-0.02	-4	-2	5.1	1.5	B	0.442	2.0	$\frac{s + 3.43,\ s\ ,\ s}{s + 0.027,\ s + 7.34,\ s + 21.6,\ s^2 + 0.158s + 5.87}$	28.5	-0.09	0.0102	0.83	-	-	-	-
PH28	1.00	-0.05	-5	-8	5.1	0	B	0.585	2.0	$\frac{s + 0.191,\ s^2 + 4.86s + 7.32}{s + 0.766,\ s + 6.82,\ s + 22.5,\ s^2 + 7.23s + 15.4}$	49.8	0.07	0.0238	0.61	3.6	18	0.84	18
PH29	0.33	-0.05	-3.0	0	10.3	0	B	0.394	4.0	$\frac{s + 3.04,\ s^2 + 0.013s + 0.110}{s + 0.067,\ s + 4.50,\ s + 23.2,\ s^2 + 0.392s + 12.1}$	50.5	0.19	0.0214	0.42	3.4	7	0.88	13
PH30	1.33	-0.2	↓	↓	2.6	↓	↓	0.433	3.5	$\frac{s + 3.14,\ s^2 + 0.056s + 0.424}{s + 0.268,\ s + 4.45,\ s + 23.1,\ s^2 + 0.410s + 11.8}$	43.6	0.20	0.0227	0.31	3.2	10	0.88	21
PH31	0.33	-0.1	-1	0	5.1	0	B	0.277	3.5	$\frac{s + 1.24,\ s^2 - 0.137s + 0.269}{s + 0.139,\ s + 2.29,\ s + 23.3,\ s^2 + 0.484s + 10.4}$	31.7	0.46	0.0186	0.51	3.3	8	0.84	23
PH32	↓	-0.02	↓	↓	20.6	↓	↓	0.444	6.5	$\frac{s + 1.23,\ s^2 - 0.201s + 0.272}{s + 0.060,\ s + 1.73,\ s + 23.7,\ s^2 + 0.597s + 14.9}$	21.8	0.60	0.0260	0.44	3.8	9	1.00	16
PH33	↓	-0.1	-3	↓	5.1	↓	↓	0.340	3.0	$\frac{s + 3.04,\ s^2 - 0.063s + 0.110}{s + 0.125,\ s + 5.03,\ s + 22.6,\ s^2 + 0.448s + 7.41}$	38.8	0.13	0.0165	0.60	2.6	11	0.80	20
PH34	↓	-0.02	↓	↓	20.6	↓	↓	0.480	5.0	$\frac{s + 3.04,\ s^2 - 0.011s + 0.110}{s + 0.043,\ s + 3.89,\ s + 23.4,\ s^2 + 0.772s + 13.0}$	39.0	0.25	0.0241	0.51	3.4	13	0.97	16
PH35	0.20	-0.09	-1	0	8.6	0	B	0.305	5.0	$\frac{s + 1.16,\ s^2 - 0.071s + 0.172}{s + 0.111,\ s + 2.57,\ s + 23.2,\ s^2 + 0.281s + 10.2}$	31.4	0.40	0.0204	0.34	3.2	5	0.86	15
PH36	0.80	-0.36	↓	↓	2.1	↓	↓	0.279	3.5	$\frac{s + 1.48,\ s^2 - 0.121s + 0.540}{s + 0.429,\ s + 2.44,\ s + 23.5,\ s^2 + 0.090s + 12.9}$	42.1	0.42	0.0224	0.08	3.6	14	0.83	24

* Factors of Δ_2 were computed using pitch (θ) loop parameters from pilot B.

TABLE A-VIII

LONGITUDINAL PARAMETERS FOR HOVERING AND LOW-SPEED FLIGHT SIMULATION OF XC-142 AND XV-4B VTOL AIRCRAFT

Parameter	XC-142	XV-4B
X_q	0.505	--
X_u	-0.153	-0.017
Z_q	-0.296	--
Z_w	-0.165	-0.017
Z_{δ_e}	0.660	--
$Z_{\lvert\delta_e\rvert}$	--	-0.393
$Z_{\lvert\delta_a\rvert}$	--	-0.473
Z_{δ_T}	--	-2.18
Z_{δ_C}	-8.44	--
M_p	--	-0.269
M_q	-0.203	-0.006
M_r	--	-0.136
M_u	0.0096	0.0045
M_w	-0.0030	-0.0011
M_{δ_P}	0.200	0.289
M_{δ_T}	--	-0.008
M_{δ_C}	0.030	--
Stability Augmentation:		
M_q	-4.70	--
M_θ	-2.35	--
Z_w	-1.35	--
Pitch Control Power, rad/sec^2	0.900	0.450 (85% rpm), 0.850 (100% rpm)
Stick Force Gradient, lb/in	1.50	1.50
Weight, lb	37,400	12,500
Thrust/Weight	1.18	1.15
I_y, slug-ft^2	126,000	11,950

TABLE A-IX

LATERAL PARAMETERS FOR HOVERING AND LOW-SPEED FLIGHT SIMULATION OF XC-142 AND XV-4B VTOL AIRCRAFT

Parameter	XC-142	XV-4B
Y_v	--	-0.130
L_p	-0.217	--
L_q	--	1.24
L_r	-0.034	--
L_v	-0.0073	-0.034
L_{δ_a}	0.333	1.37
L_{δ_r}	0.009	--
N_p	-0.020	--
N_q	--	0.128
N_r	-0.105	--
N_v	-0.0006	-0.0017
N_{δ_a}	0.009	--
N_{δ_r}	0.224	0.321
Stability Augmentation:		
L_p	-3.85	--
L_ϕ	-3.85	--
N_r	-4.70	--
Roll Control Power, rad/sec^2	1.00	1.84 (85% rpm), 3.50 (100% rpm)
Yaw Control Power, rad/sec^2	0.550	0.550 (85% rpm), 1.04 (100% rpm)
Stick Force Gradient, lb/in	1.5	1.5
Weight, lb	37,400	12,500
Thrust/Weight	1.18	1.15
I_x, slug-ft^2	191,700	2,590
I_z, slug-ft^2	286,700	12,900
I_{xz}, slug-ft^2	7,580	--

APPENDIX B

DETAILS OF CLOSED-LOOP ANALYSIS OF THE HOVERING TASK

The open- and closed-loop hovering task model equations which describe VTOL aircraft response to control inputs and turbulence are developed initially in this Appendix. The methods by which these equations and rms hovering performance measurements are used to compute adaptable pilot-model parameters are then outlined. The experiments which were conducted to verify these methods are also described. The effects of pilot-adapted pitch-loop lead on position-loop lead and the proper interpretation of position-loop lead are outlined in the concluding subsection.

A. Open- and Closed-Loop Hovering Task Model Equations

In this subsection, the open-loop equations for pitch attitude and position response to control inputs and turbulence are developed from the VTOL aircraft hovering equations of motion. These open-loop transfer functions are then used in the closed-loop equations, defined by the hovering task model, for VTOL aircraft pitch rate, pitch attitude, longitudinal velocity, and hovering position response to turbulence. These equations are used in the computation of pilot model adaptive parameters (Table A-VII). The equation for closed-loop stick response to turbulence is also developed in this section.

1. Open-Loop Hover Model Equations

A schematic of the hovering task model which is the source for the equations developed in this Appendix is presented in Sketch B-1.

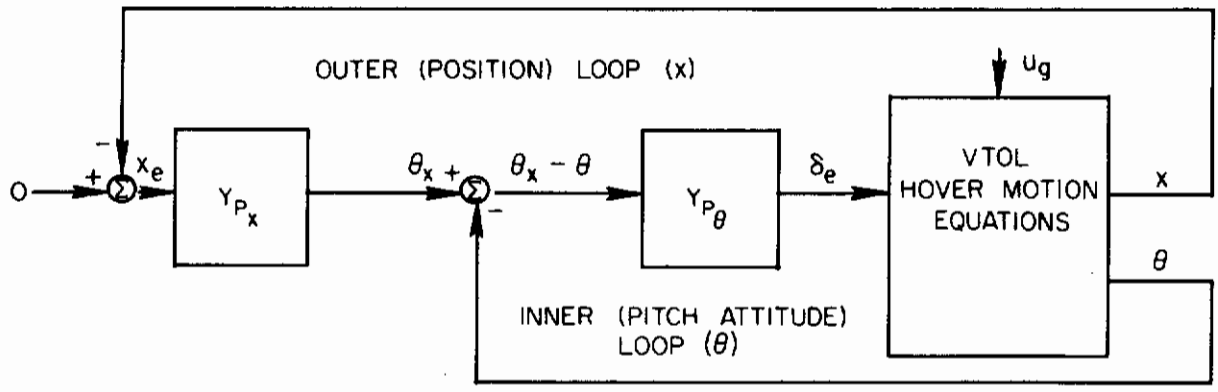

SKETCH B-1 VTOL Aircraft Hovering Task Model

The general form of the linearized equations of motion which describes the pitch attitude (θ) and longitudinal position (x) response of the simulated VTOL aircraft to control inputs and to turbulence is

$$M_u u + M_\theta \theta + M_q \dot{\theta} - \ddot{\theta} = - M_{\delta_e} \delta_e - M_u u_g$$
$$X_u u - g\theta - \dot{u} = - X_{\delta_e} \delta_e - X_u u_g \qquad \text{(B-1)}$$

The left side of the equations defines the aircraft transient response (aircraft dynamics). The right side defines the manner in which control inputs, δ_e, and turbulence, u_g, force aircraft motion. The equations have been normalized with mass and moment of inertia. The longitudinal force due to a stick command, X_{δ_e}, is usually zero for nonrotary-wing VTOL aircraft. However, for purposes of generality it will be included in the development of the equations.

The open-loop VTOL aircraft response to stick commands and turbulence is defined by the linear equations of motion (Eq. (B-1)). In transfer function notation, the open-loop pitch attitude response to stick commands, θ/δ_e, and turbulence, θ/u_g, is

$$Y_{\theta\delta_e} = \theta/\delta_e = \frac{M_{\delta_e}(s - X_u) + X_{\delta_e} M_u}{\Delta_1} \qquad \text{(B-2)}$$

$$Y_{\theta u_g} = \theta/u_g = \frac{M_u s}{\Delta_1} \qquad \text{(B-3)}$$

where:

$$\Delta_1 = s^3 - (M_q + X_u)s^2 + (M_q X_u - M_\theta)s + M_\theta X_u + M_u g \qquad \text{(B-4)}$$

and s is the Laplace operator. The open-loop transfer functions relating position response to stick commands and turbulence, x/δ_e and x/u_g, respectively, are

$$Y_{x\delta_e} = x/\delta_e = \frac{- M_{\delta_e} g - X_{\delta_e}(-s^2 + M_q s + M_\theta)}{s\Delta_1} \qquad \text{(B-5)}$$

$$Y_{x_{u_g}} = x/u_g = \frac{-X_u\left(-s^2 + M_q s + M_\theta\right) - M_u g}{s\Delta_l} \qquad \text{(B-6)}$$

Block diagram representations for the transfer functions defining open-loop VTOL aircraft response to stick commands and turbulence can be substituted into the hovering task model schematic. This involves replacing the block entitled "VTOL Hover Motion Equations" with the transfer functions as shown in Sketch B-2. The representation in Sketch B-2 aids in understanding the equations for closed-loop aircraft response to turbulence.

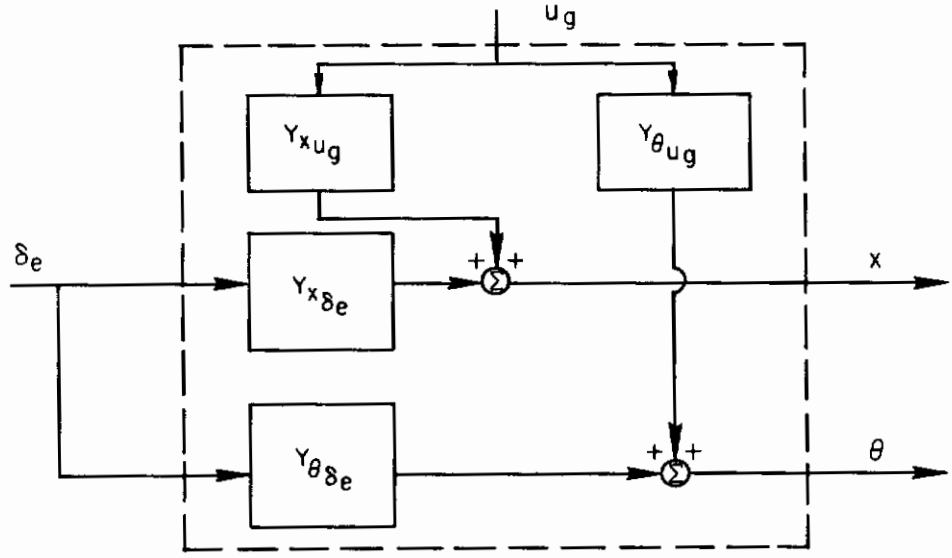

SKETCH B-2 Block Diagram Representation for the Hover Motion Equations

The open-loop position response to an attitude command (θ_x) with the inner (pitch) loop closed, designated $x/\theta_x\big|_{\theta\to\delta_e}$, must also be developed. This equation is used to compute the position (outer) loop Bode diagrams (the term $\theta\to\delta_e$ indicates that the pitch loop is closed on δ_e, i.e., that closing the pitch loop modifies the stick command). The hovering task model (Sketch B-1) indicates that the relation for $x/\theta_x\big|_{\theta\to\delta_e}$, in terms of transfer functions, is

$$x/\theta_x\Big|_{\theta\to\delta_e} = \frac{Y_{P_\theta}\, Y_{x_{\delta_e}}}{1 + Y_{P_\theta}\, Y_{\theta_{\delta_e}}} \qquad \text{(B-7)}$$

Because the pitch loop is closed, the transfer function representing the pitch-loop pilot dynamics (i.e., the pilot model) Y_{P_θ}, is included in Eq. (B-7). The pitch-loop pilot model is

$$Y_{P_\theta} = \frac{K_{P_\theta}\left(T_{L_\theta} s + 1\right) e^{-\tau_\theta s}}{T_N s + 1} \tag{B-8}$$

The transport lag $e^{-\tau_\theta s}$ is approximated with a first-order Padé approximation in all the equations that follow. This approximation is

$$e^{-\tau_\theta s} \approx \frac{1 - \tau_\theta s/2}{1 + \tau_\theta s/2} \tag{B-9}$$

It is good in the frequency domain for $\omega \leq 1/\tau_\theta$. Substituting the specified transfer functions into Eq. (B-7) results in the following equation.

$$\begin{aligned} x/\theta_x\Big|_{\theta \to \delta_e} = K_{P_\theta}\Big\{&\left[-X_{\delta_e} T_{L_\theta} \tau_\theta/2\right] s^4 + \left[X_{\delta_e} M_q T_{L_\theta} \tau_\theta/2 + X_{\delta_e}\left(T_{L_\theta} - \tau_\theta/2\right)\right] s^3 \\ &+ \left[\left(T_{L_\theta} \tau_\theta/2\right)\left(X_{\delta_e} M_\theta + M_{\delta_e} g\right) - X_{\delta_e} M_q\left(T_{L_\theta} - \tau_\theta/2\right) + X_{\delta_e}\right] s^2 \\ &- \left[\left(T_{L_\theta} - \tau_\theta/2\right)\left(X_{\delta_e} M_\theta + M_{\delta_e} g\right) + X_{\delta_e} M_q\right] s - \left[X_{\delta_e} M_\theta + M_{\delta_e} g\right]\Big\} \Big/ \Delta_2 \end{aligned} \tag{B-10}$$

where Δ_2 is defined as

$$\begin{aligned} \Delta_2 = s\Big\{&\left(T_N \tau_\theta/2\right) s^5 + \left[\left(T_N + \tau_\theta/2\right) - \left(T_N \tau_\theta/2\right)\left(M_q + X_u\right)\right] s^4 \\ &+ \left[\left(T_N \tau_\theta/2\right)\left(M_q X_u - M_\theta\right) - \left(T_N + \tau_\theta/2\right)\left(M_q + X_u\right) - K_{P_\theta} T_{L_\theta} M_{\delta_e} \tau_\theta/2 + 1\right] s^3 \\ &+ \Big[\left(T_N \tau_\theta/2\right)\left(M_\theta X_u + M_u g\right) + \left(T_N + \tau_\theta/2\right)\left(M_q X_u - M_\theta\right) + K_{P_\theta} M_{\delta_e}\left(T_{L_\theta} - \tau_\theta/2\right) \\ &\quad - K_{P_\theta} T_{L_\theta} \tau_\theta/2\left(X_{\delta_e} M_u - M_{\delta_e} X_u\right) - \left(M_q + X_u\right)\Big] s^2 \end{aligned} \tag{B-11}$$

$$+\left[\left(T_N+\tau_\theta/2\right)\left(M_\theta X_u+M_u g\right)+K_{P_\theta}\left(T_{L_\theta}-\tau_\theta/2\right)\left(X_{\delta_e}M_u-M_{\delta_e}X_u\right)\right.$$

$$\left.+\left(M_q X_u-M_\theta\right)+K_{P_\theta}M_{\delta_e}\right]s$$

$$+\left.\left[K_{P_\theta}\left(X_{\delta_e}M_u-M_{\delta_e}X_u\right)+M_\theta X_u+M_u g\right]\right\}$$

2. Closed-Loop Hover Model Equations

To compute the pilot model adapted parameters, the closed-loop hover model equations describing VTOL aircraft response to turbulence are needed. In particular, the closed-loop equations for q/u_g, θ/u_g, u/u_g and x/u_g are required. These equations are developed in this subsection along with the closed-loop equation for $\delta e/u_g$.

a. Pitch Attitude and Rate Equations

The closed-loop hovering model equation for VTOL pitch attitude response to turbulence is designated

$$\theta/u_g\Big|_{\substack{\theta\rightarrow\delta_e\\ x\rightarrow\theta_x}}$$

The terms $\theta\rightarrow\delta_e$ and $x\rightarrow\theta_x$ indicate that the pitch loop is closed on δ_e (i.e., closing the pitch loop modifies the stick command) and the position loop is closed on the attitude angle commanded by the position-loop pilot model. Carrying out the required closed-loop algebra defined by the model in Sketch B-1 results in the following relationships for $\theta/u_g\Big|_{\substack{\theta\rightarrow\delta_e\\ x\rightarrow\theta_x}}$

$$\theta/u_g\Big|_{\substack{\theta\rightarrow\delta_e\\ x\rightarrow\theta_x}}=\frac{Y_{\theta u_g}+Y_{P_\theta}Y_{P_x}\left(Y_{\theta u_g}Y_{x\delta_e}-Y_{\theta\delta_e}Y_{xu_g}\right)}{1+Y_{\theta\delta_e}Y_{P_\theta}+Y_{x\delta_e}Y_{P_\theta}Y_{P_x}}\qquad\text{(B-12)}$$

The transfer function representing the position-loop pilot dynamics (pilot model) in Eq. (B-12) is defined as

$$Y_{P_x}=K_{P_x}\frac{\left(T_{L_x}s+1\right)\left(-T_x s/2+1\right)}{\left(\tau_x s/2+1\right)}\qquad\text{(B-13)}$$

where the Padé approximation for the transport lag, $e^{-\tau_x s}$, has again been made. Substituting for the transfer functions in Eq. (B-12) results in the following relation

$$\theta/u_g\Big|_{\substack{\theta\to\delta_e\\ x\to\theta_x}} = \Big[(M_u\tau_x\tau_\theta T_N/4)s^5 + \Big\{M_u\big[\tau_x\tau_\theta/4 + T_N(\tau_x+\tau_\theta)/2\big] + K_{P_x}K_{P_\theta}T_{L_\theta}T_{L_x}\tau_x\tau_\theta\big(M_uX_{\delta_e} - M_{\delta_e}X_u\big)/4\Big\}s^4$$
$$+\Big(M_u\big[T_N+(\tau_x+\tau_\theta)/2\big] + K_{P_x}K_{P_\theta}\big(M_uX_{\delta_e} - M_{\delta_e}X_u\big)\Big\{T_{L_x}\tau_x\tau_\theta/4 + T_{L_\theta}\Big[\tau_x\tau_\theta/4 - T_{L_x}(\tau_x+\tau_\theta)/2\Big]\Big\}\Big)s^3$$
$$+\Big(M_u + K_{P_x}K_{P_\theta}\big(M_uX_{\delta_e} - M_{\delta_e}X_u\big)\Big\{T_{L_\theta}\big[T_{L_x} - (\tau_x+\tau_\theta)/2\big] + \tau_x\tau_\theta/4 - T_{L_x}(\tau_x+\tau_\theta)/2\Big\}\Big)s^2$$
$$+\Big\{K_{P_x}K_{P_\theta}\big(M_uX_{\delta_e} - M_{\delta_e}X_u\big)\big[T_{L_\theta} + T_{L_x} - (\tau_x+\tau_\theta)/2\big]\Big\}s + K_{P_x}K_{P_\theta}\big(M_uX_{\delta_e} - M_{\delta_e}X_u\big)\Big]/\Delta_3 \qquad \text{(B-14)}$$

where Δ_3 is defined as

$$\Delta_3 = (\tau_x\tau_\theta T_N)s^7/4 + \Big[\tau_x\tau_\theta/4 + T_N(\tau_x+\tau_\theta)/2 - \tau_x\tau_\theta T_N(M_q+X_u)/4$$
$$+ K_{P_\theta}K_{P_x}X_{\delta_e}T_{L_\theta}T_{L_x}\tau_x\tau_\theta/4\Big]s^6 + \Big(\tau_x\tau_\theta T_N(M_qX_u - M_\theta)/4$$
$$-\Big[\tau_x\tau_\theta/4 + T_N(\tau_x+\tau_\theta)/2\Big](M_q+X_u) + T_N + (\tau_x+\tau_\theta)/2 - K_{P_\theta}M_{\delta_e}T_{L_\theta}\tau_x\tau_\theta/4$$
$$+ K_{P_\theta}K_{P_x}X_{\delta_e}\Big\{T_{L_x}\tau_x\tau_\theta/4 + T_{L_\theta}\Big[\tau_x\tau_\theta/4 - T_{L_x}(\tau_x+\tau_\theta)/2\Big]\Big\}$$
$$- K_{P_\theta}K_{P_x}X_{\delta_e}M_qT_{L_\theta}T_{L_x}\tau_x\tau_\theta/4\Big)s^5 + \Big(\tau_x\tau_\theta T_N(M_\theta X_u + M_ug)/4 \qquad \text{(B-15)}$$
$$+\Big[\tau_x\tau_\theta/4 + T_N(\tau_x+\tau_\theta)/2\Big](M_qX_u - M_\theta) - \Big[T_N + (\tau_x+\tau_\theta)/2\Big](M_q+X_u) + 1$$
$$+ K_{P_\theta}M_{\delta_e}\Big[T_{L_\theta}(\tau_x-\tau_\theta)/2 - \tau_x\tau_\theta/4\Big] - K_{P_\theta}T_{L_\theta}\tau_x\tau_\theta(M_uX_{\delta_e} - M_{\delta_e}X_u)/4$$
$$+ K_{P_\theta}K_{P_x}X_{\delta_e}\Big\{T_{L_\theta}\Big[T_{L_x} - (\tau_x+\tau_\theta)/2\Big] + \tau_x\tau_\theta/4 - T_{L_x}(\tau_x+\tau_\theta)/2\Big\}$$
$$- K_{P_\theta}K_{P_x}X_{\delta_e}M_q\Big\{T_{L_x}\tau_x\tau_\theta/4 + T_{L_\theta}\Big[\tau_x\tau_\theta/4 - T_{L_x}(\tau_x+\tau_\theta)/2\Big]\Big\}$$

$$- K_{P_\theta} K_{P_x} T_{L_\theta} T_{L_x} \tau_x \tau_\theta \left(X_{\delta_e} M_\theta + M_{\delta_e} g\right)/4\Big) s^4 + \Big(\Big[\tau_x \tau_\theta/4 + T_N(\tau_x + \tau_\theta)/2\Big]$$

$$\left(M_\theta X_u + M_u g\right) + \Big[T_N + (\tau_x + \tau_\theta)/2\Big]\left(M_q X_u - M_\theta\right) - \left(M_q + X_u\right) + K_{P_\theta} M_{\delta_e}$$

$$\Big[T_{L_\theta} + (\tau_x - \tau_\theta)/2\Big] + K_{P_\theta}\left(M_u X_{\delta_e} - M_{\delta_e} X_u\right)\Big[T_{L_\theta}(\tau_x - \tau_\theta)/2 - \tau_x \tau_\theta/4\Big]$$

$$+ K_{P_\theta} K_{P_x} X_{\delta_e}\Big[T_{L_\theta} + T_{L_x} - (\tau_x + \tau_\theta)/2\Big] - K_{P_\theta} K_{P_x} X_{\delta_e} M_q$$

$$\Big\{T_{L_\theta}\Big[T_{L_x} - (\tau_x + \tau_\theta)/2\Big] + \tau_x \tau_\theta/4 - T_{L_x}(\tau_x + \tau_\theta)/2\Big\} - K_{P_\theta} K_{P_x}\left(X_{\delta_e} M_\theta + M_{\delta_e} g\right)$$

$$\Big\{T_{L_x} \tau_x \tau_\theta/4 + T_{L_\theta}\Big[\tau_x \tau_\theta/4 - T_{L_x}(\tau_x + \tau_\theta)/2\Big]\Big\}\Big) s^3 + \Big(\Big[T_N + (\tau_x + \tau_\theta)/2\Big]$$

$$\left(M_\theta X_u + M_u g\right) + M_q X_u - M_\theta + K_{P_\theta} M_{\delta_e} + K_{P_\theta}\left(M_u X_{\delta_e} - M_{\delta_e} X_u\right)$$

$$\Big[T_{L_\theta} + (\tau_x - \tau_\theta)/2\Big] + K_{P_\theta} K_{P_x} X_{\delta_e} - K_{P_\theta} K_{P_x} X_{\delta_e} M_q\Big[T_{L_\theta} + T_{L_x} - (\tau_x + \tau_\theta)/2\Big]$$

$$- K_{P_\theta} K_{P_x}\left(X_{\delta_e} M_\theta + M_{\delta_e} g\right)\Big\{T_{L_\theta}\Big[T_{L_x} - (\tau_x + \tau_\theta)/2\Big] + \Big[\tau_x \tau_\theta/4 - T_{L_x}(\tau_x + \tau_\theta)/2\Big]\Big\}\Big) s^2$$

$$+ \Big\{\left(M_\theta X_u + M_u g\right) + K_{P_\theta}\left(M_u X_{\delta_e} - M_{\delta_e} X_u\right) - K_{P_\theta} K_{P_x} X_{\delta_e} M_q - K_{P_\theta} K_{P_x}$$

$$\left(X_{\delta_e} M_\theta + M_{\delta_e} g\right)\Big[T_{L_\theta} + T_{L_x} - (\tau_x + \tau_\theta)/2\Big]\Big\} s - K_{P_\theta} K_{P_x}\left(X_{\delta_e} M_\theta + M_{\delta_e} g\right)$$

The closed-loop equation for VTOL aircraft pitch rate is given by

$$q/u_g \Big|_{\substack{\theta \to \delta_e \\ x \to \theta_x}} = s\theta/u_g \Big|_{\substack{\theta \to \delta_e \\ x \to \theta_x}} \tag{B-16}$$

since

$$q = \dot{\theta} = s\theta \tag{B-17}$$

Therefore, $q/u_g\Big|_{\substack{\theta\to\delta_e\\ x\to\theta_x}}$ is formed simply by adding a free s to the numerator of $\theta/u_g\Big|_{\substack{\theta\to\delta_e\\ x\to\theta_x}}$.

b. Longitudinal Position and Velocity Equations

The loop closures of the model define $x/u_g\Big|_{\substack{\theta\to\delta_e\\ x\to\theta_x}}$ in terms of transfer functions as

$$x/u_g\Big|_{\substack{\theta\to\delta_e\\ x\to\theta_x}} = \frac{Y_{x_{u_g}} + \left(Y_{x_{u_g}} Y_{\theta_{\delta_e}} - Y_{\theta_{u_g}} Y_{x_{\delta_e}}\right) Y_{P_\theta}}{1 + Y_{\theta_{\delta_e}} Y_{P_\theta} + Y_{x_{\delta_e}} Y_{P_\theta} Y_{P_x}} \tag{B-18}$$

Substituting for the transfer functions in Eq. (B-18) results in the following relation

$$\begin{aligned} x/u_g\Big|_{\substack{\theta\to\delta_e\\ x\to\theta_x}} = {} & \Big(\left(X_u\tau_x\tau_\theta T_N/4\right)s^5 + \left\{X_u\left[\tau_x\tau_\theta/4 + T_N(\tau_x+\tau_\theta)/2\right] - X_u M_q\tau_x\tau_\theta T_N/4\right\}s^4 \\ & + \left\{X_u\left[T_N + (\tau_x+\tau_\theta)/2\right] - X_u M_q\left[\tau_x\tau_\theta/4 + T_N(\tau_x+\tau_\theta)/2\right]\right. \\ & \left. - \tau_x\tau_\theta T_N(X_u M_\theta + M_u g)/4 - K_{P_\theta} T_{L_\theta}\tau_x\tau_\theta\left(X_u M_{\delta_e} - M_u X_{\delta_e}\right)/4\right\}s^3 \\ & + \left\{K_{P_\theta}\left(X_u M_{\delta_e} - M_u X_{\delta_e}\right)\left[\tau_x\left(T_{L_\theta} - \tau_\theta/2\right)/2 - T_{L_\theta}\tau_\theta/2\right] + X_u\right. \\ & \left. - X_u M_q\left[T_N + (\tau_x+\tau_\theta)/2\right] - \left(X_u M_\theta + M_u g\right)\left[\tau_x\tau_\theta/4 + T_N(\tau_x+\tau_\theta)/2\right]\right\}s^2 \\ & + \left\{K_{P_\theta}\left(X_u M_{\delta_e} - M_u X_{\delta_e}\right)\left[\tau_x/2 + \left(T_{L_\theta} - \tau_\theta/2\right)\right] - X_u M_q\right. \\ & \left. - \left(X_u M_\theta + M_u g\right)\left[T_N + (\tau_x+\tau_\theta)/2\right]\right\}s + \left[K_{P_\theta}\left(X_u M_{\delta_e} - M_u X_{\delta_e}\right)\right. \\ & \left. - \left(X_u M_\theta + M_u g\right)\right]\Big)\Big/\Delta 3 \end{aligned} \tag{B-19}$$

Because the loop closures are unchanged, the characteristic equation for $x/u_g\Big|_{\substack{\theta\to\delta_e\\ x\to\theta_x}}$ is the same (Δ_3) as that for $\theta/u_g\Big|_{\substack{\theta\to\delta_e\\ x\to\theta_x}}$ in Eq. (B-16). The closed-loop equation for VTOL aircraft longitudinal velocity (position rate) is the derivative of the equation for position.

$$u/u_g\Big|_{\substack{\theta \to \delta_e \\ x \to \theta_x}} = sx/u_g\Big|_{\substack{\theta \to \delta_e \\ x \to \theta_x}} \tag{B-20}$$

c. Closed-Loop Control Stick Response to Turbulence

The closed-loop hovering model equation for control stick response to turbulence is

$$\delta_e/u_g\Big|_{\substack{\theta \to \delta_e \\ x \to \theta_x}} = -Y_{P_\theta}\left(Y_{P_x} x/u_g\Big|_{\substack{\theta \to \delta_e \\ x \to \theta_x}} + \theta/u_g\Big|_{\substack{\theta \to \delta_e \\ x \to \theta_x}}\right) \tag{B-21}$$

Substituting for the transfer functions indicated in Eq. (B-21) results in

$$\begin{aligned}
\delta_e/u_g\Big|_{\substack{\theta \to \delta_e \\ x \to \theta_x}} = {} & \Big[\Big(-K_{P_x}K_{P_\theta}X_u T_{L_\theta}T_{L_x}\tau_x\tau_\theta/4\Big)s^6 + \Big(K_{P_x}K_{P_\theta}X_u M_q T_{L_\theta}T_{L_x}\tau_x\tau_\theta/4 \\
& - K_{P_x}K_{P_\theta}X_u\left\{T_{L_x}\tau_x\tau_\theta/4 + T_{L_\theta}\left[\tau_x\tau_\theta/4 - T_{L_x}(\tau_x+\tau_\theta)/2\right]\right\} + K_{P_\theta}M_u T_{L_\theta}\tau_x\tau_\theta/4\Big)s^5 \\
& + \Big(K_{P_x}K_{P_\theta}T_{L_\theta}T_{L_x}\tau_x\tau_\theta\left(X_u M_\theta + M_u g\right)/4 + K_{P_x}K_{P_\theta}X_u M_q\left\{T_{L_x}\tau_x\tau_\theta/4\right. \\
& \left. + T_{L_\theta}\left[\tau_x\tau_\theta/4 - T_{L_x}(\tau_x+\tau_\theta)/2\right]\right\} - K_{P_x}K_{P_\theta}X_u\left\{T_{L_\theta}\left[T_{L_x} - (\tau_x+\tau_\theta)/2\right]\right. \\
& \left. + \left[\tau_x\tau_\theta/4 - T_{L_x}(\tau_x+\tau_\theta)/2\right]\right\} - K_{P_\theta}M_u\left[T_{L_\theta}(\tau_x-\tau_\theta)/2 - \tau_x\tau_\theta/4\right]\Big)s^4 \\
& + \Big(K_{P_x}K_{P_\theta}\left(X_u M_\theta + M_u g\right)\left\{T_{L_x}\tau_x\tau_\theta/4 + T_{L_\theta}\left[\tau_x\tau_\theta/4 - T_{L_x}(\tau_x+\tau_\theta)/2\right]\right\} \\
& + K_{P_x}K_{P_\theta}X_u M_q\left\{T_{L_\theta}\left[T_{L_x} - (\tau_x+\tau_\theta)/2\right] + \left[\tau_x\tau_\theta/4 - T_{L_x}(\tau_x+\tau_\theta)/2\right]\right\} \\
& - K_{P_x}K_{P_\theta}X_u\left\{T_{L_\theta} + \left[T_{L_x} - (\tau_x+\tau_\theta)/2\right]\right\} - K_{P_\theta}M_u\left[T_{L_\theta} + (\tau_x-\tau_\theta)/2\right]\Big)s^3 \\
& + \Big(K_{P_x}K_{P_\theta}X_u M_q\left\{T_{L_\theta} + \left[T_{L_x} - (\tau_x+\tau_\theta)/2\right]\right\} - K_{P_x}K_{P_\theta}X_u \\
& + K_{P_x}K_{P_\theta}\left(X_u M_\theta + M_u g\right)\left\{T_{L_\theta}\left[T_{L_x} - (\tau_x+\tau_\theta)/2\right] + \left[\tau_x\tau_\theta/4 - T_{L_x}(\tau_x+\tau_\theta)/2\right]\right\} \\
& - K_{P_\theta}M_u\Big)s^2 + \Big(K_{P_x}K_{P_\theta}X_u M_q + K_{P_x}K_{P_\theta}\left(X_u M_\theta + M_u g\right)\left\{T_{L_\theta} + \left[T_{L_x}\right.\right. \\
& \left.\left. - (\tau_x+\tau_\theta)/2\right]\right\}\Big)s + K_{P_x}K_{P_\theta}\left(X_u M_\theta + M_u g\right)\Big]\Big/\Delta_3
\end{aligned} \tag{B-22}$$

B. Computation of the Pilot-Model Adaptive Parameters

An approach commonly used to compute pilot describing functions (the source for quasi-linear models) involves the computation of a power-spectral density function for the disturbance function and a cross-spectral density function between the disturbance function and the pilot's control stick motion. This approach has been applied frequently to one-degree-of-freedom compensatory tracking tasks, and recently techniques have been developed (Ref. 31) for applying this approach to two-degree-of-freedom compensatory tasks. The computations involved in the development of power- and cross-spectral derivatives are complex and expensive. Also, the low-frequency portion of the inner-loop describing function cannot be computed accurately (Ref. 31). The object of the UARL model studies was to establish possible trends in pilot quasi-linear model adaptive parameters which correlate with opinion. The detailed procedures involved in the spectral density computations were not justified for the limited objective of the UARL studies. Therefore, an alternate method was developed. This approach uses statistical (rms) hovering performance data from the piloted flight simulator to compute the adaptive parameters.

The equations for the hovering model (Section V) were linearized by using a first-order Padé approximation, Eq. (B-9), for the pilot model transport lags. Transfer functions were then written which define the closed-loop pitch, pitch rate, position and longitudinal velocity (position rate) response to turbulence ($\theta/u_g\Big|_{\substack{\theta\to\delta_e\\ x\to\theta_x}}$, $q/u_g\Big|_{\substack{\theta\to\delta_e\\ x\to\theta_x}}$, $x/u_g\Big|_{\substack{\theta\to\delta_e\\ x\to\theta_x}}$ and $u/u_g\Big|_{\substack{\theta\to\delta_e\\ x\to\theta_x}}$, respectively). For these computations, it was assumed that the pilot closed the pitch loop before closing the position loop. The equations describing the rms response of the model to turbulence (i.e., analytical expressions for σ_θ, σ_q, σ_x and σ_u) were developed using these closed-loop transfer functions and the analytical representation for the turbulence (Section II). For example, it can be shown that

$$\sigma_\theta^2 = \frac{2\sigma_{u_g}^2}{\omega_B} I_{B\theta} \tag{B-23}$$

where

$$I_{B\theta} = \frac{1}{2\pi j}\int_{-j\infty}^{j\infty}\left[\frac{\theta(s)}{u_g}\Bigg|_{\substack{\theta\to\delta_e\\ x\to\theta_x}}\frac{1}{(1+s/\omega_B)}\right]^2 ds \tag{B-24}$$

Equation (B-24) can be integrated using the tables contained in Appendix E of Ref. 32. An equation of the form of Eq. (B-23) can also be used to describe σ_q, σ_x, σ_u if the appropriate closed-loop transfer function ($q/u_g\Big|_{\substack{\theta\to\delta_e \\ x\to\theta_x}}$, $x/u_g\Big|_{\substack{\theta\to\delta_e \\ x\to\theta_x}}$, and $u/u_g\Big|_{\substack{\theta\to\delta_e \\ x\to\theta_x}}$, respectively) is substituted into Eq. (B-24). For a given VTOL aircraft configuration, all model parameters except the pilot model adaptive parameters are assumed to be fixed. Thus, four rms equations are provided in terms of the four pilot-model adaptive parameters which are to be computed.

A digital computer iteration program which includes the four equations describing σ_θ, σ_q, σ_x, and σ_u was written. The measured values of σ_θ, σ_q, σ_x, and σ_u (all corrected for nonzero mean wind effects) from the flight simulator are input to the program. The program iterates on the four pilot-model adaptive parameters until the computed rms values match to within 0.5% of those measured. Most of the measured rms performance data used to develop the pilot model parameters were the average of 10 simulator runs of 100-second duration each (Table A-VI) although some were averages of 15 runs.

As indicated above, the pilot-model adaptive parameters are considered to be the only model variables for a given configuration. That is, the pilot's transport lag, e.g., τ_θ, and neuromuscular lag, T_N, are considered constant for the simulated task. This assumption holds quite well for τ_θ and τ_x, but T_N has been observed to vary with changes in disturbing function frequency (Ref. 16). The filtering effect of the aircraft pitch dynamics altered the turbulence bandwidth evident to the pilot; therefore, T_N of the pilot probably changed slightly with the bandwidth. However, the results in Ref. 16 indicate that the variations in T_N can be considered second-order effects relative to the expected changes in pilot adapted parameters. The value of T_N used in this study (0.35 sec) was that given in the results of Ref. 16 for an effective disturbance bandwidth of 1 rad/sec. In that study the pilot was controlling dynamics (K/s^2 dynamics) which required him to supply lead. These conditions are similar to the pitch dynamics and turbulence characteristics (prior to the aircraft filtering) used in this study. The values for τ_θ and τ_x (0.09 and 0.08, respectively) were a result of the investigation reported in Ref. 16.

By using rms pitch rate (σ_q) instead of rms control activity (σ_{δ_e}) as one of the measured functions for computing the pilot-model adapted parameters, the effects of pilot remnant (nonlinearities) at higher frequencies on the computer parameters were reduced. For the UARL precision hovering task, the pilot remnant probably consisted primarily of extraneous commands, such as those resulting from minor pilot errors in estimation of rates and amplitudes, nervous hand motion, high-frequency "dither" inputs to test aircraft response, etc. Because the remnant is composed of extraneous stick commands, it does

not necessarily affect the pilot's ability to control. It also probably does not affect greatly the degree of stability he can achieve while controlling his aircraft. However, the presence of remnant in the data used to compute the pilot model results in Section V does affect the computed indicators of pilot capability and closed-loop system performance and stability (pilot lead, gain, crossover frequency, and phase margin). Thus, remnant can affect the interpretation of pilot capabilities and performance; it is important to reduce the effect of remnant on the computed pilot-adaptable parameters and loop-closure characteristics.

The errors in measured hovering performance introduced by pilot remnant are attenuated in two ways. First, the pilot reduces the effects of his non-linearities by operating as a high-gain servomechanism. That is, the pilot can observe the effects of some of his extraneous inputs and act to suppress them. Secondly, as mentioned previously, the filtering effects of the aircraft dynamics are used to advantage in selecting the rms performance results to be used for the computation of pilot-model adapted parameters. In this way, some of the remaining remnant is suppressed simply because it is of too high a frequency to cause significant aircraft response.

The undesirable effect of pilot remnant on hovering task model results has been pointed out, and the ways in which the remnant effects are reduced have also been discussed. An indication of the effectiveness of the mechanisms by which the error in closed-loop results from pilot remnant is reduced is given in Table B-1. This table lists the difference between the pilot

TABLE B-1

EFFECT OF PILOT ADAPTABLE PARAMETER COMPUTATION TECHNIQUE ON REDUCTION OF PILOT REMNANT EFFECT

$M_u g = 0.67$ $X_u = -0.1$ $M_q = -3$ $\sigma_{u_g} = 5.1$ $\omega_B = 0.314$ OPTIMUM M_{δ_e}

Pilot	Source	Measured σ_{δ_e}, in.	Computed σ_{δ_e}, in.	(Measured) - (Computed) in.	$\frac{\text{(Measured) - (Computed)}}{\text{(Measured)}}$ %
A	X_u Studies	0.612	0.512	0.100	16
	$M_u g$ Studies	0.562	0.469	0.093	17
	M_q Studies	0.528	0.452	0.076	14
B	X_u Studies	0.625	0.513	0.134	21
	$M_u g$ Studies	0.590	0.515	0.075	13
	M_q Studies	0.599	0.494	0.105	18

control stick activity (σ_{δ_e}) measured in the flight simulator, and that computed using the hovering task model and the pilot-model adapted parameters calculated from measurements of σ_q, σ_θ, σ_u and σ_x. The linear portion of the pilot's output and the total remnant are both present in the measured σ_{δ_e}. The computed σ_{δ_e} includes the pilot's linear output and what remains of the remnant after it has been attenuated by the two mechanisms previously described. The difference between computed and measured σ_{δ_e} provides some indication of the effectiveness of the measurement technique in reducing the error in computed pilot model parameters introduced by pilot remnant. The measured σ_{δ_e}, computed σ_{δ_e} and their differences are listed in Table B-1 for three repeated simulator tests of the same VTOL aircraft configurations. The average reduction in remnant appears to have been about 16% to 17% of the total measured pilot control stick activity. Results reported in Ref. 16 indicate that for less difficult single-loop control tasks ($\omega_{ie} \leq 1.5$ rad/sec; K/s, K/s^2 dynamics) pilot remnant is approximately 30% of the pilot's total rms control output. If this is used as a figure of merit the results in Table B-1 indicate that over half of the pilot's rms remnant is removed using the UARL measurement technique.

C. Verification of Pilot Adaptive Parameter Computation Techniques

1. Analog Computer Simulation

A simulation was developed to validate the technique for computing the pilot model adaptive parameters from measured rms data. The hovering task model was programmed on an analog computer with a preselected set of adaptive parameters in the pitch- and position-loop pilot models. The analog task model was subjected to the same simulated turbulence used to excite the aircraft configuration flown in the pilot simulation. Values of σ_θ, σ_q, σ_x, and σ_u for the analog model were measured and the average of these functions for 10 and also 20 runs of 100-second duration each were computed. Corrections were made for the effects of nonzero mean wind on the measured rms values (Section II.C.4). The technique described previously was used for computing the adaptive parameters from the measured rms results. The adaptive parameters programmed in the analog computer simulation and those recovered from 10- and 20-run averages of rms results are shown below.

	Programmed Parameters	Recovered Parameters 10 runs	20 runs
K_{P_θ}	40.2	30.7	35.3
K_{P_x}	-0.0272	-0.0268	-0.0275
T_{L_θ}	0.170	0.188	0.182
T_{L_x}	0.401	0.452	0.395

It is felt that these results validate the techniques used to recover the adaptive parameters from rms performance measurements. The results show that the pilot adaptive parameters were recovered more accurately from 20 runs than 10. In this study the pilot model parameters computed from flight simulator data are usually based on 10 runs, although some are based on 15 runs. As a result of this simulation, it was felt that the additional time to obtain more runs was not warranted since the objective was only to identify trends in the pilot model parameters with pilot opinion.

2. Pilot Model Results from Repeated Tests with the Same Configuration

The same configuration was flown on the flight simulator three times by each pilot. These identical configurations were evaluated on dates which were separated by several weeks. Therefore, the consistency of the measured rms results and recovered parameters for these repeated configurations is an indication of the accuracy of the methods and procedures used to measure data and recover pilot model parameters. The measured rms values and recovered model parameters are shown in Table B-2. These results indicate that the rms measurement techniques, pilot parameter computation methods, and the repeatability of pilot hovering performance are sufficiently accurate to permit the identification of trends in pilot parameters with pilot opinion.

D. Interpretation of Computed Position-Loop Lead

This subsection is concerned with the interpretation of computed position-loop lead and the correlation of position-loop lead with opinion. The closed-loop representation for the VTOL hovering task (Sketch B-1) assumes that the pitch-loop lead (T_{L_θ}) adapted by the pilot is also applied directly to the pilot's control of position disturbances. That is, the hovering task model is constructed so that closing the inner (pitch attitude) loop causes the pitch-loop lead term to appear in the open-loop position dynamics ($x/\theta_x\big|_{\theta \to \delta_e}$). Therefore, T_{L_θ} contributes phase angle to both the pitch open-loop dynamics (θ/δ_e) and position open-loop dynamics (pitch loop closed). Equation (B-7) is again shown below to illustrate this effect

$$x/\theta_x\Big|_{\theta \to \delta_e} = \frac{Y_{P_\theta} Y_{x_{\delta_e}}}{1 + Y_{P_\theta} Y_{\theta_{\delta_e}}} \qquad \text{(B-7)}$$

This equation defines the open-loop position dynamics (pitch loop closed) as represented by the hovering task model. Note that the pitch-loop pilot model, Y_{P_θ} -- which contains the adaptable pitch-loop lead term, T_{L_θ} -- is in the numerator of this equation. As stated previously, whatever T_{L_θ} the pilot adapts in controlling the pitch loop also supplies phase lead to the open-loop

TABLE B-2

RMS MEASUREMENTS AND PILOT ADAPTABLE PARAMETERS FROM REPEATED TESTS OF THE SAME CONFIGURATION

$M_{ug} = 0.67 \quad X_u = -0.1 \quad M_q = -3 \quad \sigma_{u_g} = 5.1 \quad \omega_B = 0.314 \quad$ OPTIMUM M_{δ_e}

Pilot	Source	σ_θ	σ_q	σ_x	σ_u	K_{P_θ}	$-K_{P_x}$	T_{L_θ}	T_{L_x}	ω_{c_θ}	PM_θ	ω_{c_x}	PM_x
A	Test Run 1	0.0306	0.0434	1.40	0.870	38.5	0.0201	0.16	0.49	3.0	8	0.86	19
	Test Run 2	0.0334	0.0464	1.53	0.952	31.4	0.0193	0.13	0.54	2.7	10	0.86	20
	Test Run 3	0.0353	0.0515	1.45	0.976	34.2	0.0211	0.13	0.44	2.7	5	0.89	16
B	Test Run 1	0.0323	0.0484	1.08	0.803	42.0	0.0268	0.18	0.39	3.2	7	1.00	15
	Test Run 2	0.0320	0.0498	1.17	0.794	37.5	0.0240	0.16	0.49	3.0	9	0.96	19
	Test Run 3	0.0330	0.0495	1.08	0.807	39.7	0.0270	0.17	0.41	3.1	8	1.00	15

position dynamics. This is characteristic of the series-closure form of multiloop pilot model chosen (Sketch B-1).

The adapted pitch-loop lead computed from measured rms data is primarily dependent on pitch control characteristics and not position control characteristics. If the pitch dynamics are unstable and a large T_{L_θ} is required to stabilize them, T_{L_θ} will contribute a large phase angle to the position loop, also. If the pitch dynamics are stable and a small T_{L_θ} is adapted, a small phase angle from T_{L_θ} will be contributed to the position dynamics. Remember that this contribution from T_{L_θ} is also made to the open-loop position dynamics $(x/\theta_x|_{\theta \to \delta_e})$ whether these dynamics need a large amount of adapted lead compensation or not. For example, consider a configuration where the pitch dynamics are lightly damped and require a large T_{L_θ}, but the open-loop position dynamics (without the phase contribution from T_{L_θ}) are relatively well damped. Then, when the phase contribution from T_{L_θ} is added, the open-loop position dynamics may be provided with as much phase angle, or more, than is needed to provide good closed-loop position stability. For such a configuration, T_{L_x} would not be needed to provide stability. Consequently its value would be quite small. Such a case is PH36 in Table A-VII. It is apparent, then, that the T_{L_x} computed for the hovering task model is dependent on the value of T_{L_θ} needed to stabilize the open-loop pitch dynamics (θ/δ_e). In fact, the T_{L_x} computed is only that value which is needed to supplement the phase contribution from T_{L_θ} in providing closed-loop position stability.

The configurations for the M_ug studies discussed in Sections IV and V will be used to illustrate the effect of T_{L_θ} on T_{L_x} for pilot B. These configurations are listed as PH6 through PH9 in Table A-VII. Pilot B, when closing the position loop for these configurations, achieved a rather consistent degree of stability. That is, position-loop phase margin (PM_x) remained about 19 degrees for all values of M_ug (Table A-VII). He accomplished this, of course, by adding lead to compensate for the lag of the aircraft dynamics and inherent pilot lags in the region of position loop crossover frequency (assumed here to be $\omega_{c_x} = 1.0$ rad/sec) and thus provided the $PM_x \sim 19°$. The phase lag contributed by Δ_2 (the denominator of $x/\theta_x|_{\theta \to \delta_e}$) and the inherent pilot lags at $\omega_{c_x} = 1.0$ rad/sec were quite consistent when M_ug was varied. This is shown in the following table in the column entitled "Initial Phase Lag" (this column is the total phase lag plus 180 deg to put the "Initial Phase Lag" in a form which can be compared with PM_x).

M_ug	Initial Phase Lag	T_{L_θ}	Initial Phase Lag Plus Phase Lead from T_{L_θ}	T_{L_x}	Initial Phase Lag Plus Phase Lead from T_{L_θ} and T_{L_x} (PM_x)
0	-17	0.01	-16	0.72	19
0.33	-16	0.10	-10	0.53	18
0.67	-16	0.17	- 7	0.49	19
1.00	-17	0.20	- 6	0.50	21

The third column in the list shows the value of T_{L_θ} adapted in the M_ug studies for pilot B. In the series model T_{L_θ} contributes phase lead angle in the $x/\theta_{x|\theta \rightarrow \delta_e}$ closure. The fourth column shows the phase lag from Δ_2 and the pilot lags after the phase lead angle contribution from T_{L_θ} has been added to it. Thus, the phase angle in the fourth column becomes smaller (less negative) with M_ug because the phase angle contributed from T_{L_θ} increases with M_ug while the "Initial Phase Lag" (second column) is relatively unchanged. The fifth column in the listing shows the value of T_{L_x} computed for the M_ug study and the sixth column shows PM_x (the resultant phase angle plus 180 deg) at the assumed crossover frequency of ω_{c_x} = 1.0 rad/sec. Position-loop phase margin PM_x is, of course, the sum of the "Initial Phase Lag" in the second column plus the phase angle contributed from both T_{L_θ} and T_{L_x}. Note that PM_x was nearly constant for the M_ug studies.

Since both the "Initial Phase Lag" (second column) and also position-loop phase margin (PM_x, column 6) were nearly constant with M_ug, the computed lead results from the M_ug study are a good example of the dependence of T_{L_x} on the magnitude of T_{L_θ}. As pitch-loop disturbances increased with M_ug, the pilot had to adapt more T_{L_θ} in order to respond to them and also maintain pitch closed-loop stability. This is shown in the list. Since T_{L_θ} increased with M_ug, the phase lead angle it contributed to the nearly constant "Initial Phase Lag" (second column) also increased. Thus, as shown in the fourth column, the magnitude of the sum of the "Initial Phase Lag" and the phase lead contributed by T_{L_θ} decreased (became less negative). Since the value in the fourth column decreased, the phase contribution from T_{L_x} necessary to result in the nearly constant PM_x also had to decrease with M_ug. This is shown in the listing. As T_{L_θ} increased, there was a corresponding decrease in T_{L_x} indicating that T_{L_x} is quite dependent on the value of T_{L_θ}.

The pilot makes no distinction as to the source for the lead he supplies in the position loop. He is aware that a certain level of lead must be supplied for closed-loop position stability and it is this lead term which affects his opinion. This effective lead term ($T_{L_{x_{eff}}}$) which the pilot is actually supplying to the position loop is that value which provides the same phase angle contribution at crossover frequency as T_{L_θ} and T_{L_x} combined. This combined phase angle contribution is

$$\alpha = \tan^{-1}\left(T_{L_{x_{eff}}}\omega_{c_x}\right) = \tan^{-1}\left(T_{L_\theta}\omega_{c_x}\right) + \tan^{-1}\left(T_{L_x}\omega_{c_x}\right) \qquad \text{(B-25)}$$

At M_ug = 0.67, for example, the effective lead which the pilot is supplying in controlling position is $T_{L_{x_{eff}}}$ = 0.72 sec. As mentioned previously, it is this effective lead term which correlates with pilot opinion.

In summary, then, the pilot makes no distinction as to how he provides the necessary lead in the position loop. He simply supplies it. The hovering task model, however, is constructed so that it supplies T_{L_θ} to the pitch and

position loops. Therefore, T_{L_x} is computed to supplement T_{L_θ} as necessary to give the position-loop phase margin which the measured data indicated the pilot used. Consequently, T_{L_x}, alone, cannot be regarded as an indicator of the pilot's opinion of position-loop control difficulty. Instead, the $T_{L_{x_{eff}}}$ should be used for this purpose.

Unclassified
Security Classification

DOCUMENT CONTROL DATA - R&D
(Security classification of title, body of abstract and indexing annotation must be entered when the overall report is classified)

1. ORIGINATING ACTIVITY (Corporate author) United Aircraft Research Laboratories 400 Main Street East Hartford, Connecticut 06108	2a. REPORT SECURITY CLASSIFICATION Unclassified 2b. GROUP N/A

3. REPORT TITLE
Fixed-Base Flight Simulator Studies of VTOL Aircraft Handling Qualities in Hovering and Low-Speed Flight

4. DESCRIPTIVE NOTES (Type of report and inclusive dates)
Final Report -- August 1966 through August 1967

5. AUTHOR(S) (Last name, first name, initial)
Miller, David P.
Vinje, Edward W.

6. REPORT DATE	7a. TOTAL NO. OF PAGES	7b. NO. OF REFS
	198	32

8a. CONTRACT OR GRANT NO.	9a. ORIGINATOR'S REPORT NUMBER(S)
AF 33(615)-3736	F910482-12
b. PROJECT NO. 698 DC	
c.	9b. OTHER REPORT NO(S) (Any other numbers that may be assigned this report) AFFDL-TR-67-152
d.	

10. AVAILABILITY/LIMITATION NOTICES
This document is subject to special export controls and each transmittal to foreign governments or foreign nationals may be made only with prior approval of AFFDL(FDCC), Wright-Patterson AFB, Ohio 45433 .

11. SUPPLEMENTARY NOTES	12. SPONSORING MILITARY ACTIVITY
N/A	AFFDL(FDCC) Wright-Patterson AFB, Ohio 45433

13. ABSTRACT A systematic investigation of VTOL longitudinal and lateral handling qualities in hovering and low-speed flight was conducted in a fixed-base simulator. The effects of rate damping and attitude stability augmentation on handling qualities for a range of speed-stability and drag parameters, turbulence levels, and several other factors were studied. Pilots selected optimum control sensitivity, prepared written comments and assigned pilot opinion ratings for each configuration. The results for minimum satisfactory handling qualities are correlated with the aircraft and stability augmentation parameters and compared with existing and suggested requirements for VTOL handling qualities. Suggested criteria for aircraft dynamic characteristics and minimum response to control inputs that are based on the flight simulator data are presented. Root-mean-square performance data for a precision hovering task were obtained for a range of aircraft, stability augmentation and turbulence level parameters. Pilot model adapted parameters for a multi-loop representation of the hovering task were computed from these rms performance data and correlated with pilot opinion.

Results show that the stability augmentation and optimum control sensitivity requirements for satisfactory handling qualities are dependent on the gust-sensitivity of the aircraft. The generalized results show little correlation with existing or suggested criteria. Instead they indicate that the aircraft speed-stability parameters must be considered in the development of handling qualities specifications. The rms hovering performance was dependent primarily on

DD FORM 1-JAN 64 1473

Unclassified
Security Classification

14. KEY WORDS	LINK A		LINK B		LINK C	
	ROLE	WT	ROLE	WT	ROLE	WT
Fixed-base simulation data VTOL aircraft handling qualities Hovering and low-speed flight Stability augmentation requirements						

INSTRUCTIONS

1. ORIGINATING ACTIVITY: Enter the name and address of the contractor, subcontractor, grantee, Department of Defense activity or other organization *(corporate author)* issuing the report.

2*a*. REPORT SECURITY CLASSIFICATION: Enter the overall security classification of the report. Indicate whether "Restricted Data" is included. Marking is to be in accordance with appropriate security regulations.

2*b*. GROUP: Automatic downgrading is specified in DoD Directive 5200.10 and Armed Forces Industrial Manual. Enter the group number. Also, when applicable, show that optional markings have been used for Group 3 and Group 4 as authorized.

3. REPORT TITLE: Enter the complete report title in all capital letters. Titles in all cases should be unclassified. If a meaningful title cannot be selected without classification, show title classification in all capitals in parenthesis immediately following the title.

4. DESCRIPTIVE NOTES: If appropriate, enter the type of report, e.g., interim, progress, summary, annual, or final. Give the inclusive dates when a specific reporting period is covered.

5. AUTHOR(S): Enter the name(s) of author(s) as shown on or in the report. Enter last name, first name, middle initial. If military, show rank and branch of service. The name of the principal author is an absolute minimum requirement.

6. REPORT DATE: Enter the date of the report as day, month, year; or month, year. If more than one date appears on the report, use date of publication.

7*a*. TOTAL NUMBER OF PAGES: The total page count should follow normal pagination procedures, i.e., enter the number of pages containing information.

7*b*. NUMBER OF REFERENCES: Enter the total number of references cited in the report.

8*a*. CONTRACT OR GRANT NUMBER: If appropriate, enter the applicable number of the contract or grant under which the report was written.

8*b*, 8*c*, & 8*d*. PROJECT NUMBER: Enter the appropriate military department identification, such as project number, subproject number, system numbers, task number, etc.

9*a*. ORIGINATOR'S REPORT NUMBER(S): Enter the official report number by which the document will be identified and controlled by the originating activity. This number must be unique to this report.

9*b*. OTHER REPORT NUMBER(S): If the report has been assigned any other report numbers *(either by the originator or by the sponsor)*, also enter this number(s).

10. AVAILABILITY/LIMITATION NOTICES: Enter any limitations on further dissemination of the report, other than those imposed by security classification, using standard statements such as:

(1) "Qualified requesters may obtain copies of this report from DDC."

(2) "Foreign announcement and dissemination of this report by DDC is not authorized."

(3) "U. S. Government agencies may obtain copies of this report directly from DDC. Other qualified DDC users shall request through _____."

(4) "U. S. military agencies may obtain copies of this report directly from DDC. Other qualified users shall request through _____."

(5) "All distribution of this report is controlled. Qualified DDC users shall request through _____."

If the report has been furnished to the Office of Technical Services, Department of Commerce, for sale to the public, indicate this fact and enter the price, if known.

11. SUPPLEMENTARY NOTES: Use for additional explanatory notes.

12. SPONSORING MILITARY ACTIVITY: Enter the name of the departmental project office or laboratory sponsoring *(paying for)* the research and development. Include address.

13. ABSTRACT: Enter an abstract giving a brief and factual summary of the document indicative of the report, even though it may also appear elsewhere in the body of the technical report. If additional space is required, a continuation sheet shall be attached.

It is highly desirable that the abstract of classified reports be unclassified. Each paragraph of the abstract shall end with an indication of the military security classification of the information in the paragraph, represented as *(TS)*, *(S)*, *(C)*, or *(U)*.

There is no limitation on the length of the abstract. However, the suggested length is from 150 to 225 words.

14. KEY WORDS: Key words are technically meaningful terms or short phrases that characterize a report and may be used as index entries for cataloging the report. Key words must be selected so that no security classification is required. Identifiers, such as equipment model designation, trade name, military project code name, geographic location, may be used as key words but will be followed by an indication of technical context. The assignment of links, rules, and weights is optional.

13. Abstract (Continued) position-loop disturbances. Changes in pitch-loop dynamics and disturbance level had little effect on hovering performance even when they resulted in large changes in pilot opinion rating. Results of the studies of pilot model adapted parameters show that pilot opinion correlates well with a combination of adapted lead and aircraft gust sensitivity.